NINTH INTERNATIONAL BENCHMARK WORKSHOP ON NUMERICAL ANALYSIS OF DAMS

St.Petersburg, Russia, 22-24 June 2007

PROCEEDINGS

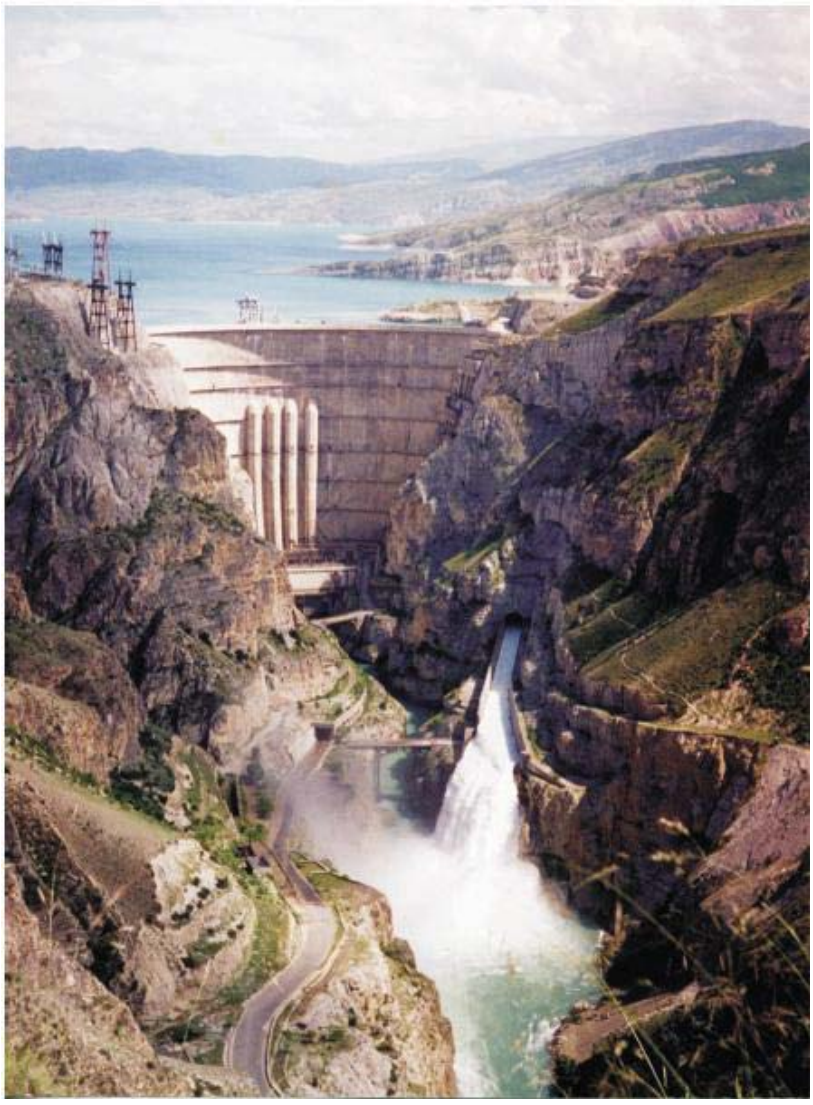

PROCEEDINGS

NINTH INTERNATIONAL BENCHMARK WORKSHOP ON NUMERICAL ANALYSIS OF DAMS

St.Petersburg, Russia,
22-24 June 2007

Organized by
ICOLD
Technical Committee on Computational Aspects
of Analysis and Design of Dams

Publishing coordinators:
Vyacheslav Glagovsky and Elena Gibyanskaya

Cover photo: Chirkeiskaya HPP dam

Printed in Russia

Published by Vedeneev All-Russian Research Institute of Hydraulic Engineering, Inc.

Printed: Dom Shuan, Ltd.
21, Gzhatskaya St., Saint Petersburg, 195220, Russia

The B.E.Vedeneev VNIIG, Inc.
21, Gzhatskaya St., Saint Petersburg, 195220, Russia
phone: +7 812 535-5445,
fax: +7 812 535-6720
e-mail: vniig@vniig.ru
web site: www.vniig.ru

ISBN 978-5-85529-129-2

FOREWORD

The Ninth International Benchmark Workshop on Numerical Analysis of Dams was held on 22 -24 of June, 2007, in St.Petersburg, Russia. Previous Workshops were successfully held in Bergamo, Italy (1991 and 1992), Paris, France (1994), Madrid, Spain (1996), Denver-Colorado, USA (1999), Salzburg, Austria (2001), Bucharest, Romania (2003) and Wuhan, China (2005).

The Workshop was organized by the Technical Committee on Computational Aspects of Analysis and Design of Dams of the International Commission on Large Dams (ICOLD) and Vedeneev All-Russian Research Institute of Hydraulic Engineering, Inc. («Vedeneev VNIIG»).

It was sponsored by Russian National Committee on Large Dams, Unified Energy System of Russia (RAO UESR), Federal Hydrogeneration Company HydroOGK, NP "Gidroenergetika Rossii".

The official supporting magazine was "The International Journal on Hydropower and Dams".

The purpose of the Workshop was to provide a critical examination of the computational methods and software used for dam analysis. For this purpose some specific problems in concrete and embankment dams were formulated and the participants were invited to provide solution of the problems that will be comparatively evaluated during the Workshop. In this way, the most appropriate computational approach for each specific problem can be recommended.

Consistent with previous Workshops, there were three themes, two of them focused on a dam type, as follows: concrete dams (Theme A) and embankment dams (Theme B), the third theme C was dedicated to the methods of numerical modeling of dams. The problems, formulated by different organizations, had been examined and approved by ICOLD Technical Committee. The problems provided for each of the three themes mentioned above were the following: analysis of the elastic behaviour of an arch-gravity dam after the first impounding (formulator: Dr Ignacio Escuder Bueno, co-formulator: Francisco Blazquez, Spain), stress-strain state of high rock-fill dam with a central ground core at large amplitude of operation water level changes (formulator: Dr. Stanislav Panov, Russia) and the Open Theme - Advanced Numerical Modelling for Dams (formulator: Alain Carrère, France).

The Workshop was dedicated to the analysis of results in solving the technical themes A and B, discussions on the theme C focused on the methods of numerical modeling of dams. The presentation of the results by the contributors for each technical theme was preceded by the presentation of the theme by formulator. Finally, each formulator presented a comparison of the results and conclusions.

More than 40 specialists from 12 countries took part in the Workshop; they are Austria, Canada, France, Italy, Japan, Macedonia, Netherlands, Romania, Russia, Sweden, Switzerland and United States of America. The participants made 16 oral presentations and reports on three main themes which had been proposed by the organizers for consideration. This volume contains the formulation of problems, synthesis reports concerning the solutions of the problems and the papers submitted by participants. Some papers reported on the Workshop only as oral presentations are included in the volume too.

Information about the one-day tour to Volhovskaya HPP (one of the oldest HPP in Russia) with visiting the historical and cultural place Staraya (Old) Ladoga organized on 24 of June is also included.

The organizers hope that the papers published in this volume will be useful for scientific researchers who deal with problems of numerical analysis of dams.

Scientific Committee of the Ninth International Benchmark Workshop on Numerical Analysis of Dams

Chairman:
A. Carrere (France)

Vice-Chairman
G. Mazza (Italy)

Members
C.Bossoney (Switzerland)
S.H.Chen (China)
D.Curtis (Canada)
M.Fanelli (Italy)
V.B.Glagovsky (Russia)
Y.P.Liapichev (Russia)
G.Manueco (Spain)
E.Matheu (USA)
A.Popovici (Romania)
S.N.Soheili (Iran)
Y.Uchita (Japan)
G.Zenz (Austria)

Organizing Committee
A.Carrere (ICOLD representative)
G.Mazza (Italy)
Ignacio Escuder Bueno (Spain)
Francisco Blazquez (Spain)
E.Bellendir (Russia)
V.Glagovsky (Russia)
A.Khrapkov (Russia)
A.Pak (Russia)
S.I.Panov (Russia)

CONTENTS

THEME A

Concrete Dams

International Commission On Large Dams

Committee on Computational Aspects of Analysis and Design of Dams

9th Benchmark Workshop on Numerical Analysis of Dams

22 -24 June, 2007 - St.Petersburg, Russia

THEME A - Concrete Dam

ANALYSIS OF THE ELASTIC BEHAVIOR OF AN ARCH-GRAVITY DAM

Formulator: **Dr. Ignacio Escuder Bueno**
iescuder@hma.upv.es
UNIVERSIDAD POLITECNICA DE VALENCIA
Dpto. Ingenieria Hidraulica Camino de Vera S/N
Valencia 46022 (Spain)

Co-Formulator: **Francisco Blazquez**
Canal de Isabel II. Madrid, Spain.

Foreword

Records obtained from dam instrumentation are crucial in order to interpret the structure behavior and be able to assess its safety. However, due to the uncertainties involved in the process of installing such instruments, the way readings are collected, the nature of the instruments and their conservation state, measurements can be not as reliable as expected. In fact, measurements can be misunderstood, can lead to make the wrong decisions and, in some cases, can make dam engineers to develop some degree of skepticism about their importance. Numerical modelling can be a helping tool but also adds some additional uncertainties if they are not carefully and rigorously used: construction data should be examined, constitutive models properly chosen, etc.

In summary, combination of a good knowledge of the instruments, an appropriate conservation of instrumentation and reading procedure, a realistic data management program and the implementation of numerical models is a very important task that has to be carefully undertaken due to all the involved uncertainties. But also, the behavior itself of a dam, is a source (sometimes the main one) of uncertainties.

In this context, the study of the behavior of La Acena Arch Gravity Dam is proposed.

Picture of the Dam

Aim of the theme

In particular, La Acena Dam is an arch gravity structure, and belongs to the Madrid water supply system operated by the company Canal de Isabel II. The study of its behaviour has been divided according to chronological order and the source of the readings:

a) First impounding (February 1999 to May 2001)

The instrumentation and monitoring system of the dam was aimed to displacement, joint performance, stresses and seepage control. The analysis of data recorded during first impounding resulted in the following outcomes:

- Maximum displacement toward the abutments (tangential) was 3.75 mm, reached when the reservoir was at maximum normal operating level.
- Radial displacements (upstream to downstream) were in a range between 1.23 cm and 1.8 cm, with slight differences between blocks. Maximum recorded joint movement was 1.88 mm.
- Maximum seepage flow (40 l/min) also occurred for the maximum normal operating level. The maximum value for a single block was 1.7 l/min.

b) Movements after first impounding

Movements recorded after first impounding by means of four plumblines revealed an apparently significant increase of downstream displacements (around 4 cm).

The exercise proposed aims at analysing the stress-strain behavior of the dam and interpreting the recorded displacement at the crest and its pattern, as related to water level and temperature time histories.

Main lines of the Theme

The exercise consist in building a model that explains the elastic behaviour of the dam (detailed geometry, water level and temperature - exterior and interior- time series will be provided).

The model (2D or 3D; Finite Element or Finite Difference; etc.) will be selected by the participants, that should try to explain the elastic behaviour of the dam.

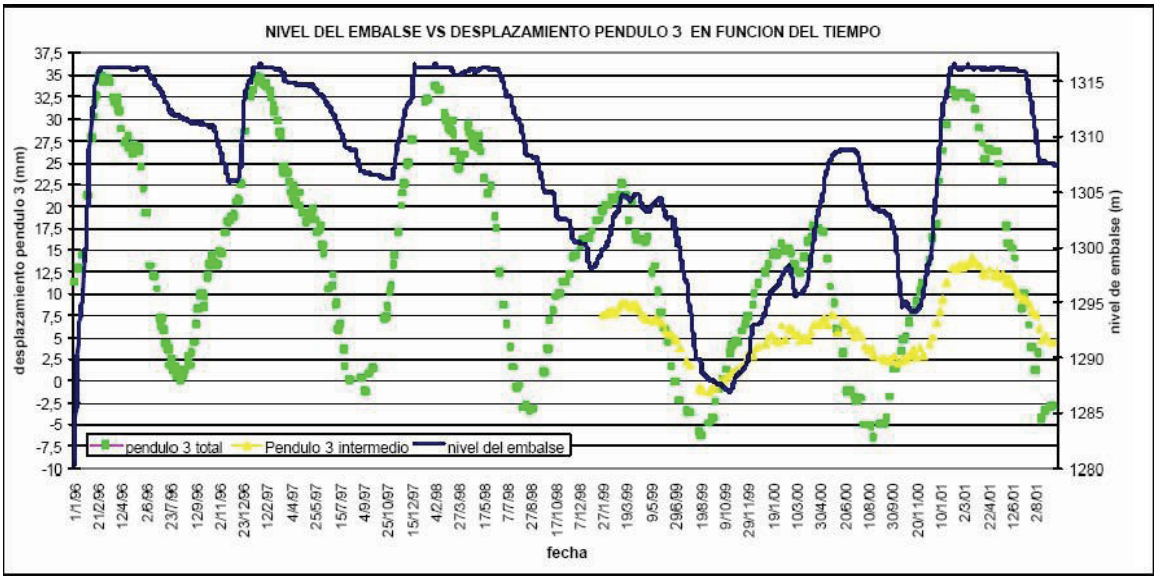

Figure. Recorded behaviour (to be explained by the model)

Legend: Water level in blue (elevation in meters y-axes on the right)

Incremental horizontal displacements from lower gallery to the crest in green (displacement in millimeters, y-axes on the left)

Incremental horizontal displacements from lower gallery to intermediate gallery in yellow (displacement in millimeters, y-axes on the left)

LESSONS LEARNED IN THE ANALYSIS OF THE ELASTIC BEHAVIOR OF AN ARCH-GRAVITY DAM PERFORMED BY SEVEN INDEPENDENT ENGINEERING TEAMS

Ignacio Escuder Bueno

(Universidad Politecnica de Valencia, Spain)

Francisco Blazquez Prieto

(Canal de Isabel II, Madrid, Spain)

Ignacio Escuder Bueno (CE, MSc, PhD) is currently Professor at Universidad Politecnica de Valencia (UPV, Spain) and permanent member of the Spanish National Committee on Large Dams (SPANCOLD). He is consultant on different aspects of dam engineering and his major research field is devoted to Risk Analysis as applied to Dam Safety.

Francisco Blazquez Prieto (CE) is currently a chief engineer at Canal de Isabel II, the water supply company of Madrid (Spain) and permanent member of the Spanish National Committee on Large Dams (SPANCOLD). He is in charge of the safety of the dams in his company and his major research field is devoted to Seismic Aspects of dam engineering.

ABSTRACT

The analysis of the behavior of an arch-gravity dam, whose main features and outcomes are herein presented, has been performed by seven independent engineering teams: Universidad Politecnica de Valencia (Spain), CESI Ricerca (Italy), Coyne-et-Bellier (France), Tokyo Electric Power Service Company (Japan) in cooperation with the University of Colorado (USA), TNO DIANA BV (The Netherlands), Civil Engineering School of Skopje (Republic of Macedonia) and Technical University of Civil Engineering of Bucharest (Rumania).

The case corresponds to material designated “Theme A” at the Ninth International Benchmark Workshop on Numerical Analysis of Dams, celebrated in Saint Petersburg (Russia) in June, 2007, organized by the ICOLD Committee on Computational Aspects of Analysis and Design of Dams.

Among many lessons learned, those related to the capabilities of the different implemented models, the differences observed in numerical results, and the analysis of all sources of uncertainty are specifically addressed in this article.

1. INTRODUCTION

As is currently widely accepted in dam engineering, proper assessment of the behavior and safety of these critical infrastructures requires an appropriate conservation of instrumentation and reading procedure, a realistic data management program, and the implementation of numerical models. Besides these very important tasks that have to be carefully undertaken due to all the involved uncertainties, the behavior of the dam itself is a source (sometimes the main one) of uncertainty. The role of benchmarks, allowing comparisons of results using different constitutive models, computer codes, etc., can be very relevant to an improved understanding and assessment of the uncertainties involved in cases like the one herein presented. This particular case was formulated by the authors of the article, and corresponds to material designated as "Theme A" at the Ninth International Benchmark Workshop on Numerical Analysis of Dams, celebrated in Saint Petersburg (Russia) in June 2007, organized by the ICOLD Committee on Computational Aspects of Analysis and Design of Dams.

The seven participants (P) in "Theme A" have contributed significantly to a better understanding of the capabilities of different codes and modelling strategies, as well as to the improvement of our understanding of the degree to which different ways of considering certain load hypothesis may affect the final results. Also, through all their contributions, some key conclusions can be established regarding the needs of future modelling and site investigation and also regarding the balanced program of works needed in both modelling and site investigation to minimize uncertainties and maximize the efficiency of the investment. The names of the participants and their papers are listed below (Table 1), together with the reference (P1 to P7) assigned to each in this article.

REF.	TITLE OF THE CONTRIBUTION	AUTHORS	COMPANY / INSTITUTION
P1	Analysis Of The Elastic Behavior Of An Arch-Gravity Dam	Eduardo Echeverria[1] Ignacio Escuder[2]	[1]Universidad Politecnica de Valencia and OFITECO, Spain. [2]Universidad Politecnica de Valencia, Spain.
P2	FEM Analyses For The Interpretation Of The Structural Behavior Of La Aceña Dam	Massimo Meghella Piero Masarati	Cesi Ricerca Spa, Milan, Italy
P3	Analysis Of The Elastic Behavior Of An Arch-Gravity Dam	T. Bourgoin C. Noret-Duchëne	Coyne-et-Bellier, Gennevilliers, France
P4	Analysis Of The Elastic Behavior Of La Aceña Arch-Gravity Dam	Gjorgi Kokalanov Ljubomir Tancev Stevcho Mitovski	Civil Engineering Faculty, Skopje, Republic of Macedonia
P5	Elastic Analysis Of An Arch-Gravity Dam Behavior Using Merlin	Yoshinori Yagome[1] Yoshihisa Uchita[1] Victor Sauoma[2]	[1]Tokyo Electric Power Service Co., Inc, Japan [2]University of Colorado, USA.
P6	Elastic Analysis Of An Arch-Gravity Dam Using Diana	Gerd-Jan Schreppers Giovanna Lilliu	TNO DIANA BV, Delft, The Netherlands
P7	Numerical Simulation Of An Arch-Gravity Dam Behavior During Operation	Adrian Popovici Radu Sarghiuta	Technical University of Civil Engineering of Bucharest, Romania

Table 1. List of Contributions

The formulators, who are the authors of the article, work at the Universidad Politecnica de Valencia and at the Canal de Isabel II (water supply company in Madrid which owns the dam) respectively. They worked together on the document, “First Review And General Analysis Of The Safety Of The Dam”, with OFITECO (a Spanish engineering consulting firm specializing in dam engineering), the firm in charge of that contract.

2. SCOPE OF THE WORK

The studied structure, La Aceca Dam, is an arch-gravity dam operated by the “Canal de Isabel II”, the company in charge of the Madrid (Spain) water supply system. It is a symmetrical arch-gravity dam defined by a circular arch with a radius of 150 m. for the upstream face and an aperture equal to 90 sexagesimal degrees. The crest arch (without right and left abutments) has a development of 235.6 m and a maximum height of 66 m. The upstream face is defined by a cylindrical surface, and the cantilevers have variable thickness with altitude. The thickness of the crown cantilever ranges from 4 m on top to 28.8 m on the bottom. The dam (arch and abutments) is divided into 19 cantilevers separated by joints.

The following picture (Figure 1) shows the structure from downstream.

Figure 1. View Of The Dam (From Downstream)

The joints of the dam were sealed in February of 1989. A year later, during the first impounding of the dam (February 1990 to May 1991), the instrumentation and monitoring system was aimed to measure stresses and displacements of the dam body, performance of joints, and seepage. The analysis of data recorded in that particular period resulted in the following outcomes:

- Maximum displacement toward the abutments (tangential) was 3.75 mm, reached when the reservoir was at maximum normal operating level.

- Radial displacements (upstream-downstream) were in a range between 12.3 mm and 18 mm, with slight differences between blocks. The maximum recorded relative movement in any of the joints was 1.88 mm.

- Maximum seepage flow (40 l/min) also occurred during the maximum normal operating level. The maximum measured through a single block was 1.7 l/min.

Movements recorded after first impounding by means of four plumb lines have consistently shown a range of radial displacement of approximately 40 mm. The exercise proposed aimed at analyzing the stress-strain behavior of the dam, and interpreting the recorded displacement from 1999 to 2001 (the pattern of behavior has remained constant since then), as related to water level and temperature time histories.

In particular, all seven participants were asked to justify their numerical tool (finite difference, finite element or any other type), their geometric model (cell sizes and location) and all constitutive models, as a prior step to proceeding with the two parts of the problem: 1) by calculating displacements for a series of particular dates according to the given data in the block where the “Plumb line 3” is installed, and 2) by varying any of the characteristics of the analysis in order to get values for displacement as similar as possible to those recorded by “Plumb line 3” (see location in Figure 2), followed by an engineering interpretation of the meaning of such changes in the calculation model.

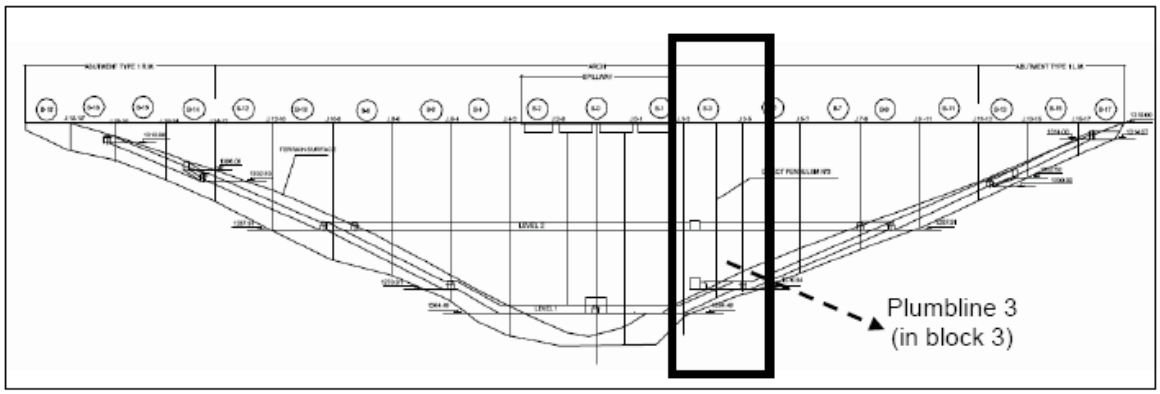

Figure 2. Location Of Plumb line 3.

3. SUMMARY OF GIVEN DATA

The available data provided to all participants in various magnetic formats (dwg, excel, etc.) were related to the geometry of the dam, the geology of the foundation, the mechanical characteristics of the concrete and rock, temperature data, and detailed records of movements related to water levels from January 1999 to November 2001. A selection of the given data is provided by means of the following figures and tables.

In particular, Figure 3 shows the cross section of the dam at block Number 3, where Pendulum 3 is located. Figure 4 represents the geology of the foundation, and Figure 5 represents the radial displacements measured by direct Pendulum 3. In addition, Table 2 summarizes the static properties of the materials, Table 3 contains the historical monthly average temperatures near the dam site, and Table 4 is a selection of temperatures (^{o}C) recorded on the dam’s body during first impounding.

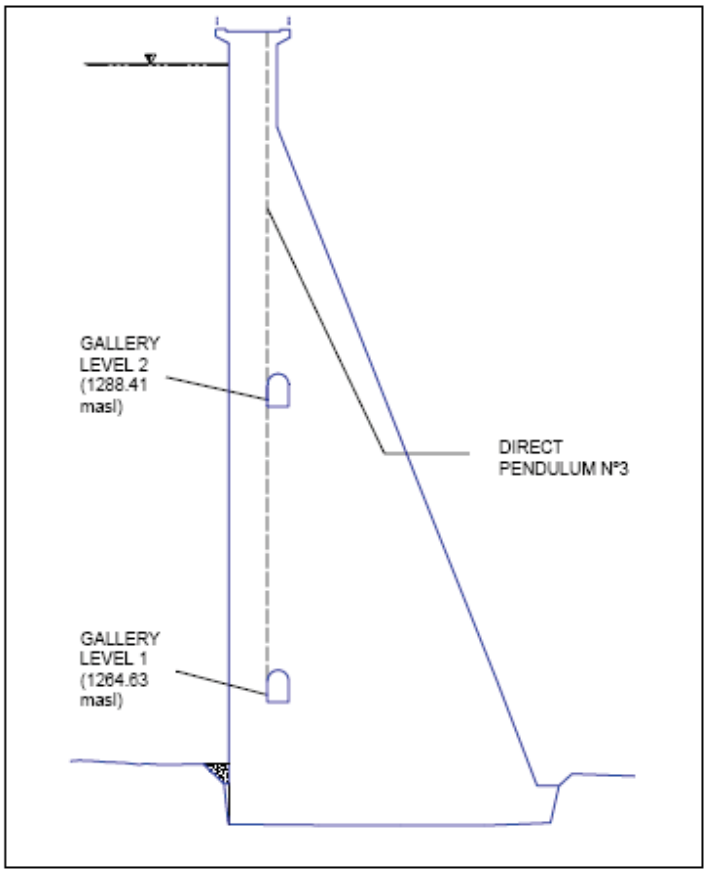

Figure 3. Cross-Section Of The Dam

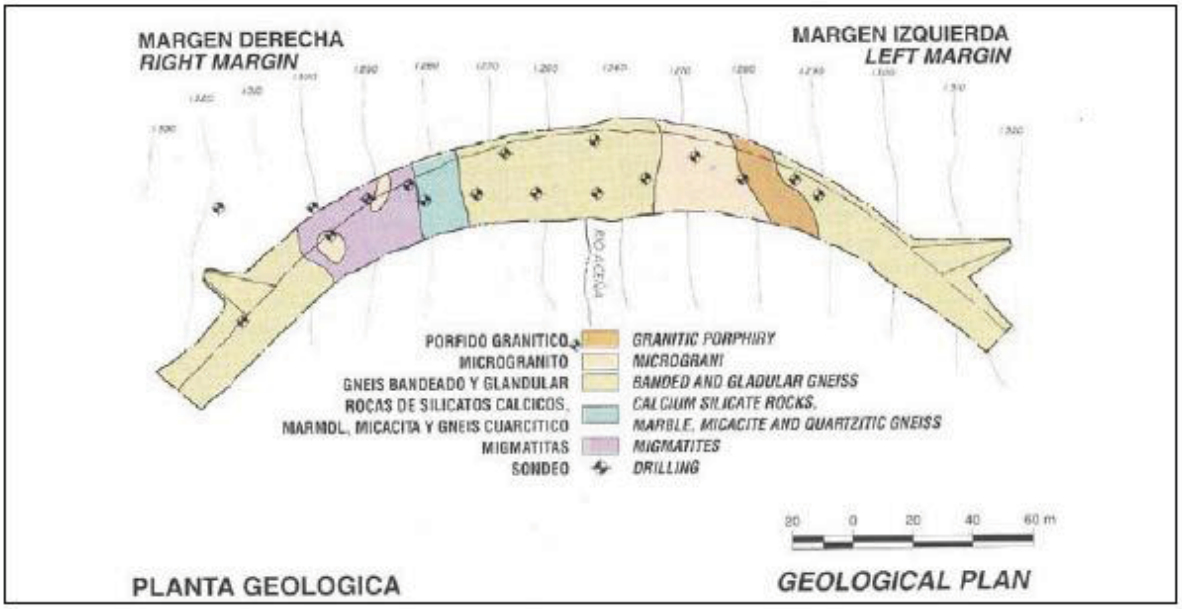

Figure 4. Geological Characteristics Of The Foundation

PROPERTY	FOUNDATION	DAM BODY
Specific weight	22 KN/m^3	23.6 KN/m^3
E (Young Modulus)	10000 MPa	20000 MPa
Poisson´s Ratio	0.2	0.2
Coefficient of thermal expansion	0	10^{-5} ºC^{-1}

Table 2. Static Properties Of Materials

Month	J	F	M	A	M	J	J	A	S	O	N	D
Temperature (ºC)	2.9	3.7	5.9	8.2	12.0	16.1	20.0	19.6	16.3	11.0	5.9	3.2

Table 3. Historical Monthly Average Temperatures Near The Dam Site

DATE	07/02/1990	26/04/1990	26/12/1990	31/01/1991	22/03/1991	04/05/1991
WATER LEVEL	Empty reservoir	1280 (masl)	1293.6 (masl)	1296.5 (masl)	1311 (masl)	1316 (full reservoir)
B3/DS/1283	8.7	10.2	8.9	7.8	9.8	11.3
B3/CE/1283	14.1	12.1	15.9	13.8	12.7	11
B3/CE/1309	3.8	7.8	3.9	2.8	5.3	8.3

Table 4. Selection Of Temperatures (ºC) Recorded On Dam's Body During First Impounding

Legend:

Bi = Block "i"

DS/CE/US: location of the thermal resistance inside the block (Downstream/Center/Upstream)

1BCD = thermal resistance elevation in masl.

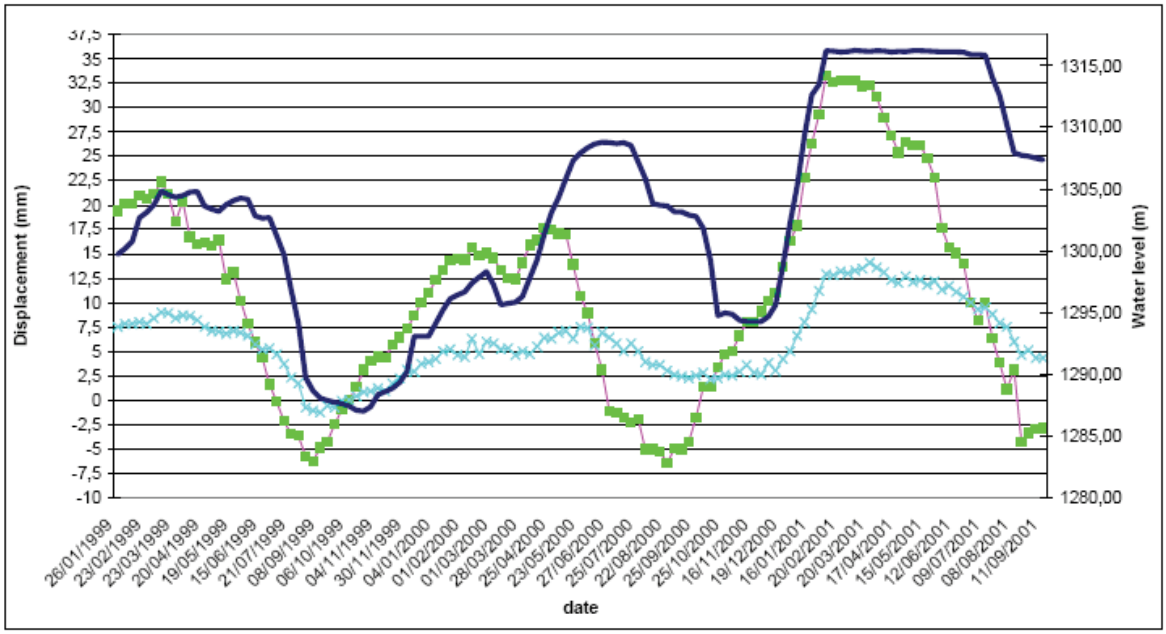

Figure 5. Radial Displacements Form Direct Pendulum 3

Legend:

Water level in dark blue (elevation in meters above sea level)

Incremental horizontal displacements from lower gallery to the crest in green (displacement in millimetres; Positive = Downstream direction)

Incremental horizontal displacements from lower to intermediate gallery in light blue (displacement in millimetres; Positive = Downstream direction)

In any case, as many participants remarked after analyzing the given data, it was anticipated that measurements provided might not be sufficient to grant a sound interpretation of dam behavior. In particular, the following lack or incompleteness of information was highlighted:

a) Inflow/Outflow seasonal regime of the reservoir (water temperatures to assign to the wet face of the dam model, etc.)

b) The influence of thermal radiation and daily air temperatures, given particular dam face exposures.

c) The shortness of the observation period, which might compromise the ability to identify trends and repeatable situations.

d) The synthetic and generic nature of measurements relevant to the first impounding, particularly those relevant to joint displacements, such as:

- Maximum joint “movement” recorded was 1.88 mm, but no information on either the type of movement--opening or sliding--or the external conditions of its occurrence were provided

- The exact locations of the thermometers inside the dam body are not reported, making it difficult to identify the internal temperature patterns inside the dam body

within the first impounding period.

e) The eventual spatial variability of the elastic parameters of the dam and its foundation.

4. CHARACTERISTICS OF THE MODELS

Despite the fact that the formulators provided a particular model geometry generated from the software SAP2000, all participants used different codes and many of them changed the features of the mesh. These main features are briefly commented upon bellow:

- The P1 Solution is based on an analysis performed with SAP 2000 NL V.7.0. The model was built by means of 53038 joints, 11654 within the dam body, and 45740 elements, 9327 within the dam body. The element used is defined as “solid”, an eight joint and six plane faces element. The size of the element has been defined by the need to be able to reproduce the thermal gradient through the thickness of the dam body. The width has been divided into five elements, thus implying an average size of three meters for the element.

- P2 Contributors used their in-house developed FEM Code CANT-SD to analyze the linear-elastic FEM model of the dam-foundation system. The same FEM mesh as the one provided by the formulators was used for all analyses.

- P3 Team carried out the structural model with the help of the software COQEF, developed by Coyne-et-Bellier. COQEF models the dam by means of thick shell elements. The elements of the mesh are made up of rectangles defined by 8 nodes and triangles defined by 6 nodes. Foundation elements are VOGT elements defined by a line with 3 nodes. In order to get a reasonable mesh size, only 578 nodes were selected to build the dam model.

- P4 used computer software SOFiSTiK for stress-strain analyses. The finite element mesh was generated using SOFiSTiK automatic mesh generator. Three types of element were used to model the dam’s body: BRIC, QUAD and SPRING elements. The BRIC element is a general six-sided element with eight nodes. The plane element, QUAD, is a general quadrilateral element with four nodes. In order to simulate the behavior of the interfaces of the dam (joints between concrete blocks, dam-foundation interaction), SPRING elements were also introduced. This complex modelling of the dam resulted in a finite element mesh with 10.383 finite elements and 56.638 nodes.

- P-5 Analysis was performed by the computer code MERLIN, which has the support of a window-based pre-processor, KUMONOSU, used to generate the 2D and 3D meshes. In the stress analysis, interface elements were used between the dam and the foundation (it was assumed that the monoliths were rigidly connected). For the most sophisticated model (3D including joints), the total number of nodes was 33871, allocating 16163 inside the dam body.

- P-6 conducted the study using DIANA Finite Element software and Midas FX+ as DIANA pre-/post-processor. The dam body was initially schematized by means of a parameterized cylinder at the upstream face, a parameterized cone at the downstream face, and a parameterized ring at the top. Boolean operators applied to these parameterized geometrical shapes lead to the final geometry of the dam body. The element size was set at 2 m for the elements in the dam, and at 25 m for the elements at the boundaries of the foundation. A tetrahedron mesh was generated

automatically. The mesh contained 32562 elements in the foundation, and 12742 elements in the dam.

- P7 used ANSYS computer code. The finite element back-analysis of the dam's behavior was performed in bi-(2D) and three-dimensional (3D) hypotheses. The dam body was discretized with the SOLID 45 element type, using four rows of elements on the dam thickness. This element is defined by 8 nodes and is linear, isoparametric with incompatible modes included. The volume of rock foundation extended in every direction was about 1.5 Hd (Hd – dam maximum height), and was meshed with tetrahedral solid element (SOLID45). Finally, the total number of SOLIDS used in the 3D model was 16772.

Concerning the load hypothesis, basic differences were found among teams that did or did not consider the uplift pressure as an acting force, and also among those that modelled temperatures in different ways (see Figure 6 as an example provided by P2). Another difference factor is that some of the participants also performed a statistical model to analyze the given recorded data. Main characteristics of the load hypothesis, together with the just-reviewed model features, are summarized in Table 5.

	CODE	DETERMINISTIC MODEL	TEMPERATURE MODEL	UPLIFT
P1	SAP 2000	3D. 53038 Joints	Steady and linear	YES
P2	CANT-SD	3D. 53038 Joints	Transient and with water temperature delay	NO
P3	COQ-EF	3D. 578 Nodes	Stucky	…...
P4	SOFiSTiK	3D. 56638 Nodes	Reproducing construction records	……
P5	MERLIN	2D+3D. 4113 Nodes	Steady and linear	YES
P6	DIANA	3D. 45304 Elements	Transient	……
P7	ANSYS	2D+3D. 16772 Elements	Transient	……

Table 5. List Of Models And Features

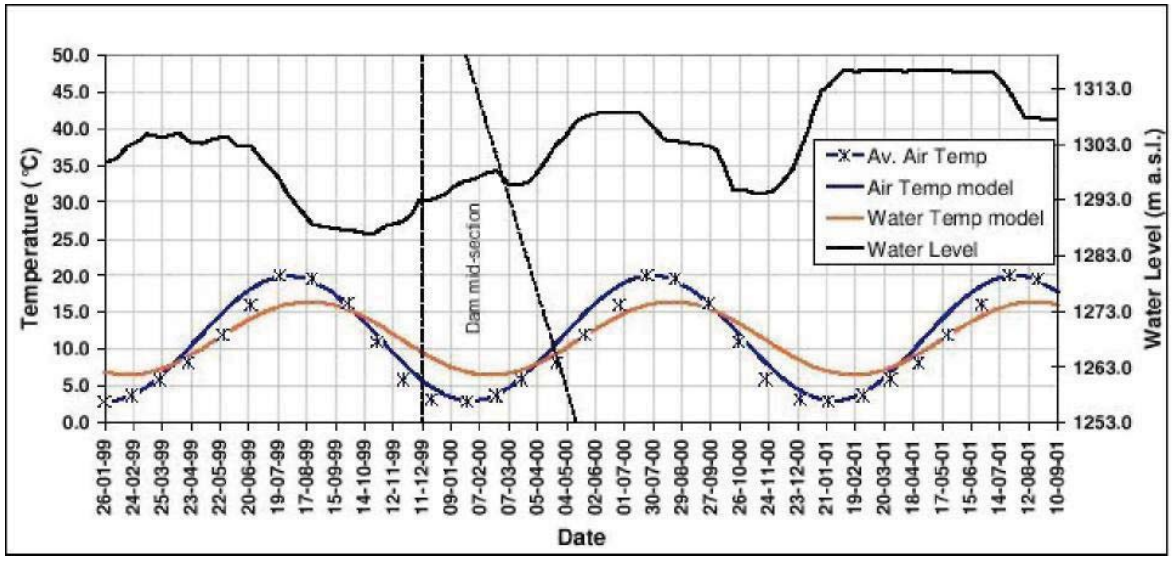

Figure 6. Example Of Input Temperatures Considered (P2)

Finally, Figure 7 provides a view of all the models previously introduced.

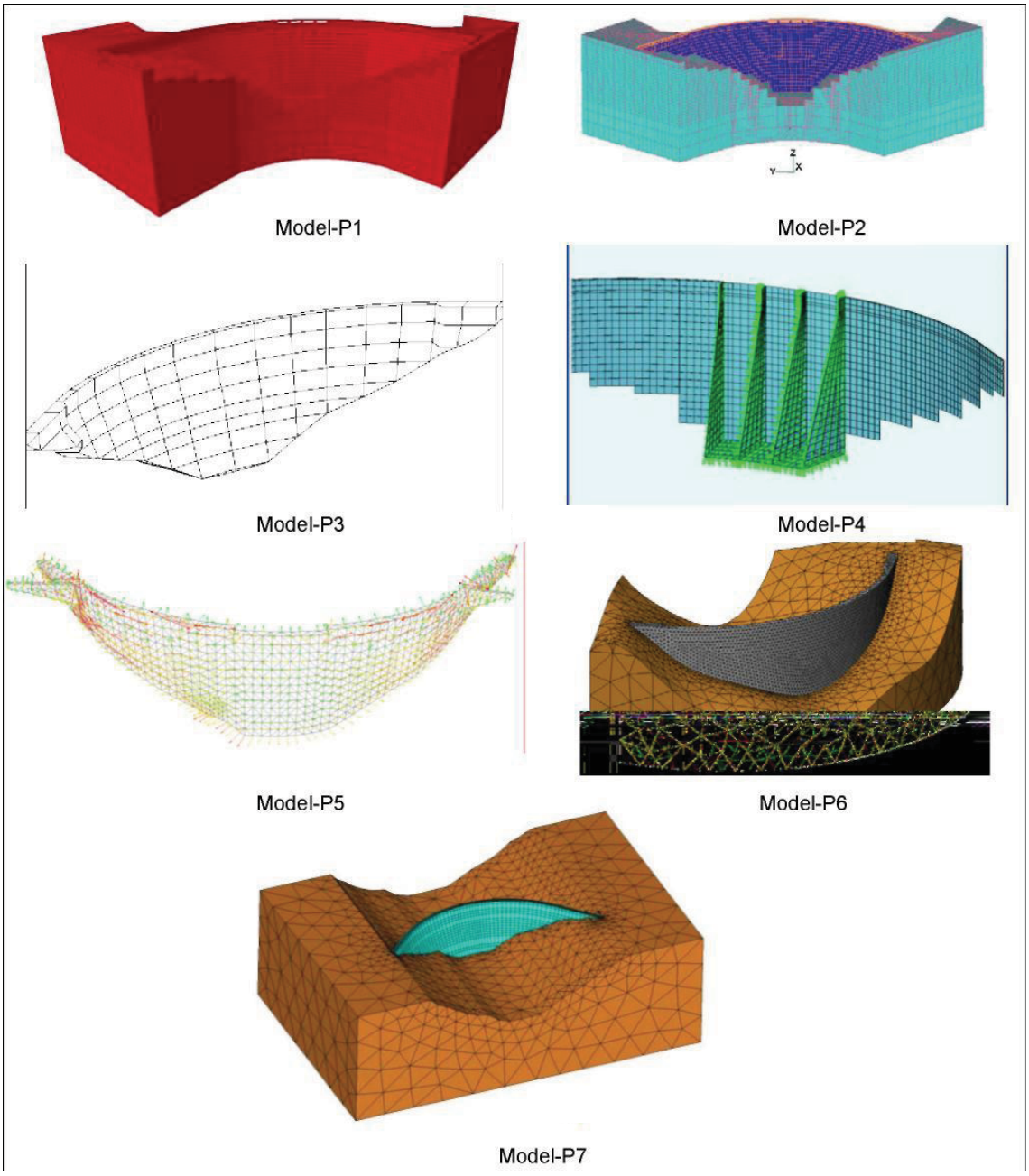

Figure 7. View Of The Models

5. COMPARISON OF NUMERICAL RESULTS

A comparison of the different numerical results obtained by the teams using the set of given parameters is given bellow (Figure 8 and Table 6).

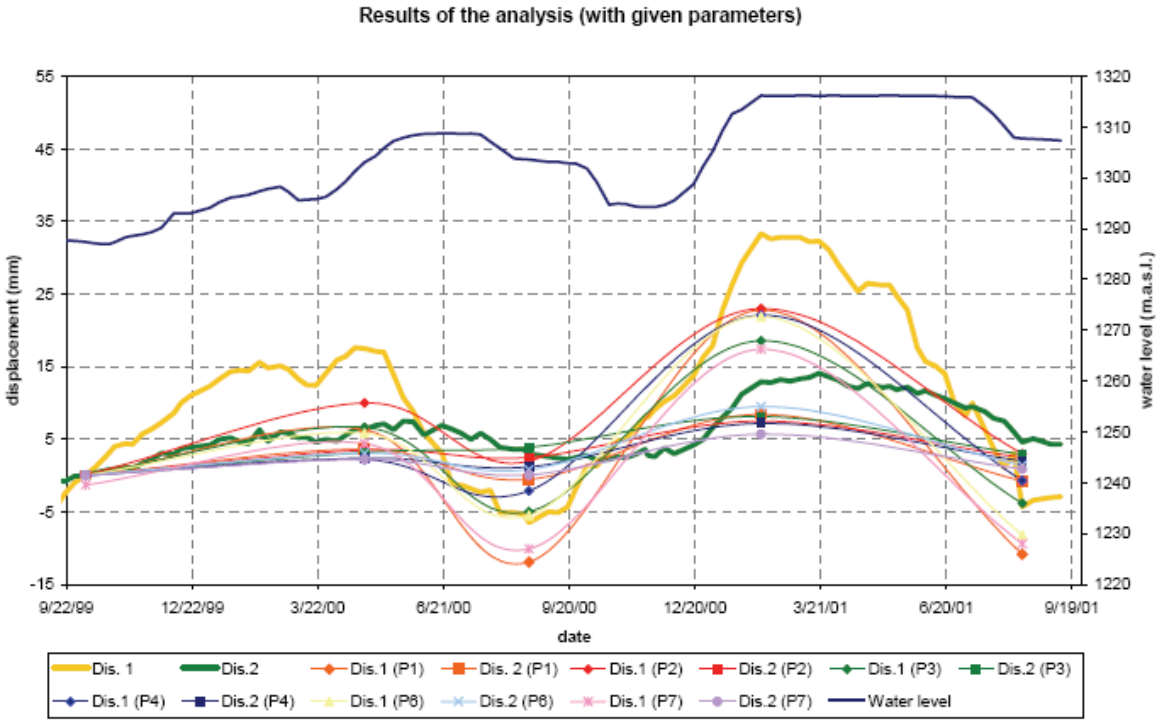

Figure 8. Comparison Of Numerical Results (Using The Given Parameters)

DATE/DISPLACEMENTS(mm)	06/10/1999	25/04/2000	22/08/2000	06/02/2001	14/08/2001
Recorded-D.Crest	**0,00**	**17,50**	**-6,50**	**33,30**	**-4,40**
Recorded-D.Gallery	**0,00**	**6,30**	**3,00**	**12,90**	**4,60**
P1-Crest	0,00	6,30	-11,93	22,77	-10,85
P1-Gallery	0,00	3,61	-0,53	8,43	-0,75
P2-Crest	0,00	10,00	2,00	23,00	3,00
P2-Gallery	0,00	3,50	2,50	7,50	2,50
P3-Crest	0,00	6,63	-4,97	18,58	-3,85
P3-Gallery	0,00	3,18	3,90	8,11	2,92
P5-Crest	0,00	2,20	-2,10	22,10	-0,70
P5-Gallery	0,00	2,40	1,20	7,20	2,00
P6-Crest	0,00	5,80	-5,50	21,90	-8,20
P6-Gallery	0,00	3,10	0,80	9,50	1,40
P7-Crest	-1,30	4,40	-10,10	17,40	-9,40
P7-Gallery	0,00	2,20	0,10	5,70	0,90

Table 6. Numerical Results (Using The Given Parameters)

Figure 9 and Table 7 compare the best fitted results achieved by the teams after performing their sensibility analysis.

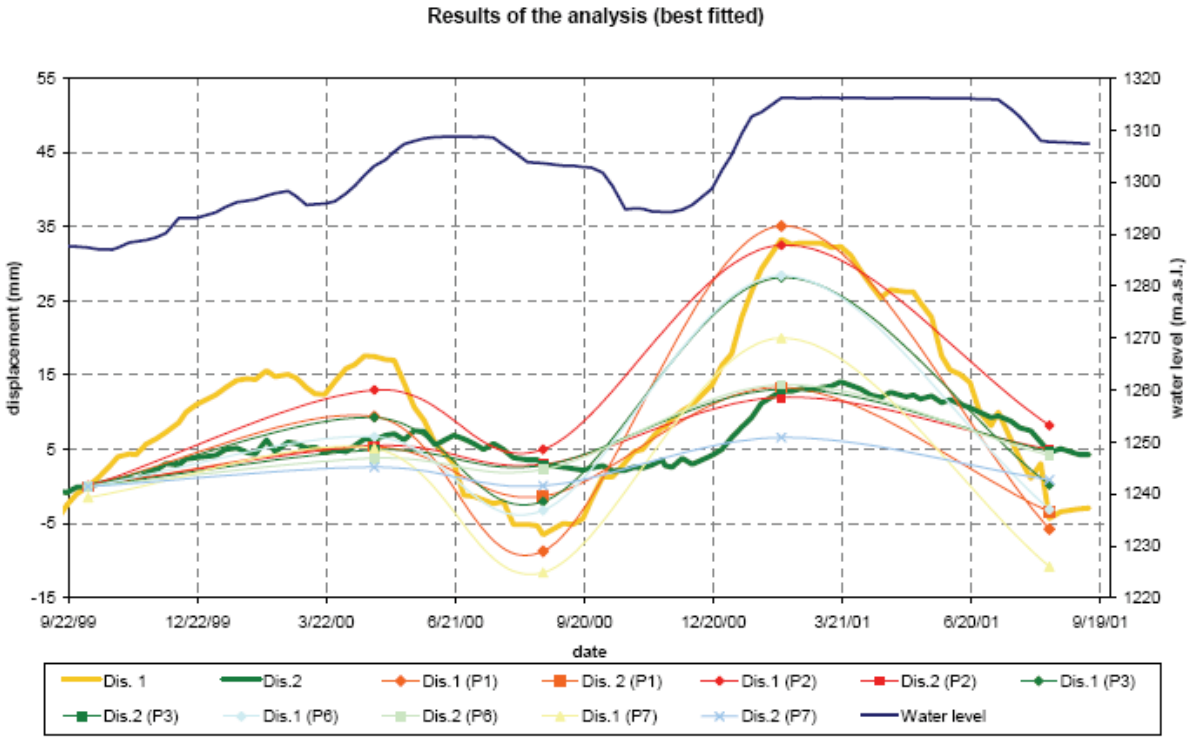

Figure 9. Comparison Of Numerical Results (Best-Fitted)

DATE/DISPLACEMENTS(mm)	06/10/1999	25/04/2000	22/08/2000	06/02/2001	14/08/2001
Recorded-D.Crest	**0,00**	**17,50**	**-6,50**	**33,30**	**-4,40**
Recorded-D.Gallery	**0,00**	**6,30**	**3,00**	**12,90**	**4,60**
P1-Crest	0,00	9,43	-8,70	35,10	-5,72
P1-Gallery	0,00	5,36	-1,31	13,36	-3,42
P2-Crest	0,00	13,00	5,00	32,50	8,25
P2-Gallery	0,00	5,50	3,00	12,00	5,00
P3-Crest	0,00	9,30	-2,02	28,13	0,23
P3-Gallery	0,00	4,92	2,86	13,08	4,71
P6-Crest	0,00	6,70	-3,20	28,40	-3,10
P6-Gallery	0,00	3,80	2,30	13,70	4,20
P7-Crest	-1,50	5,10	-11,60	20,00	-10,80
P7-Gallery	0,00	2,60	0,10	6,60	0,90

Table 7. Numerical Results (Best Fitted)

6. LESSONS LEARNED BY SENSIBILITY ANALYSIS

The main findings from the various participants who performed a sensibility analysis are summarized below.

P1. Two parameters were varied in order to better explain the behavior of the dam: the concrete's Young Modulus and the consideration, or not, of the uplift pressure. It was found that, when the concrete's Young Modulus is divided by two, the results of the analysis are quite similar to the real measures; consequently, the variation of this parameter captures the

structural behavior of the dam. Additionally, since the uplift effect was found to be not very important, its influence on the final result is negligible. The results of these analyses are presented below (Table 8 and Figure 10)

Date	Comparison of obtained displacements in the Crest (in mm)				
	Dis 1	Dis 1.1	Dis 1.2	Dis 1.3	Dis 1.4
06/10/1999	**0,00**	0,00	0,00	0,00	0,00
25/04/2000	**17,50**	6,30	9,42	6,30	9,42
22/08/2000	**-6,50**	-11,93	-8,69	-11,93	-8,69
06/02/2001	**33,30**	22,77	35,09	22,77	35,09
14/08/2001	**-4,30**	-10,85	-5,72	-10,82	-5,72

Table 8. Results Of P1 Sensibility Analysis

Where:
Dis 1 (mm): Monitoring data from Plumb line 3
Dis 1.1 (mm): Dis 1 obtained using given data:
Dis 1.2 (mm): Dis 1 obtained without considering uplift effect
Dis 1.3 (mm): Dis 1 obtained using Young Modulus divided by two.
Dis 1.4 (mm): Dis 1 obtained without considering uplift effect and using Young Modulus divided by two.

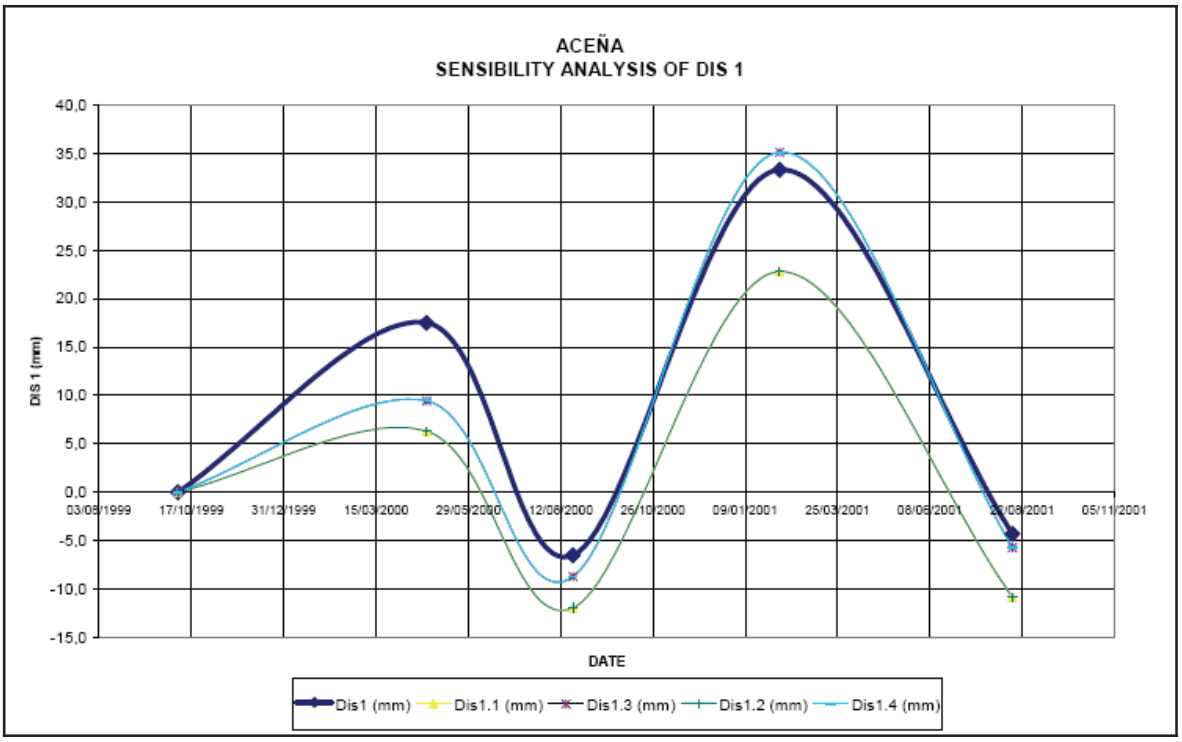

Figure 10. Results of P1 sensibility analysis

P2. The team altered the given stiffness so that both the Young Modulus of the dam and of its foundation was halved. In the results presented below (Figure 11 and Figure 12), it appears that some non-linear effects may have been activated in the upper part of the dam

during particular periods (summer), which may be in accordance with measurements of joint movements recorded during the first reservoir impounding and indicate the need to properly include the joints' behavior in a future model.

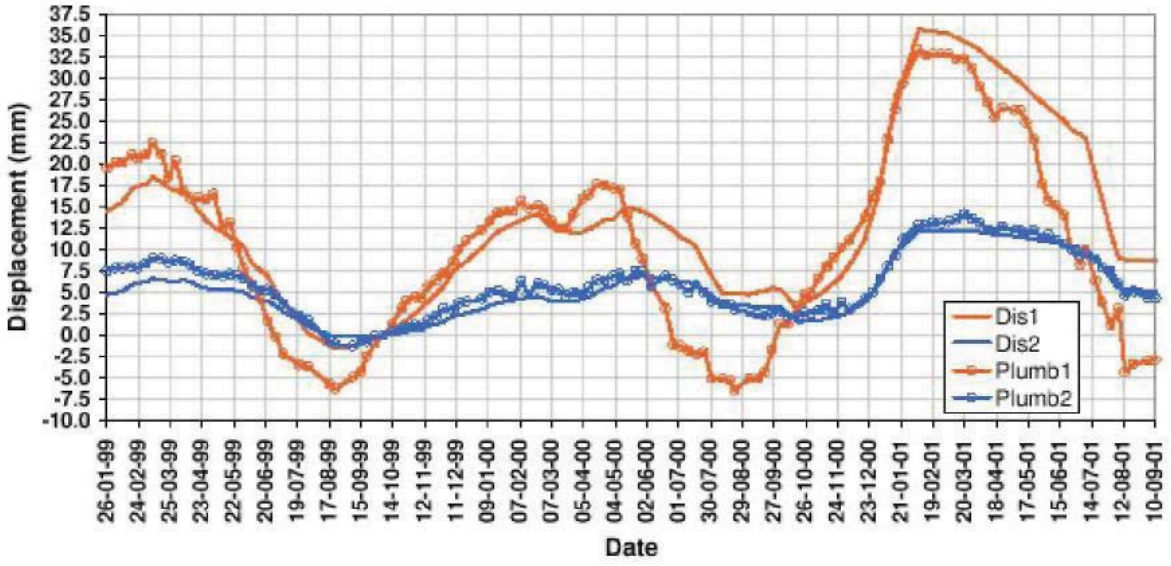

Figure 11. Displacements Calculated For Pendulum 3 (Both E Divided By 2). Dis1 (From Lower Gallery To The Crest) And Dis 2 (From Lower To Intermediate Gallery)

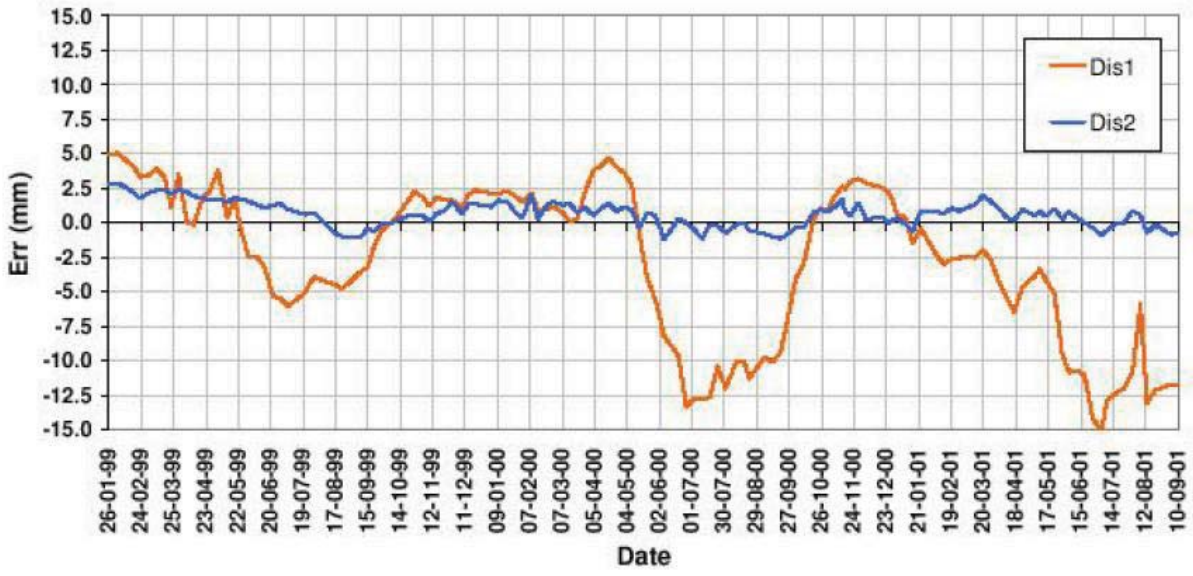

Figure 12. Error For Pendulum 3 (Module E Divided By 2). Difference Between Measured And Calculated Displacements (Dis1 & Dis 2)

P3. The team determined the best set of coefficients corresponding to the smallest differences between the recorded and the calculated displacements by the least-squares method. The best simulation was obtained with a Concrete Young Modulus of Ec = 11.8 GPa with a standard deviation equal to 1.8 GPa, a Concrete Young Modulus/Rock Young Modulus ratio unchanged (so that the Rock Young Modulus was defined by Er = 5.9 GPa), and a coefficient of thermal expansion α = 9.5*10-6 °C^{-1} with a standard deviation of 1.5*10-6 °C^{-1}. In consequence, the dam has a more flexible behavior than the behavior corresponding to the supposed material mechanical properties. The real amplitude of movements of this arch-gravity dam can be modelled only with an important increase in the dam flexibility (i.e. with an important decrease of its concrete Young Modulus); thus, a non-linear phenomenon may appear in the behavior of the dam and be responsible for this increase in flexibility.

The following table and figure present the results of calculations with these adjusted mechanical properties (Table 9 and Figure 13)

Date	water level	air temperature	Dis1 Recorded	Dis 1 Calculated	Dis 2 Recorded	Dis 2 Calculated
	(masl)	(°C)	(mm)	(mm)	(mm)	(mm)
06/10/1999	1287,4	9,82	0,00	0,00	0,00	0,00
25/04/2000	1303,09	7,57	17,50	8,32	6,30	4,18
22/08/2000	1303,61	19,36	-6,50	-3,48	3,00	2,02
06/02/2001	1316,2	5,80	33,30	25,27	12,90	11,12
14/08/2001	1307,73	20,16	-4,30	-1,41	4,60	3,52

Table 9. Results of P2 Sensibility Analysis

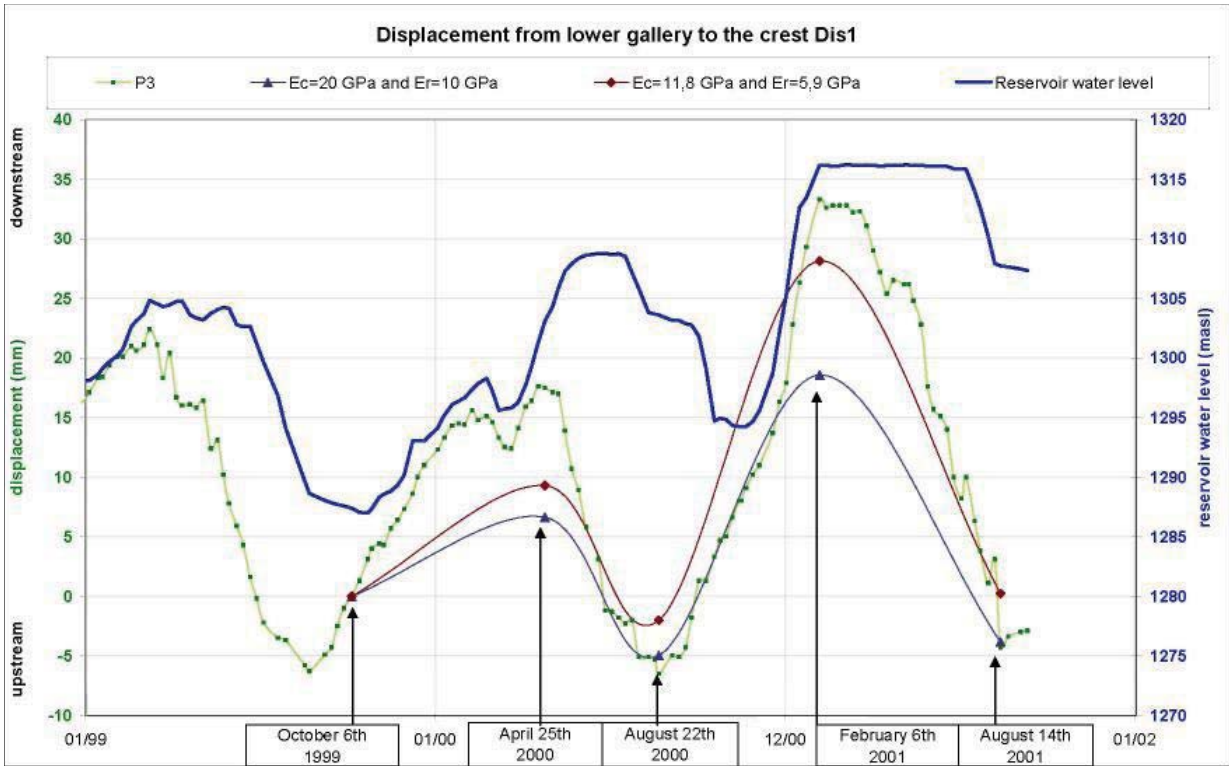

Figure 13. Results of P2 Sensibility Analysis

P5. The team considered a series of variations for the Young Modulus in 2D models: 5000MPa, 10000MPa, and 20000MPa in the foundation; 15000MPa, 20000MPa and 5000MPa in the dam. However, a 3D parametric study was not performed, and two only cases were analyzed. Relative displacements of Pendulum 3 for this analysis are shown in Figure 14.

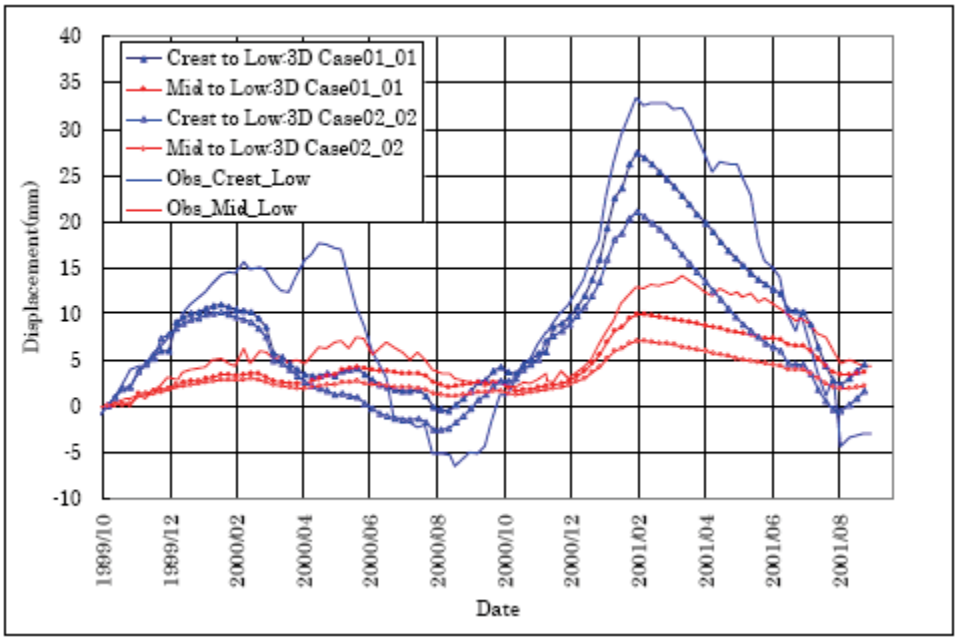

Figure 14. Relative Displacements of Pendulum (3D)

Where Case01_01 corresponds to Young Modulus of dam =15000MPa and Young Modulus of foundation = 5000MPa, while Case02_02 corresponds to Young Modulus of dam =20000MPa and Young Modulus of foundation = 10000MPa.

An additional analysis was performed for a range of concrete coefficients of thermal expansion from 0.7 to 1.3x10-5/^{o}C, while keeping the other parameters equal to those of Case01_01. Results are shown in Figure 15. It is worth noting that an increase in the coefficient of thermal expansion results in little change in the relative displacement from the intermediate to lower gallery. It is suspected that this is due to the assumed constant water temperature on the upstream face.

P6. In order to achieve a better fitting of the measured displacements, some parameters of the model were varied as follows: a lower stiffness of the foundation was considered, the temperature of the dam was assumed constant over the year in the core of the dam, and the water temperature was varied over the year.

First, the stiffness of the foundation was assumed equal to 0.2 GPa. In this case, the calculated relative horizontal displacements showed reasonable agreement with the measured target displacements. The largest differences occurred at the load situation corresponding to 25/04/2000. Such differences may be caused by an erroneous assumption concerning water or environment temperature. For example, the month of April in 2000 may have been colder than the average over the years, as is considered in the analysis. The corresponding calculated horizontal displacements are summarized in Table 10.

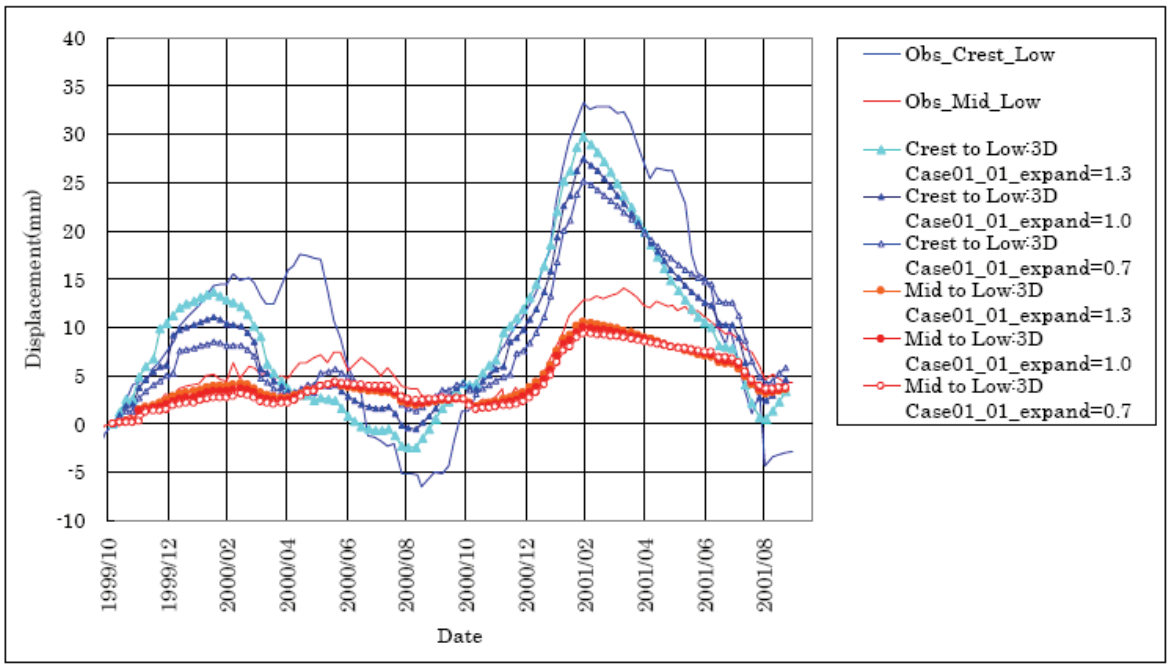

Figure 15. Relative Displacements (3D) For Parameter of Coefficient Of Thermal Expansion

Date	Target (D1)	Target (D2)	Analysis (D1)	Analysis (D2)
06/10/1999	0.0	0.0	0.0	0.0
25/04/2000	17.5	6.0	6.7	3.8
22/08/2000	-5.0	3.0	-3.2	2.3
06/02/2001	32.0	13.0	28.4	13.7
14/08/2001	1.0	7.5	-3.1	4.2

Table 10. Relative Horizontal Displacements in mm: Between Bottom Gallery and Crest (D1); Between Bottom and Middle Gallery (D2)

Second, the temperature in the core of the dam body was assumed constant and equal to 11є C during the whole year. The core of the dam body was defined as the portion of the volume at a distance greater than 3 m from the outer surfaces of the dam. In this case, the temperature was assigned to all nodes falling in the core of the dam body, while the temperature at nodes falling outside were determined from the steady-state thermal analysis. As seen in Table 11, the differences between these results and results obtained with the original model are small, especially for the relative displacement between the bottom gallery and crest of the dam.

Third, the water temperature was considered equal to 14єC at the load situations 06/10/1999, 22/08/2000 and 14/08/2001 (in the summer or close to summer), and equal to 5єC at the load situations 25/04/2000 and 06/02/2001 (in the spring or in winter). Nevertheless, the assumption of variable water temperature over the year does not lead to a better fitting of the measured displacements. The calculated displacements are presented in Table 12.

Date	Target (D1)	Target (D2)	Analysis (D1)	Analysis (D2)
06/10/1999	0.0	0.0	0.0	0.0
25/04/2000	17.5	6.0	5.6	2.8
22/08/2000	-5.0	3.0	-5.4	1.1
06/02/2001	32.0	13.0	21.3	9.0
14/08/2001	1.0	7.5	-7.7	1.9

Table 11. Relative Horizontal Displacements (in mm) Between Bottom Gallery and Crest of the Dam (D1); Between the Bottom And Middle Gallery (D2)

Date	Target (D1)	Target (D2)	Analysis (D1)	Analysis (D2)
06/10/1999	0.0	0.0	0.0	0.0
25/04/2000	17.5	6.0	2.7	2.5
22/08/2000	-5.0	3.0	-4.6	0.3
06/02/2001	32.0	13.0	18.7	9.0
14/08/2001	1.0	7.5	-7.2	0.1

Table 12. Relative Horizontal Displacements (in mm) Between Bottom Gallery and Crest of the Dam (D1); Between Bottom and Middle Gallery (D2).

P7. In order to reduce the difference between recorded/computed displacements, the stiffness of the dam-foundation system was diminished, using new material mechanical characteristics to the inferior limit usually accepted for this type of dam. The new mechanical characteristics are presented in the Table 13. The displacements computed with the new material mechanical characteristics are presented in the Table 14. However, the new results did not reach the recorded displacements except for Dis1 in 22.08.2000 and 14.08.2001. The performance of the computed displacements versus the recorded ones would be improved taking into account a better evaluation of the dam body temperatures.

Date	Target (D1)	Target (D2)	Analysis (D1)	Analysis (D2)
06/10/1999	0.0	0.0	0.0	0.0
25/04/2000	17.5	6.0	6.7	3.8
22/08/2000	-5.0	3.0	-3.2	2.3
06/02/2001	32.0	13.0	28.4	13.7
14/08/2001	1.0	7.5	-3.1	4.2

Table 14. Results of P7 Sensibility Analysis

7. SOME LESSONS LEARNED BY STATISTICAL MODELLING

Statistical models, which correlate structure behavior variables and external factors, have been used increasingly during recent years. Their use is not as complex as for deterministic models, making forecasting of future behavior easier for various load situations. They are

also very useful for checking consistency of data or identifying abnormal values of any variable values over time.

Only participants one (P1) and three (P3) used statistical modeling, and the main characteristics of these models together with relevant knowledge gained through such modeling are presented below.

P1 first used software, AUSMODEL (developed by OFITECO), which calculates the set of empirical relations that better explain the so-called "control variable" readings (e.g., movements, pore pressures, strains, seepage, etc.) in terms of time (from a chosen origin), head water, temperatures and rainfall.

Effects on the control variable related to time (irrecoverable), or related to any of the other external variables, can be isolated. The program also allows identification of "unexplained" behavior and its tendency. The results, as given in Figure 16 for displacements from foundation to the gallery, did not show irrecoverable movements.

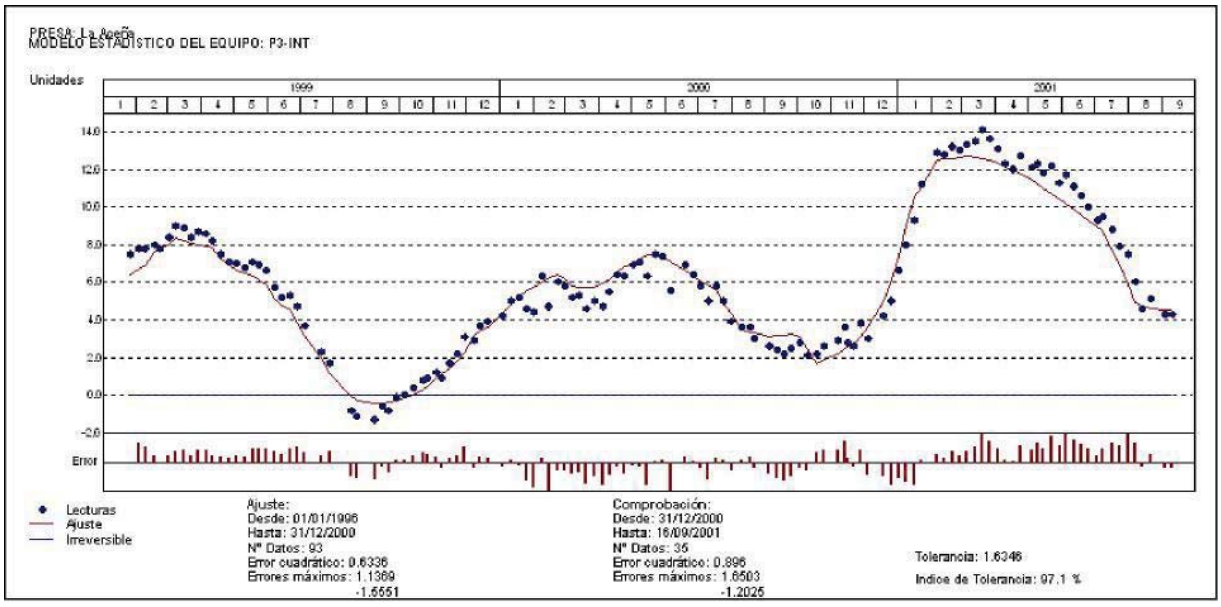

Figure 16. Model Fitted By AUSMODEL to Movements from Foundation to the Gallery

In addition, as another way to estimate how external variables such as water level and temperature are influencing the structural behavior of the dam, three statistical analyses were performed with "Statgraphics plus V.5.0" (water level and temperature separately and coupled). The results of the regression analysis of the joint influence of water level and environment temperature on the displacements from foundation to crest (Dis 1) are defined by the equation that fits the model:

$$Dis1 = 207864.0 - 318.952wlev + 0.122366wlev^2 - 5.10044Temp + 0.739249Temp^2 - 0.0555234Temp^3 + 0.00137341Temp^4$$

Where "wlev" is water level and "Tem" is external temperature.

Since the P-value in the ANOVA table is less than 0.01, there is a statistically significant relationship between the variables at the 99% confidence level. The R-Squared statistic indicates that the model as fitted explains 84.1215% of the variability in Dis1. In conclusion it is noteworthy that the coupled effect of thermal and hydraulic loads explains a significant

amount of the movement of La Aceca Dam. However, the remaining 15% should be explained by other variables.

P3 applied the HST method (developed by Coyne-et-Bellier) for the three displacements recorded by direct Pendulum 3: horizontal displacement from lower gallery to the crest, called Dis1; horizontal displacement from lower to intermediate gallery, called Dis2; and horizontal displacement from intermediate gallery to the crest, called Dis3.

For the first displacement, 343 observations were available between 03/01/1996 and 11/09/2001. For the others, only 130 observations are available between the first of January 1996, and the eleventh of September 2001. CONDOR software (developed by Coyne-et-Bellier) calculates the best model for each displacement, using hydrostatic functions (Z, Z2, Z3, Z4), seasonal functions (cosS, sinS, sin2S and sinS*cosS), temporal functions (T, exp. (-T) or discontinuous step function. The best models were composed with one “H” function Z and all four seasonal “S” functions. For all models, the temporal functions did not improve the interpretation of dam movements. More specifically:

- The residual standard deviation for the displacement Dis1 is equals to 2.8 mm, which corresponds to a correct explanation coefficient of 75.5 %. The models for the other displacements Dis2 and Dis3 have residual standard deviations, respectively, as high as 0.8 mm and 2.4 mm. Their explanation coefficients are equal to 78 % and 70.5 %.

- The influence of the seasonal effect on Dis1 is 27 mm, with the maximum at mid-August and the minimum at the beginning of February. The influence of the hydrostatic effect is 44 mm when the reservoir water level varies from elevation 1253 masl. (empty reservoir) to elevation 1316 masl. (full reservoir).

- For Dis2, the influence of the seasonal effect is 3.7 mm with the maximum at the end of August and the minimum at the beginning of March; the influence of the hydrostatic effect equals to 22 mm for the same range of reservoir water level as Dis1.

- The influence of the seasonal effect on Dis3 is 20 mm, with the maximum at the beginning of August and the minimum at the beginning of March; the influence of the hydrostatic effect is 18 mm.

On the other hand, CONDOR detected an anomaly in the horizontal displacement from lower gallery to the crest (Dis1), which occurred between 18/08/1999 and 28/09/1999, inclusive. The explanation of this phenomenon may be that the reservoir water level was very low during the summer of the year 1999. The water elevation went down from 1299.65 to 1288.05 masl between 06/07/1999 and 08/08/1999. So the dam recorded an important displacement in the upstream direction probably due to the thermal effect. After the month of November 1999, the reservoir water level rose to a usual elevation, and the corrected value of Dis1 became normal again.

7. CONCLUSIONS

All independent teams have reached the series of conclusions that are given bellow. Though they are in a sense very similar, some particularities that enrich the overall conclusions are presented at the end of the article.

P1. Although the statistical analysis of the input data shows that 85% of the movement of the dam can be explained by the coupled action of water pressure and temperature, the results of the analysis emphasize the fact that there must be another factors influencing the mechanical behavior of the dam. In particular, the numerical model represents properly the trend of the real movements of the dam, but the real magnitude is captured only if the

stiffness assumed for the concrete is reduced.

P2. The main conclusion to be drawn from the comparison of numerical results and recorded data indicates a need to properly include joint behavior in a future FEM model. Such a simulation might be gradually approached starting, for instance, by considering the central dam blocks free to move as independent cantilevers, and modelling the actual non-linear effects of the structural joints with proper FEM elements. The comparison of calculated and measured behavior should include the joints' relative displacements, if the relevant measurements are available. If not, monitoring them in terms of opening, sliding and extension is strongly recommended. Finally, in cases in which the comparison is still not deemed acceptable, the assumptions made on the external temperatures models should be critically reviewed.

P3. After performing a prior statistical model to check for abnormalities on the records, the structural model allowed an explanation of the non-linear behavior of the dam. It could not, however, be used alone to describe the non-linear phenomena, possibly due to the opening of joints under exceptional hydrostatic loads, and due to the high deformability of foundation rock. Monitoring and a precise investigation into the displacements of joints and foundation are necessary to a complete and perfect understanding of the non-linear response of the arch-gravity dam.

P4. In order to explain the dam's complete behavior and to answer all questions, it is necessary to do a very complex model, including simulation of the real construction procedure, introduction of all joints between concrete blocks with non-linear constitutive law, application of all loads with the real loading history, and, while the same time, calibrating the model using the measured data. In our opinion, fulfilment of these requirements is possible, but the process is both effort- and time-intensive.

P5. The two main conclusions are 1) 2D analysis captured the dam response almost exactly except for the time period 2000/04 and 2000/10, when it appeared that the arch effect was clearly operating, and 2), results for the relative displacement from intermediate to lower gallery in 2D analysis indicated the need for a smaller elastic modulus. Improved results could be obtained with the availability of an exact history of the air temperature, the dam body temperature (including summer values), and more information regarding local radiation.

P6. The major role in the displacements measured in the dam was played by the effect of thermal expansion, which dominates the effect of hydrostatic loading. Temperature distribution in the core of the dam body has a relatively minor effect. A reduced stiffness of the foundation results in a better fit of the measured displacements, which can be reasonably well predicted even under the simplistic assumptions of linear elastic material behavior. In any case, better results may be expected when more detailed information concerning the input parameters are known: real profile of the ground surface, foundation stiffness, development of water temperature, and environmental temperature.

P7. The computed displacements in the 3D finite element model using ANSYS computer code and mechanical/thermal material characteristics recommended by the formulator are generally smaller than the corresponding displacements recorded at Pendulum 3. The computed displacements in the 2D model are closer to the corresponding displacements recorded at Pendulum 3, than those computed in the 3D model. After improving the results by diminishing the stiffness properties, it can also be concluded that data on dam body temperatures are a very coarse approximation of the real temperatures.

In summary, despite all the various assumptions, load hypothesis, models, etc., conclusions of almost all participants include:

- Either dam body and/or foundation rock may be less stiff than expected.
- Temperatures can not be properly modelled with the available data.
- Non-linear effects, particularly sliding in the joints, may be influencing the behavior.
- Irrecoverable movements have not been identified.

Finally, the authors (formulators) wish to note that Canal de Isabel II, according to the recommendations of the "First Review And General Analysis Of The Safety Of The Dam" (OFITECO, 2004), is undertaking an extension of the investigation of the dam, by providing topographical control of the movements and by drilling the dam core and the foundation to gain information on the mechanical parameters of the materials.

The results of the Benchmark strongly support the need and efficiency of an investment in the capabilities of numerical modelling to achieve a better knowledge of the materials and behavior of the dam, resulting in a consistent reduction of the uncertainties identified by the formulators and participants.

ACKNOWLEDGEMENTS

Special thanks are given to all the participants and their firms or institutions for their valuable and considerable effort, and to the Canal de Isabel II, which provided a very interesting study case. Also special thanks to Dr. Glagovski, as responsible representative of the Benchmark organization, and to the other members of the ICOLD Committee on Computational Aspects of Analysis and Design of Dams (chaired by Mr. Alain Carrere and vice-chaired by Mr. Guido Mazza). Finally, the first author has been able to participate in the Benchmark in the context of the project "Aplicacion del analisis de riesgos a los programas de conservacion, mantenimiento, rehabilitacion y gestion de la seguridad de presas y embalses. BIA2006-08948" sponsored by the Spanish Ministry of Education and Science (30%) and FEDER funds of the European Union (70%).

REFERENCES

Note: all seven individual papers with the contributions from the participants will be ready by the end of 2007, as part of the "Proceedings on the Ninth International Benchmark Workshop on Numerical Analysis of Dams (Russia, 2007)"

UPV SOLUTION

Eduardo ECHEVERRÍA GARCÍA
Civil Engineer
POLYTECHNICAL UNIVERSITY OF VALENCIA

Ignacio ESCUDER BUENO
PhD, M.Sc, Civil Engineer
POLYTECHNICAL UNIVERSITY OF VALENCIA

1. Statement of the problem.

La Aceña Dam is an arch gravity structure and belongs to the Madrid water supply system operated by the company Canal de Isabel II. The study of its behaviour has been divided according to chronological order and the source of the readings:

a) First impounding (February 1990 to May 1991)

The instrumentation and monitoring system of the dam was aimed to displacement, joint performance, stresses and seepage control. The analysis of data recorded during first impounding resulted in the following outcomes:

- Maximum displacement toward the abutments (tangential) was 3.75 mm, reached when the reservoir was at maximum normal operating level.

- Radial displacements (upstream-downstream) were in a range between 1.23 cm and 1.8 cm, with slight differences between blocks. Maximum joint movement recorded was 1.88 mm.

- Maximum seepage flow (40 l/min) also occurred for the maximum normal operating level. The maximum value for a single block was 1.7 l/min.

b) Movements after first impounding

Movements recorded after first impounding by means of four plumblines revealed an apparently significant increase of the range of displacements (around 4 cm).

The exercise proposed aims at analysing the stress-strain behavior of the dam and interpreting the recorded displacement at the crest and its pattern, as related to water level and temperature time histories.

Using the given data the formulator asks for the participants to calculate the following displacements:

Date	Dis1 (mm)	Dis 2 (mm)
06/10/1999	0	0
25/04/2000		
22/08/2000		
06/02/2001		
14/08/2001		

Where

Dis1: Incremental horizontal displacements from lower gallery (gallery level 1 in plan P11.dwg) to the crest in mm. (at Plumbine N.3 Location; See Block 3 and corresponding cross section in P11.dwg)

Dis2: Incremental horizontal displacements from lower to intermediate gallery (gallery level 2 in planes) in mm. (at Plumbine N.3 Location; See Block 3 and corresponding cross section in P11.dwg).

Following table summarizes static material mechanical properties:

Property	FOUNDATION	DAM BODY
Especific weight	22 kN / m^3	23.6 kN / m^3
E (Young modulus)	10000 Mpa	20000 Mpa
Poisson´s Ratio	0.2	0.2
Coef. of thermal exp. A	0	10^{-5} $^oC^{-1}$

Table: Material static properties

Note: Any other needed property may be used if justified by the participant.

Following table shows historical monthly average temperatures in Peguerinos (near La Aceña´s Dam)

Month	E	F	M	A	M	J	J	A	S	O	N	D
Temperature (ºC)	2.9	3.7	5.9	8.2	12.0	16.1	20.0	19.6	16.3	11.0	5.9	3.2

Note: joints were sealed in February of 1989

2. Justification of calculation procedures

2.1. Software used.

The solution proposed is based in an analysis performed with SAP 2000 NL V.7. SAP 2000 NL is a finite element program developed in Berkeley University, California. This software uses the finite element method for the solution of any type of problem concerning structural analysis. It allows the researcher carrying out static and dynamical calculations and also nonlinear analysis.

2.2. Description of the constructed model.

Figure 1 shows the model of The Aceña dam constructed for its analysis with SAP 2000 NL.

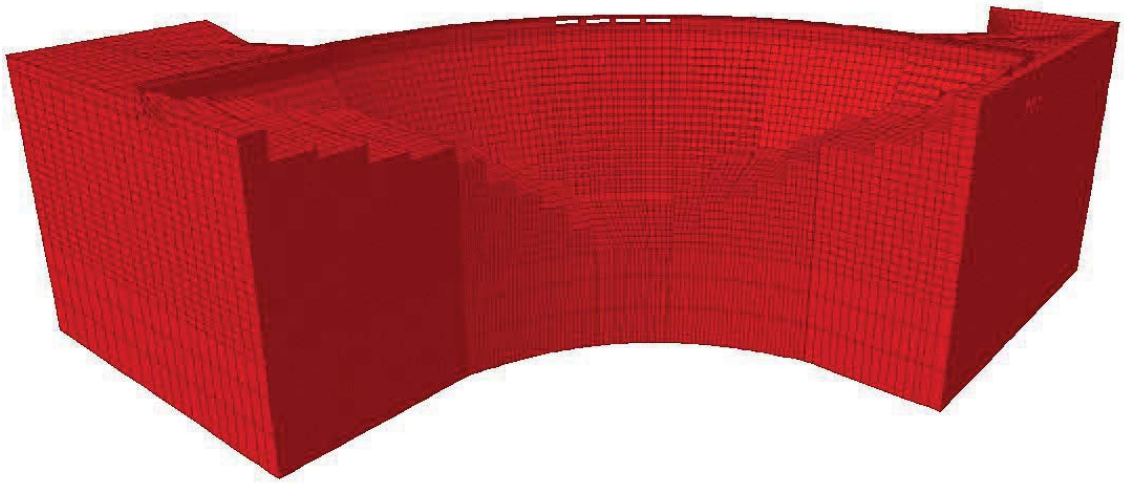

Figure 1. Numerical model built

This model consists of:

- 53038 joints of which 11654 represents the dam body.
- 45740 elements of which 9327 represents the dam body.

A solid type element has been used, an eight joint and six plane faces element which is used in SAP 2000 NL for three dimensional structures analysis. The size of the element has been defined by the necessity of being able to reproduce the thermal gradient through the thickness of the dam body. The width has been divided into five elements. This division

implies an average size of three meters for the element. Therefore, this is the distance between two consecutive horizontal planes. At the foundation this distance gets a little bit larger.

All these considerations take us to the final model.

Each element is associated to a material with isotropic properties, which are the following:

- Young Modulus (E)
- Shear Stiffness
- Poisson's ratio
- Thermal expansion ratio

The joints which form the bottom part of the foundation have been considered restrained in all directions, while in the lateral boundaries of the model only the horizontal displacements have been restrained and the vertical displacements have been left free to better reproduce the real behaviour of the structure-foundation system.

2.3. Statistical analysis of recorded data.

As a preliminary approach, in order to determine how external variables such as water level and temperature are influencing the structural behaviour of La Aceña Dam, three statistical analyses have been performed with "Statgraphics plus V.5.0".

The relationship between the displacements recorded by the plumbline nº3 (disp1) and the water level reservoir (wlev) have been statistically modelled by a multiple regression analysis. The following table shows the main results of this analysis:

Multiple Regression – disp1

```
Multiple Regression Analysis
-----------------------------------------------------------------------------
Dependent variable: disp1
-----------------------------------------------------------------------------
                                    Standard          T
Parameter               Estimate      Error       Statistic        P-Value
-----------------------------------------------------------------------------
CONSTANT               1.02886E7   1.5735E7       0.653864         0.5180
wlev                    -17886.0    27491.6      -0.650598         0.5201
wlev^2                   7.93491    12.2581       0.647322         0.5222
wlev^8                       0.0        0.0      -0.627455         0.5350
-----------------------------------------------------------------------------

                          Analysis of Variance
-----------------------------------------------------------------------------
Source             Sum of Squares     Df  Mean Square    F-Ratio      P-Value
-----------------------------------------------------------------------------
Model                     2497.37      3      832.458      10.99       0.0000
Residual                  2348.76     31      75.7666
-----------------------------------------------------------------------------
Total (Corr.)             4846.14     34

R-squared = 51.5333 percent
R-squared (adjusted for d.f.) = 46.843 percent
Standard Error of Est. = 8.7044
Mean absolute error = 7.00455
Durbin-Watson statistic = 0.168615 (P=0.0000)
Lag 1 residual autocorrelation = 0.90858
```

The output shows the results of fitting a multiple linear regression model to describe the relationship between disp1 and the water level (wlev). The equation of the fitted model is

Disp1 = 1.02886E7 - 17886.0xwlev + 7.93491xwlev^2 - 5.47729E-20xwlev^8

Since the P-value in the ANOVA table is less than 0.01, there is a statistically significant relationship between the variables at the 99% confidence level.

The R-Squared statistic indicates that the model as fitted explains 51.5333% of the variability in Disp1. So the water level has a significant influence in the variability of recorded data.

In a second analysis, the study of the relationship between Disp1 and the external temperature has been performed by means of a similar analysis. Its results are given in the table below:

Multiple Regression – disp1

```
Multiple Regression Analysis
-----------------------------------------------------------------------------
Dependent variable: disp1
-----------------------------------------------------------------------------
                                     Standard          T
Parameter                Estimate        Error       Statistic        P-Value
-----------------------------------------------------------------------------
CONSTANT                  370.731        374.716       0.989364         0.3313
Temp                      -310.26        311.405      -0.996321         0.3279
Temp^2                    107.861        103.014        1.04705         0.3044
Temp^3                   -18.9842        17.6344       -1.07655         0.2912
Temp^4                    1.85828        1.69762        1.09464         0.2833
Temp^5                  -0.102554      0.0925844       -1.10768         0.2778
Temp^6                 0.00298168      0.0026676        1.11774         0.2735
Temp^7             -0.0000354745   0.0000315229       -1.12536         0.2703
-----------------------------------------------------------------------------

                           Analysis of Variance
-----------------------------------------------------------------------------
Source             Sum of Squares     Df  Mean Square    F-Ratio      P-Value
-----------------------------------------------------------------------------
Model                      3108.1      7      444.015       6.90       0.0001
Residual                  1738.04     27      64.3717
-----------------------------------------------------------------------------
Total (Corr.)             4846.14     34

R-squared = 64.1356 percent
R-squared (adjusted for d.f.) = 54.8375 percent
Standard Error of Est. = 8.0232
Mean absolute error = 5.74557
Durbin-Watson statistic = 1.01547 (P=0.0005)
Lag 1 residual autocorrelation = 0.438346
```

The equation of the fitted model is:

Disp1 = 370.731 - 310.26xTemp + 107.861xTemp^2 - 18.9842xTemp^3 +

+1.85828xTemp^4 - 0.102554xTemp^5 + 0.00298168xTemp^6 - 0.0000354745xTemp^7

Since the P-value in the ANOVA table is less than 0.01, there is a statistically significant relationship between the variables at the 99% confidence level.

The R-Squared statistic indicates that the model as fitted explains 64.1356% of the variability in disp1. So there is a higher influence of external temperature in the dam displacements than the water level effect.

Finally, a regression analysis of the coupled influence of water level and environment temperature has been done. The results of this analysis are shown at the following table:

Multiple Regression – disp1

```
Multiple Regression Analysis
-----------------------------------------------------------------------------
Dependent variable: disp1
-----------------------------------------------------------------------------
                                     Standard          T
Parameter               Estimate         Error       Statistic        P-Value
-----------------------------------------------------------------------------
CONSTANT                207864.0       77970.3        2.66595         0.0126
wlev                    -318.952       119.139       -2.67714         0.0123
wlev^2                  0.122366     0.0455113         2.6887         0.0119
Temp                    -5.10044       9.92675      -0.513808         0.6114
Temp^2                  0.739249       1.45244       0.508971         0.6148
Temp^3                -0.0555234     0.0852161       -0.65156         0.5200
Temp^4                0.00137341    0.00173033       0.793724         0.4340
-----------------------------------------------------------------------------

                          Analysis of Variance
-----------------------------------------------------------------------------
Source             Sum of Squares     Df  Mean Square    F-Ratio      P-Value
-----------------------------------------------------------------------------
Model                    4076.64      6      679.441      24.72       0.0000
Residual                 769.495     28       27.482
-----------------------------------------------------------------------------
Total (Corr.)            4846.14     34

R-squared = 84.1215 percent
R-squared (adjusted for d.f.) = 80.719 percent
Standard Error of Est. = 5.24232
Mean absolute error = 3.3742
Durbin-Watson statistic = 0.978026 (P=0.0000)
Lag 1 residual autocorrelation = 0.505545
```

The output shows the results of fitting a multiple linear regression model to describe the relationship between disp1 and the joined effect of environment's temperature and water level at reservoir. The equation of the fitted model is

$$Disp1 = 207864.0 - 318.952*wlev + 0.122366*wlev^2 - 5.10044*Temp +$$
$$+0.739249*Temp^2 - 0.0555234*Temp^3 + 0.00137341*Temp^4$$

Since the P-value in the ANOVA table is less than 0.01, there is a statistically significant relationship between the variables at the 99% confidence level. The R-Squared statistic indicates that the model as fitted explains 84.1215% of the variability in Disp1.

To conclude we can say that the coupled effect of thermal and hydraulic loads explains a significant amount of the movement of La Aceña Dam. However the 15% remaining should be explained by other variables.

2.4. Input Loads considered

2.4.1. Self-weight.

Self-weight as a load is automatically generated by SAP 2000 NL. This load is evenly distributed on the element's volume and is equal to its specific weight. It always acts on the global –Z direction.

We can see at the graphic given below the vertical stresses (in MPa) obtained due to exclusively the self-weight.

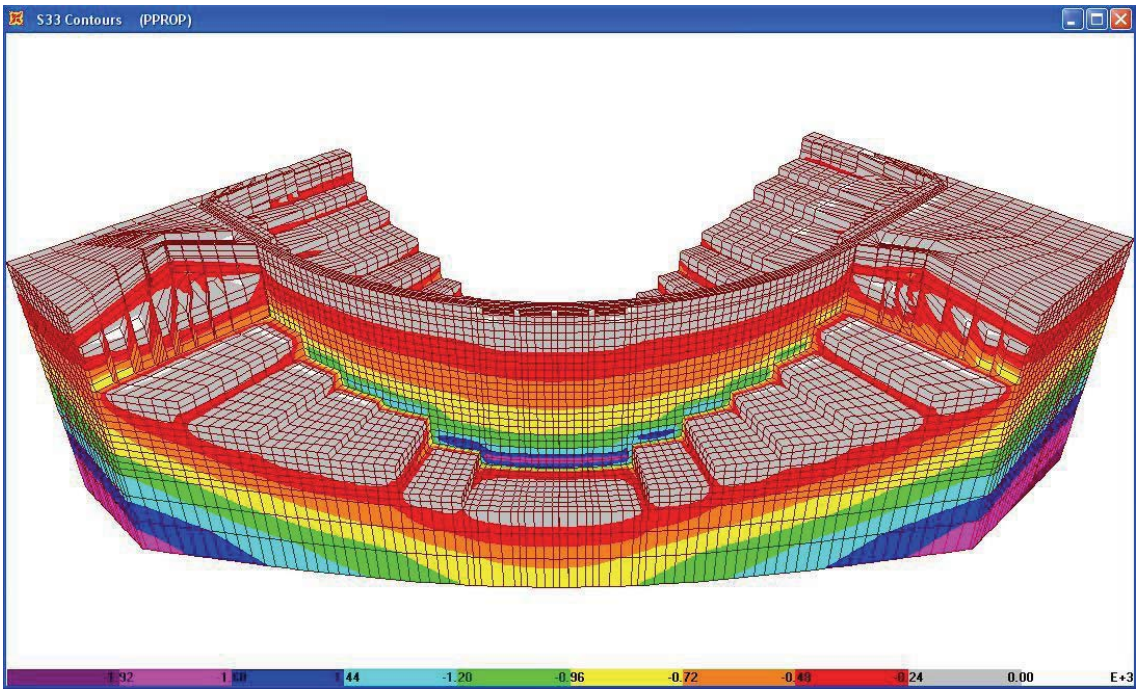

2.4.2. Water pressure.

The water pressure has been considered as a surface force perpendicular to the wet face, with a value of 10H KN/m2, being H the difference in height between the reservoir water level and the height of the point considered for applying the force.

So the water pressure has been applied as a point load which concentrates the resulting water pressure on the faces of the four elements which the joint is linked to divided by four.

A different load case has been generated for each date of the analysis. Figure 2 shows the water pressure applied at the maximum water level case (06th of February 2001).

2.4.3. Uplift Pressure.

It has been supposed a hydraulic gradient between upstream and downstream faces in order to consider the uplift pressure. This hydraulic gradient is generated from the upstream wet face to the downstream wet face with different elements involved in each water level.

The specific weight of the elements located in this theoretical wet area has been considered to be the submerged one ($\gamma' = \gamma - \gamma\omega$).

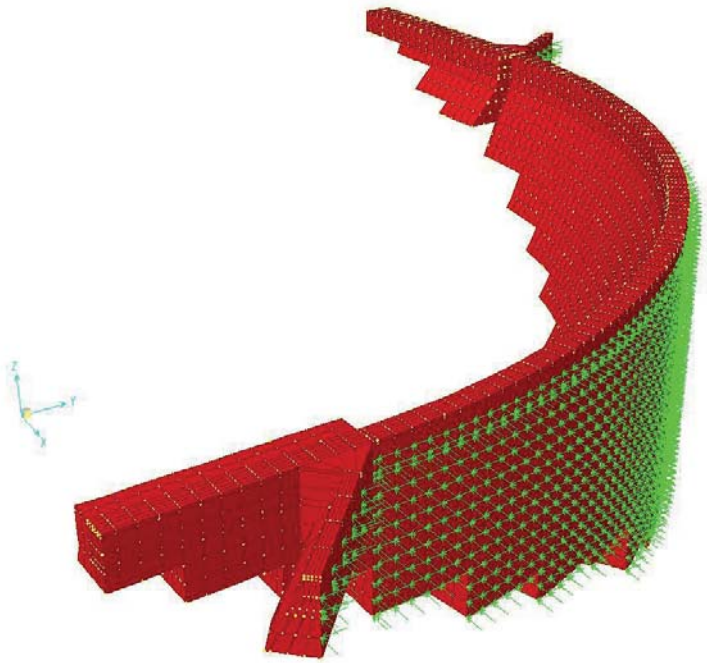

Figure 2. Water pressure applied at Maximum water level case.

2.4.3. Uplift Pressure.

To analyze each case a thermal field has been created at the entire dam's body, subjected to the following boundary conditions:

i. The wet face has a temperature of 4ºC.

ii. The dry face and the head of the dam has an environment temperature.

Because of this increase of temperature has been assigned for each element, calculated as the difference between its own temperature and the average temperature of the month in which the joints were sealed which is February.

We can assume that from this date the dam works as a monolithic structure and is the origin of displacements form the dam's body.

3. Straight comparison with displacements at DP 3

3.1. Dis1

The following table shows the comparison between dis1 measured at the crest for the plumbline N^{er} 3 and dis 1 obtained by numerical analysis:

Date	Dis 1obtained (mm)	Dis 1 recorded (mm)
06/10/1999	0,000000	0,000000
25/04/2000	6,300916	17,500000
22/08/2000	-11,938325	-6,500000
06/02/2001	22,773277	33,300000
14/08/2001	-10,856314	-4,300000

The trend of this model is the same as the recorded data but the ranges of the calculated displacementes are smaller than the real ones. However this suggests that a sensibility analysis of one or more parameters involved in the model the elastic behaviour of La Aceña Dam could be of great help to explain the results.

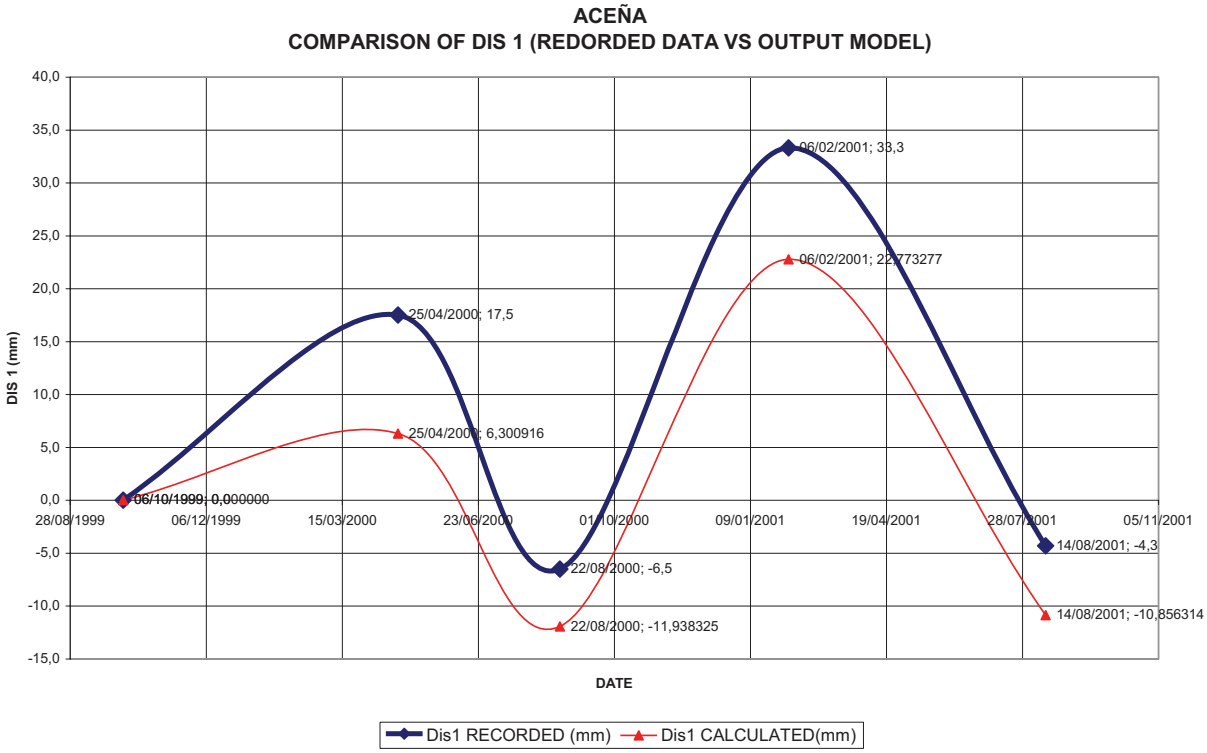

3.2. Dis2

The comparison of displacements measured in the gallery at level two against the model ones is practically the same as Dis 1. The model has the same trend. There are smaller displacements towards upstream than the real ones but these displacements are larger towards downstream direction.

The following table shows the comparison between dis2 measured at the dam's body for the plumbline Ner 3 and dis 1 obtained by numerical analysis with Sap 2000 NL :

Date	Dis 2 obtained(mm)	Dis 2 recorded (mm)
06/10/1999	0,000000	0,000000
25/04/2000	3,612815	6,300000
22/08/2000	-0,532962	3,000000
06/02/2001	8,436903	12,900000
14/08/2001	-0,752728	4,600000

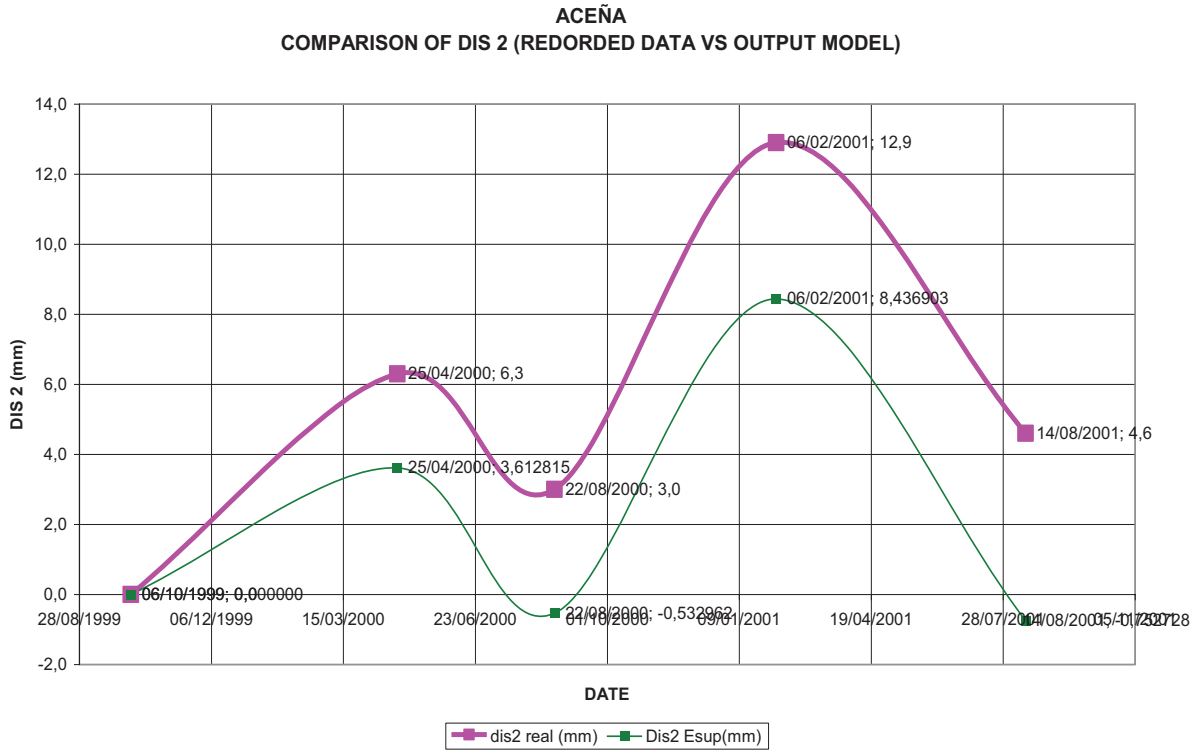

4. Sensibility Analysis

Two parameters have been varied in order to explain the behaviour of the dam:

1) The concrete's Young Modulus.
2) The uplift which has been neglected.

The results of these analyses are presented below.

4.1. Dis1

The results of Dis 1 in each analyzed hypoyhesis are presented in the table below:

Date	comparison of obtained results for dis 1 (mm)				
	Dis 1	Dis 1.1	Dis 1.2	Dis 1.3	Dis 1.4
06/10/1999	0,00000000	0,00000000	0,00000000	0,00000000	0,00000000
25/04/2000	17,50000000	6,30091628	9,42506499	6,30114275	9,42646424
22/08/2000	-6,50000000	-11,93832505	-8,69565984	-11,93791644	-8,69565984
06/02/2001	33,30000000	22,77327666	35,09837747	22,77356160	35,09781948
14/08/2001	-4,30000000	-10,85631450	-5,72263445	-10,82883267	-5,72071962

Where:

- Dis 1 (mm): Monitoring data from plumbline nº3
- Dis 1.1 (mm): Dis 1 obtained using given data:
- Dis 1.2 (mm): Dis 1 obtained without considering uplift effect
- Dis 1.3 (mm): Dis 1 obtained using Young modulus divided by two.
- Dis 1.4 (mm): Dis 1 obtained without considering uplift effect using and using Young modulus divided by two.

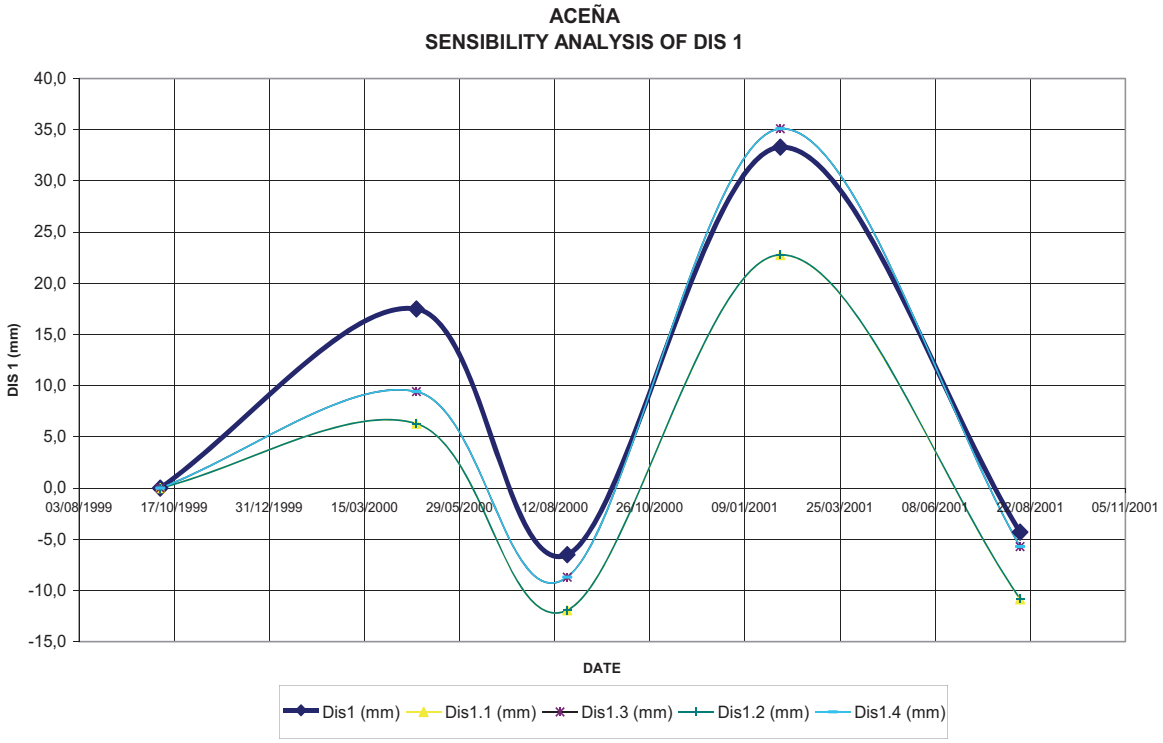

As we can see at the graph when the concrete's Young modulus is divided by two the results of the analysis are quite similar to the real measures so the variation of this parameter captures the structural behaviour of the dam. The uplift effect is not very important thus its influence on the final result because is negligible. So the best fit is obtained by dividing the Young Modulus by two.

4.2. Dis2

The displacements calculated at intermediated gallery for each case presents the same situation as Dis1 does:

Date	comparison of obtained results for dis 2 (mm)				
	Dis 2	Dis 2.1	Dis 2.2	Dis 2.3	Dis 2.4
06/10/1999	0,00000000	0,00000000	0,00000000	0,00000000	0,00000000
25/04/2000	6,30000000	3,61281525	3,61281525	5,36072402	5,36106333
22/08/2000	3,00000000	-0,53296248	-0,53296248	-1,30525438	-1,30554395
06/02/2001	12,90000000	8,43690281	8,43690281	13,35566412	13,35514317
14/08/2001	4,60000000	-0,75272837	-0,75300598	-3,41746631	-3,41831201

Where:

- Dis 2 (mm): Monitoring data from plumbline nº3
- Dis 2.1 (mm): Dis 2 obtained using given data:
- Dis 2.2 (mm): Dis 2 obtained without considering uplift effect
- Dis 2.3 (mm): Dis 2 obtained using Young modulus divided by two.
- Dis 2.4 (mm): Dis 2 obtained without considering uplift effect using and using Young modulus divided by two.

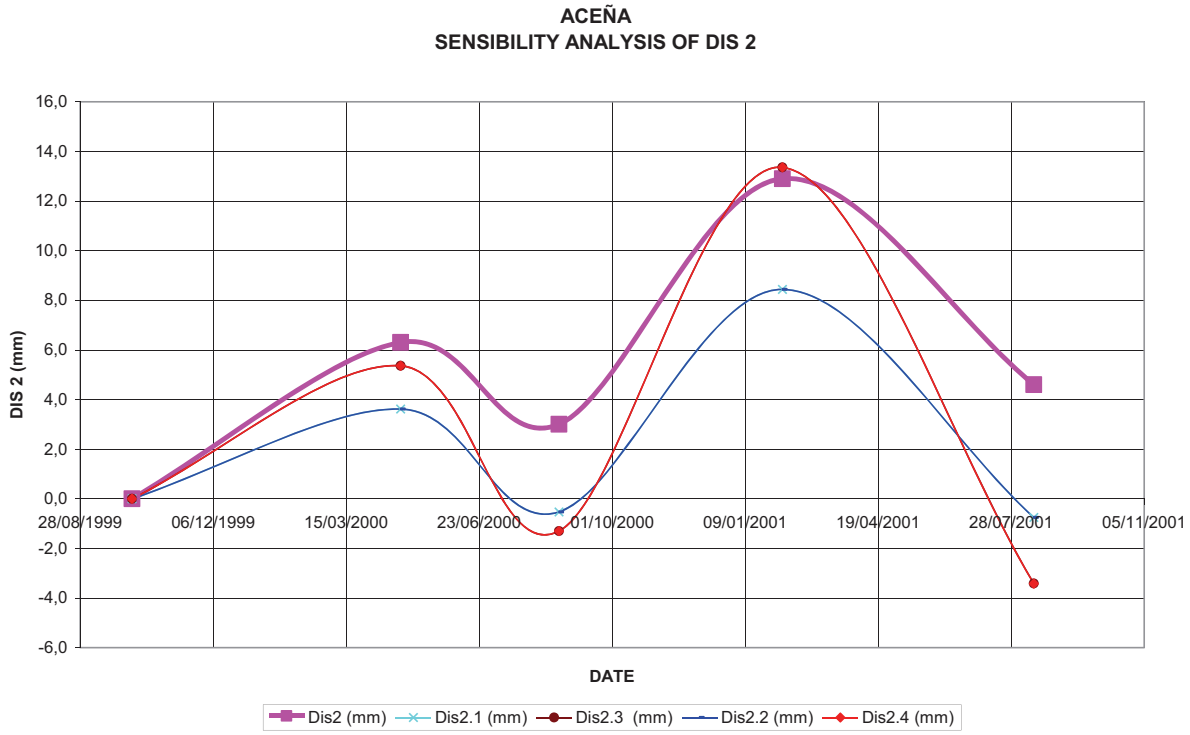

When applying the same changes the behaviour is represented quite well and there's very little influence due to the uplift effect.

5. Summary of results

The table below shows the results of the entire analyzed hypothesis:

Date	comparison of obtained results for Dis 1 (mm)				
	Dis 1	**Dis 1.1**	**Dis 1.2**	**Dis 1.3**	**Dis 1.4**
06/10/1999	0,00000000	0,00000000	0,00000000	0,00000000	0,00000000
25/04/2000	17,50000000	6,30091628	9,42506499	6,30114275	9,42646424
22/08/2000	-6,50000000	-11,93832505	-8,69565984	-11,93791644	-8,69565984
06/02/2001	33,30000000	22,77327666	35,09837747	22,77356160	35,09781948
14/08/2001	-4,30000000	-10,85631450	-5,72263445	-10,82883267	-5,72071962
Date	**comparison of obtained results for Dis 2 (mm)**				
	Dis 2	**Dis 2.1**	**Dis 2.2**	**Dis 2.3**	**Dis 2.4**
06/10/1999	0,00000000	0,00000000	0,00000000	0,00000000	0,00000000
25/04/2000	6,30000000	3,61281525	3,61281525	5,36072402	5,36106333
22/08/2000	3,00000000	-0,53296248	-0,53296248	-1,30525438	-1,30554395
06/02/2001	12,90000000	8,43690281	8,43690281	13,35566412	13,35514317
14/08/2001	4,60000000	-0,75272837	-0,75300598	-3,41746631	-3,41831201

The following graphic shows the comparison between UPV best fitted solution (Case 4) and the recorded data

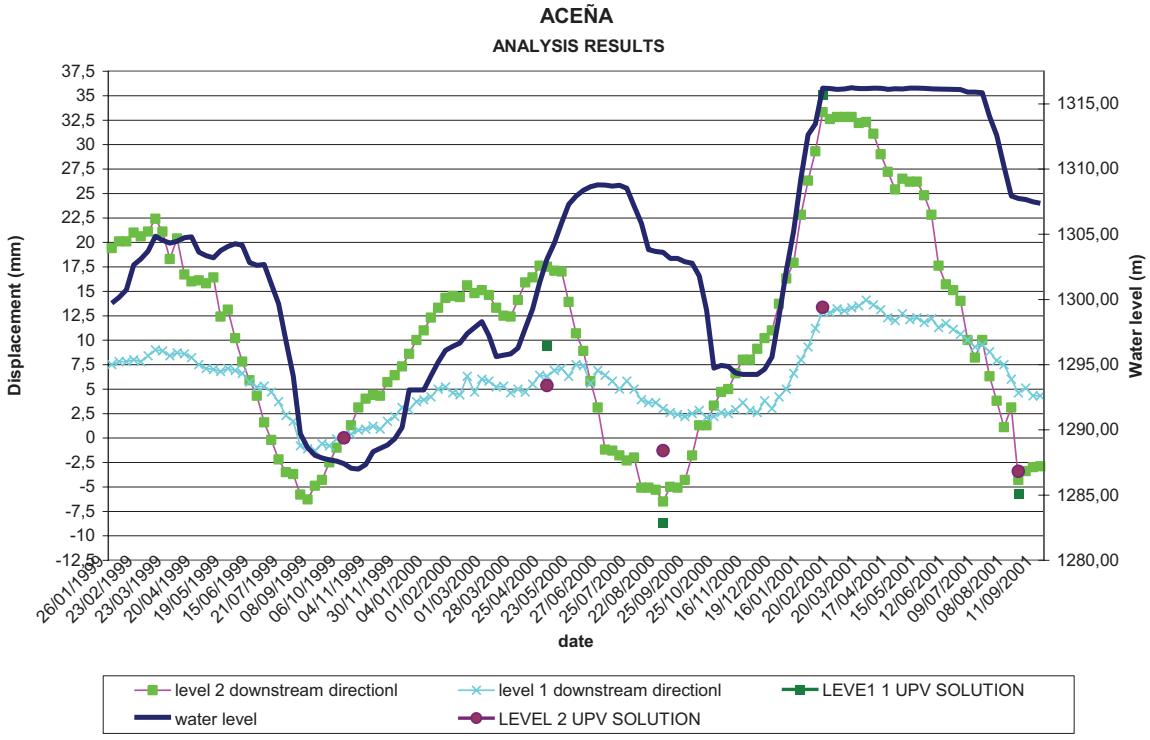

In conclusion, although the statistical analysis of the input data shows that 85% of the movement of the dam can be explained by the coupled action of water pressure and temperature, the results of the analysis emphasize the fact that there must be another factors influencing the mechanical behavior of the dam. In particular, the numerical model represents properly the trend of the real movements of the dam, but the real magnitude is captured only if the stiffness assumed for the concrete is reduced.

FEM ANALYSES FOR THE INTERPRETATION OF THE STRUCTURAL BEHAVIOUR OF LA ACECA DAM

By

Massimo Meghella, Piero Masarati

CESI RICERCA Spa, Milan, Italy

Summary

In the frame of the ICOLD - 9th Benchmark Workshop on Numerical Analysis of Dams, the proposed Theme A on the "*Analysis of the elastic behaviour of an arch-gravity dam*" [1] has been approached by using CANT-SD, a FEM code developed by CESI RICERCA for the structural analysis of dams. Due to the information incompleteness about the actual thermal boundary conditions (no reservoir temperatures are available) and the insufficient knowledge of the measured behaviour (block 3 plumbline measurements only), several analyses have been carried out in order to investigate both the influence of each single load component and of the materials parameters on the observed behaviour. In addition , a system identification process aimed at modelling the external temperature conditions to apply to the upstream/downstream faces of the FEM model of the dam in order to simulate the measured behaviour has been attempted. Finally, through a suitable combination of each single load component with a properly calibrated set of elastic parameters and boundary temperature conditions a possible interpretation of the measured structural behaviour has been provided.

Keywords: Finite Element Method, Linear Elasticity, Back Analysis, System Identification, Thermal Analysis, Structural Diagnostic.

1. Introduction

According to the purpose of Theme A of the 9th Benchmark Workshop on numerical analysis of dams [1], in the present paper the analysis of the elastic behaviour of La Aceca dam, aimed at interpreting the structural behaviour as provided by the plumbline #3 measurements, is presented and discussed.

The authors, on the basis of the data provided by the formulators, used their in house developed FEM Code CANT-SD [2], to analyse the linear-elastic FEM model of La Aceca dam-foundation system.

In the foreword of Theme A, the formulators claimed: "Records obtained from dam instrumentation are crucial in order to interpret the structure behaviour and be able to assess its safety. However, due to the uncertainties involved in the process of installing such instruments, the way readings are collected, the nature of the instruments and their conservation state, measurements can be not as reliable as expected. In fact, measurements *can be misunderstood, can lead to make the wrong decisions and, in some cases, can make dam engineers to develop some degree of skepticism about their importance. Numerical*

modelling can be a helping tool but also adds some additional uncertainties if they are not carefully and rigorously used: construction data should be examined, constitutive models properly chosen, etc. In summary, combination of a good knowledge of the instruments, an appropriate conservation of instrumentation and reading procedure, a realistic data management program and the implementation of numerical models is a very important task that has to be carefully undertaken due to all the involved uncertainties. But also, the behavior itself of a dam, is a source (sometimes the main one) of uncertainties". In addition to the above statements, widely recognized and shared by the dam engineering community, "*completeness"* and "*redundancy"* of measurements should be properly assured in order to improve the knowledge of dam-reservoir-foundation system and to shrink all sources of uncertainties.

In this case, the provided measurements might not be sufficient to grant a sound interpretation of the dam behaviour. In particular the following lacks or incompleteness of information can be highlighted:

a) Inflow/outflow seasonal regime of the reservoir and in particular the water temperatures to assume on the wet face of the dam model;

b) The influence of thermal radiation and daily air temperatures, given the particular dam faces exposure (Fig. 1);

c) The observation period might be too short to identify trends and repeatable situations;

d) The measurements relevant to the first impounding are quite synthetic and generic, in particular those relevant to joint displacements (e.g. maximum joint "movement" recorded was 1.88 mm, but no information on both type of movement - opening or sliding - and external conditions of its occurrence were provided. The exact locations of the thermometers inside the dam body are not reported, making it difficult to identify the internal temperature patterns inside the dam body developed during the first impounding period)

Nevertheless several analyses have been carried out in order to investigate both the influence of each single load component and of the materials parameters. Finally, through a thorough analysis of the results a possible interpretation of the measured structural behaviour has been provided.

2. Model assumptions

According to the formulators requests the FEM model of the dam has been assumed as linear-elastic, so all single load effects may be easily combined, through the superimposition effects principle, that holds for linear problems. Moreover, in order to further limit the analysis complexity and the overall model uncertainties, uplift pressures have not been considered. These assumptions considerably simplify all analysis steps and ease the interpretation of the results, but, on the other hand, they might imply an unrealistic representation of the real behaviour of the dam, that may be in particular significantly influenced by the non-linear effects due to the joints relative displacements. The temperatures distributions inside the dam body have been calculated through a FEM thermal conduction analysis, by assuming the sinusoidal models of the external temperatures (air and water) described in §2.2.

Fig. 1. Google Earth view of LA Aceca dam

2.1. Fem Mesh and input parameters

The same FEM mesh as the one provided by the formulator has been used for all the analyses (Fig. 2).

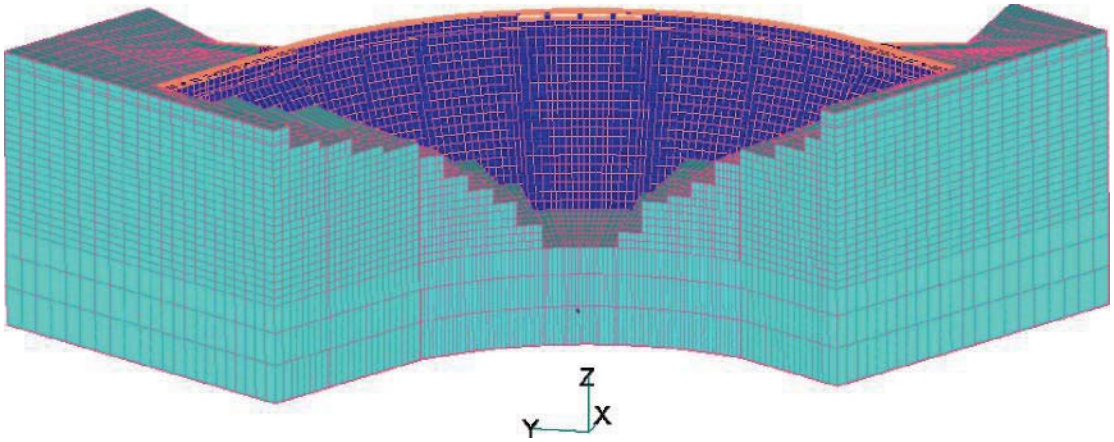

Fig. 2. FEM mesh of the dam-foundation system

The mesh consists of 53038 nodes, 9328 linear brick elements for the dam block, 36413 linear brick elements for the rock foundation.

In the following table the material mechanical properties (as provided by the formulators) and the thermal parameters (as adopted by the authors from literature values) are summarized:

PROPERTY	FOUNDATION	DAM BODY
Specific Weight	22 KN / m^3	23.6 KN / m^3
E (Young Modulus)	10000 MPa	20000 MPa
Poisson.S Ratio	0.2	0.2
Coeff. of thermal Expansion	0	10-5 ϵC^{-1}
Thermal Conductivity *(literature value)*	-	104650 J /(days m °C)
Thermal Capacity *(literature value)*	-	2093000 J / (m^3 °C)

Table 1. Input parameters

2.2. Loads and loading combinations

Since the *superimposition effects principle* holds for linear problems, each single load effects (dead weight, hydrostatic pressures, temperature effects) has been separately calculated and further combined. The external temperature variation has been modelled as sinusoidal functions on the basis of the measured average monthly air temperatures (Fig. 3).

In particular, as no water temperatures measurements are available, the relevant temperature cycles has been deducted from the air temperature cycles, considering

that for reservoirs physically and climatically similar to the one under examination [3], it has been observed that the water temperature amplitude typically is around 60% of the air amplitude and the relevant cycles are delayed 1 month with respect to the air cycle.

The temperature time histories (air and water) have been uniformly applied on the proper dam faces (dry and wet) and through the conductivity analysis the temperature distributions inside the dam body have been calculated for each time step (10 days) to be subsequently used for the structural analyses. Figs. 4 and 5 show the temperatures distributions corresponding respectively to the time when the maximum upstream (August 2000) and downstream (February 2001) displacements occur.

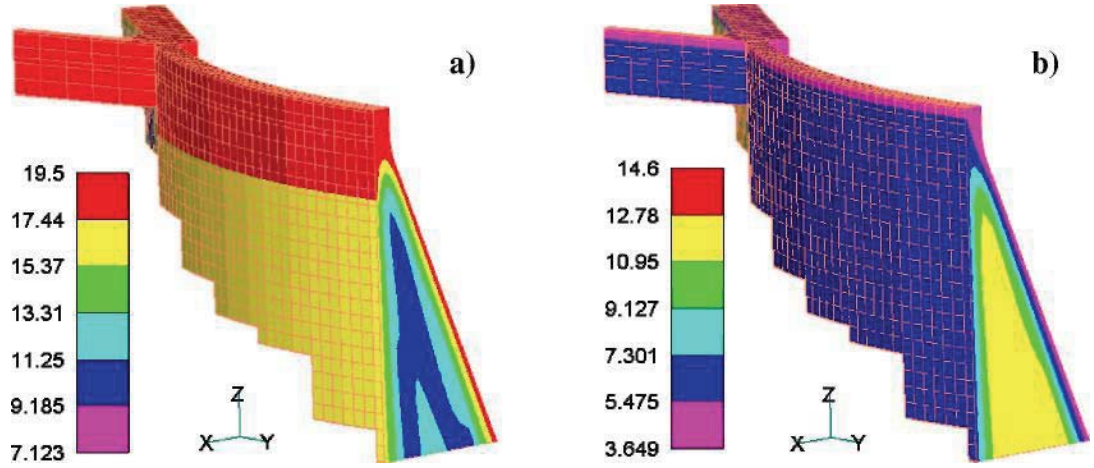

Fig. 4. Temperatures distributions: a) August 2000; b) February 2001

The average monthly air temperature (3.7 °C) correspondent to the cold period when the dam structural joints were sealed (February 1989) has been assumed as the reference temperature (when no thermal stresses occur).

2.3. System identification process

As previously stated (§1), the level of uncertainty in modelling the behaviour of La Aceca dam is quite high and the displacement measurements provided by the Plumbline #3 are difficult to interpret with so many variables and simplified assumptions in play. So, in order to validate some preliminary assumptions on the external temperature models, a set of back analyses aimed at identifying the sinusoidal parameters of the external temperature distributions (periods, amplitudes, phases) have been carried out. The identification process is based on the comparison of the measured and calculated displacements, for a set of 11 couples of top displacement values (A-A',…K-K'), each characterized by the same water level (Fig. 5). In this way the variation of the system response is influenced by the variation of the external temperatures only.

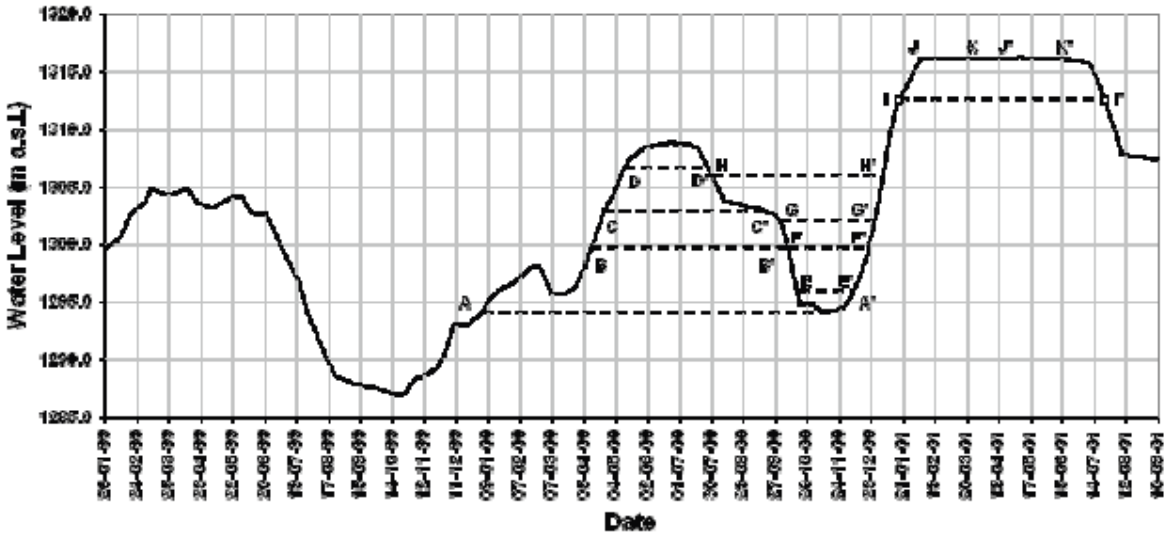

Fig. 5. Selected couples with same water level

Unfortunately the identification process provided unrealistic values for the parameters of the external temperature cycles (in particular of the water). That might be due to the following reasons:

- Wrong assumptions on the structural model: the non-linear effects due to the possible joint movements have not been considered and might be significant.

- Wrong assumptions on the external temperatures models: 1) sinusoidal functions might not be appropriate to model the water temperatures; 2) the latter might vary over the height (as usually is the case in summer, when the water stratification occur [4]); 3) the influence of thermal radiation and daily air temperatures, given the particular dam faces exposure, might be significant.

-

3. Results

In Figs. 6 and 7 the single load effects (Dis1 and Dis2), respectively due to the hydrostatic pressures and the temperatures loads are reported. The combination of the two effects are reported and compared with the correspondent measurements in Fig. 8.

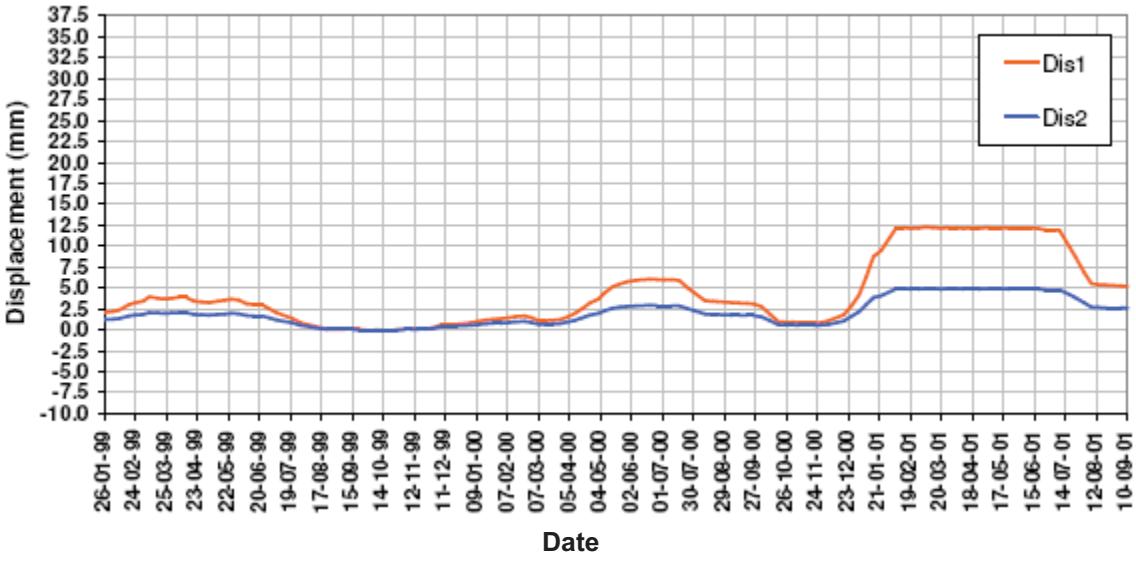

Fig. 6. Displacements calculated for pendulum n. 3 (pressure effect only). Dis1 (from lower gallery to the crest) and Dis2 (from lower to intermediate gallery)

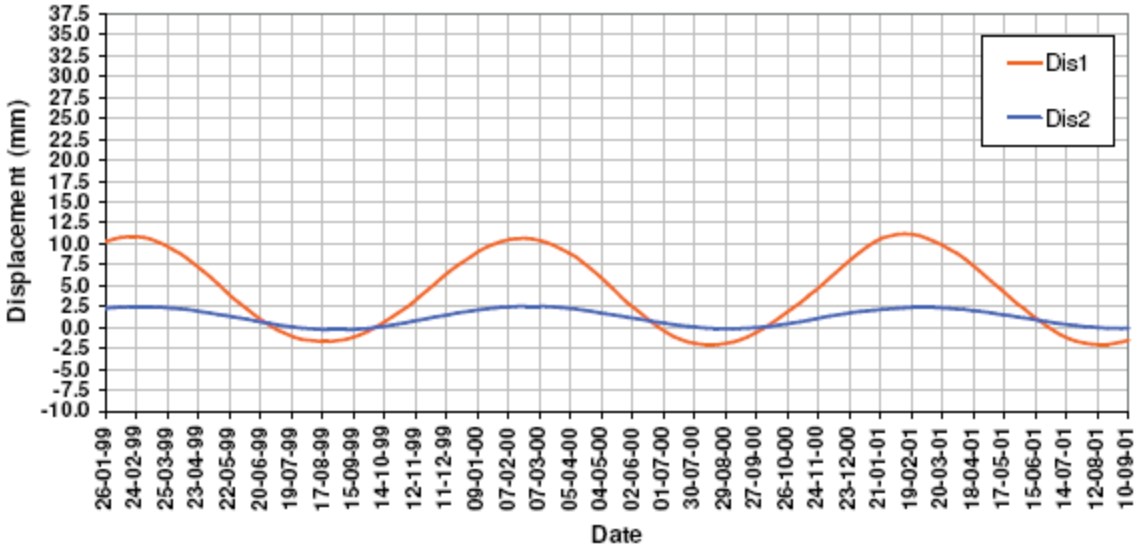

Fig. 7. Displacements calculated for pendulum n. 3 (thermal effect only). Dis1 (from lower gallery to the crest) and Dis2 (from lower to intermediate gallery)

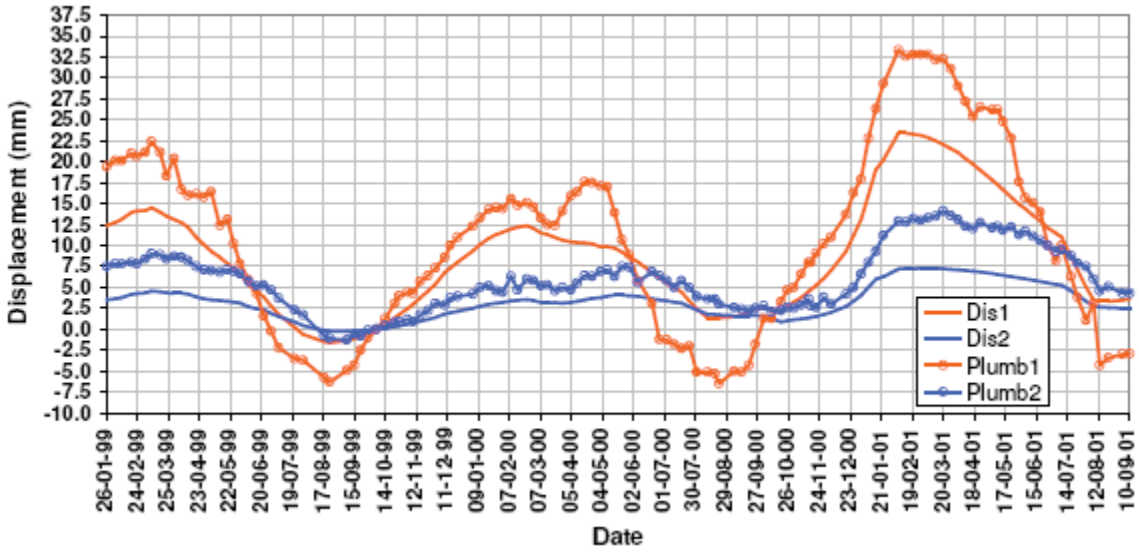

Fig. 8. Calculated (Dis1, Dis2) vs. measured (Plumb1, Plumb2) displacements for pendulum n. 3.

It can be noticed that the calculated displacements are mostly much lower than the measured one. That implies that the overall stiffness of the system has been overestimated.

Then, a further attempt to tune the model stiffness was to halve both the Young modulus of the dam and of its foundation and the correspondent results are reported in Fig. 9.

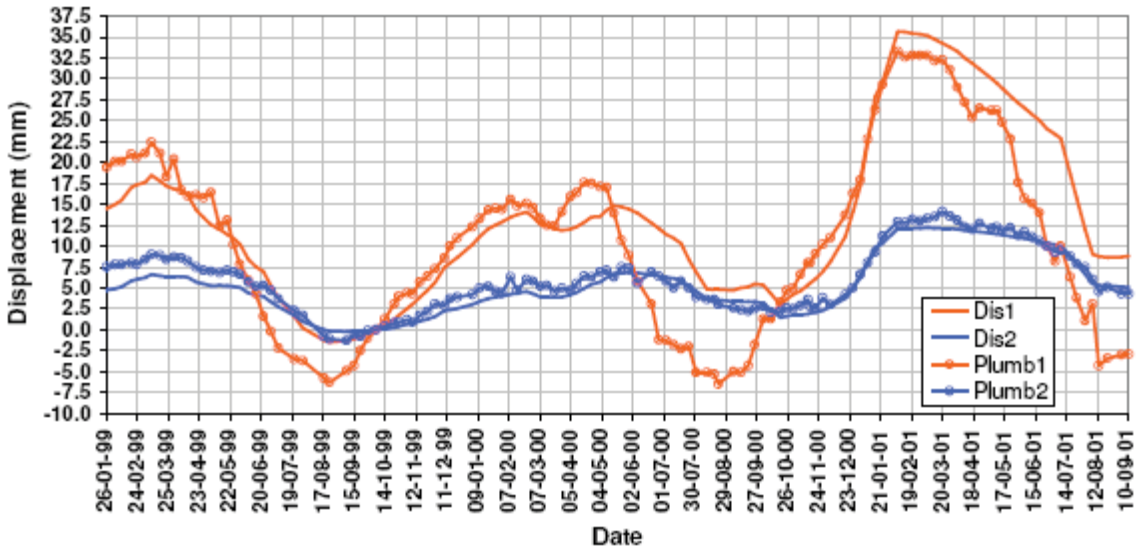

Fig 9. Calculated (Dis1, Dis2) vs. measured (Plumb1, Plumb2) displacements for pendulum n.3. (both E divided by 2).

In this case the comparison has definitely improved and, even if the top displacement (Dis1) comparison is still not acceptable, the intermediate one (Dis2) is quite good and it can be better appreciated in Fig. 10, where the difference between the measured and the calculated displacements are reported.

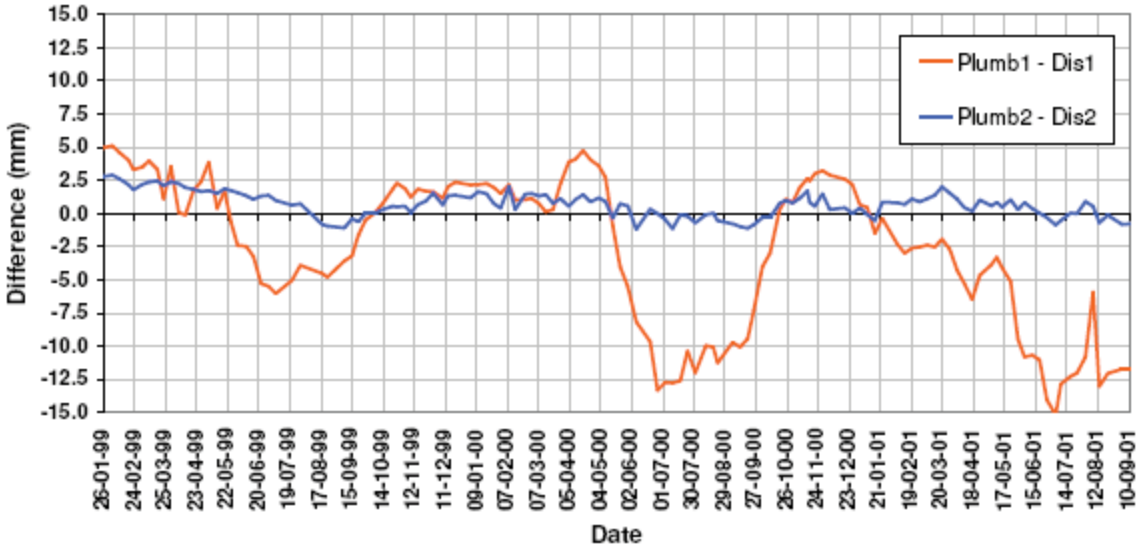

Fig. 10. Difference between measured and calculated displacements for pendulum n.3 (modulie divided by 2).

These results might be justified by the fact that some non-linear effects occur in the upper part of the dam during the same period of the year (summer), being reasonably due to the activation of sliding displacements of the joints, that obviously the linear-elastic model of the dam is not able to simulate. That confirms the first evidence resulting from the identification process previously described and is in line with the measurements of the joint “movements”, as recorded during the first reservoir impounding [1].

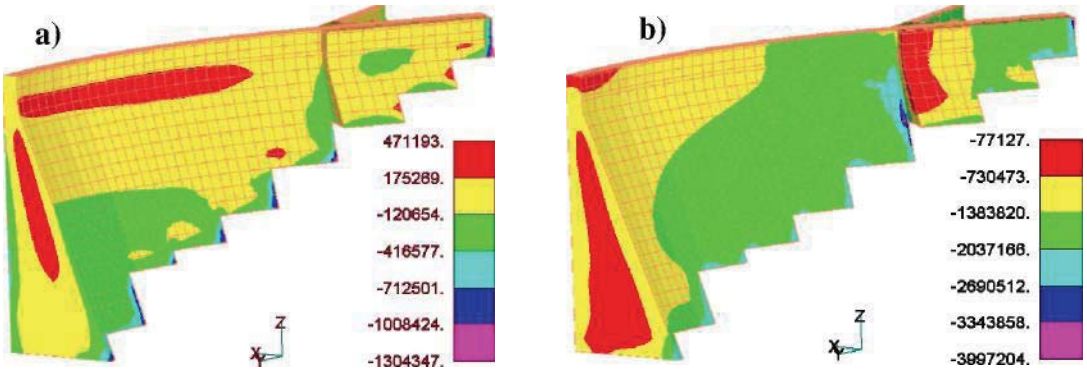

Fig. 11. Stress distributions on August 2000: a) Max Princ. Stress [Pa]; b) Min Princ. Stress[Pa]

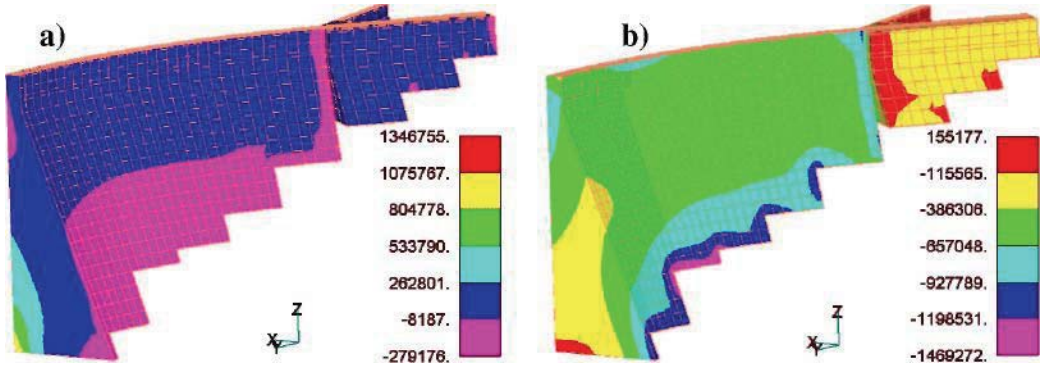

Fig. 12. Stress distributions on February 2001: a) Max Princ. Stress [Pa]; b) Min Princ. Stress [Pa]

Finally, the stress patterns in terms of principal stresses corresponding to the time when the maximum upstream (August 2000) and downstream (February 2001) displacements occur, are reported in Figs. 11 and 12 respectively, showing that both the maximum tensile (1.35 MPa) and the maximum compressive (3.99 MPa) stresses are compatible with the correspondent expectable strengths estimates.

4. Conclusions

The Theme A of the 9th B-W on Numerical Analysis of Dams has been approached by using CANT-SD, a FEM code developed by CESI RICERCA for the structural analysis of dams.

Despite the limited knowledge of the actual structural behaviour, the linear-elastic analyses and the system identification process previously described allowed, through a thorough comparison between calculated and measured displacements of block #3, a possible interpretation of the measured structural behaviour.

The main conclusion of the comparison indicates the need to properly include the joints behaviour in a future FEM model, which simulation might be gradually approached starting, for instance, from considering the central dam blocks free to move as independent cantilevers, to model the actual non-linear effects of the structural joints with proper FEM elements. The comparison of calculated and measured behaviour should include the joints relative displacements, if the relevant measurements are available. If not, the monitoring of them, in terms of opening, sliding and extension, is strongly recommended.

Finally, in case the comparison still would not be acceptable, the assumptions made on the external temperatures models should be critically reviewed in light of what discussed in § 2.3.

References

[1] Escuder Bueno, I., Blazquez Prieto, F - Theme A formulation "*Analysis of the elastic behaviour of an arch-gravity dam*", 9th Benchmark Workshop on Numerical Analysis of Dams, St.Petersburg, Russia, 22 -24 June, 2007.

[2] Masarati, P., Meghella, M., "*The FEM computer code CANT-SD for non-linear static and dynamic analysis of dams*", Enel.Hydro rep. n. 6045, Milan, 2000.

[3] Garofalo, E., Gilli, L., "*Gestione dei serbatoi idroelettrici e tutela qualitativa dei corpi idrici: utilizzo integrato di misure in continuo e modelli per simulazioni revisionali*", L'Acqua-Associazione Idrotecnica Italiana (*in press*).

[4] Loffler H., Hutchinson G. E.,. "*The thermal classification of lakes*", Proc. Nat. Acad., Washington D.C., 42: 84-86 Sci, 1956.

ANALYSIS OF THE ELASTIC BEHAVIOUR OF AN ARCH-GRAVITY DAM

T. BOURGOUIN, C.NORET-DUCHÊNE
COYNE ET BELLIER, 9 allée des Barbanniers, 92632 Gennevilliers, France

ABSTRACT

The measurements of the pendulum n°3, corresponding to the crest deflection of LA ACENA arch-gravity dam were studied over the 1999-2001 period, in order to explain the recorded movements of the dam. The Hydrostatic/Seasonal/Time statistical method (HST) and a structural model were used together to interpret the monitoring data. The HST model was prepared with the help of CONDOR software, developed by COYNE-ET-BELLIER. The statistical tool provided the readings of the pendulum as an expression, which depends only on hydrostatic and seasonal functions. To complete the analysis of the behaviour of LA ACENA dam, a structural model was created by the mean of the COQEF code, developed by COYNE-ET-BELLIER and specially dedicated for the calculations of arch dams. This deterministic method allowed an adjustment of mechanical properties of the dam (Young modulus, coefficient of thermal expansion). Two possible sets of parameters were found, which may explain the observed behaviour of the dam.

Key words: monitoring, arch-gravity dam, deterministic method, statistical method, finite elements

1. INTRODUCTION

The present exercise aimed at analysing and interpreting the behaviour of the arch-gravity dam called “LA ACENA” using observations recorded during the period 1999-2001. The study of its behaviour was allowed by means of movements recorded by the plumbline N°3. The authors decided to use two methods in order to describe and to understand the behaviour of the dam. The first one is a structural method, using a finite elements model and the second method is based on a statistical analysis.

The structural method was carried out with the help of the software COQEF, developed by COYNE-ET-BELLIER especially for quick 3D modelling of arch dams.
COQEF models the dam by means of thick shell elements. The elements of the mesh are made up with rectangles defined by 8 nodes and with triangles defined by 6 nodes. Foundation elements are VOGT elements defined by a line with 3 nodes.

This software can model various loadings on dam like weight, hydrostatic pressure and thermal loadings. In particular it can be used to calculate dam weight, when joints are not yet sealed. COQEF code is able to calculate the deformations and the strains (principal strains, shear strains and normal strains) in dam body.

Various combinations of loadings have been used to calculate the horizontal displacements at Plumbline n°3 located in the block 3 for the selected dates.

The statistical method was performed with the help of the software called CONDOR. This software is developed by Coyne-et-Bellier for the interpretation of monitoring data. This software refers to the Hydrostatic/Seasonal/Time (HST) method developed by "Electricité de France" (EDF) for dams monitoring. The authors used the temporal working mode of this software. The temporal analysis allowed finding a mathematic relation between readings from the pendulum n°3 and dam parameters like hydrostatic, seasonal and temporal parameters.

2. PART 0. Justification of the model

2.1 Presentation of LA ACENA dam

LA ACENA dam is a symmetrical arch-gravity dam defined by a circular arc with a radius of 150 m for the upstream face and an aperture equal to 90 hexadecimal degrees. The crest arc (without right and left abutments) has a development of 235.6 m and the maximum height of the dam is 66 m.
The upstream face is defined by a cylindrical surface and the cantilevers have a variable thickness with altitude. The thickness of the crown cantilever range from 4 m on top to 28.8 m on the bottom. The dam (i.e. arch and abutments) is divided into 19 cantilevers separated by joints.

2.2 Preparation of the structural model

A file dedicated to COQEF was prepared with the nodes of the dam mesh. These nodes have been extracted from the file JOINTS.txt provided by the formulator.
In order to get a reasonable mesh size, only 578 nodes were selected to build the dam model. There is only one material for all elements, namely the concrete. Nodes at the dam basis represent the interface foundation/dam body.

The dam mesh is built with 17 cantilevers and 9 arcs. The elements at the base of the dam are made up with triangular elements. The flat base at the crown of the dam is also modelled with two small triangular elements. *(See fig.1 and fig.2).*

Other views of the mesh are given in appendix.

The shape of the abutments was derived from the mesh provided by the Formulator. While respecting a basic geometry, the thickness of abutments is larger than the one of the arch. To keep the thickness of abutments, the mesh was locally modified. *(fig.3)*

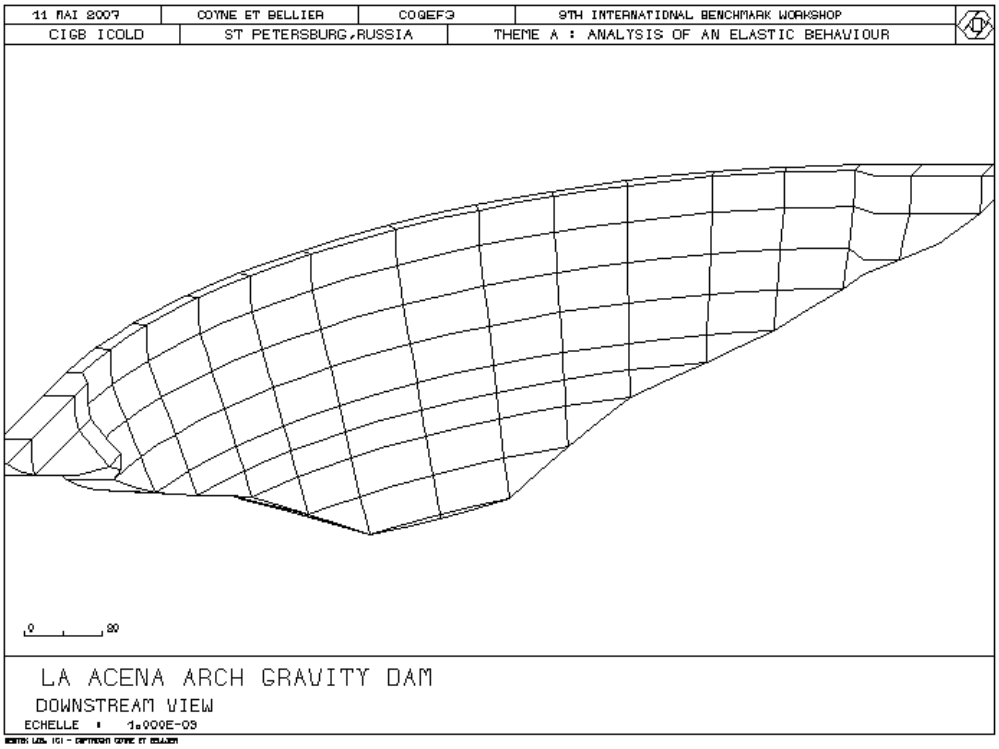

Figure 1: Downstream view of the mesh

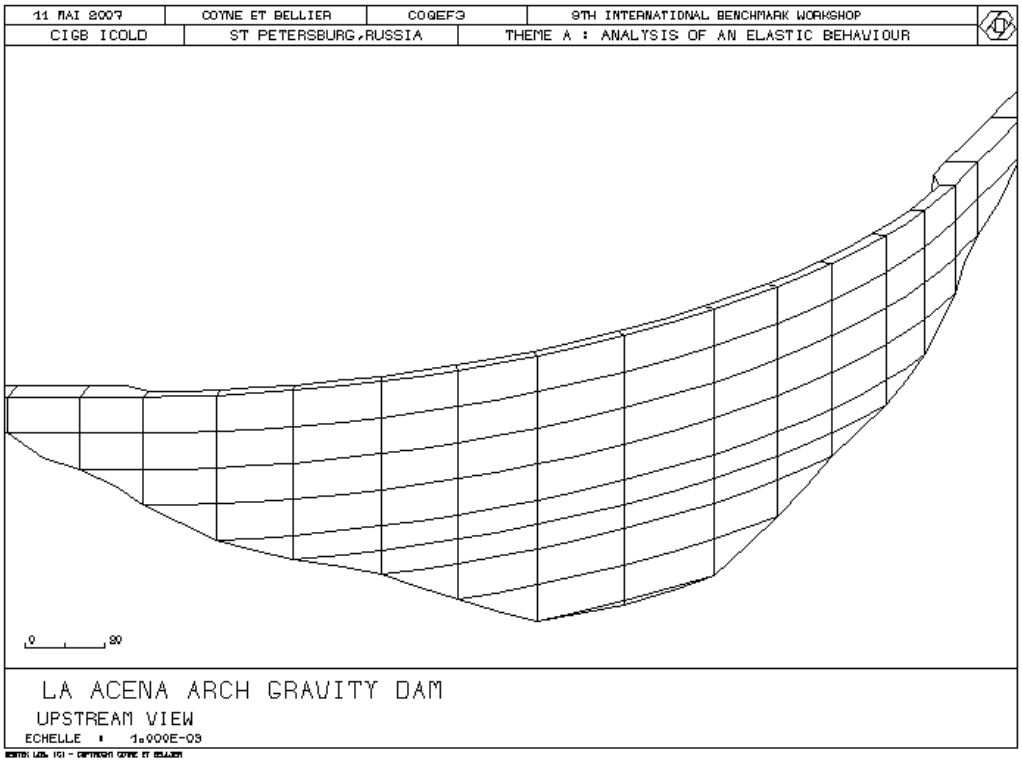

Figure 2: Upstream view of the mesh

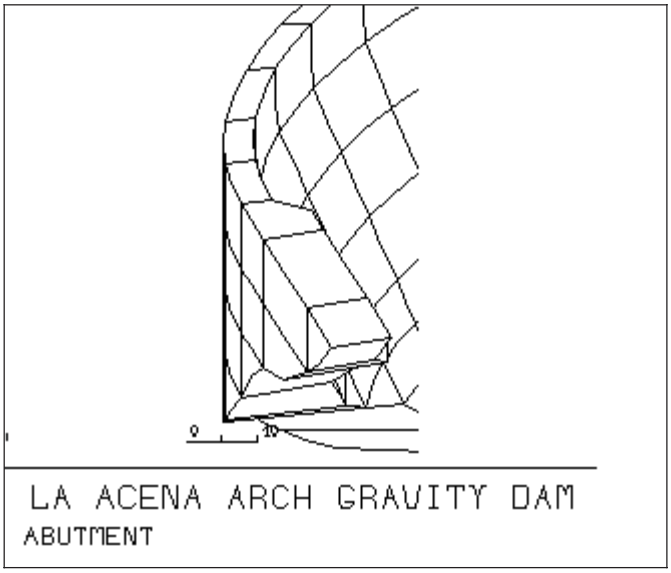

Figure 3: Right abutment

For the calculations in part 1, the mechanical properties of the materials suggested by the Formulator were used:

Property	DAM BODY	FOUNDATION
Specific weight	23.6 kN / m^3	22 kN / m^3
E (Young modulus)	20 GPa	10 GPa
Poisson´s Ratio	0.2	0.2
Coef. of thermal exp. A	10^{-5} ºC^{-1}	0

Structural calculations were carried out with several loading cases. These cases are combinations of:

- dam weight with independent cantilevers (i.e. the joints are not sealed)
- dam weight with monolithic dam (i.e. the joints are sealed)
- hydrostatic pressure at different levels
- thermal load of a specific day with temperatures according to the reservoir water level

The temperatures given by the Formulator and recorded in the dam body during the first impounding can not be used for the calculation of thermal loads. In fact chemical reactions happened during the first impounding and the recorded temperatures can not represent the future temperatures inside the dam body. So the Authors had to determine the temperatures distribution in the dam body from the given air temperatures.

The thermal load was drastically simplified:
- Variations of temperature in the dam body were considered linear from upstream to downstream, following Stucky's simplification [REF. 1].
- The downstream and the upstream faces of the dam are faced with sinusoidal variations of temperature. These sinusoidal temperature distributions are calculated for each downstream and upstream node, taking into account their location (water, air) and elevation. The sinusoids have the same period but their amplitude varies according to their location and elevation.

The air temperature sinusoid was calculated by equalling the surface under it with the surface under the mean temperature curve (see §2.3.2).

We observed that Stucky's hypothesis didn't fit well with the given temperature during April and May.

2.3 Preparation of the statistical analysis

Another file was created with the characteristics of the dam (reservoir water level, dam height, date of measurement) and with the horizontal displacements read by the pendulum n°3.

2.3.1 Variations of the reservoir water level

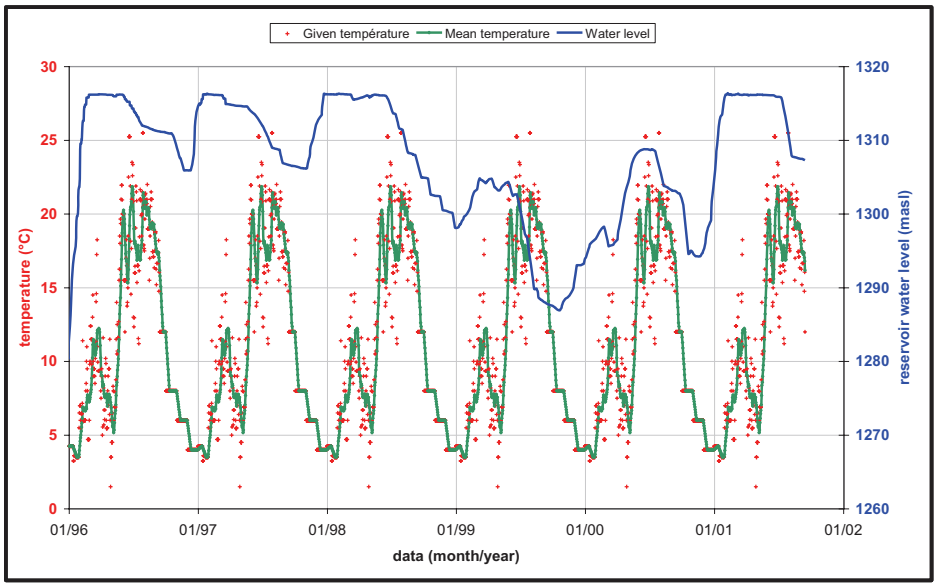

Figure 4: Variations of the reservoir water level and temperature

During the study period, the reservoir presented various levels: the water level during year 1999 is very low whereas the dam is faced with an important rise of the water level in 2001 (fig.4). So there is little correlation between the reservoir water level and the seasons. The explanation coefficient of the reservoir water level by mean of seasonal parameter is only 0.15 high and justifies the independence of hydrostatic and seasonal functions.

2.3.2 Variations of temperature

According to the given data, the air temperature follows perfectly a periodic yearly variation. There are sometimes huge differences between air temperatures for days running.

The figure 4 shows that the temperatures are the same from year to year over the period 1996-2001. It seems very unlikely that air temperature evolution be identical during these 6 years: the temperature data are not the result of direct readings.

The Authors calculated a "mean temperature", which is an average over the previous ten days temperatures; it is represented on figure 5. The large rose points represents the days selected for the present exercise.

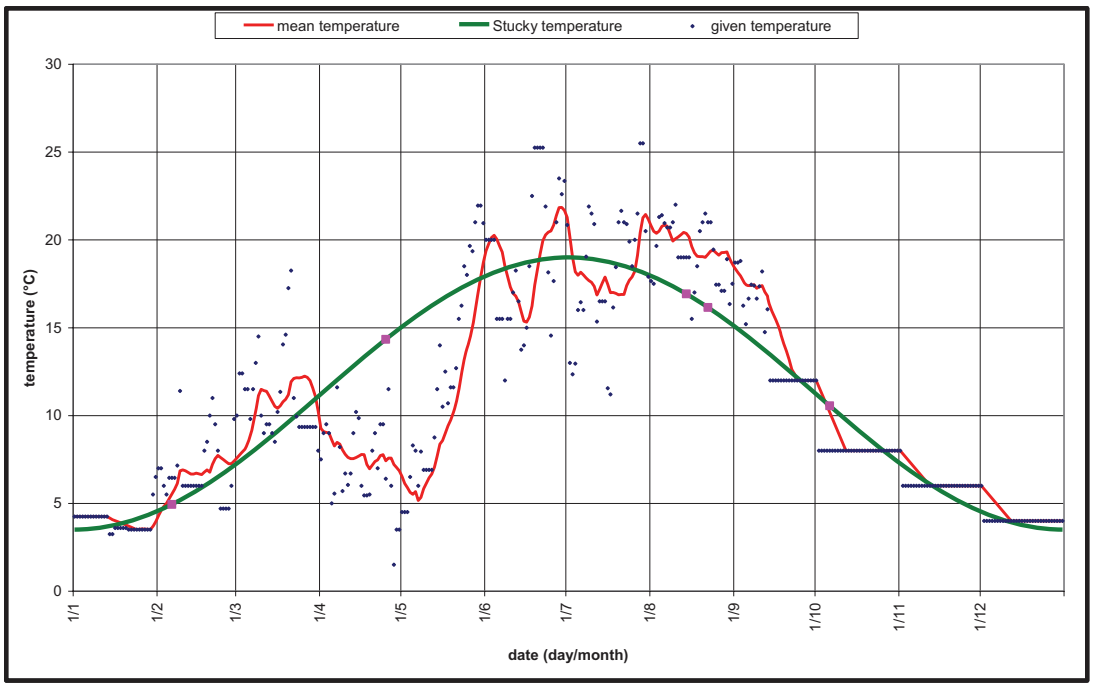

Figure 5: air temperature: raw, mean and sinusoid

2.4 Results of HST model

(HST method is explained in Appendix.)

The HST method was applied for the three displacements recorded by direct pendulum n°3:
- Horizontal displacement from lower gallery to the crest called Dis1
- Horizontal displacement from lower to intermediate gallery called Dis2
- Horizontal displacement from intermediate gallery to the crest called Dis3

For the first displacement, 343 observations are available between 03/01/1996 and 11/09/2001. For the others only 130 observations are available between the first of January 1996 and the eleventh of September 2001.
CONDOR software calculates the best model for each displacement, using hydrostatic functions (Z, Z^2, Z^3, Z^4), seasonal functions (cosS, sinS, $\sin^2$S and sinS*cosS), temporal functions (T, exp. (-T) or discontinuous step function.

2.4.1 Selected models

The best models were composed with one “H” function Z and all four seasonal “S” functions. For all models, the temporal functions do not improve the interpretation of dam movements.

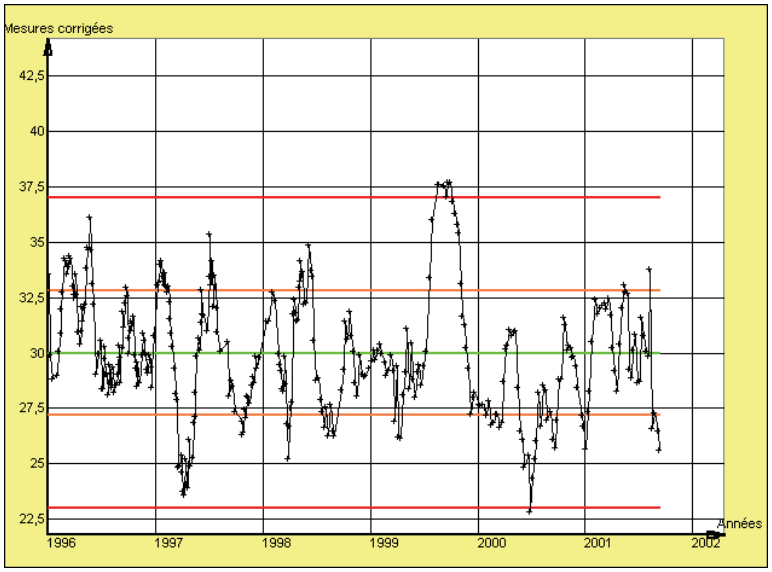

Figure 6: variations of corrected values of Dis1

The residual standard deviation for the displacement Dis1 equals to 2.8 mm which corresponds to a correct explanation coefficient of 75.5 percent. The models for the other displacements Dis2 and Dis3 have a residual standard deviation respectively as high as 0.8 mm and 2.4 mm. Their explanation coefficients equal to 78 percent and 70.5 percent.

The influence of the seasonal effect on Dis1 is 27 mm, with the maximum at mid-August and the minimum at the beginning of February. The influence of the hydrostatic effect is 44 mm when the reservoir water level varies from elevation 1253 m.a.s.l. (empty reservoir) to elevation 1316 m.a.s.l. (full reservoir).

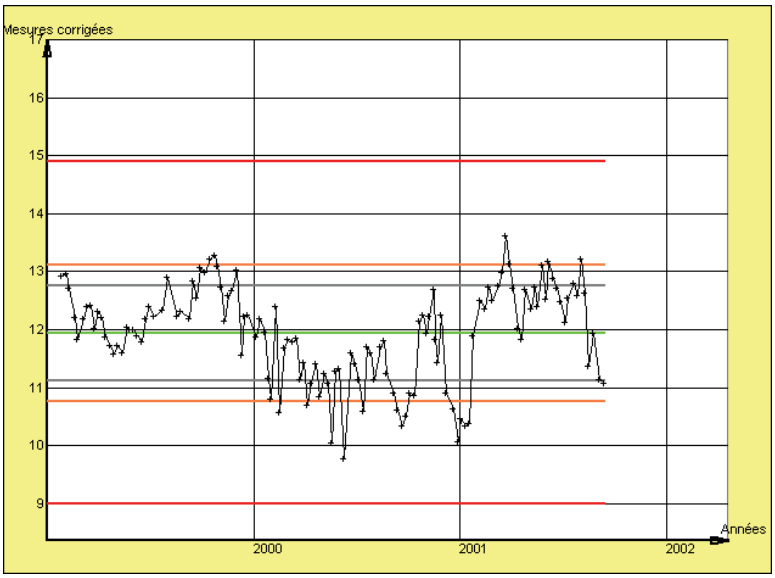

Figure 7: variations of corrected values of Dis2

For Dis2 (fig.7), the influence of the seasonal effect is 3.7 mm with the maximum at the end of August and the minimum at the beginning of March, the influence of the hydrostatic effect equals to 22 mm for the same range of reservoir water level than Dis1.

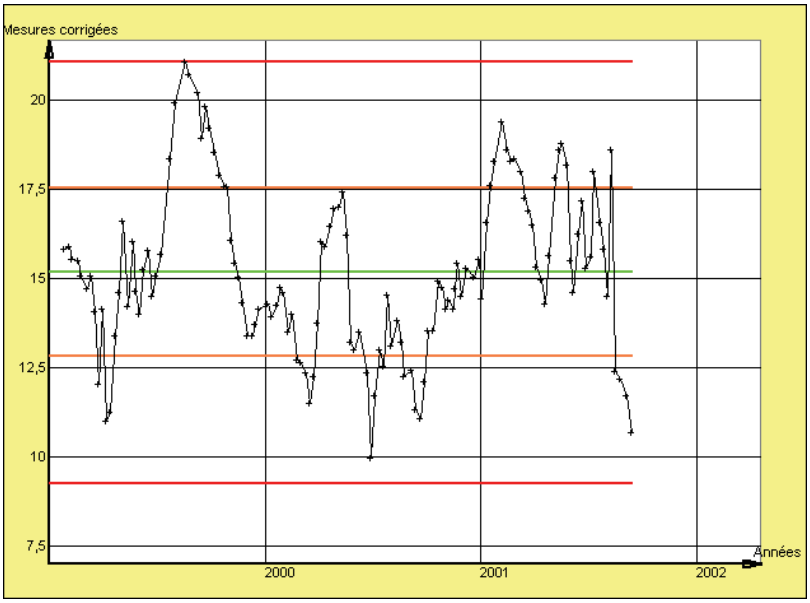

Figure 8: variations of corrected values of Dis3

The influence of the seasonal effect on Dis3 is 20 mm, with the maximum at the beginning of August and the minimum at the beginning of March, the influence of the hydrostatic effect is 18 mm.

2.4.2 Abnormal monitoring data

CONDOR detected an anomaly in the horizontal displacement from lower gallery to the crest (Dis1), which occurred between 18/08/1999 and 28/09/1999 inclusive. This anomaly can be seen on figure 6. The quick rising of corrected values of Dis1 is about 8 mm in one month.
The explanation of this phenomenon may be that the reservoir water level was very low during the summer of the year 1999. The water elevation went down from 1299.65 to 1288.05 m.a.s.l between 06/07/1999 and 08/08/1999. So the dam recorded an important displacement in the upstream direction probably due to the thermal effect. After the month of November 1999 the reservoir water level raised at a usual elevation and the corrected value of Dis1 became normal again.

There is no variation between average displacements before and after this date. Considering this fact we can suppose that the anomaly has not influenced the temporal behaviour of La ACENA Dam. This anomaly showed an imperfect adjustment of the created model.

2.4.3 Model formulation

The model calculated by CONDOR is expressed as a function of:
- the relative reservoir level Z=(MaxRWL-RWL)/Dam Height
- the season angle, rounded from 0 at January 1st to 360 at December 31st

Dis 1 (mm) = 29.9945	constant
• -44.2689 * Z	Hydrostatic functions Z=(1316.5 – water level) / 66
• -9.886 * [1-cos(S)] • 8.3575 * sin(S) • 0.5992 * $\sin^2$(S) • -4.5114 * sin(S) * cos(S)	Seasonal functions S = [0 ; 360]

The explanation coefficient is as high as 75.5 %, which corresponds to a correct model over the short period of measurement.

Dis 2 (mm) = 11.9388	constant
• -21.9494 * Z	Hydrostatic functions Z=(1316.5 – water level) / 66
• -1.2780 * [1-cos(S)] • 1.7878 * sin(S) • -0.6379 * sin(S) * cos(S)	Seasonal functions S = [0 ; 360]

The explanation coefficient for Dis2 is as high as 78 %.

Dis 3 (mm) = 15.0347	constant
• -17.2141 * Z	Hydrostatic functions Z=(1316.5 – water level) / 66
• -8.1095 * [1-cos(S)] • 6.0398 * sin(S) • 2.8335* $\sin^2$(S) • -3.8115 * sin(S) * cos(S)	Seasonal functions S = [0 ; 360]

The explanation coefficient for Dis3 is 70.5 %.

3. PART 1. Calculation of displacements recorded by pendulum n°3

For each selected date, the authors simulated recorded conditions (reservoir water level, temperature in dam body,) and calculated the following displacements:

- Dis 1 : horizontal displacement from lower gallery to the crest at pendulum n°3 (block 3)
- Dis 2 : horizontal displacement from lower to the intermediate gallery at pendulum n°3 (block 3)

The program TRACEF, bound to COQEF, allowed drawing the deformations of the dam.

The Formulator suggested in the present exercise that the measurements of 6th October 1999 are equal to 0. Consequently the calculated displacements for the other days (25/04/2000, 22/08/2000, 06/02/2001, and 14/08/2001) are to be considered as the difference of simulated displacements with the one of the 6th of October.

Another possibility could have been to equalize the average recorded displacements and the average calculated displacements.

For the present study, the authors decided to follow the method suggested by the Formulator and have made equal the recorded and the calculated displacements on the 6th October of the year 1999.

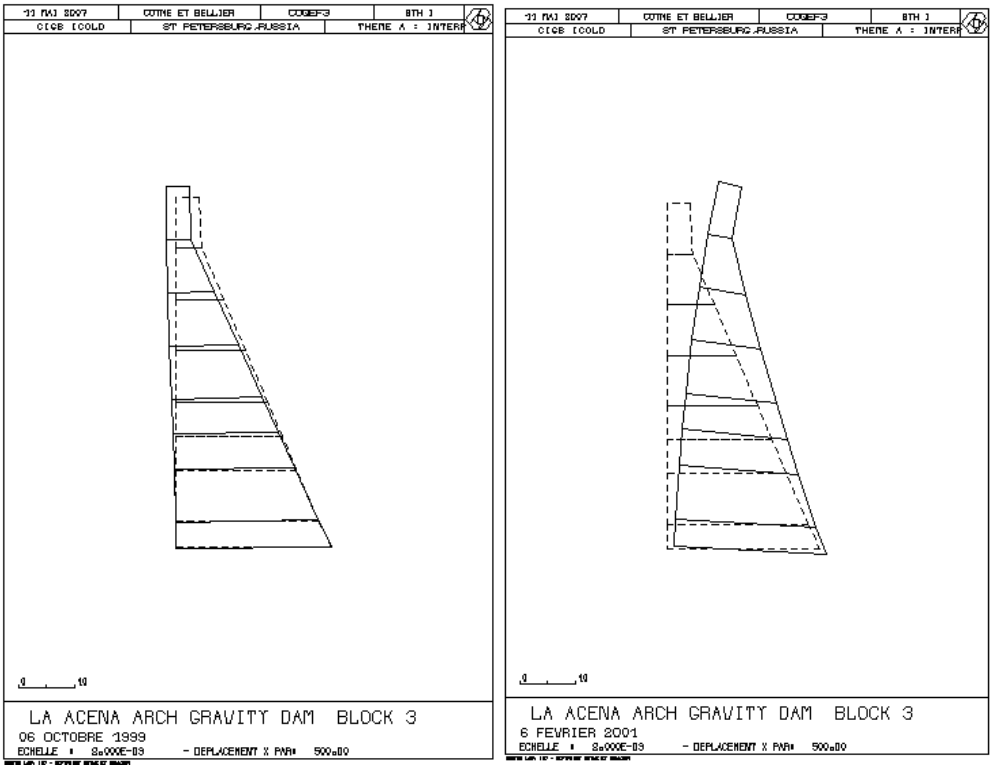

Figure 9: calculated displacement at block 3 on October 6th 1999 and February 6th 2001

The following table shows the calculated displacements:

Date	water level (masl)	air temperature (°C)	Dis1 recorded (mm)	Dis 1 calculated (mm)	Dis 2 recorded (mm)	Dis 2 calculated (mm)
06/10/1999	1287,40	9,82	0,00	0,00	0,00	0,00
25/04/2000	1303,09	7,57	17,50	6,63	6,30	3,18
22/08/2000	1303,61	19,36	-6,50	-4,97	3,00	3,90
06/02/2001	1316,2	5,80	33,30	18,58	12,90	8,11
14/08/2001	1307,73	20,16	-4,30	-3,85	4,60	2,92

The following graphics show the comparison between the calculated and the recorded displacements with dam parameters on the selected days:

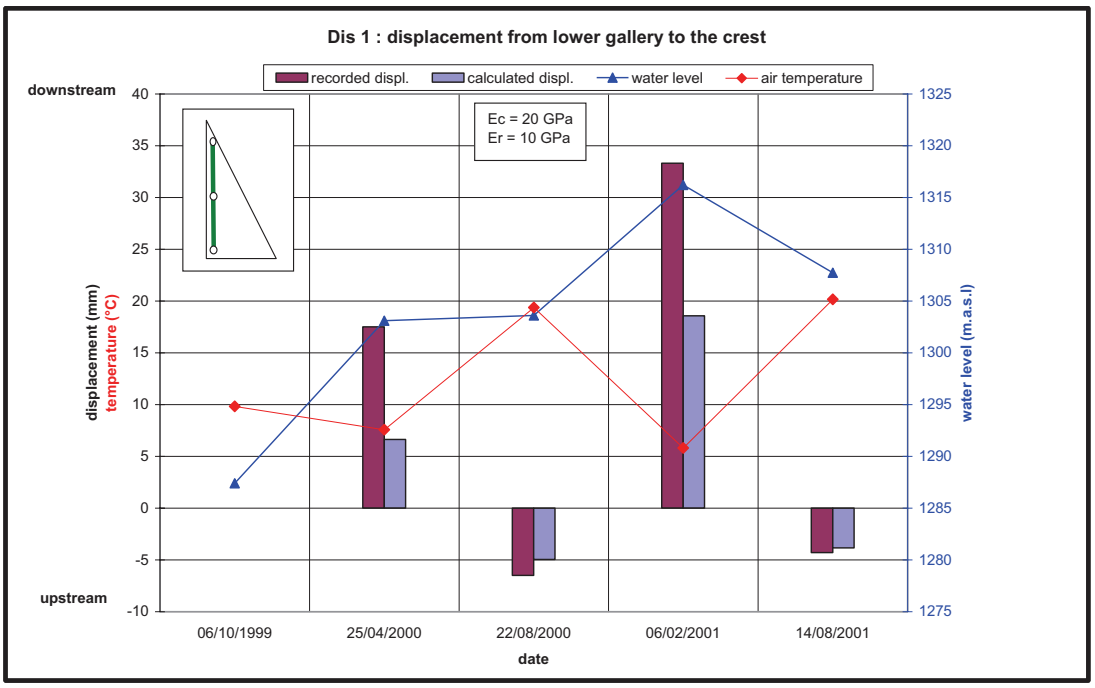

Figure 10: comparison between recorded and calculated displacements Dis1

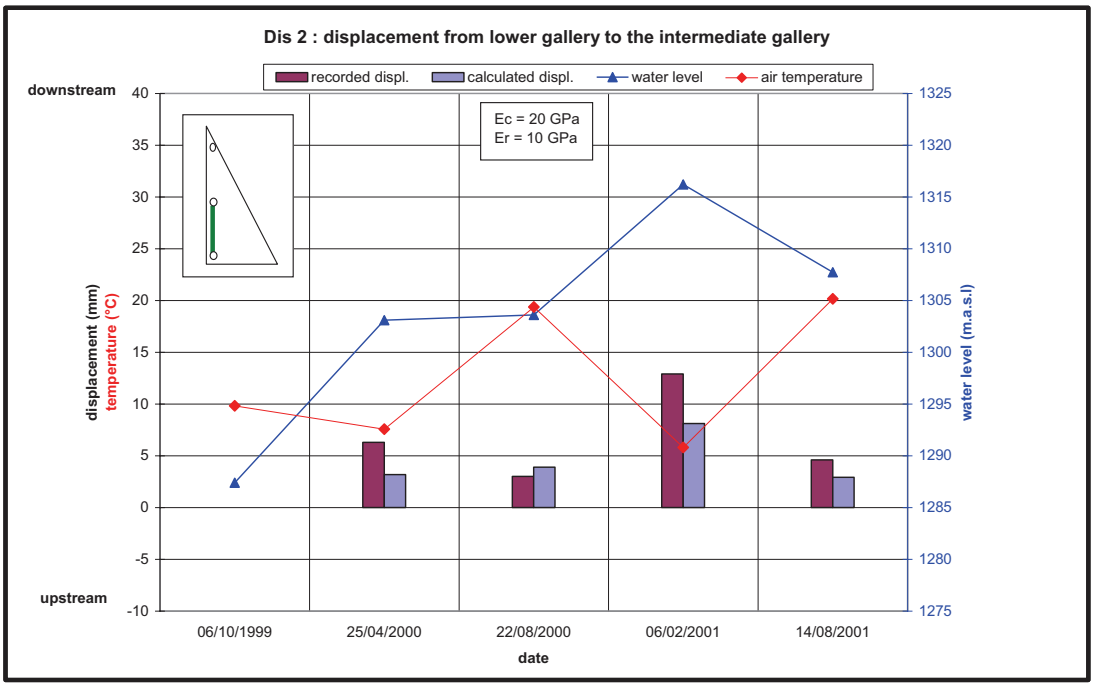

Figure 11: comparison between recorded and calculated displacements Dis2

The calculated displacements do not exactly correspond to the displacements recorded by the pendulum n°3. The range of calculated displacements is less large than the range of measurements. The dam has a more flexible behaviour than the one predicted by the model. So Young modulus (in concrete or in foundation) seems to be overestimated.

The standard deviation of the difference between recorded displacements and calculated displacements for the dimension Dis1 equals to 6.7 mm. For Dis2, the standard deviation of the difference between recorded displacements and calculated displacements is 1.6 mm.

As the displacement due to hydrostatic variations depends only on the Young modulus, the difference between the crest displacement calculated with CONDOR for the maximum of reservoir water level (44 mm) and the crest displacement calculated with COQEF (15 mm) indicates the inadequacy of the first concrete Young modulus estimation.

4. PART 2. Analysis of recorded data

The displacements obtained in part 1 showed that the given mechanical properties seem to be not correct.

We showed with the help of CONDOR that there is no time drift in the behaviour of La Acena Dam. So displacements of the pendulum N°3 can be calculated as the sum of two functions:

- An hydrostatic displacement, depending on the concrete Young modulus Ec
- A thermal displacement, depending on the coefficient of thermal expansion α and the concrete Young modulus Ec. This function corresponds to the seasonal function of CONDOR.

We determined the best set of coefficients (Ec, Er and α) corresponding to the smallest differences between the recorded and the calculated displacements by the least-squares method.

The best simulation was obtained with:
- Concrete Young modulus **Ec = 11.8 GPa** with a standard deviation equal to1.8 GPa
- Concrete Young modulus/Rock Young modulus ratio remains unchanged. So the Rock Young modulus is defined by : **Er = 5.9 GPa**
- Coefficient of thermal expansion **α = 9.5*10^{-6} °C^{-1}** with a standard deviation of 1.5*10^{-6} °C^{-1}

The following table presents the results of calculations with these adjusted mechanical properties:

Date	water level (masl)	air temperature (°C)	Dis1 recorded (mm)	Dis 1 calculated (mm)	Dis 2 recorded (mm)	Dis 2 calculated (mm)
06/10/1999	1287,40	9,82	0,00	0,00	0,00	0,00
25/04/2000	1303,09	7,57	17,50	9,30	6,30	4,92
22/08/2000	1303,61	19,36	-6,50	-2,02	3,00	2,86
06/02/2001	1316,2	5,80	33,30	28,13	12,90	13,08
14/08/2001	1307,73	20,16	-4,30	0,23	4,60	4,71

The following graphics show a comparison between the recorded and calculated displacements with the adjusted parameters:

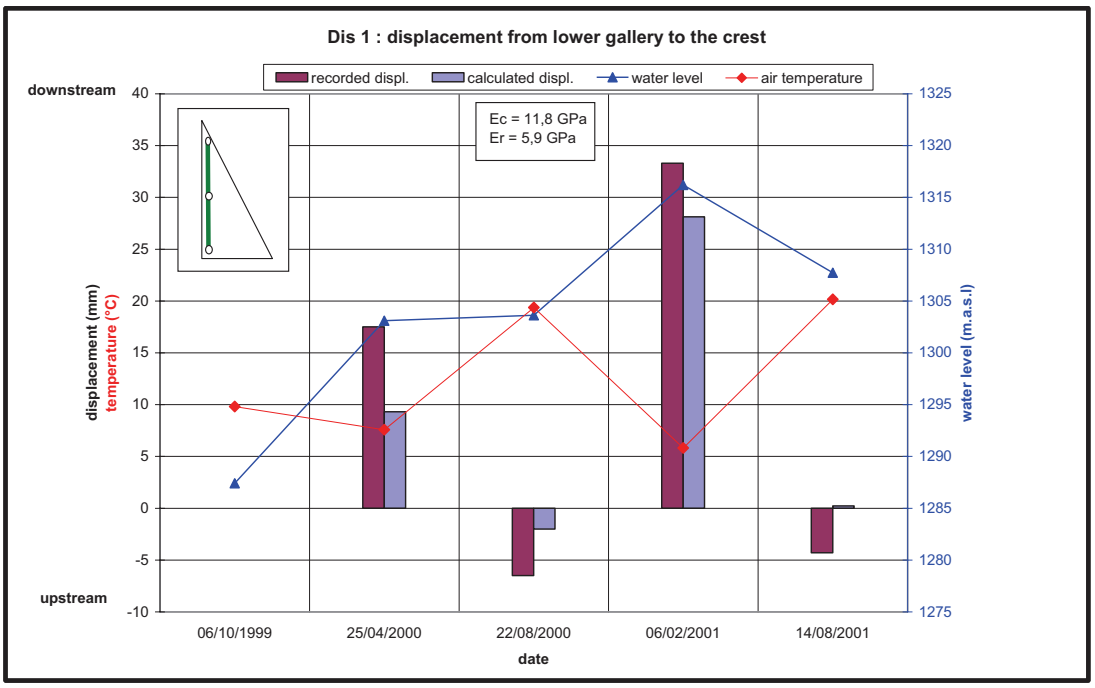

Figure 12: Comparison between recorded and calculated displacements Dis1

The differences between the recorded and the calculated values may be explained by the approximation in the thermal loads. We already mentioned the fact that the given temperatures may be average data. Thus the applied thermal loads may not represent the real thermal effects. It can be seen in particular for the displacements from lower gallery to the crest on the 25th of April when the temperature is far away from Stucky's temperatures.

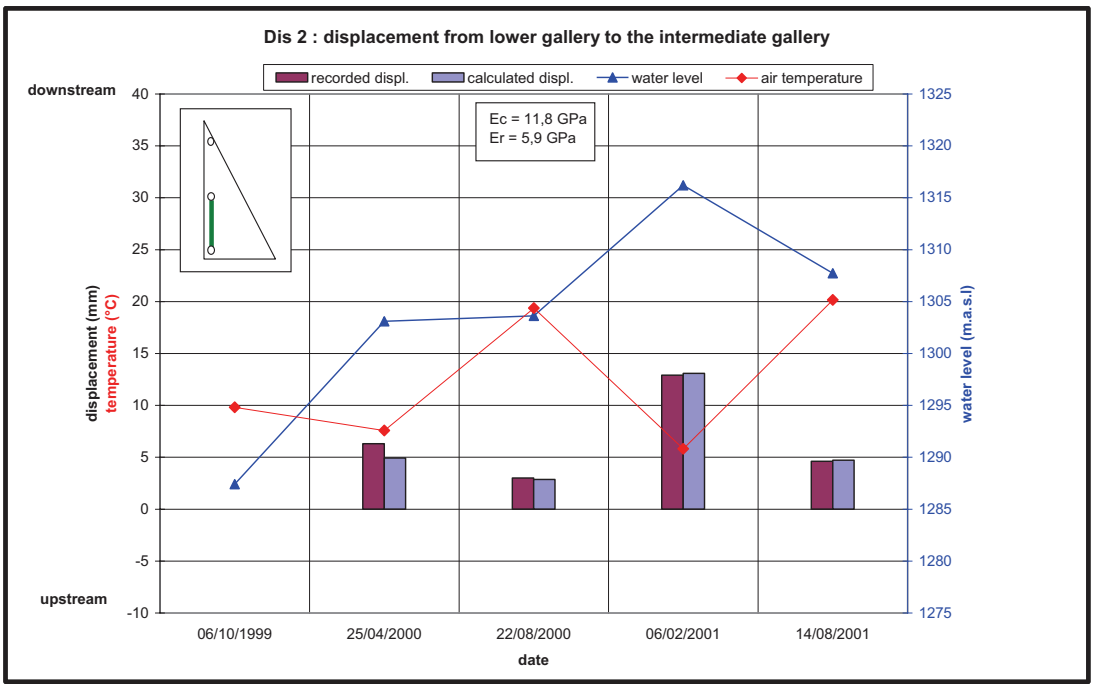

Figure 13: Comparison between recorded and calculated displacements Dis2

With the adjustment of mechanical parameters, the standard deviation decreases from 6.7mm to 5.1mm. This new model is 23.9 % better than the other one calculated in Part one.

For Dis2, The standard deviation of the difference between recorded displacements and calculated displacements become as low as 0.6 mm, which correspond to an improvement of the model calculated in Part one equal to 63.7%.

The model of Dis2 is better than the one of Dis1. This could be explained by the fact that the lower part of the dam is less sensitive to thermal loadings, which are not well-known.

The following graphics show the effect of parameters adjustment on the calculated displacements.

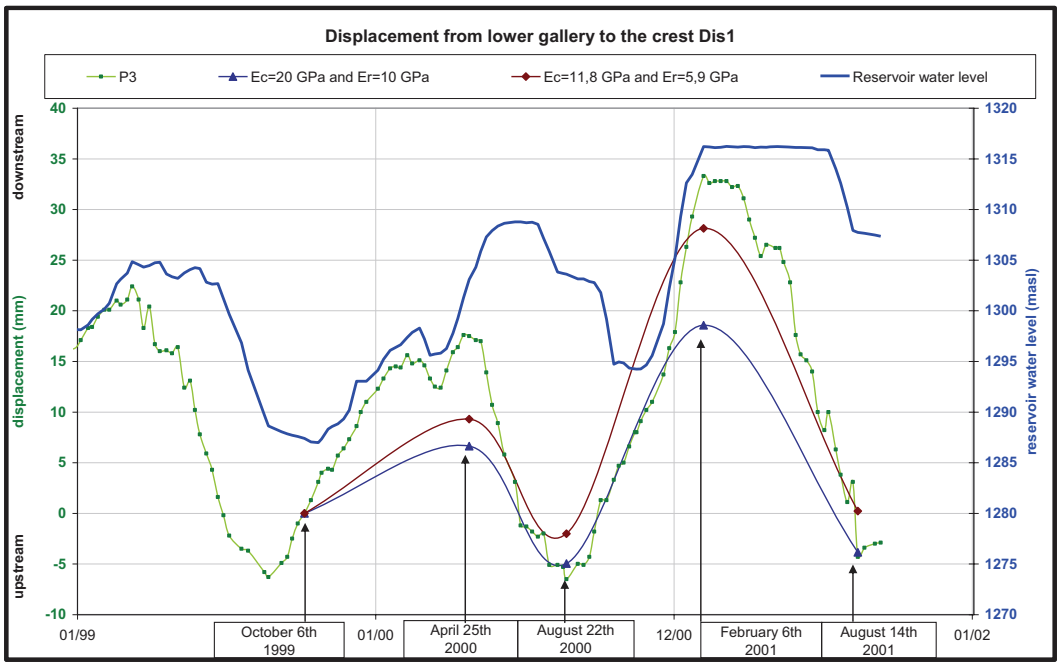

Figure 14: Comparison between Dis1 calculated in part 1 and Dis1 calculated in part 2

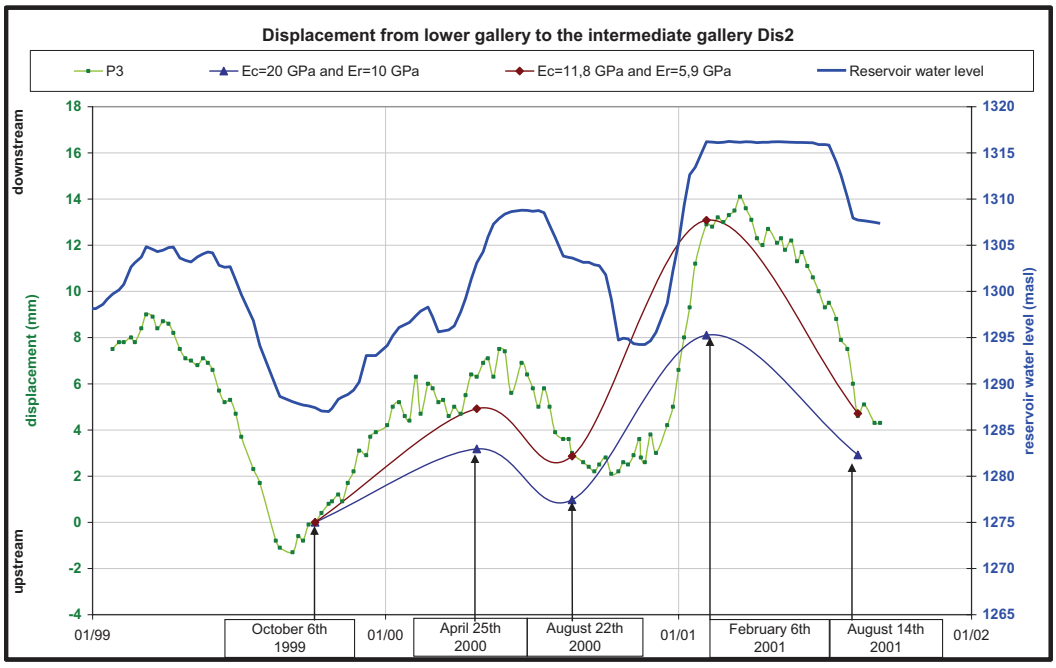

Figure 15: Comparison between Dis2 calculated in part 1 and Dis2 calculated in part 2

So the dam has a more flexible behaviour than the behaviour corresponding to the supposed material mechanical properties. The real amplitude of movements of this arch-gravity dam can be modelled only with an important increase of the dam flexibility i.e with an important decrease of his concrete Young modulus (Ec=11.8 GPa). A non-linear phenomenon may appear in the behaviour of La ACENA dam and be responsible for this increase of flexibility.

This unexpected high global deformability may be due to the opening of joints between blocks of the dam. The opening of these joints can involve an additional displacement, which drops down the general Young modulus of the dam. The consequence is that the dam behaves like a more flexible dam.

A particular monitoring of these joints at different levels should be able to clarify whether there is physical evidence of this assumption, or not.

The best model is obtained with a very deformable Foundation characterized by rock Young modulus equal to 5.9 GPa. According to the geological map given by the Formulator the most important part of the foundation of LA ACENA Dam is composed of banded and glandular gneiss. The Young modulus of the foundation (Er = 5.9 GPa) seems too small for this type of material, except if the foliation or fracturation of the foundation rock is high. A geological inspection of the foundation should validate or refute this other assumption.

So, two phenomenons can be formulated together in order to explain the behaviour of LA ACENA arch gravity dam:
- A non linear explanation like the opening of vertical joints, which decreases the young modulus in dam body.
- A weakness of the foundation rock, which behaves like a very deformable rock.

CONCLUSION

For this present theme A, statistical and structural models were used together with success to interpret the behaviour of LA ACENA arch-gravity dam.

The structural model completed the statistical method. It allowed the adjustment of material properties in order to characterize the increase of dam flexibility. This model allowed to explain the non-linear behaviour of LA ACENA dam but it can not be used alone to describe the non linear phenomenon, maybe due to the opening of joints under exceptional hydrostatic loads and due to the high deformability of the foundation rock. A monitoring and a precise investigation into the displacements of joints and foundation are necessary to complete and to understand perfectly the non-linear response of LA ACENA arch-gravity dam. The return to the statistical method would be able to help the monitoring of these joints.

The statistical method and the structural method must be used together in order to do a complete analysis of an arch dam, each one having a precise role. The first one described the correlations between measurements and hydrostatic, seasonal, time parameters and the second one was used to adjust the mechanical properties to the observed dam movements and to explain the specific dam behaviour.

REFERENCES

[1] A.Stucky, “Thermal problems about dams construction” (“problèmes thermiques posés par la construction des barrages reservoirs”)

[2] A.Carrère, M.Colson, B.Goguel, C.Noret, “Modelling: a means of assisting interpretation of readings” (“la modélisation : outil d’aide à l’interprétation des mesures), Q78 R 63 20th ICOLD Congress, Beijing 2000.

[3] E. Bourdarot, A.Carrère, L.Mei, M.Hoonaker “Combined Contributions of monitoring and modelling for the analysis of dam behaviour” (“Apports combines de l’auscultation et de la modélisation pour l’analyse et la comprehension du comportement du barrage“) Q78 R64 20th ICOLD Congress, Beijing 2000.

[4] J.L.Seraphim, R.W. Clough, “Arch dams”, chapter 18: observed and interpreted linear and non linear behaviour.

APPENDIX

Presentation of the Hydrostatical-Seasonal-Time method (HST)

Output of the software CONDOR for the displacement Dis1 from lower gallery to the crest

Output of the software CONDOR for the displacement Dis2 from lower gallery to the intermediate gallery

Presentation of COQEF mesh program

Calculated displacements (Ec = 11.8 GPa and Er = 5.9 GPa)

Presentation of the Hydrostatical-Seasonal-Time method (HST)

Electricité de France (EDF) originally developed the statistical method HST more than thirty years ago, in order to monitor the largest French dams.

The HST method is used by the means of readings of instruments installed on the dams to:
- appreciate reversible behaviour of the dam (linked to the reservoir level and seasonal parameter corresponding to the thermal effects and the effects of seasonal rains on the dam),
- qualify the scatter of readings,
- detect and describe significant time evolution in the dam.

To qualify the effects of each parameters on the dam behaviour independently, the raw measurement collected from instruments is separated into one-variable functions through a multi linear regression.
So the raw measurement (MR) is modelled by the following expression:

$MR = f(Z) + g(S) + h(T) + R$

Where Z is the normalised reservoir level ($Z = \frac{Max(WL) - WL}{Height}$), S the seasonal parameter (rounded from 0 at January 1st to 360 at December 31st), T the time and R the residual or unexplained divergence)

The corrected measurement MC is obtained by subtracting reversible effects (hydrostatic and seasonal effects) from the raw measurement:

$MC = MR - f(Z) - g(S) = h(T) + R$

Scatter in raw and corrected measurements are characterized by the standard deviations (VaB and Vac) of these readings from their mean values. These standard deviations are involved in the definition of the global coefficient of correlation CgC (specially used by statisticians) and of the global coefficient of explanation CgE (dear to engineers). These coefficients prove the quality and the validity of the model. Their expression is the followings:

$$CgC = \sqrt{1 - \left(\frac{VaC}{VaB}\right)^2} \quad \text{and} \quad CgE = 1 - \frac{VaC}{VaB}$$

The linearly-varying global coefficient of explanation is easier to understand than the global coefficient of correlation. It represents directly the part of variations in raw measurements that can be explained by the created model.

The width of the band of scatter of the raw and corrected measurements can be expressed by 5 corresponding standard deviations. In fact 95% of the readings are located in this band equal to ± 2.5 standard deviations.

This HST method allows a quick diagnostic of a measurement by comparing its corrected value with the previous corrected values. If the residual for this reading is within ± 1 residual standard deviation band, the reading is considered as “normal”. If it is between ± 1 and ± 2.5 residual standard deviations, the reading is deemed to be “doubtful but acceptable”. Outside this range, all readings are defined as “abnormal”.

This quick diagnostic makes it possible to check immediately if the anomaly is due to an erroneous reading, to a problem with a spatially isolated instrument or groups of instruments or due to a more serious reason like a significant time drift in the dam behaviour. Also the

method HST allows knowing whether this time drift deviation gets larger over time and generate a new model including the discovered time effects.

Coyne-et-Bellier has developed the software CONDOR, which proposes a user-friendly interface for HST-method.

Output of the software CONDOR for the displacement Dis1 from lower gallery to the crest

Coyne et Bellier
Bureau d'Ingénieurs Conseils

La Acena arch gravity Dam
displacement recorded by direct

CONDORpc version Windows
interprétation de l'auscultation

Grandeur Dis1 (mm, déplacement haut à bas)

Modèle HST actif du 01/06/2007 16:49:46

Données

Nombre de séries de mesures valides utilisées : 343
Date de la première série : 03/01/1996
Date de la dernière série : 11/09/2001
Durée de la période : 5,69 années

Résultats statistiques

Ecart-type des mesures brutes:	EctB = 11,415 mm
Ecart-type des écarts avec le modèle:	EctC = 2,795 mm
Coefficient global de corrélation:	CgC = 0,970
Coefficient global d'explication:	**CgE = 75,5 %**
Amplitude maximale des déplacements dus à l'effet saisonnier:	25,897
Amplitude maximale des déplacements dus à l'effet hydrostatique (sur variation de 10 m):	7,968

Formulation du modèle

					Coefficients de Student-Fisher	Coefficients de participation
Dis1 (mm)		=	29,9945			
+	Z	*	-44,2689	} *correction*	31,530	26,880
+	Z²	*		} *selon la*		
+	Z3	*		} *cote de*		
+	Z4	*		} *retenue*		
+	(1-CosS)	*	-9,8886	} *correction*	42,710	27,000
+	SinS	*	8,3575	} *selon*	35,210	38,970
+	Sin²S	*	0,5992	} *la*	1,370	0,246
+	SinS.CosS	*	-4,5114	} *saison*	10,620	0,907
+	T/Tbt	*		} *correction*		
+	(T/Tbt)²	*		} *selon le*		
+	Exp(-T/Tbt)	*		} *long terme*		
+	{ D>=DDM }	*		} *terme de marche*		

Constantes de la formulation

Zphe = 1316,500
Tbt = 1 (en années)
DDM =
Hbr = 63,500
Dinit =

Notations

Z : creux relatif: (0 = plein, 1 = vide), calculé par la formule: Z=(Zphe-H)/Hbr ,avec
. Zphe : cote des plus hautes eaux, et
. Hbr : hauteur du barrage,
H : cote de la retenue lors de la mesure courante,
S : saison, comptée de 0 au 1er janvier à 360 au 1er janvier suivant,
T : temps en années à partir de la date initiale Dinit (correspondant ou non à la mise en eau),
Tbt : constante de temps,
DDM : date de marche à partir de laquelle la correction du terme "de marche" est appliquée,
D : date (et heure) de la mesure courante.

Mesures corrigées en H et en S, et modèle temporel

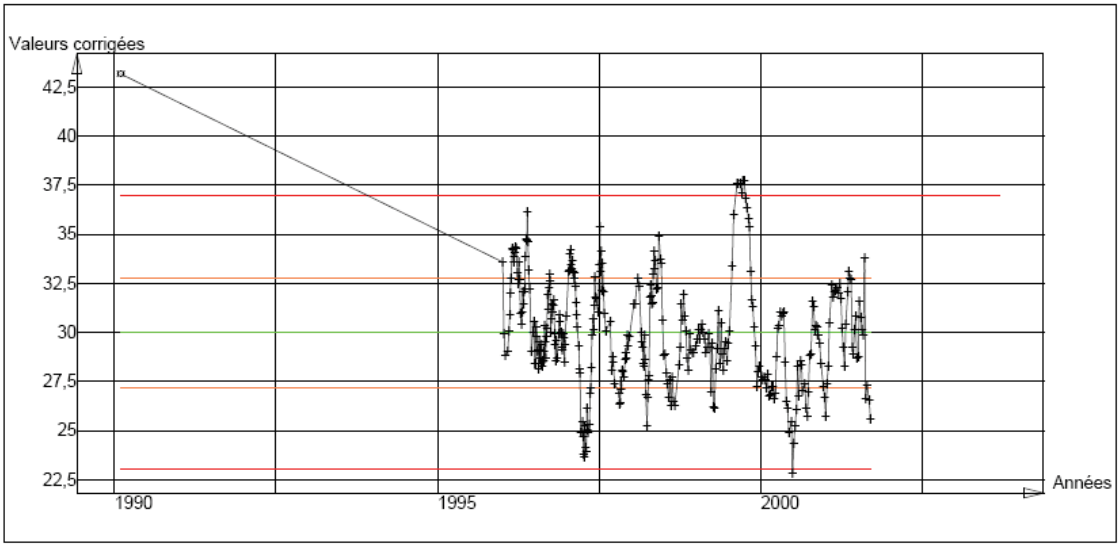

Correction saisonnière

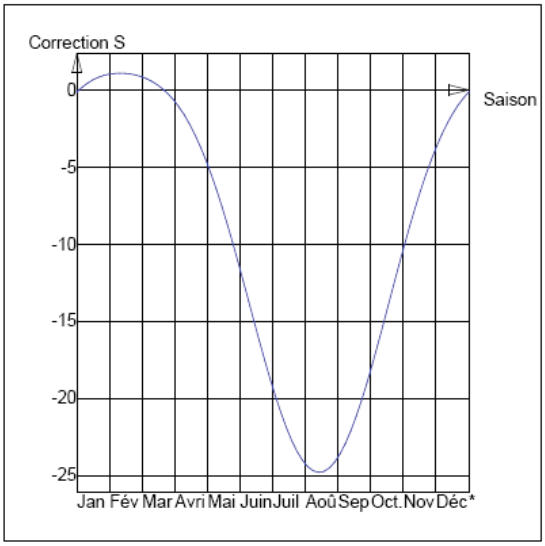

Correction hydrostatique

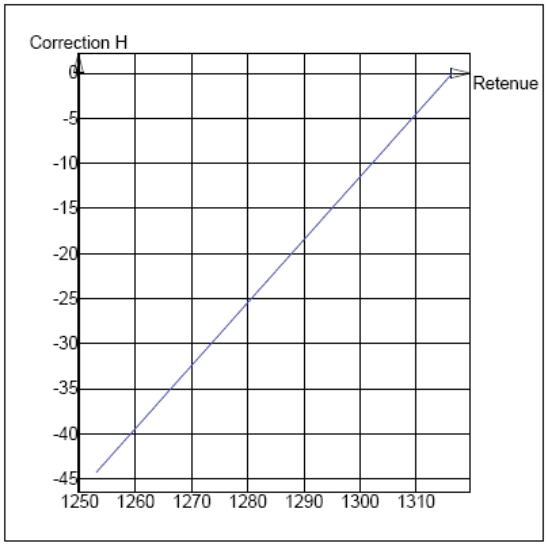

Output of the software CONDOR for the displacement Dis2 from lower gallery to the intermediate gallery

Coyne et Bellier
Bureau d'Ingénieurs Conseils

La Acena arch gravity Dam
displacement recorded by direct

CONDORpc version Windows
interprétation de l'auscultation

Grandeur Dis2 (mm, déplacement moyen à bas)

Modèle HST actif du 01/06/2007 16:50:29

Données

Nombre de séries de mesures valides utilisées : 129
Date de la première série : 26/01/1999
Date de la dernière série : 11/09/2001
Durée de la période : 2,63 années

Résultats statistiques

Ecart-type des mesures brutes:	EctB = 3,749 mm
Ecart-type des écarts avec le modèle:	EctC = 0,826 mm
Coefficient global de corrélation:	CgC = 0,975
Coefficient global d'explication:	**CgE = 78,0 %**
Amplitude maximale des déplacements dus à l'effet saisonnier:	4,420
Amplitude maximale des déplacements dus à l'effet hydrostatique (sur variation de 10 m):	3,951

Formulation du modèle

					Coefficients de Student-Fisher	Coefficients de participation
Dis2 (mm)	=	11,9388				
+	Z *	-21,9494	}	*correction*	31,680	71,680
+	Z² *		}	*selon la*		
+	Z3 *		}	*cote de*		
+	Z4 *		}	*retenue*		
+	(1-CosS) *	-1,2780	}	*correction*	10,660	-1,841
+	SinS *	1,7878	}	*selon*	14,540	25,460
+	Sin²S *		}	*la*		
+	SinS.CosS *	-0,6379	}	*saison*	3,085	-0,163
+	T/Tbt *		}	*correction*		
+	(T/Tbt)² *		}	*selon le*		
+	Exp(-T/Tbt) *		}	*long terme*		
+	{ D>=DDM } *		}	*terme de marche*		

Constantes de la formulation

Zphe = 1316,500
Tbt = 1 (en années)
DDM =
Hbr = 63,500
Dinit =

Notations

Z : creux relatif: (0 = plein, 1 = vide), calculé par la formule: Z=(Zphe-H)/Hbr ,avec
. Zphe : cote des plus hautes eaux, et
. Hbr : hauteur du barrage,
H : cote de la retenue lors de la mesure courante,
S : saison, comptée de 0 au 1er janvier à 360 au 1er janvier suivant,
T : temps en années à partir de la date initiale Dinit (correspondant ou non à la mise en eau),
Tbt : constante de temps,
DDM : date de marche à partir de laquelle la correction du terme "de marche" est appliquée,
D : date (et heure) de la mesure courante.

Mesures corrigées en H et en S, et modèle temporel

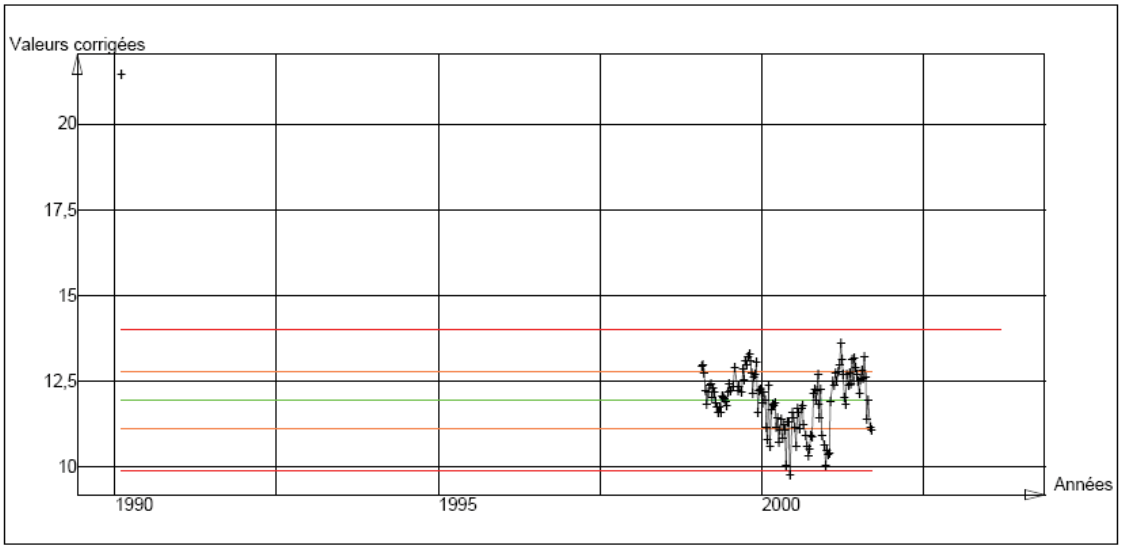

Correction saisonnière

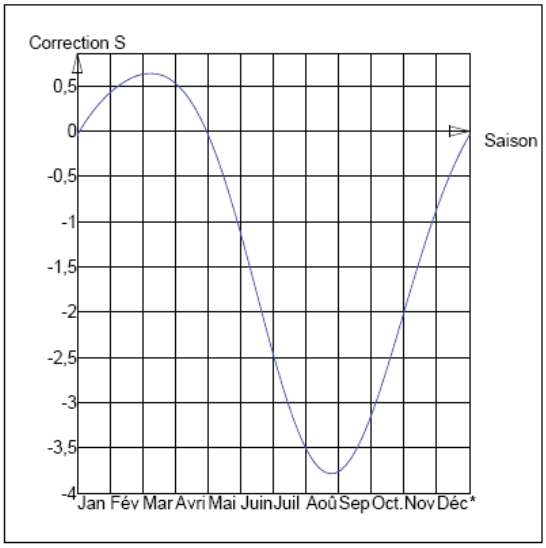

Correction hydrostatique

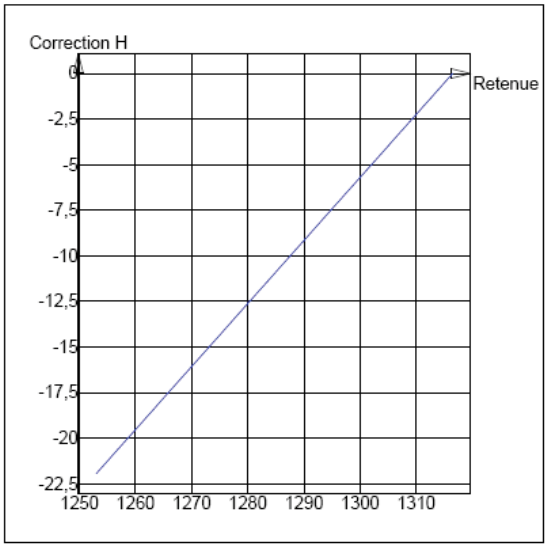

Presentation of COQEF mesh program

COQEF was developed by Coyne-et-Bellier for implementation of arch dams calculations by using finite element method. Dam body is modelled with thick shell elements. These elements can be either rectangular or triangular to describe the dam body and the foundation is made up with VOGT elements.

COQEF builds a quick mesh of arch dams with only 5 input data. These data are expressed as a polynomial function with the variable z corresponding to the vertical level. This polynomial represent the following geometric data:

- Distance of crown cantilever centre line from setting out line

- Polar radius
- Angle of logarithmic spiral
- Half thickness of horizontal arch at crown cantilever
- Increase of half thickness of horizontal arch with the curve length

This mesh gives immediately a very good approximation of the dam shape.

In the framework of this exercise, a mesh was already provided by the formulator. So the authors built the COQEF mesh of La Acena dam by selecting nodes from the given file JOINTS.txt

The input data are the coordinates of every upstream and downstream node. COQEF use quadratics finite elements. So there are medium nodes on arcs and on cantilevers between nodes located at the intersection of arcs and cantilevers. Each cantilever has two more nodes than the previous cantilevers from abutment to the crown. Considering this fact, the program will calculate the number of built cantilevers.

The elements are definitively constructed by calculating the curvilinear coordinates of nodes, by their thickness from nodes coordinates, then by joining nodes and finally by associating to these elements a material and its mechanical properties (Young modulus, Poisson's ratio).
With this program, the dam mesh can be drawn by TRACEF3, which is a program compatible with the COQEF code.

Then, combinations of loads (hydrostatic pressure, thermal load and dam weight) can be applied to this created structural model in order to calculate the stress and the displacement in the structure.

The mesh of La Acena arch-gravity dam, using COQEF code, is represented on the following pictures:

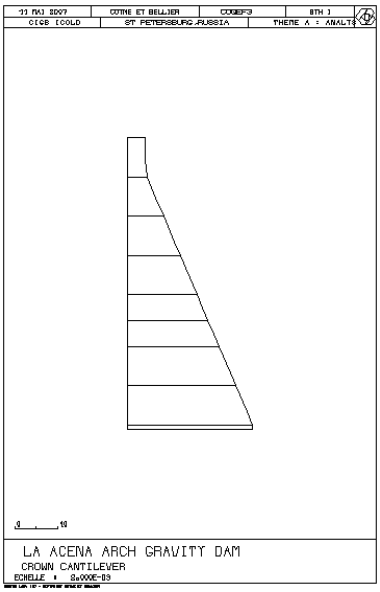

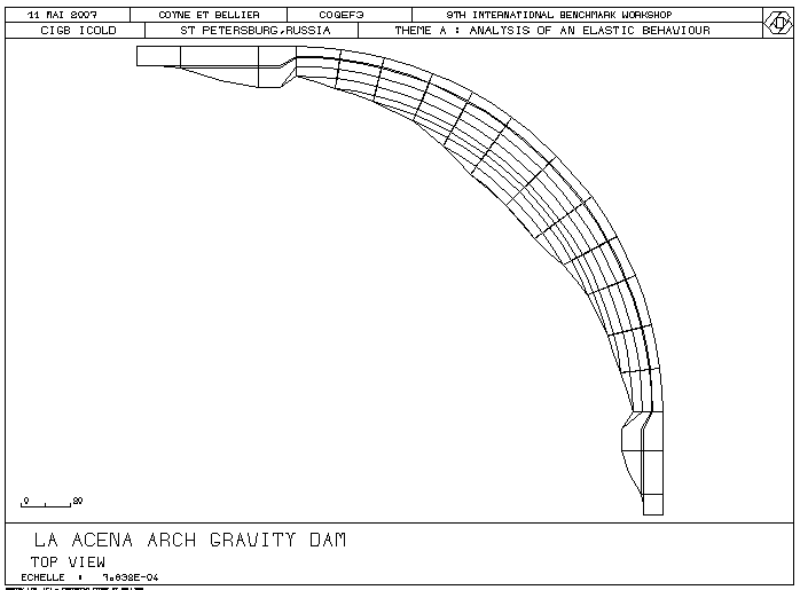

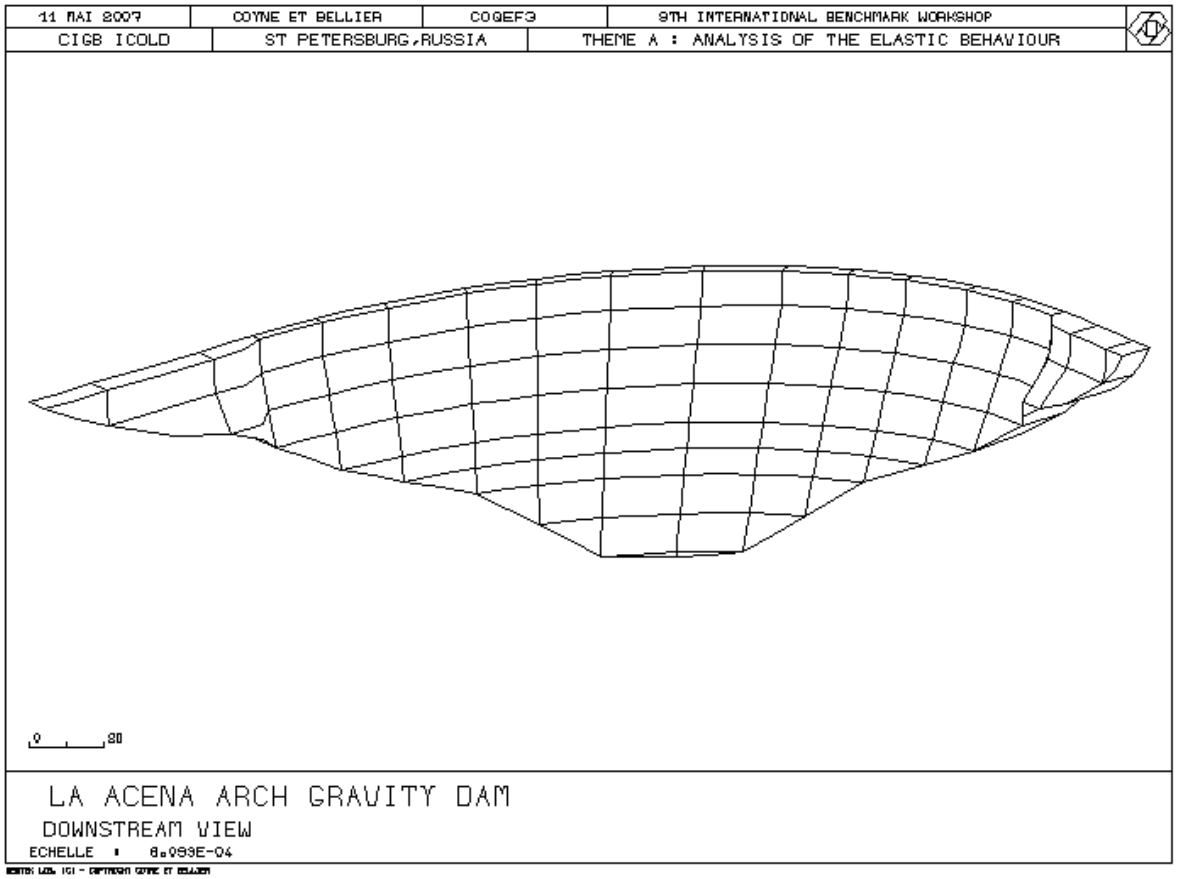
11 MAI 2007
COYNE ET BELLIER
COQEF3
9TH INTERNATIONAL BENCHMARK WORKSHOP
CIGB ICOLD
ST PETERSBURG,RUSSIA
THEME A : ANALYSIS OF THE ELASTIC BEHAVIOUR
0
80
LA ACENA ARCH GRAVITY DAM
DOWNSTREAM VIEW
ECHELLE : 8.093E-04

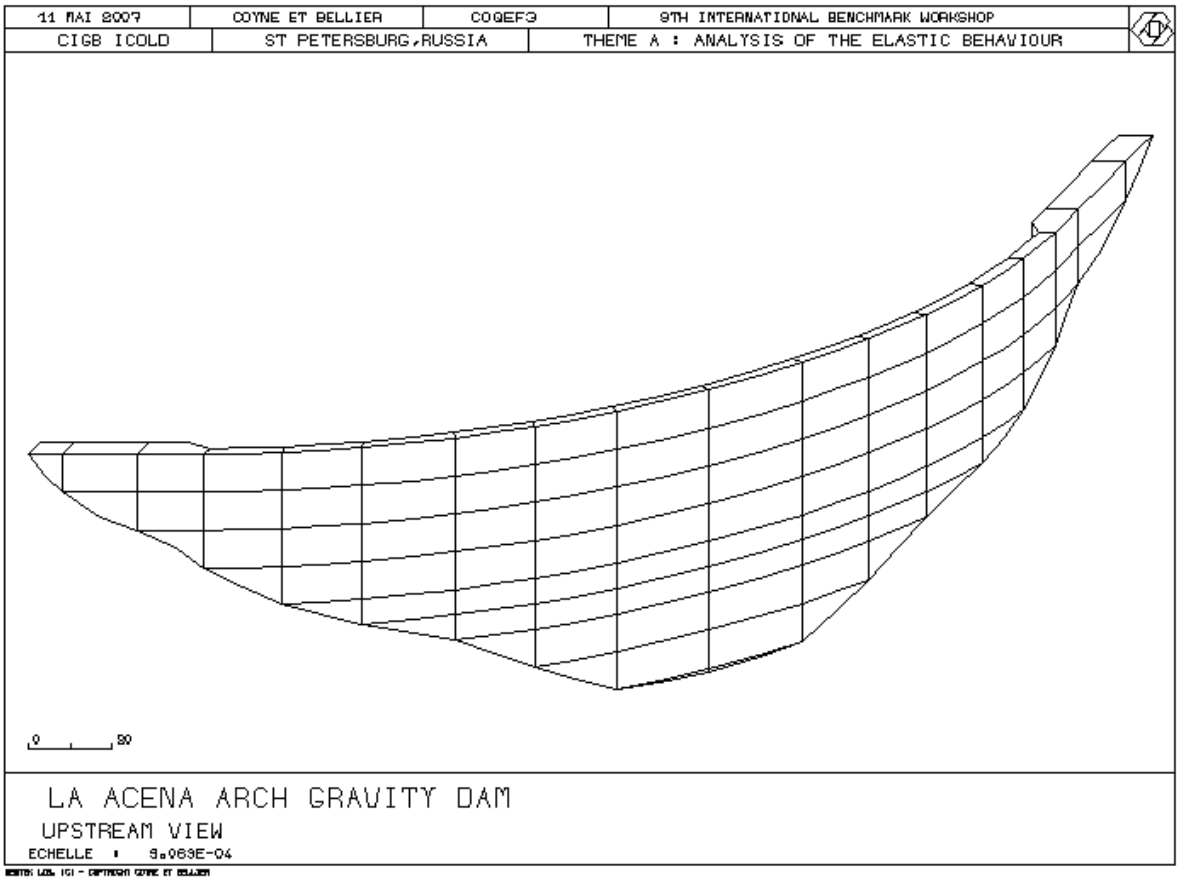
11 MAI 2007
COYNE ET BELLIER
COQEF3
9TH INTERNATIONAL BENCHMARK WORKSHOP
CIGB ICOLD
ST PETERSBURG,RUSSIA
THEME A : ANALYSIS OF THE ELASTIC BEHAVIOUR
0
80
LA ACENA ARCH GRAVITY DAM
UPSTREAM VIEW
ECHELLE : 9.063E-04

Calculated displacements (Ec = 11.8 GPa and Er = 5.9 GPa)

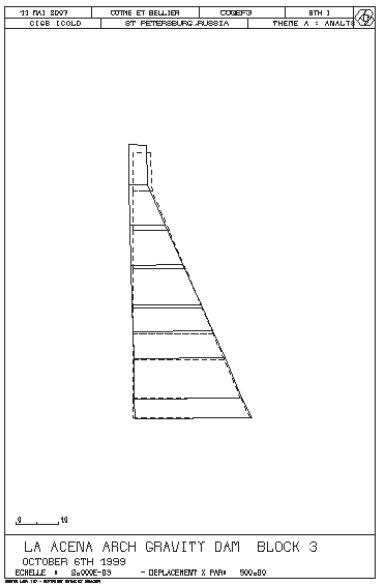

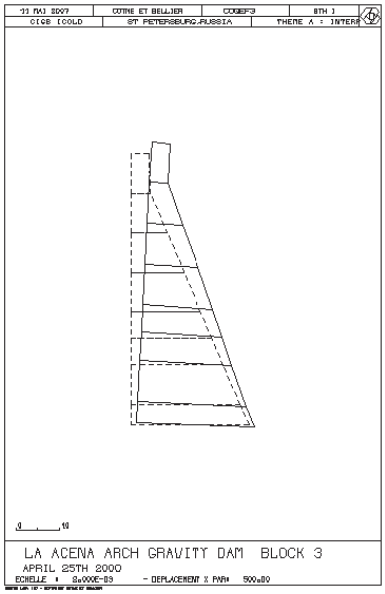

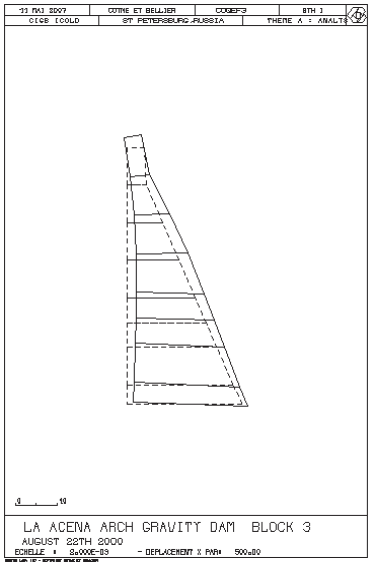

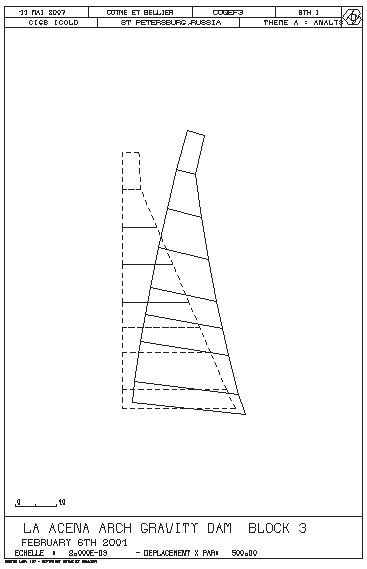

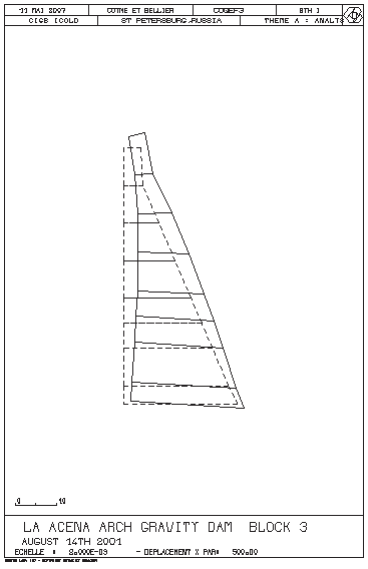

ANALYSIS OF THE ELASTIC BEHAVIOUR OF LA ACEÑA ARCH-GRAVITY DAM

Gjorgi KOKALANOV,
Professor, Faculty of Civil Eng., Skopje, Republic of Macedonia

Ljubomir TANČEV,
Professor, Faculty of Civil Eng., Skopje, Republic of Macedonia

Stevcho MITOVSKI,
Assistant, Faculty of Civil Eng., Skopje, Republic of Macedonia

1. Introduction

La Aceña dam is a large arch gravity dam, around 66 m high above the foundation, belonging to the Madrid water supply system. The main aim of this analysis is to gain data for the deformation-stress state of the dam, following the history of the behaviour of the structure (related to water level and temperature time histories), by means of numerical experiments. These data would serve for comparison with the measured results that will be followed by interpretation of the obtained data and in the end conclusions concerning the obtained results and the behaviour of the dam.

2. Description of the three dimensional numerical model of analysis

2.1 General part

The used computer software SOFiSTiK for stress-strain analyses, produced in Munich (Germany), is based on the finite element method. It has a wide range of possibilities for simulation of dam behaviour and inclusion in the analyses of all necessary fenomena, important for real simulation of the dam behaviour, such as: an automatic discretization of the dam body taking into account the iregularities in the geometry of the dam base, application of different constitutive models for materials, simulation of the dam body construction and reservoir filling in increments, and so on. The program has rich possibilities for presentation of the output results. In our work, mainly plane graphical presentation was used, showing the output results in the main cross sections, as well as in longitudinal section.

2.2 Discretization of the dam body

Using the given data 3-dimensional (3D) mathematical model of the dam was build. The given data didn't suit the SOFiSTiK format, and Visual Basic computer program was written. The program transformed the receiving data in appropriate format. In other to simulate the construction stages, the body of the dam was built in 23 increments. Every layer was approximately 3m high. Fig. 1 shows the general view of the dam body together with the surrounding rock foundation.

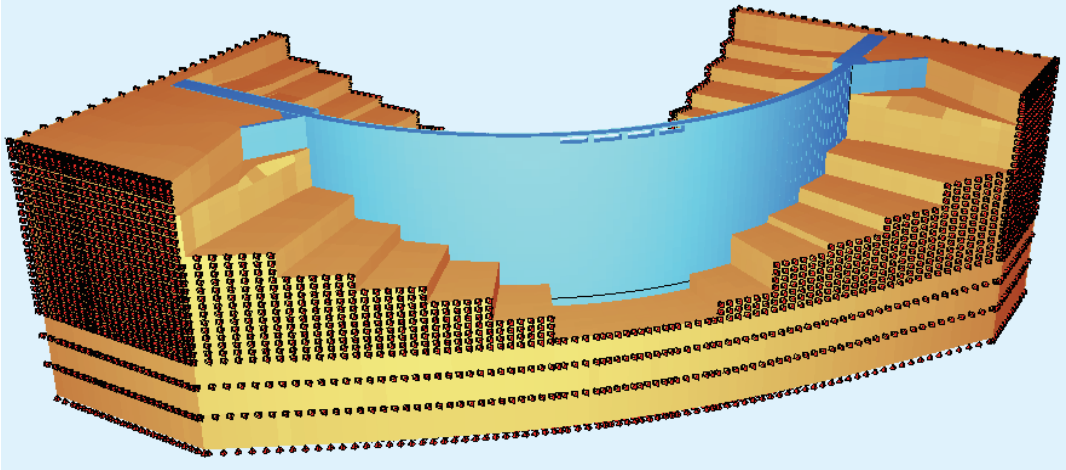

Figure 1. General view of the 3-D model of the dam-foundation system

The finite element mesh was generated using SOFiSTiK automatic mesh generator. Three types of element were used to model the dam's body: BRIC, QUAD and SPRING elements. The solid element of SOFiSTiK is the BRIC element (Fig. 2), a general six-sided element with eight nodes.

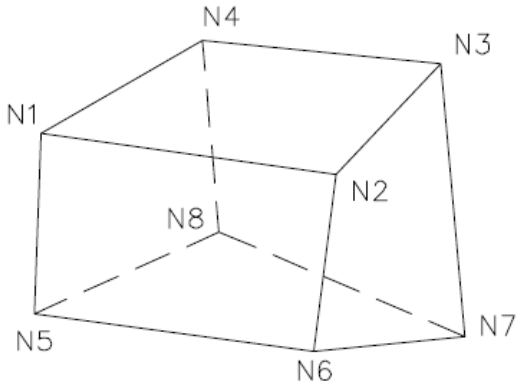

Figure 2. BRIC element

The plane element QUAD (Fig. 3) is a general quadrilateral element with four nodes. In other to simulate the behaviour of the interfaces of the dam (joints between concrete blocks, dam-foundation interaction), spring elements are introduced.

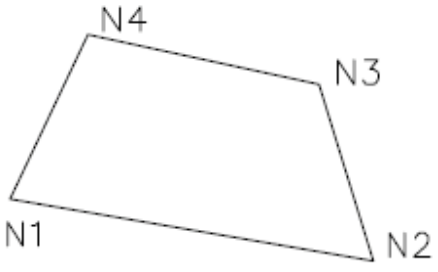

Figure 3. QUAD element

The surfaces of the BRIC element can be described by special QUAD-elements, which can also be employed for the display of stresses in BRIC-elements. The QUAD-elements are introduced in order to simplify the process of generation the water pressure loads and coupling springs between blocks.

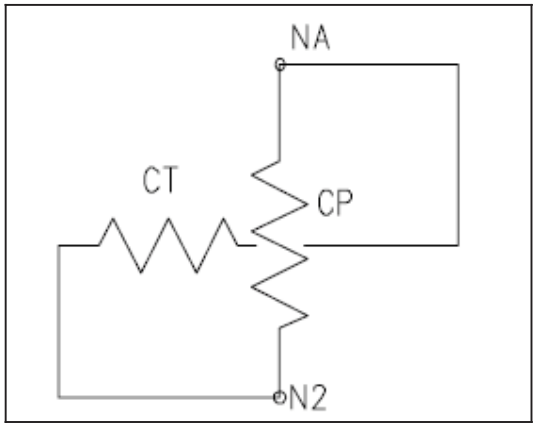

Figure 4. SPRING element

Springs can be defined as support conditions or as coupling springs between two nodes. The spring is defined by means of a principal direction and two spring constants. The spring constants CP and CT are assigned to the principal and the lateral direction, respectively. If a friction coefficient and/or cohesion are input, the lateral spring can not sustain forces greater than:

Friction_coeff. · Compressive_force + Cohesion

The element's geometry is checked by the program for node numbering order, re-entrant corners and side ratios smaller than 1:5. This complex modelling of the dam resulted in finite element mesh with 10.383 finite elements and 56.638 nodes. This talks enough of the complexity of the numerical solution and the possible difficulties that can appear during the execution.

2.3 Constitutive relationship and parameters of the materials

The choice of the parameters for the materials is one of the most important questions in the numerical analyses of dams. In this analysis linear-elastic constitutive stress-strain relationship was applied for all materials used in the model. The properties of the materials used in the analyses are given in Table 1 (according to the appendix for material data).

Table 1. Parameters of the materials applied in the numerical analyses

PROPERTY	FOUNDATION	DAM BODY
specific weight	22 kN/m^3	23.6 kN/m^3
E (Young modulus)	10000 Mpa	20000 Mpa
Poisson´s Ratio	0.2	0.2
Coef. of thermal exp. A	0	10^{-5} $^oC^{-1}$

In the second stage of the analyses some calibration of the material properties was done. The material properties were changed so the displacements in the appropriate node match the values given with the benchmark.

2.4 Loading of the dam

According to the given data, appropriate water presser and temperature loads were created. SOFiSTiK has very efficient tools for load generation. With the VOLU-statement, a loading on volumes, group of BRIC-elements or all QUAD-elements within the volume is enabled. The changes of the pressure load along tree edges are specified. All referenced elements of the group or the volume will be loaded. The selection of elements is only by a sheared cube (Fig.5), defined by three selectable directions p_1–p, p_3–p_2, p_5–p_4, which must not be collinear.

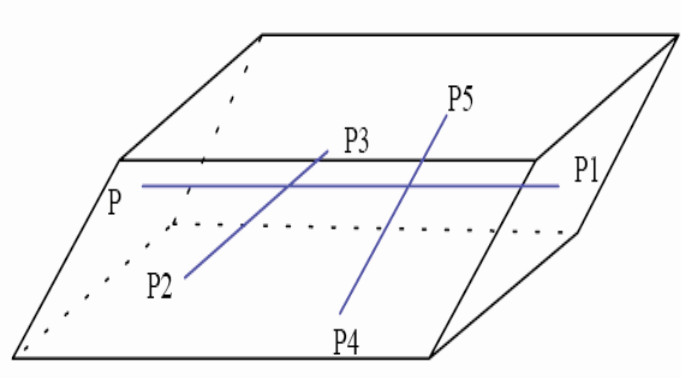

Figure 5. Sheared cube

For transfer of the water pressure loads, some QUAD elements faces the upstream of the dam's body was created (Fig.6). This elements has only geometrical values, they have no contribution on the total structure stiffness. Referencing these QUAD elements in the VALU statement cause simple transfer of the water pressure in appropriate node loads.

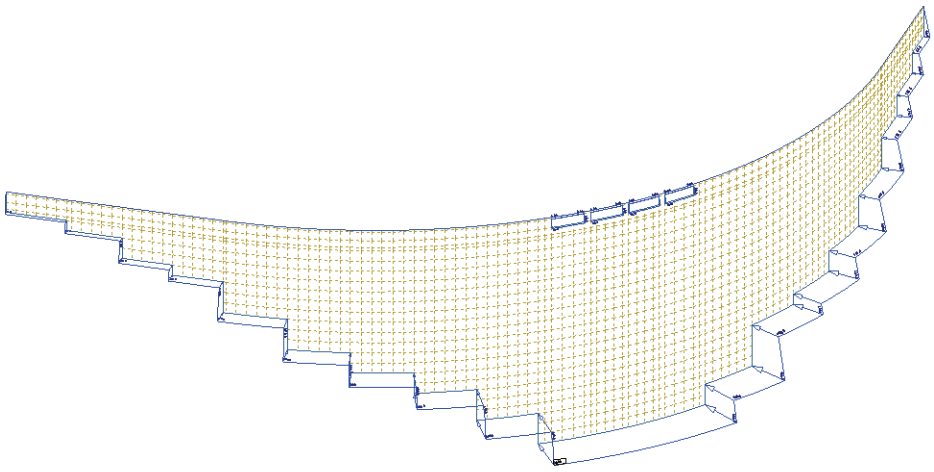

Figure 6. Water load applied on the longitudinal section of the dam

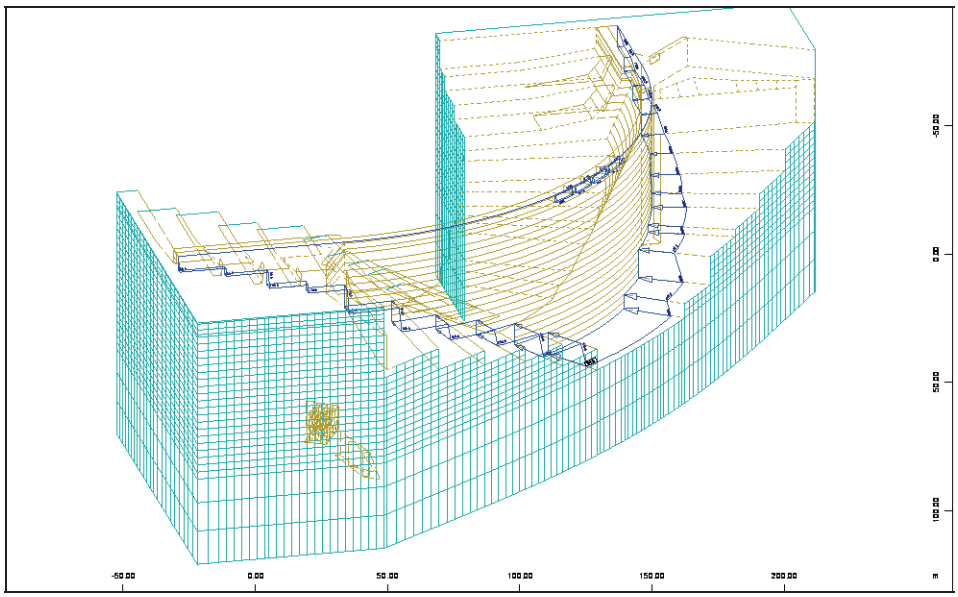

Figure 7. Water load applied on the 3-D model of the dam

The water load is applied as hydrostatic pressure in increments combined with the temperature load. Figure 7 shows the applied water load on the dam.

Previous investigations made on similar objects showed that the temperature distribution is not uniform inside the dam's body. In the core of the dam the temperature is almost uniform. Near to the faces it is dramatically changed (Fig.8a.). SOFiSTiK supported only uniform temperature in the BRIC elements. Having in mind the temperature distribution and SOFiSTiK possibility of temperature presentation, we decided to create three different zones for temperature distribution. One at the upstream side, the other at the core, and the third at the downstream side of the dam body (Fig. 8b).

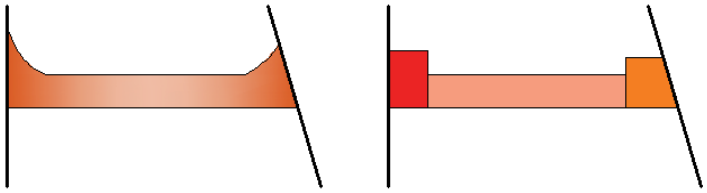

Fig. 8a. Temperature distribution

Fig. 8b. Temperature approximation

The temperature load is applied in accordance with the data from the appendix for temperature and the height of the thermometers installed in the dam body. In the intermediate part of the dam (in the BRIC elements), in dependence from the location of the thermometers, there is a steady distribution of the temperature in longitudinal direction, while in the ends of the dam upstream and downstream, there is a difference in the temperature values compared with the intermediate part because of the influence of the water and the environment. The

distribution of the temperature in one cross section is shown on Fig. 9, while Figure 10 shows the temperature distribution on the 3-D model of the dam.

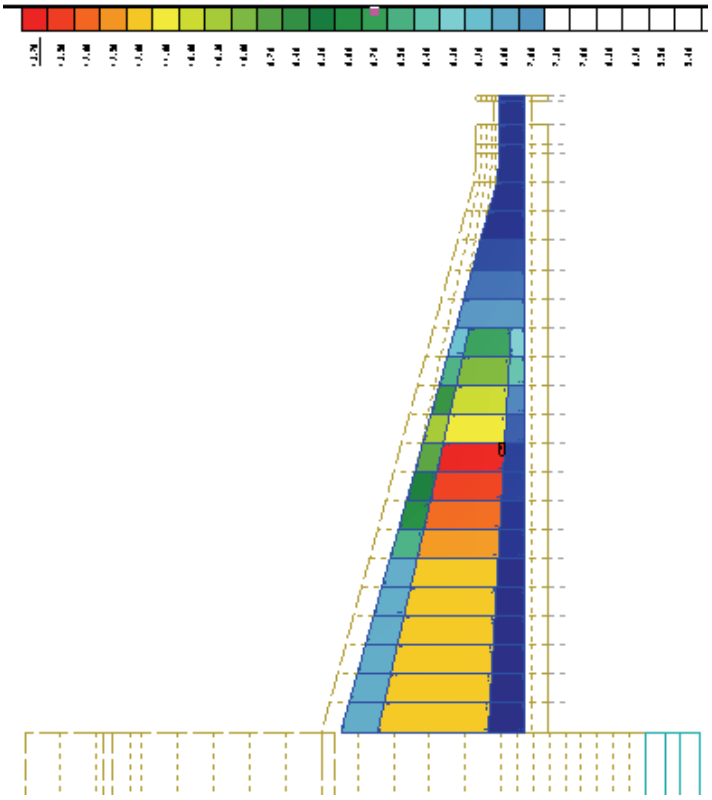

Figure 9. Temperature distribution in cross-section of the dam body

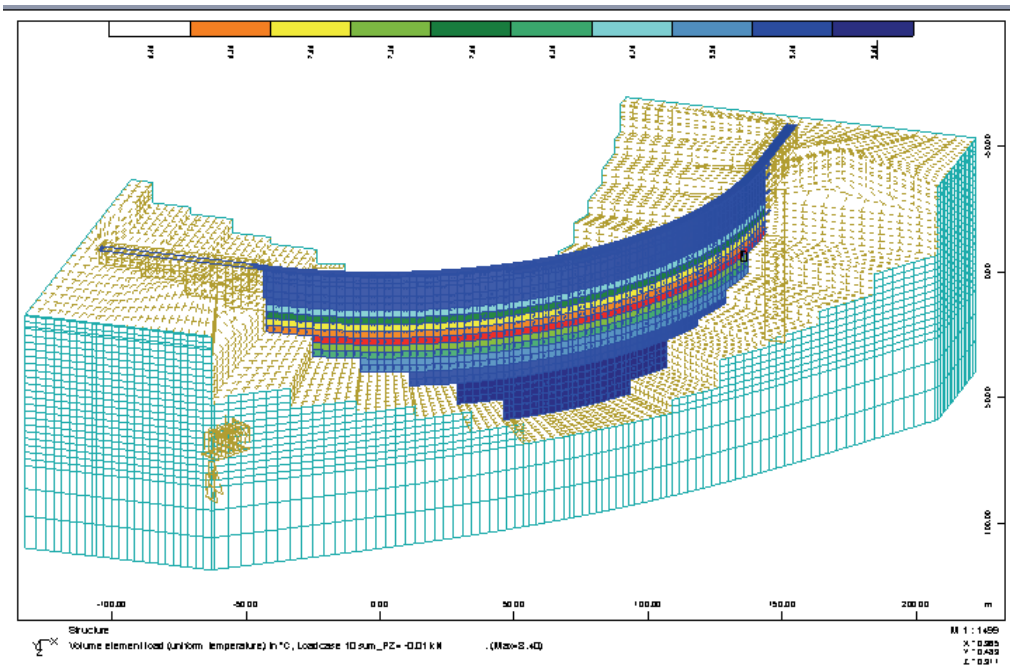

Figure 10. Temperature distribution on the 3-D model of the dam-foundation system

2.5 Analyses

The dam was analyzed on statically action of water pressure loads and temperature. The results from the analyses showed that the chosen mathematical model is to stiff. The deformations in the considering nodes were much lower than the measured ones. In our opinion the reason for this inconvenience was that the body of the dam was modelled as continuous one. In realty the dam was constructed in blocks with working joints between them. There is some sliding between blocks at the contact that make the structure more flexible. So, we decided to redesign the previous mathematical model and to create model that would have a real behaviour on the contact of the blocks. In the new mathematical model the dam's body was constructed of several blocks. Each block was built in 23 increments. The blocks were made of BRIC elements, Fig. 11. On the contact faces between blocks, distributed coupling spring elements were introduced. These springs have one longitudinal and two transversal stiffness. SOFiSTiK has very nice tool for generation of this type of springs. Two structural areas that face the block body should be generated. Simply referencing these areas and introducing the spring's properties would generate appropriate springs in the nodal points of the area.

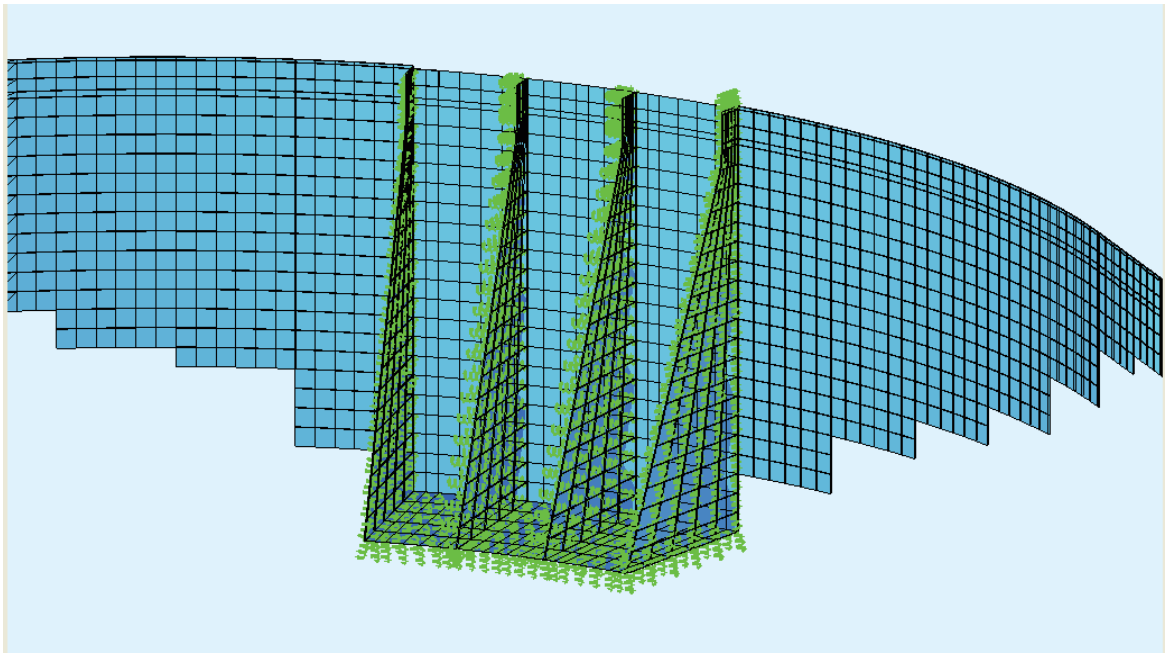

Figure 11. Distribution of the coupling springs

Similar coupling springs at the contact of the dam with terrain should be created. With introduction of the coupling springs two contact phenomenon are taken under consideration: sliding between blocks and sliding between dam and terrain. In this study case the properties of the springs were estimated by calibrations. We change the transversal stiffness of the spring until the maximum displacement in the joint match the recorded data. The longitudinal stiffness should be a large number. This large stiffness should ensure the contact of the faces of blocks. In the reality the stiffness of the springs should be taken form experimental data.

3. Results obtained from the analyses

- Using the above described methodology and parameters, the following results of the displacements were obtained:

- Due to the death load (self weight of the dam), maximum vertical settlement appears at the dam crest in the main dam cross section with the value of 7.46 mm (Fig. 12), while the maximum displacement is located in the same level, with value of 3.78 mm (Fig 13).

- The influence of the temperature changes was analysed using the data given at the beginning of the formulation of the problem. In our report only the radial displacements from temperature load for one increment, for the period 07.02.1990-24.04.1990, are given (for the longitudinal dam section), Figure 14. The maximum calculated value for this increment is 2.06 mm and is located at the dam crest. Later on, much more date concerning temperature changes and measured displacements were supplied by the Formulator, but due to limited time and complexity of the problem, it was impossible to perform completely new analyses. Namely, to satisfy all requirements and to get real results, it is necessary to simulate the construction of the dam in more increments (blocks), to apply spring elements in all joints, and, which is very important, to introduce the non-linear behaviour of the interfaces, based on the experimental data.

- The influence of the water load was analysed for the period of 72 days, in which water height in the reservoir aroused approximately from 16 to 52 m above the dam foundation. Under these conditions, the radial displacements in the dam body reached the value of 16 mm, Fig. 15 and 16. In the same time, the maximum value of the vertical displacement is slightly above 3 mm and is located at the middle of the highest dam cross section, Fig. 17. The Radial displacements for this load case are also shown on the longitudinal dam section, with the maximum value of 16.3 mm, Figure 18. This value, together with the appropriate incremental value obtained by temperature load, gives the total maximum radial displacement of approximately 18 mm, given by the Formulator of the problem. To obtain this value, we have changed previously formulated model, introducing spring elements in the middle blocks of the dam (Figure 11), with appropriate stiffness parameters, and calibrating the elasticity modulus for the concrete (it was increased by 60%).

4. Conclusions

From the performed and above described analyses, following main conclusions could be drawn out:

4.1 SOFiSTiK software is a powerful tool for complex three-dimensional stress-strain analyses of dams. It has rich possibilities for modelling of the system dam body – foundation, for application of different constitutive laws, as well as for complex load influences.

4.2 Calibrating the previously done model, using some of the advanced features of SOFiSTiK software, it was possible to explain some of the results obtained by the measurements performed in the service period of 66 m high arch-gravity La Aceña Dam, in Spain. But, to explain the complete behaviour, and to answer all questions, it is necessary to do very complex model, with simulation of the real construction procedure, introduction of all joints between concrete blocks with non-linear constitutive law, application of all loads with the real loading history, and, in the same time, calibrating the model using the measured data. In our opinion, it

is possible to fulfil these requirements, but this job requires much effort, and it is time consuming.

4.3 Despite the rapid progress of the computer techniques, to perform a three-dimensional stress-strain analysis of such a complex structure, as a dam is, it is not yet an easy task.

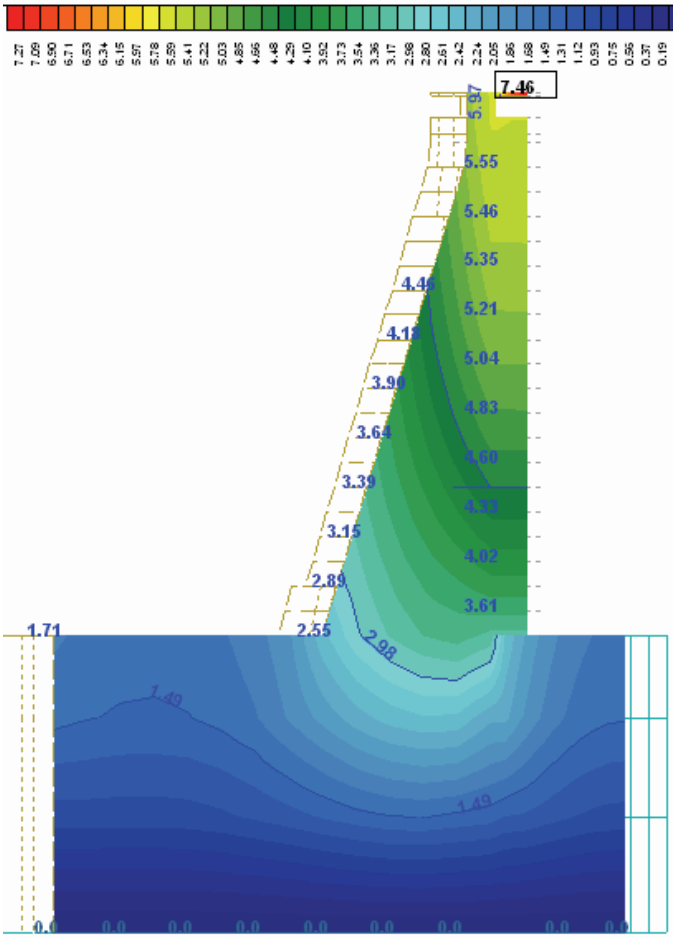

Figure 12. Vertical displacements in the main dam cross section caused by the dead load of the dam [mm], Y= (0.0 ÷ 7.46) mm

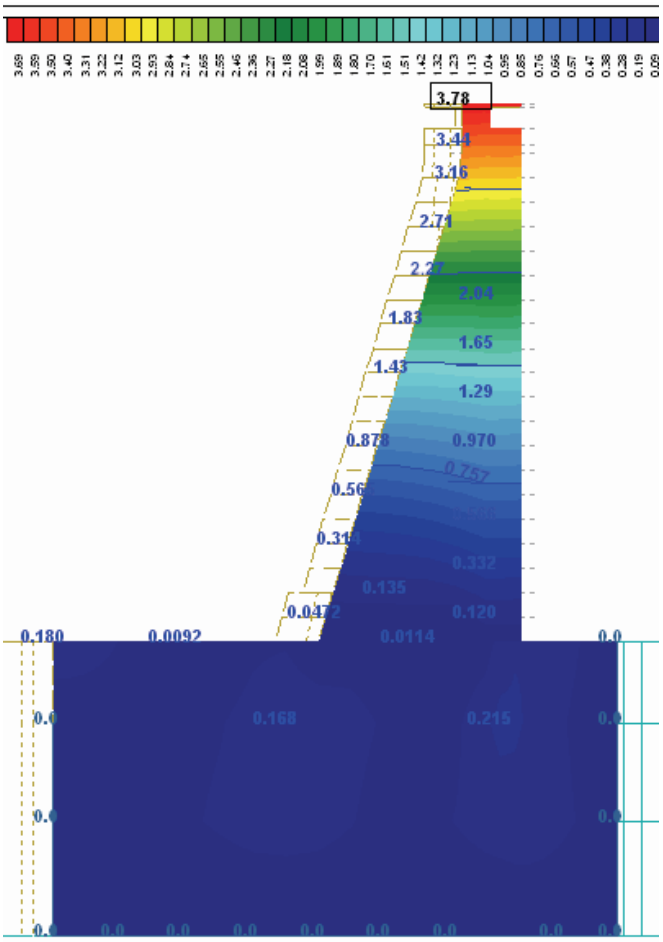

Figure 13. Radial displacements in the main dam cross section caused by the dead load of the dam [mm], R= (0.0 ÷ 3.78) mm

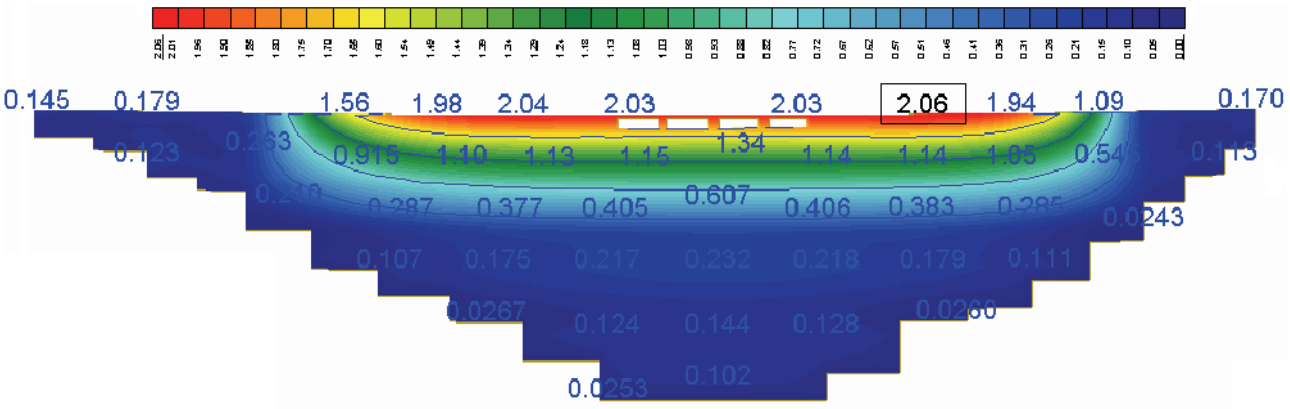

Figure 14. Incremental radial displacements from temperature load in the longitudinal dam section (for one increment, for the period 07.02.1990-24.04.1990) [mm], R= (0.0 ÷ 2.06) mm

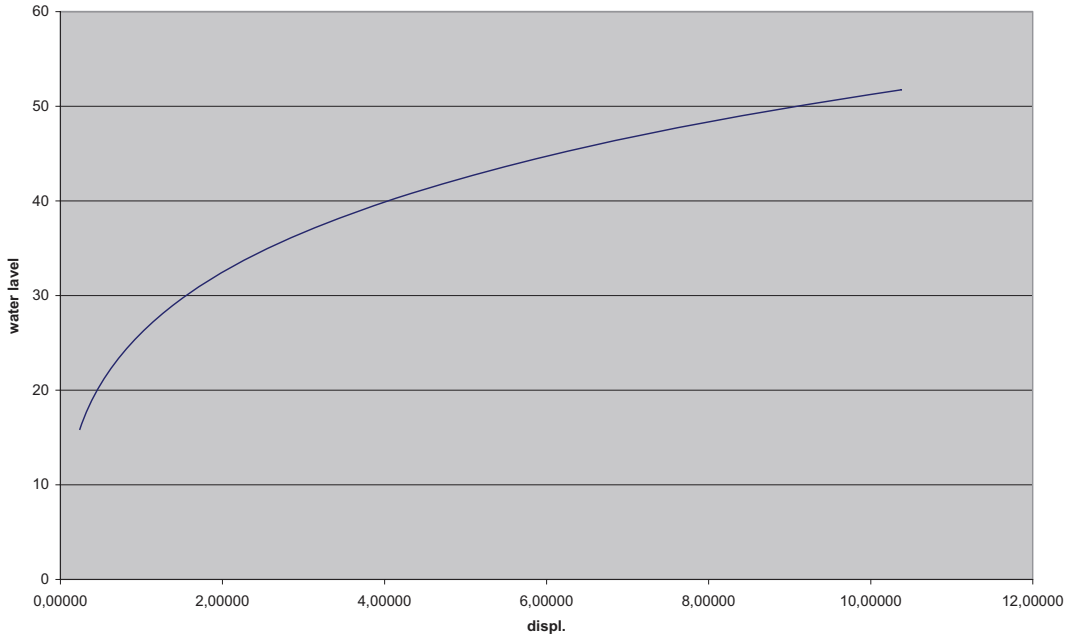

Figure 15. Values of the radial displacements in the central dam cross section depending on the reservoir water height during the period of reservoir filling. The water heights are given in meters above the foundation, the displacement in mm.

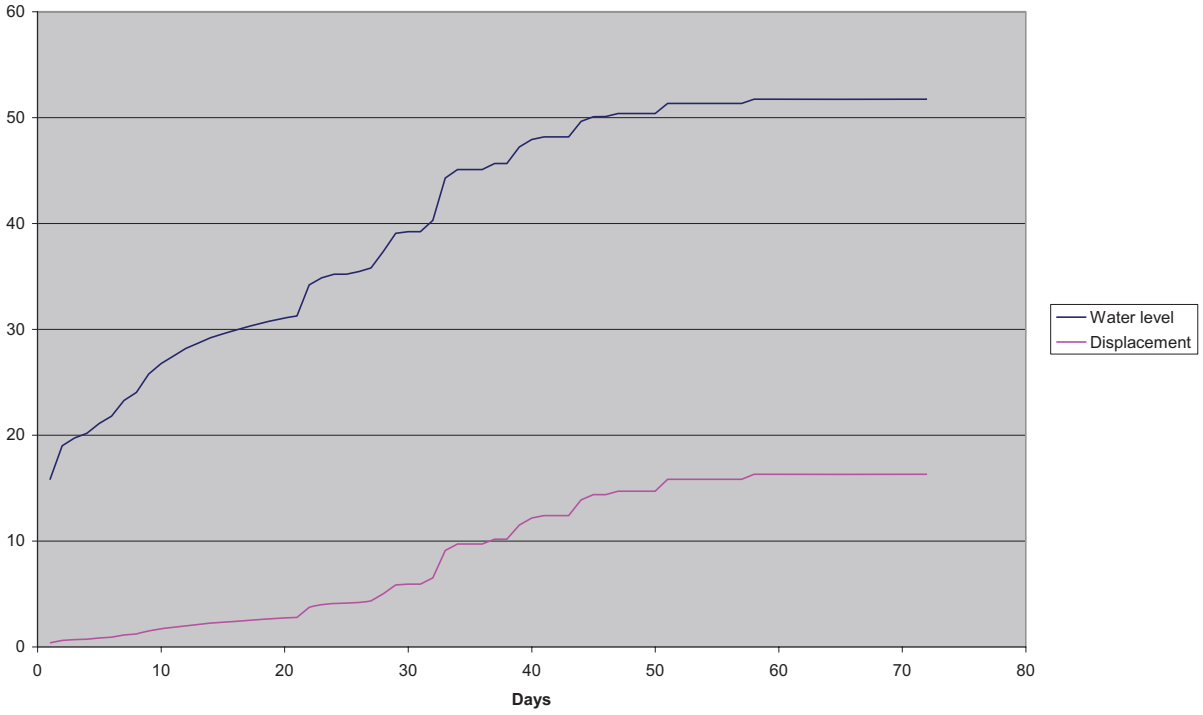

Figure 16.Values of the radial displacements in the central dam cross section depending on the reservoir water height during the period of reservoir filling in 73 days. The water height and the displacements shared the vertical axes – respectively in m and mm.

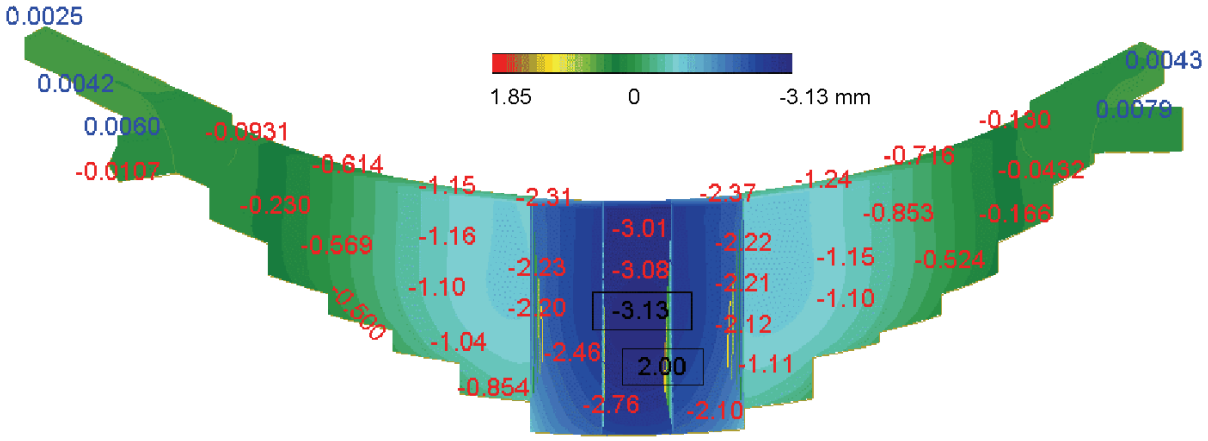

Figure 17. Values of the vertical displacements in the longitudinal dam section, caused by the water pressure during the period of reservoir filling (see Fig. 4 and 5). The values are given in mm. – means displacement downward, + upward.

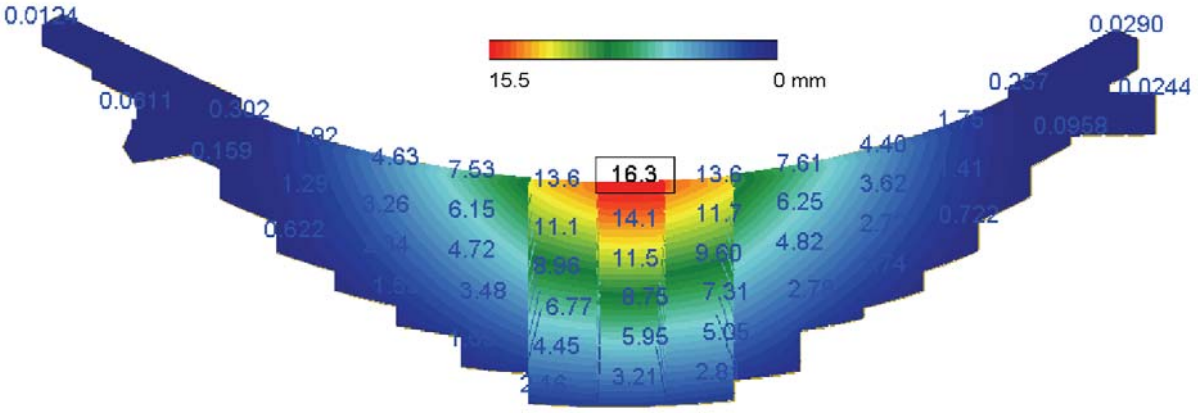

Figure 18. Values of the radial displacements in the longitudinal dam section, caused by the water pressure during the period of reservoir filling (see Fig. 4 and 5). The values are given in mm. + means displacement to downstream direction.

ELASTIC ANALYSIS OF AN ARCH-GRAVITY DAM BEHAVIOR USING MERLIN

Yoshinori Yagome
Department of Hydraulic Power Engineering, Tokyo Electric Power Service Co., Inc.
Yoshihisa Uchita
Specialist, Construction Engineering Center, Tokyo Electric Power CO., Inc.
Victor Saouma
Professor, Department of Civil Engineering, University of Colorado

SUMMARY: A Parametric study of an arch-gravity (Aceña) dam for thermal stress using Merlin is reported. We first performed a 2D and 3D thermal analysis based on the recorded dam and ambient mean monthly air temperature. Then, the determined temperatures were used for a subsequent 2D and 3D stress analysis which accounted for pool level fluctuation. Whereas we were unable to perfectly match the observed upstream response of the summer (April – September), we had a nearly perfect match with the downstream response in winter (October – March).

1. INTRODUCTION

Dam instrumentation records are essential for the evaluation of a dam behavior. However, field measurements are often tainted by uncertainties. Similarly, numerical models can be equally important to assess the dam response, and to possibly better understand the cause of experimental uncertainties. Yet, all numerical models start with an assumption, and the analysis results must be examined with great caution. Henceforth, ideally field observations and numerical analysis should go hand in hand. In this paper, we report the analysis of Aceña dam which has been assigned by the organizers of the 9th Benchmark Workshop on Numerical Analysis of Dams. When the dam was first impounded, maximum joint displacements were 1.88 mm, yet subsequent measurements with the four plumblines gave displacements of the order of 4 cm.

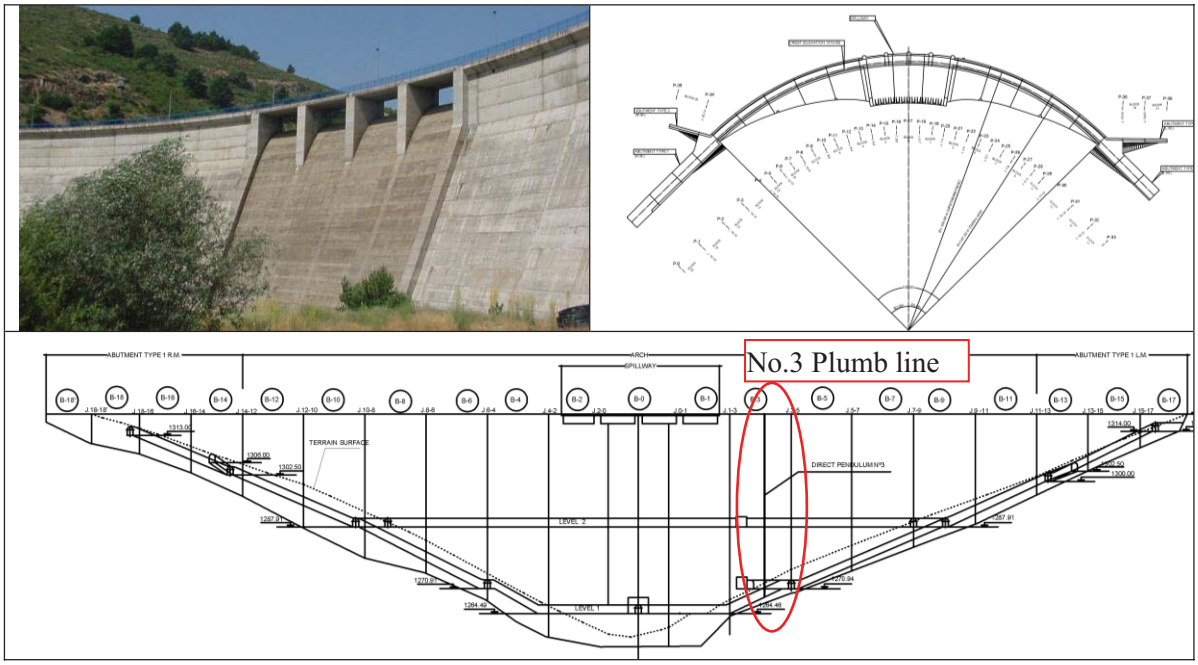

Fig. 1 Aceña Dam; Picture and Geometrical Layout

2. PROGRAM DESCRIPTION

Analysis was performed by the computer code MERLIN (http://civil.colorado.edu/~saouma/Merlin) which has been in continuous development for over 12 years. Merlin, probably one of the most sophisticated analytical tools for dam analysis, has numerous features essential for the modeling of dams. Amongst them: 2D-3D, static and dynamic, linear and nonlinear (numerous nonlinear constitutive models for fracture mechanics based discrete and smeared cracks for concrete and rock), fluid elements, automatically adjustable static and dynamic uplift pressures, sophisticated models for radiation damping, restart capabilities and ability to transfer static analysis reactions to nodal dynamic loads, possibility to incrementally modify the elastic properties, amongst others. Such an analysis could not be possible without the support of a window-based preprocessor, KUMONOSU. These interactive tools understand the "language of dams", and enable the user to discretize very complex dam geometry and boundary conditions and loads in a relatively short time. Finally, the window based graphical postprocessor enables the analysis to "data mine" the results, and efficiently extract from the analysis essential figures for a technical report. Whereas practically all the standard features of finite element post-processors are found in Spider, the program can also automatically perform the 3D deconvolution of an earthquake record, compute and display factors of safety, and can be used with any finite element code.

3. MODEL DESCRIPTION

3.1 Mesh Generation

First, KUMONOSU was used to generate the 2D and 3D meshes, based on the files supplied by the organizers, for the analyses. In the stress analysis, interface elements were used between the dam and the foundation (it was assumed that the monoliths were rigidly connected), Table 1.

Table 1 Numbers of Node and Element for each Analysis

Numbers	2D		2D with Joint		3D		3D with Joint	
	Dam	All	Dam	All	Dam	All	Dam	All
Node	864	1806	864	1882	4153	10563	4153	8950
Element	1582	3369	1582	3377	16153	52196	16163	33871
Increment	297	101	297	101	297	101	297	101
CPU time(hr)	0.1	0.5	0.1	0.5	0.5	4.0	0.5	5.0

*Note CPU spec is Pentium(R) D 3.4GHz

The Elastic Modulus of the dam body was set to 20,000 MPa, a mass density of 2.36 kN/m^3, a Poisson ratio of 0.2 and a coefficient of thermal expansion of $10^{-5}/^0$C. The rock foundation had an elastic modulus of 10,000 MPa, a zero mass density, and a Poisson ratio of 0.2. For thermal analysis, only the dam was modeled, and computed nodal temperatures were then assigned to the corresponding nodes in the stress analysis (in which the foundation was now modeled) along with the hydrostatic load.

The stress analysis was subjected to thermal load, self weight of the dam, hydrostatic and uplift pressures. For the uplift, it was assumed that the upstream pressure is equal to the corresponding hydrostatic pressure, that the pressure is reduced by 20% at the drain location, and that the downstream pressure is zero. Henceforth, a linearly varying uplift pressure was assumed in the absence of a crack. Should the analysis open a crack, then the uplift distribution will be automatically altered and there will be a constant uplift along the crack, and then back to the linearly varying

distribution along the uncracked ligament.

Since the supplied temperature record did not include summer temperatures, the initial 2D analysis first replicated the observed temperatures, and then the 3D analysis was performed.

Both linear analysis, and nonlinear ones (in which nonlinear interface elements were placed between the dam and the foundation) were performed. Fracture mechanics based interface elements, weak in tension and shear strong in compression, were used between the dam and the foundation.

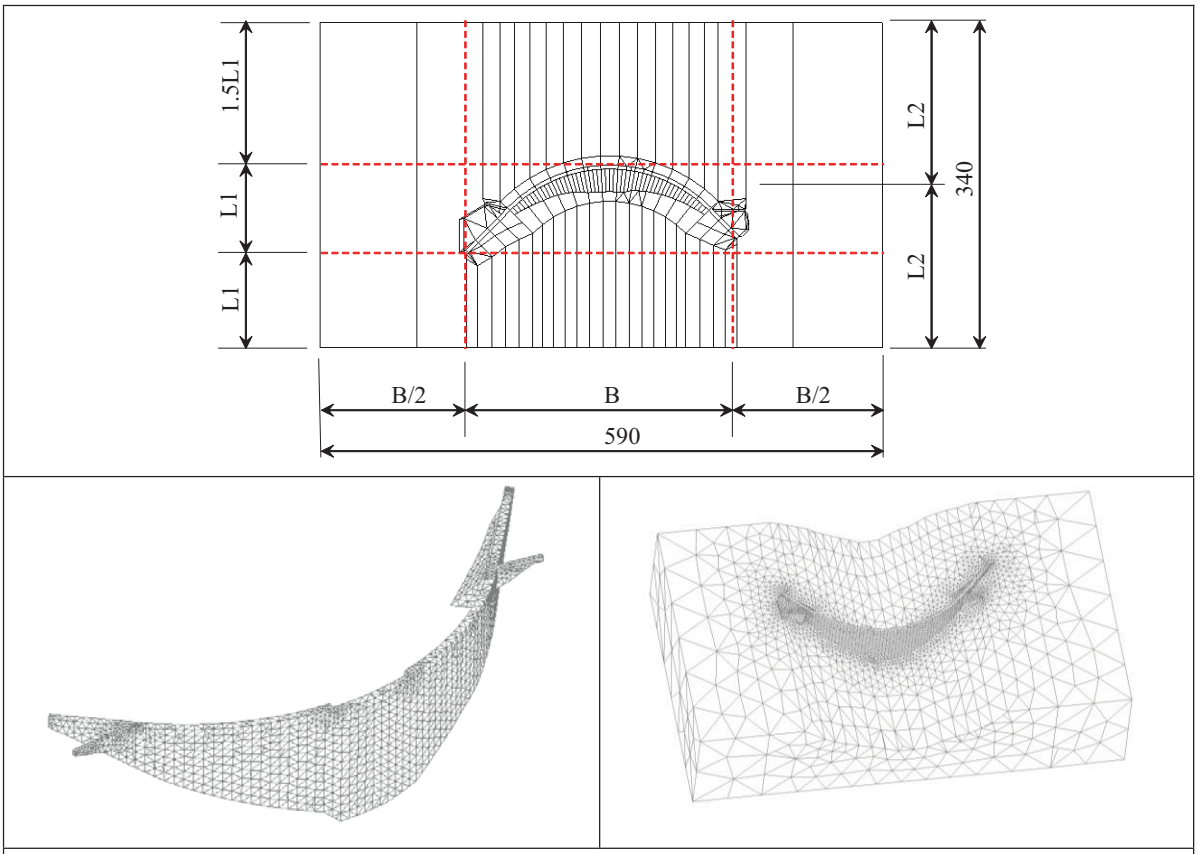

Fig. 2 Finite Element Mesh (3D)

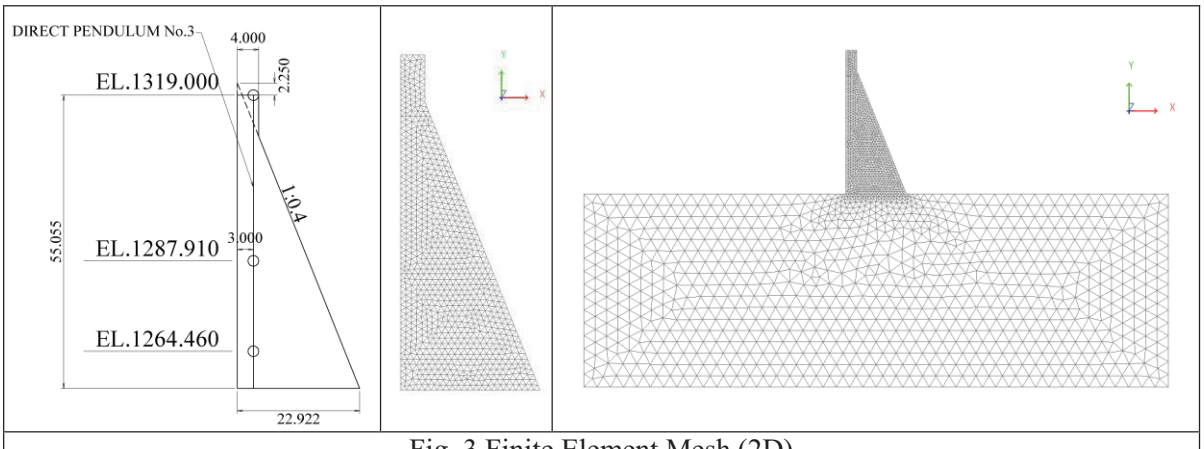

Fig. 3 Finite Element Mesh (2D)

3.2 Thermal Load

3.2.1 Air temperature

Table 2 summarizes the average monthly temperature in the city of Pegeuerinos which is close to the dam.

Table. 2 Historical Monthly Average Temperatures in Peguerinos

Month	J	F	M	A	M	J	J	A	S	O	N	D
Temperature (°C)	2.9	3.7	5.9	8.2	12.0	16.1	20.0	19.6	16.3	11.0	5.9	3.2

Assuming that the temperature was representative of the mid-month, a simple linear regression was performed to obtain the yearly temperature harmonic variation as shown in Fig. 4.

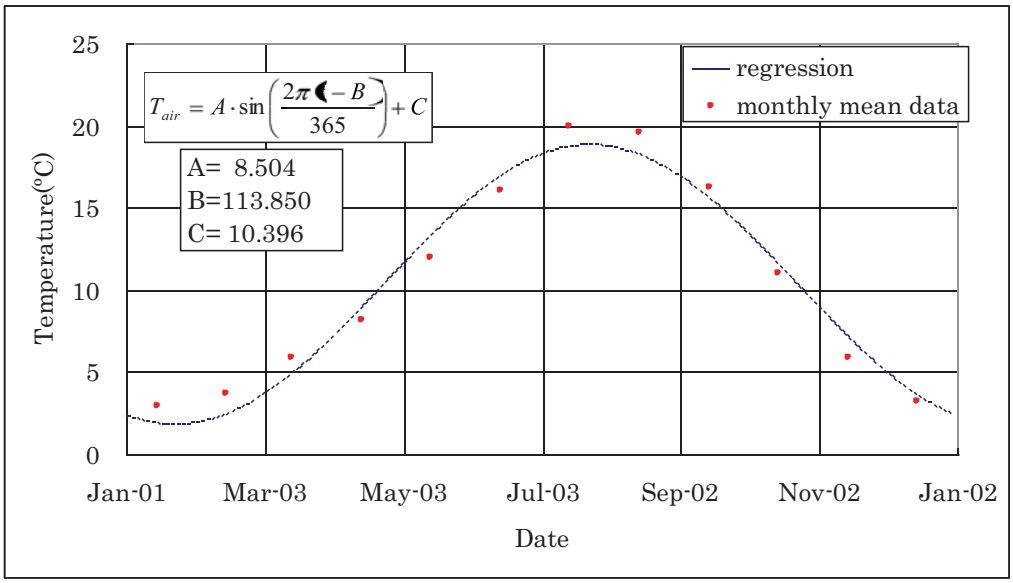

Fig. 4 Regression for air temperature data

3.2.2 Dam body temperature

(1) Upstream surface

Fig. 5 shows the recorded temperature on the upstream face. Based on Fig.5 we assumed upstream face temperature is constant: average temperature 7.4°C.

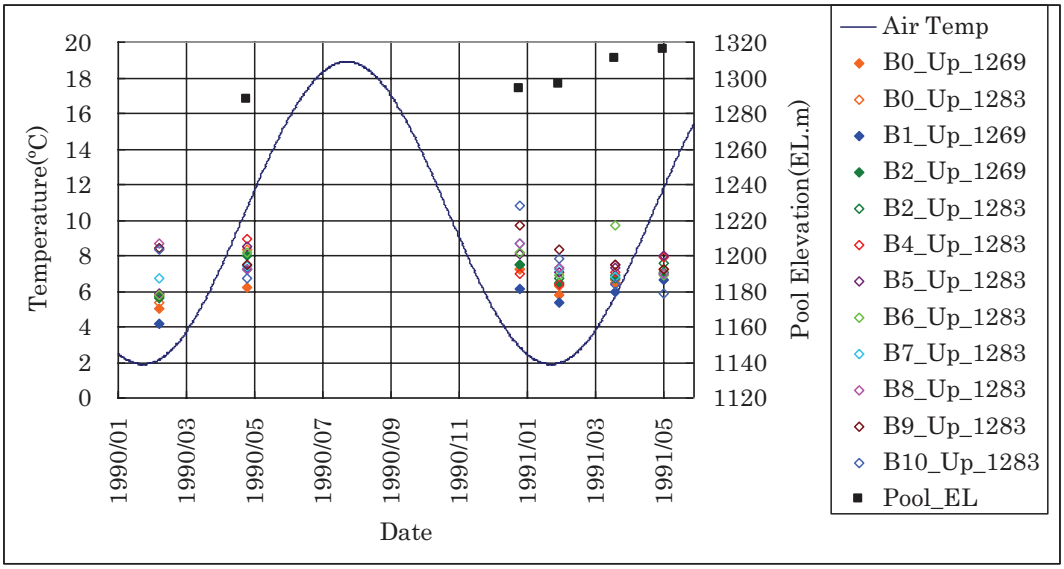

Fig. 5 Observed data of upstream surface

(2) Downstream surface

Fig. 6 shows the downstream face temperature variation; however no data is available for the April-December. Again a simple regression analysis was performed, and it turned out that the concrete temperature is slightly lower than the air temperature; usually this is not the case due to radiation. Thus, it was arbitrarily decided that the downstream surface temperature would be determined as the average of the difference (=3°C) between air temperature and the downstream surface temperature, Fig. 7.

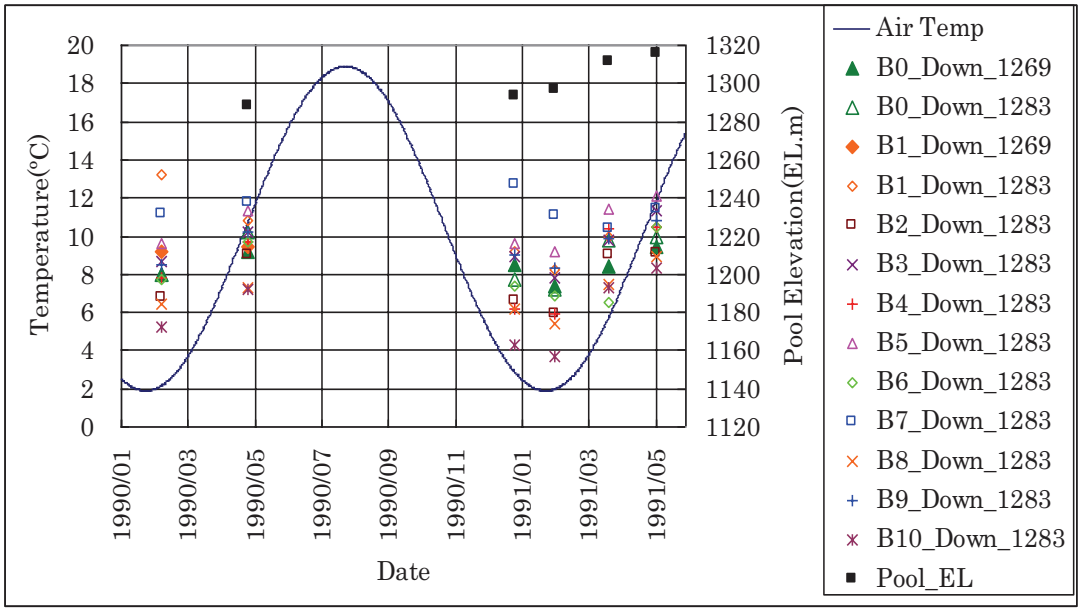

Fig. 6 Observed data of downstream surface

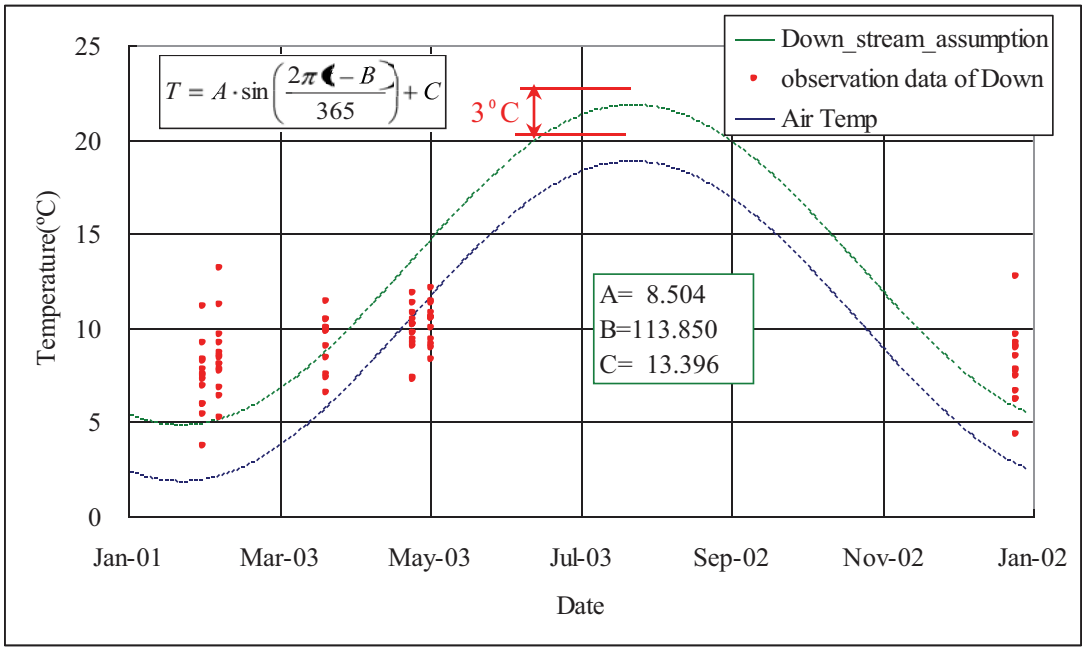

Fig. 7 Observed data and assumption for downstream surface

(3) Dam body center

Again temperature inside the dam body (B0 – B4) and the pool elevation are shown in Fig. 8. We note that two major trends emerge. The dam center temperatures with high elevation (EL1309) seem to be primarily influenced by the air temperature. The other, corresponding to lower elevations (EL. 1,283-1,269), dam center temperatures seem to be more influenced by the water level than the ambient air temperature. Since data from the center of the dam are only slightly affected by the external temperature, it was decided to consider an average temperature (12.2oC) for the initial temperature of the dam center based on the lower part (EL. 1283,1269) before impounding.

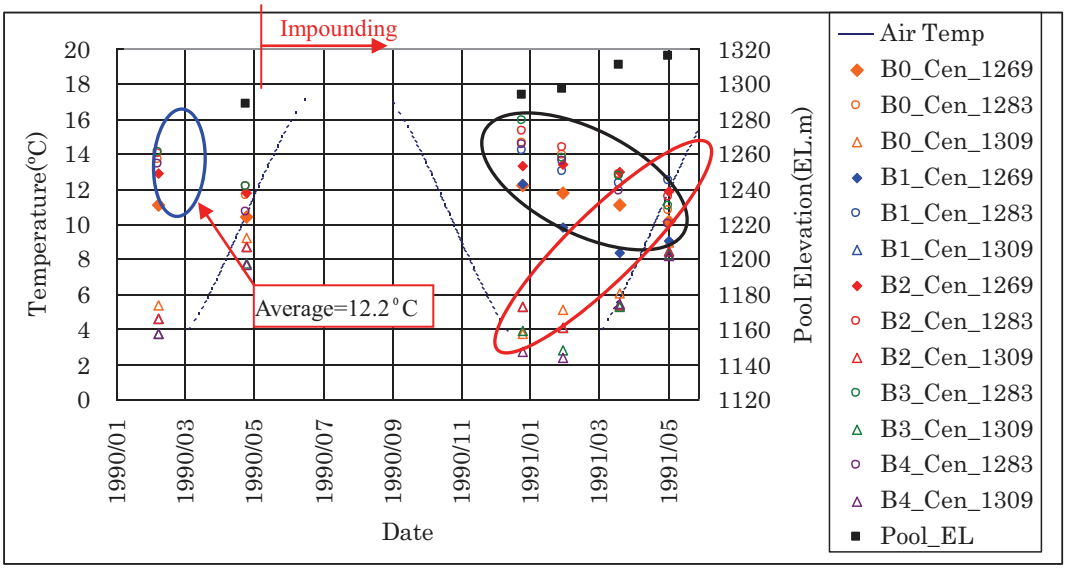

Fig. 8 Observation data of dam center (B0 - B4)

3.2.3 Final setting temperature data

The final temperatures of the adopted models are thus shown in Fig. 9. The temperature was cycled for 3 years of transient analysis, after which a steady state solution was determined.

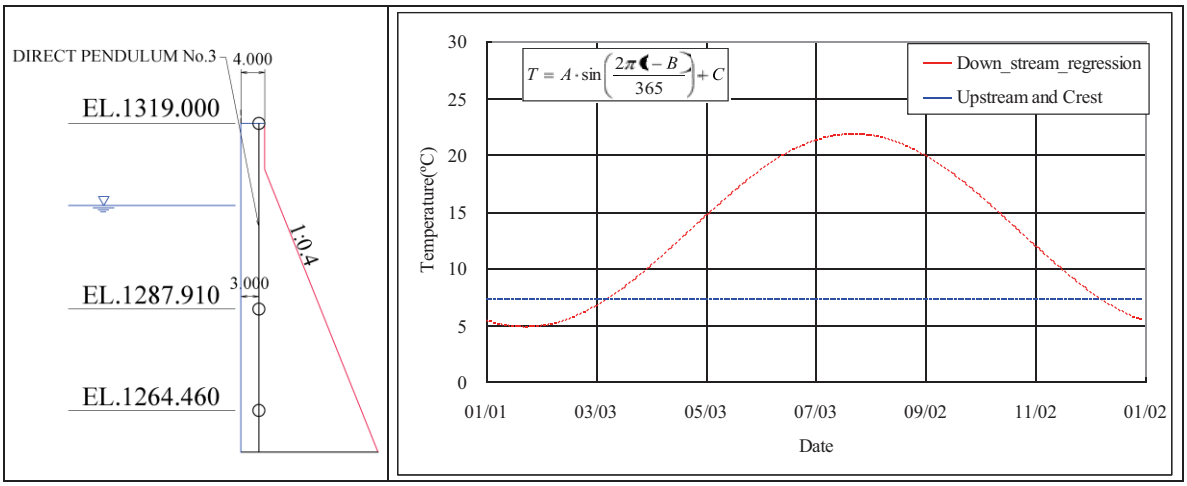

Fig. 9 Final setting temperature data

3.3 Pool elevation fluctuation

Since the daily pool elevation was not provided, interpolations was performed to obtain the weekly variation. 2D analysis was then performed for 2, 4 and 7 days, yielding practically the same results.

4. ANALYSIS RESULTS FOR PART-1

4.1 2D analysis result

Relative displacements, corresponding to pendulum No.3 are shown in Fig. 10. We observe that our numerical predictions are indeed very close to the recorded winter observations, but fail to favorably correlate for the summers of 2000 and 2001. On the other hand, comparison for the intermediate and lower gallery is almost identical to the observed ones.

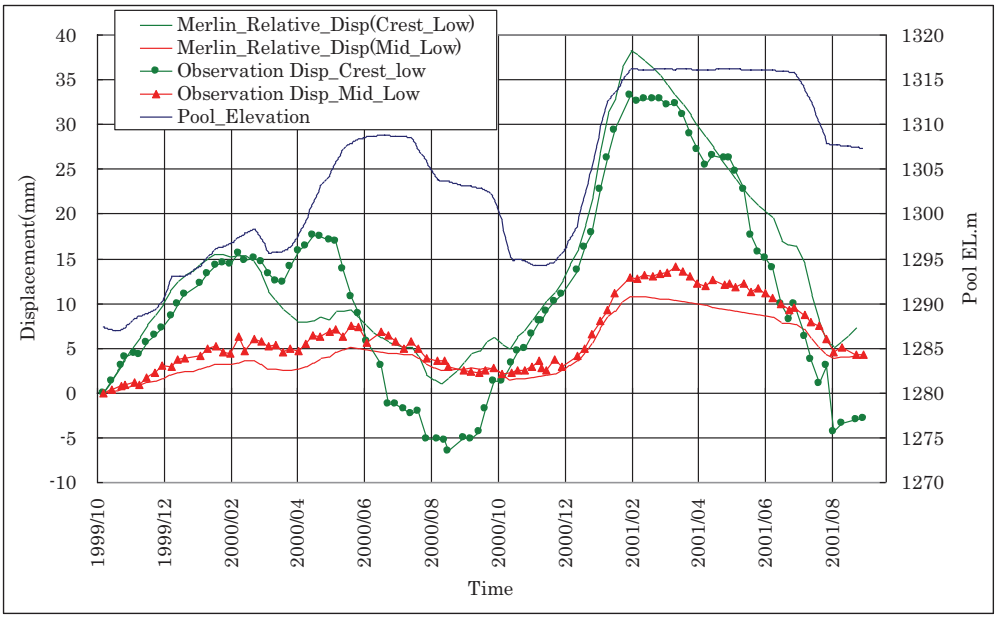

Fig. 10 Relative displacement of No.3 pendulum (2D)

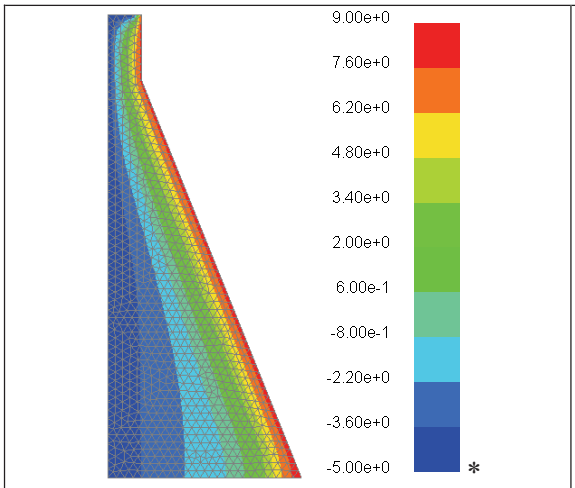

Fig. 11 Temperature contour (2000/08/02)

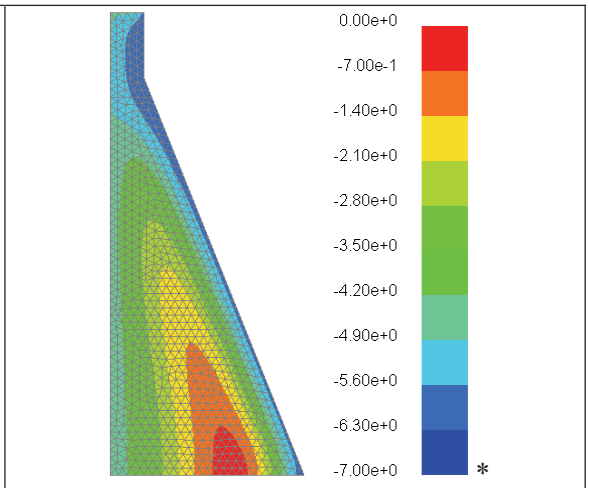

Fig. 12 Temperature contour (2001/01/31)

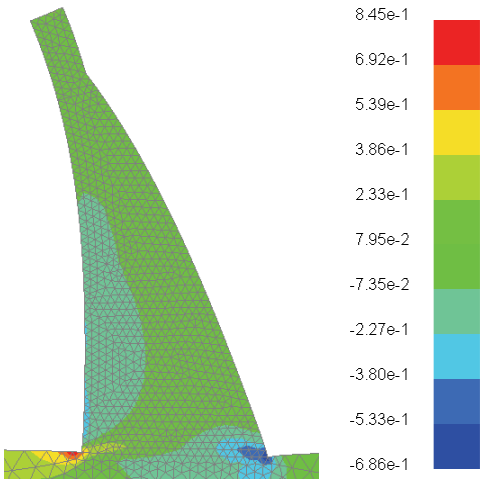

(MPa)

Fig. 13 Maximum principal stress contour (2000/08/02)

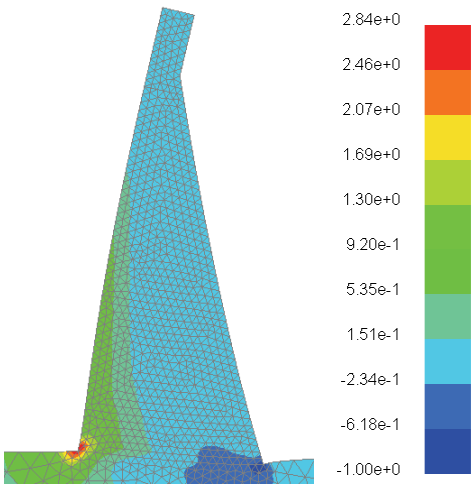

(MPa)

Fig. 14 Maximum principal stress contour (2001/01/31)

* Note that these are the thermal gradients with respect to the base temperature of 12.2°C.

4.2 3D analysis result

Again, comparison of relative displacements, as recorded by pendulum No.3, is shown in Fig. 15. We note that the displacements are smaller than those obtained from the 2D due to the arch effects and the three-dimensionality of the structure.

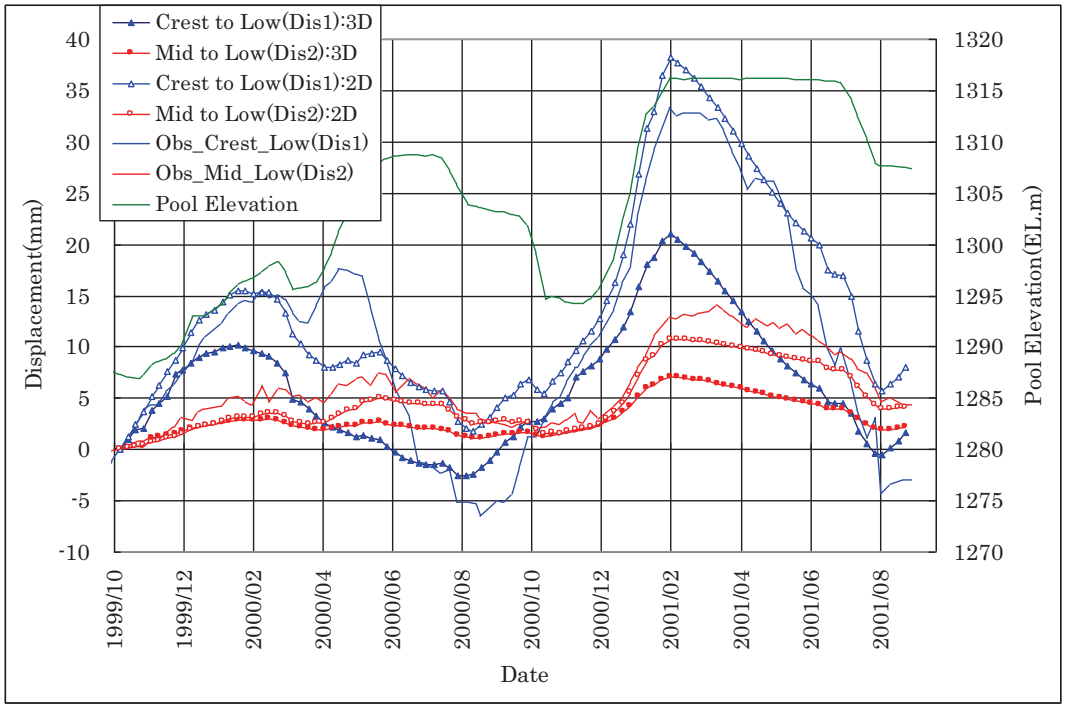

Fig. 15 Relative displacement of No.3 pendulum (2D,3D)

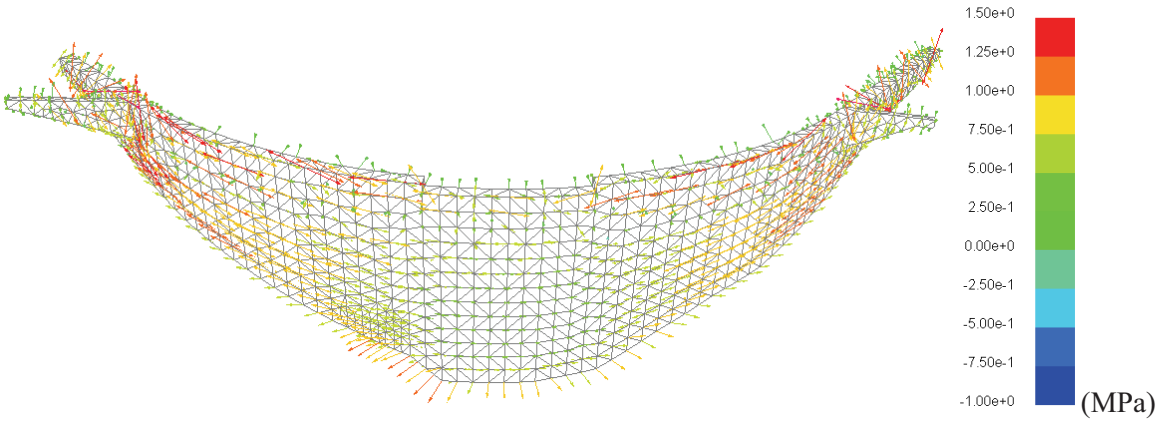

Fig. 16 Maximum principal stress vector (2000/08/02)

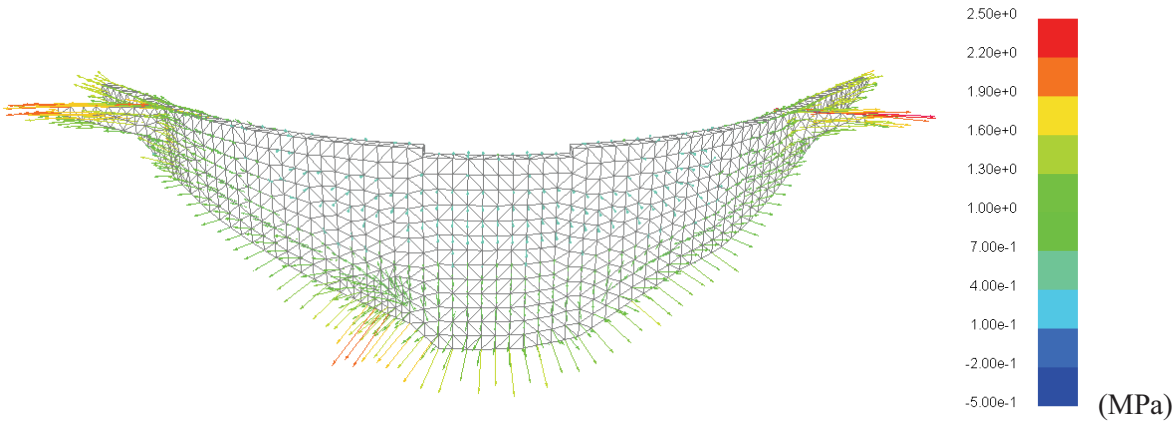

Fig. 17 Maximum principal stress vector (2001/01/31)

4.3 Analysis result for Part1 problem

Summary of this first part of the analysis is shown in Table. 3

Table. 3 Analysis Result For Part1

Date	Observation		2D		3D	
	Dis1 (mm)	Dis2 (mm)	Dis1 (mm)	Dis2 (mm)	Dis1 (mm)	Dis2 (mm)
1999/10/06	0.0	0.0	0.0	0.0	0.0	0.0
2000/04/25	17.5	6.3	8.5	3.8	2.2	2.4
2000/08/22	-6.5	3.0	1.7	2.6	-2.1	1.2
2001/02/06	33.3	12.9	38.0	10.7	22.1	7.2
2001/08/14	-4.3	4.6	5.2	4.0	-0.7	2.0

5. ANALYSIS RESULTS FOR PART-2 PROBLEM

5.1 Parameter analysis of Young modulus

5.1.1 2D analysis

In this study, we considered the following variations for the Young modulus: a) Foundation: 5,000MPa,10,000MPa(Basic),20,000MPa;Dam:15,000MPa,20,000MPa(Basic), 5,000MPa;Table. 4.

Table. 4 Combination of young modulus

Dam / Foundation	15,000MPa	20,000MPa	25,000MPa
5,000MPa	Case01_01	Case01_02	Case01_03
10,000MPa	Case02_01	Case02_02	Case02_03
20,000MPa	Case03_01	Case03_02	Case03_03

Analysis results for the relative displacement of the crest with respect to the lower gallery and of intermediate to lower gallery are shown in Fig. 18 and Fig. 19 respectively.

For the crest-lower gallery relative-displacement Case02_02 represents the proper approximation, whereas results for Case01_01, Case02_01, Case03_01 do have a big difference from observed displacement during 2000/04-2006/06 and 2000/06-2006/08 .

Results suggest that the displacements caused by the static water pressure are larger than those induced by the thermal expansion during 2000/04-2000/06. We guess that the actual temperature is far different from assumed one.

For the intermediate to lower gallery relative displacement, and as expected, both Case01_02 and Case01_01 represent the average case which is close to the observed data.

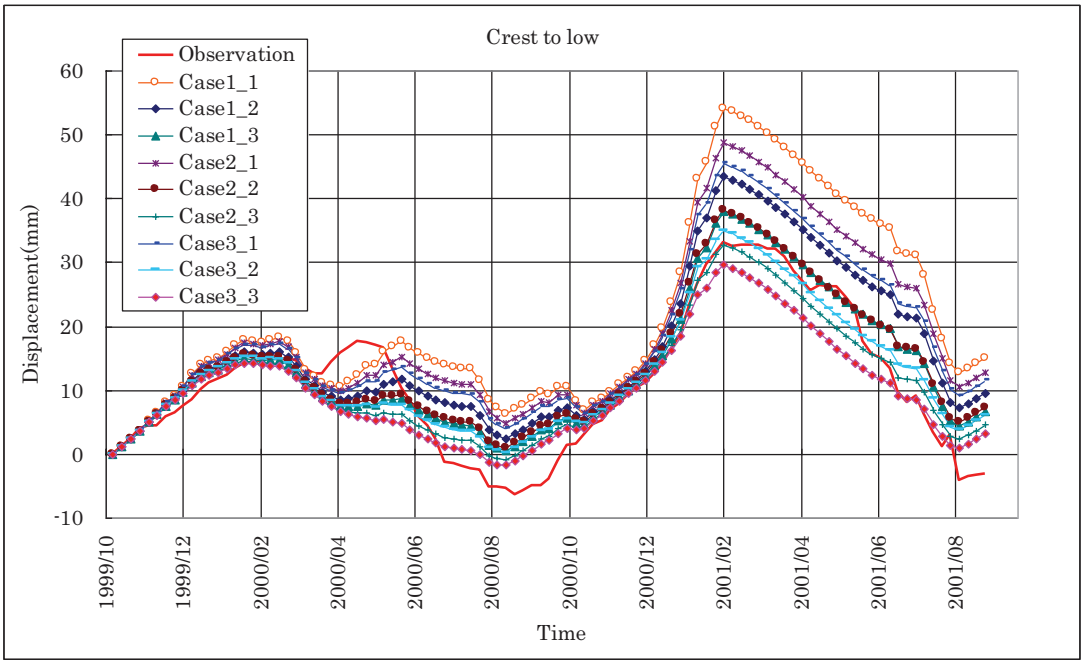

Fig. 18 Relative displacements of Pendulum (Crest to Low)

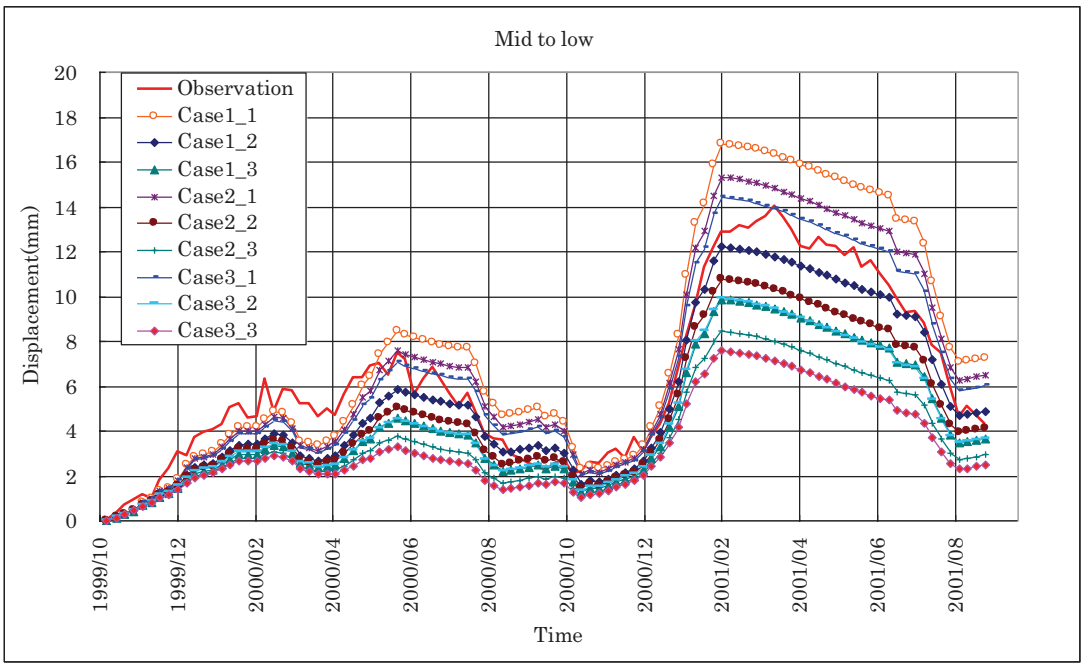

Fig. 19 Relative displacements of Pendulum (Mid to Low)

5.1.2 3D analysis

Because of the large computational time, we did not perform a 3D parametric study; hence we limited ourselves to a 3D analysis of Case01_01 which had the largest displacement in 2D. Relative displacements of pendulum for this analysis are shown in Fig. 20

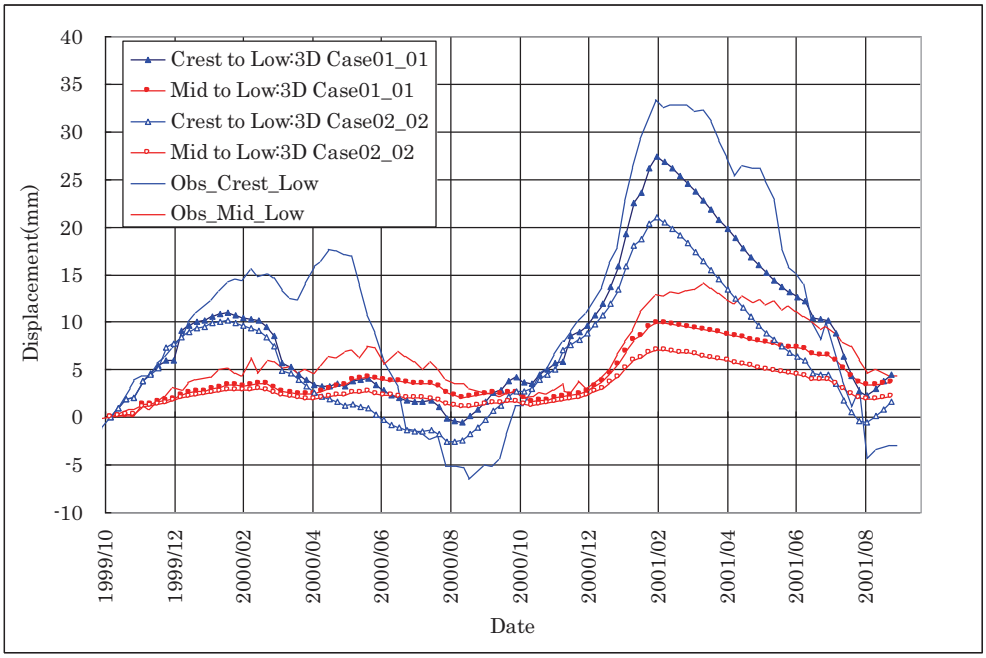

Fig. 20 Relative displacements of pendulum (3D)

5.2 Other parameters analysis

5.2.1 Coefficient of thermal expansion: 3D analysis

Analyses have thus far been performed for a concrete coefficient of thermal expansion equal to $1.0x10^{-5}/^{o}C$, however this value usually ranges from 0.7 to $1.3x10^{-5}/^{o}C$. Thus, we performed additional analysis using this range of values while keeping the other parameters equal to those of Case01_01 (young modulus of dam =1.5e+04MPa, young modulus of foundation =5.0e+03MPa). Results are shown in Fig. 21. We note that an increase in the coefficient of thermal expansion does not change much the relative displacement from the intermediate to lower gallery. We suspect that this is due to the assumed constant water temperature on the upstream face.

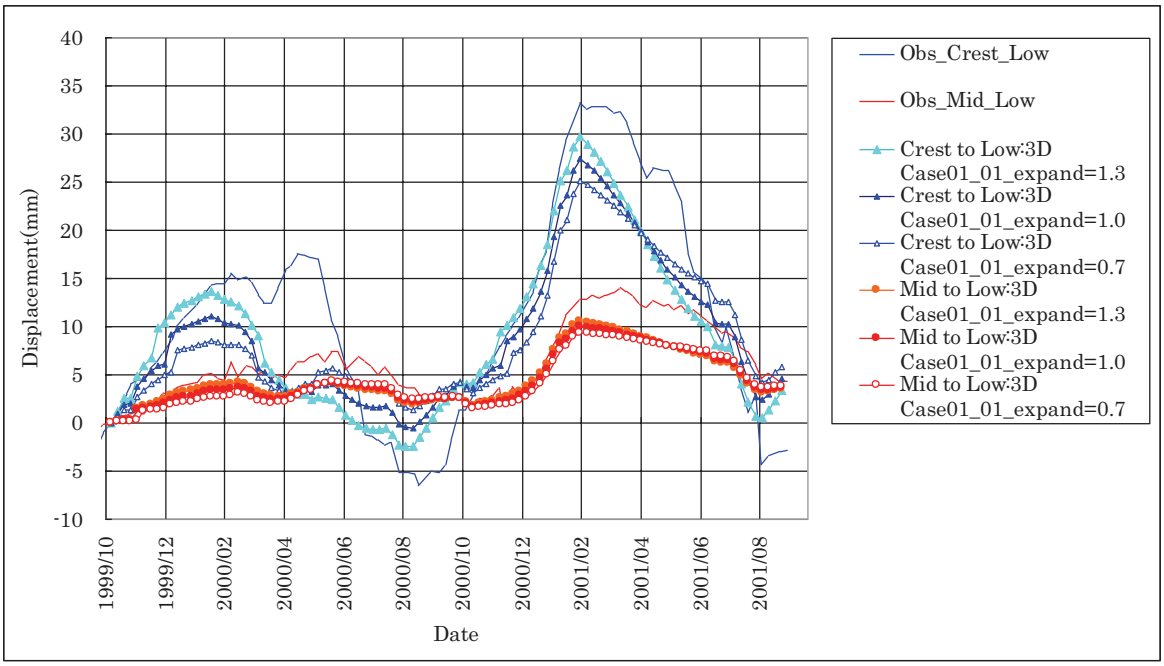

Fig. 21 Relative displacements (3D) for parameter of coefficient of thermal expansion

6. CONCLUSION

The following conclusions can be drawn from this analysis:

1. 2D analysis captured almost exactly the dam response except for the time period 2000/04 and 2000/10. There does not seem to be much arch action in this dam.
2. Results for the relative displacement from intermediate to lower gallery in 2D analysis point to a smaller elastic modulus.
3. Improved results could be obtained if we were provided with the exact history of the air temperature, the dam body temperature (including summer values), and more information regarding local radiation.

ELASTIC ANALYSIS OF AN ARCH-GRAVITY DAM USING DIANA

Gerd-Jan Schreppers, Giovanna Lilliu
TNO DIANA BV, Schoemakerstraat 97, 2628 VK Delft, The Netherlands
www.tnodiana.com

SUMMARY: Modelling and analysis with DIANA Finite Element Software of the La Aceca arch-gravity dam are presented in this paper. Comparison between calculated and measured displacements shows reasonable agreement. Thermal expansion of the dam as well as foundation properties appears to have major impact on the calculated results. The different analyses reported in this study provide insight in the effect of e.g. water temperature, environment temperature and foundation stiffness on the deformations of the dam.

1. INTRODUCTION

In the 9th meeting of the ICOLD Benchmark Workgroup on Numerical Analysis of Dams the case of the La Aceca arch-gravity dam was discussed. This paper describes the contribution of TNO DIANA to this workshop. In the analysis, material is considered linear elastic and the only loads applied to the dam are hydrostatic pressure and thermal expansion. Although a finite element mesh was already provided by the formulator of the benchmark, a new finite element mesh was built using midas FX+ for DIANA preprocessor. The sequence of steps for generating the finite element model of the dam is described in detail in the sequel of this paper.

2. PROGRAM DESCRIPTION

The study was conducted using DIANA Finite Element software and midas FX+ for DIANA pre-/post-processor. DIANA, which is developed by TNO DIANA BV, is present in the market for more than 20 years. DIANA is a general purpose 3-dimensional finite element program with functionality for dynamic and nonlinear stress analysis of concrete and soil/rock structures. Specific functionality for analysis of dams is present in the program, such as: phased construction, heat-stress analysis, groundwater flow-stress analysis, young hardening concrete.

3. MODEL DESCRIPTION

The hexahedron model, which was provided by the formulator of the benchmark, is displayed in Figure 1. This model is defined using 8-noded hexahedron elements. The number of elements is 36397 in the foundation, and 9327 in the dam. Some of the elements are badly shaped. The ground surface is modeled as a stair-case, which is not realistic. Such type of mesh does not allow for mesh-adaptations in the study. In Figure 2 an additional light blue-transparent surface, which represents the ground surface, is added to the original model. This ground surface is defined automatically in midas FX+ for DIANA by mapping a vertex-face to the nodes of the ground surface in the original model.

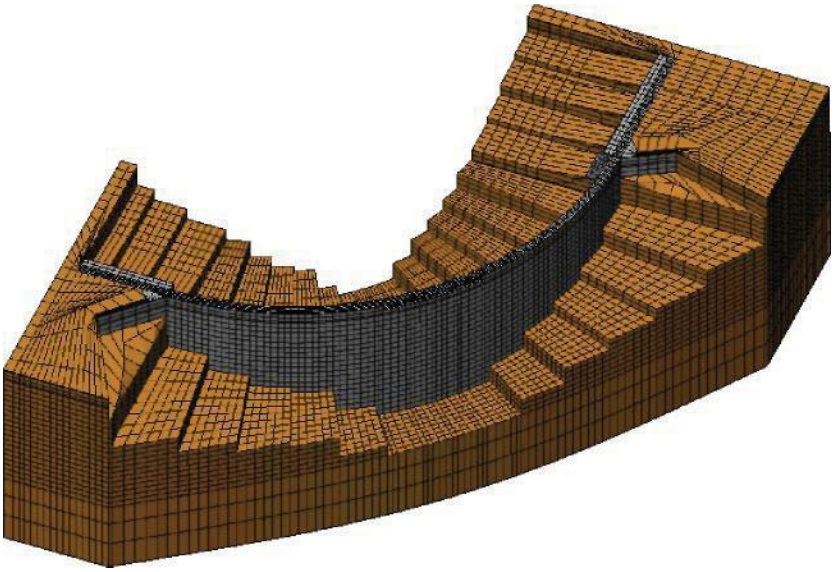

Figure 1: Hexahedron model provided by the formulator of the benchmark: in brown are the elements that model the foundation, in grey the elements that model the dam body.

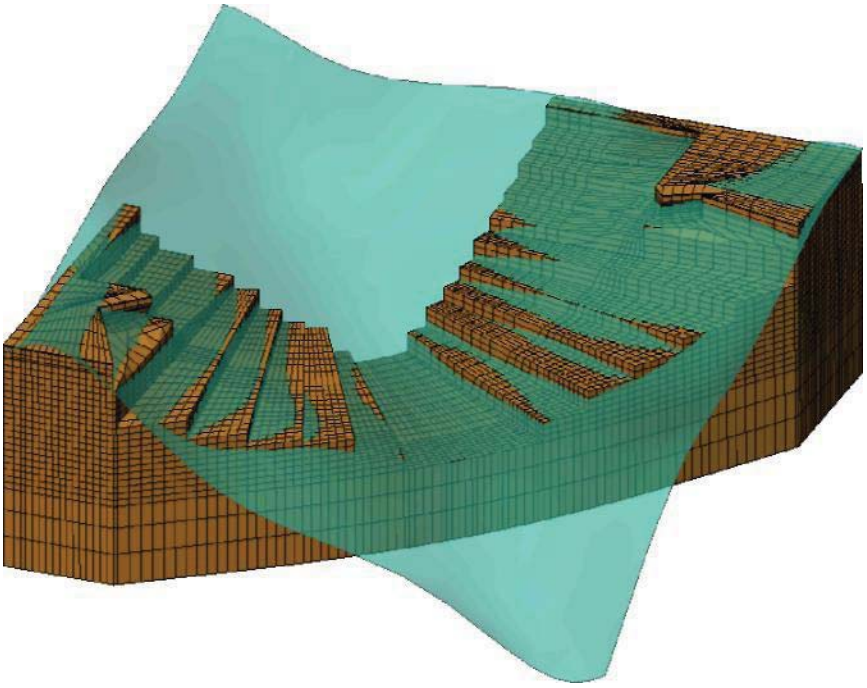

Figure 2: Hexahedron model with foundation elements only and mapped ground surface (in light blue-transparent).

The dam body is initially schematized by means of a parameterized cylinder at the upstream face and a parameterized cone at the downstream face, and a parameterized ring at the top. Boolean operators applied to these parameterized geometrical shapes lead to the final geometry of the dam body, which is displayed in light blue-transparent in Figure 3. In a similar manner, the abutments are schematized by means of parameterized boxes, which are shown in yellow in Figure 3.

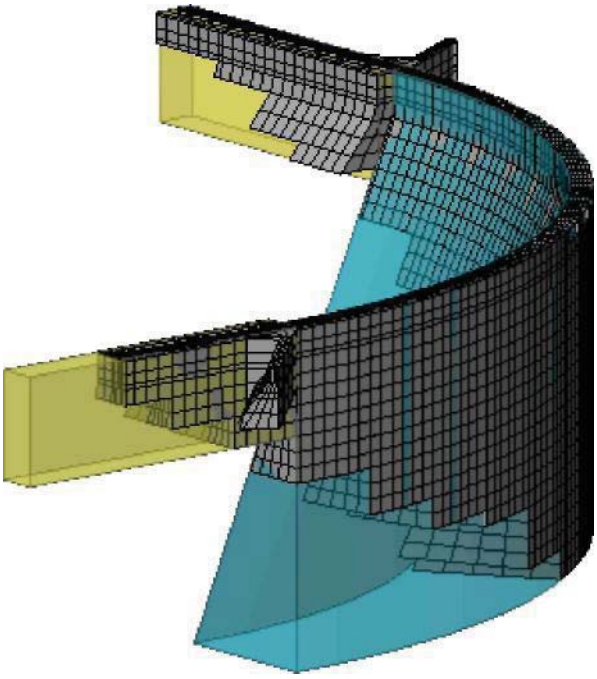

Figure 3: Schematization of the dam geometry: the dam body is shown in blue-transparent; the abutments are shown in yellow- transparent.

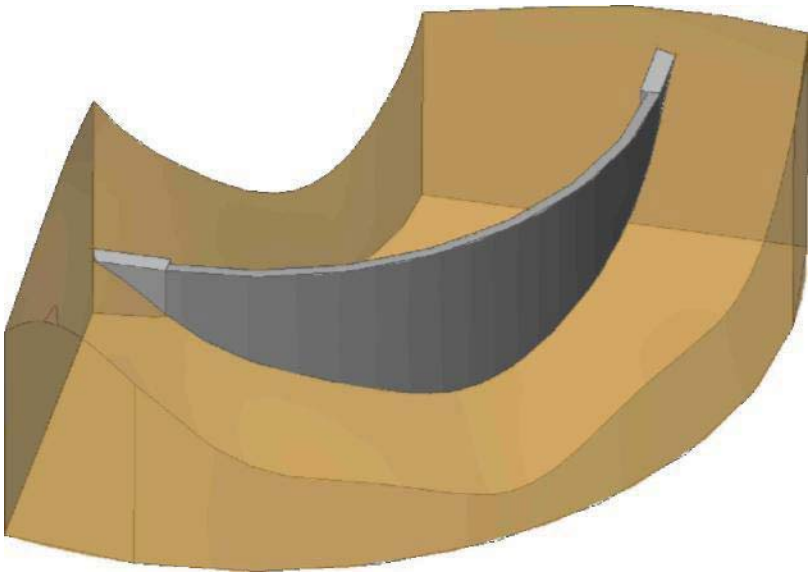

Figure 4: Geometry of foundation (in brown-transparent) and dam (in grey) after trimming the dam schematized in Figure 3 with the ground surface shown in Figure 2 .

The final geometry is obtained trimming the dam schematized in Figure 3 with the ground surface shown in Figure 2 and removing the portion of the dam that falls under the ground surface. The boundaries of the foundation, which is shown in brown-transparent in Figure 4, are

defined by its inner/outer radii, bottom surface and end surfaces. Before generating the mesh, an appropriate mesh division is assigned to each part of the model. The element size is set at 2 m for the elements in the dam, and at 25 m for the elements at the boundaries of the foundation. A tetrahedron mesh is generated automatically. The mesh, which is shown in Figure 5 and Figure 6 (upstream and downstream view, respectively), contains 32562 elements in the foundation, and 12742 elements in the dam.

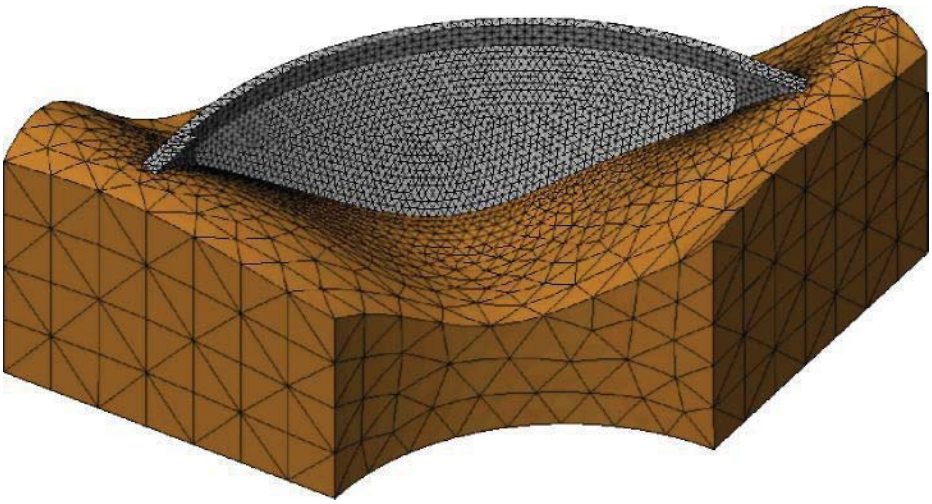

Figure 5: Upstream view of the finite element mesh

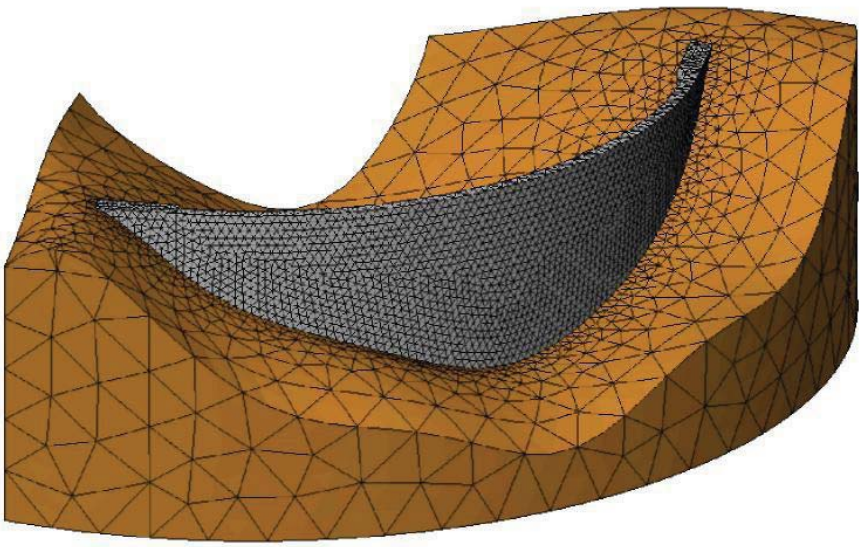

Figure 6: Downstream view of the finite element mesh.

The finite element mesh is composed of 10-noded quadratically interpolated tetrahedron elements.

The following material parameters are assumed:

	Dam	Foundation
Young's modulus (GPa)	20.0	10.0
Poisson's ration (-)	0.2	0.2
Linear thermal expansion ($^oC^{-1}$)	1.0E-5	0.0

The loads considered in the analysis are the hydrostatic pressure on the upstream portion of the dam and the foundation, and the thermal expansion that accounts for changes in temperature of the dam body. The five load situations considered in the analysis are those identified as target in the benchmark:

Date	Water level (m)	Environment temperature (^oC)
06/10/1999	1288	11.0
25/04/2000	1300	8.2
22/08/2000	1304	16.1
06/02/2001	1316	3.7
14/08/2001	1310	19.6

The hydrostatic pressure is defined by means of a space function, which defines the hydrostatic pressure at different altitudes. Such pressure is assigned to all elements of the upstream ground surface, and to the elements of the upstream dam that are in contact with the water. The program computes automatically the values of hydrostatic pressure at each node of the elements. Uplift is neglected. Figure 7 displays a detailed view of a cut-away of the finite element mesh, with the hydrostatic pressures visualized by means of arrows located at the nodes of each element.

Figure 8 displays a cross section of the dam and the corresponding water level, which varies in time as indicated in the table above.

In this paper it is initially assumed that the water temperature remains constant, and equal to 5^oC for each loading situation. The environment temperature varies in time accordingly to the table above. This table indicates the averaged monthly temperatures registered in the neighbouring city of Peguerinos. It should be emphasized that these averages are computed on a time span of several years, and do not correspond to the actual temperature at the date indicated in the table. These temperatures are prescribed as boundary conditions in all nodes of the portion of the outer surface of the dam, which is exposed to the air (see Figure 8). The temperatures at the bottom of the dam and inside the dam are automatically calculated by the software.

The analysis is conducted in DIANA by means of a so called staggered heat-stress analysis. This type of analysis consists of a sequence of heat flow and stress analysis. The temperatures derived from the heat flow analysis are automatically applied to the model as external load in the sequent stress analysis, together with the hydrostatic pressure. The heat flow analysis can be steady-state (as in this benchmark case study) or transient. The quadratically interpolated elements are automatically converted to linearly interpolated elements in the heat flow analysis.

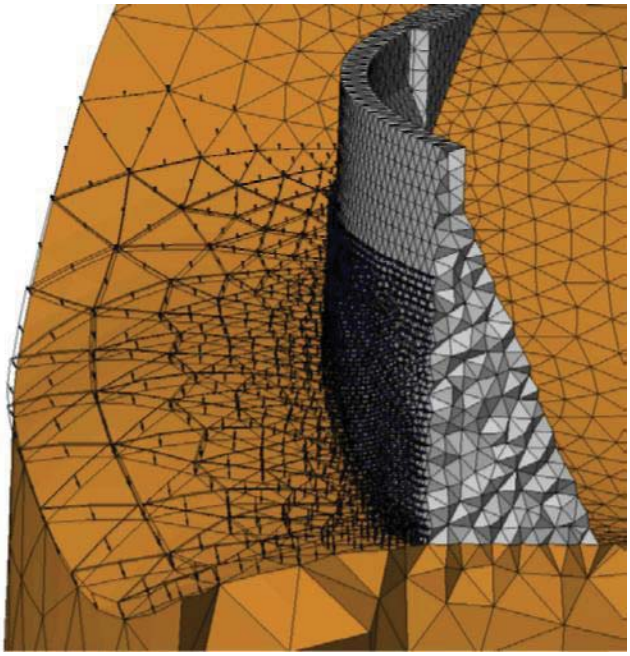

Figure 7: Cut-away of the finite element mesh: the hydrostatic load is visualized by means of arrows normal to the face of the elements.

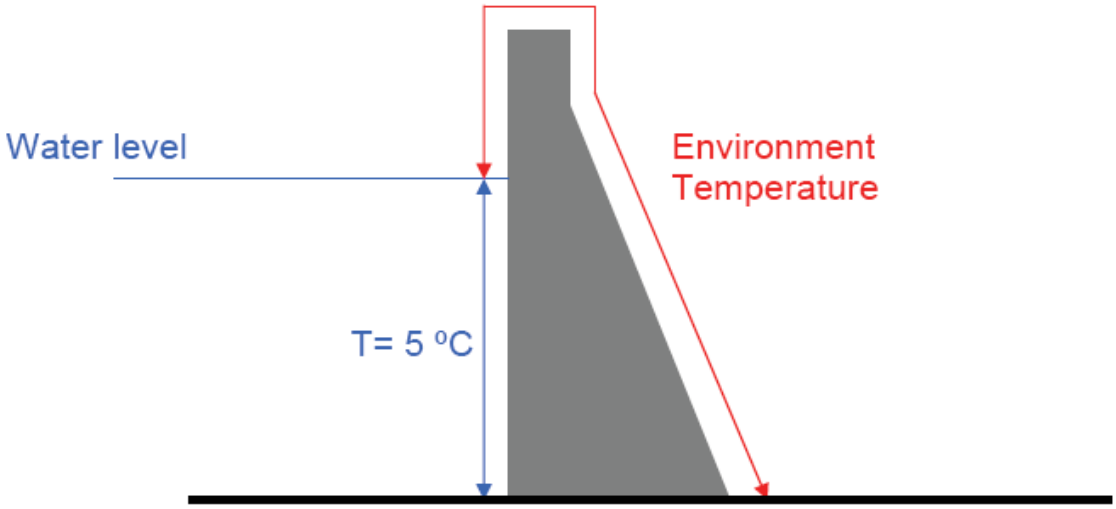

Figure 8: Typical load combination in a cross section of the dam: the water level defines the portion of the cross section subjected to hydrostatic pressures; the remaining part of the cross section is subjected to prescribed temperatures.

For the stress analysis, the side surfaces and the bottom surface of the foundation are supported in the normal direction.

The analyses are conducted using first the set of parameters as defined in this paragraph (PART I), and changing this set of parameters afterwards (PART II).

4. ANALYSIS RESULTS FOR PART 1

In PART I of this benchmark study, the adopted parameters are those defined in paragraph 3. The calculated temperature profiles for the 5 load situations are given in Figures 9a to 9e (the same colour scale is used for all load situations).

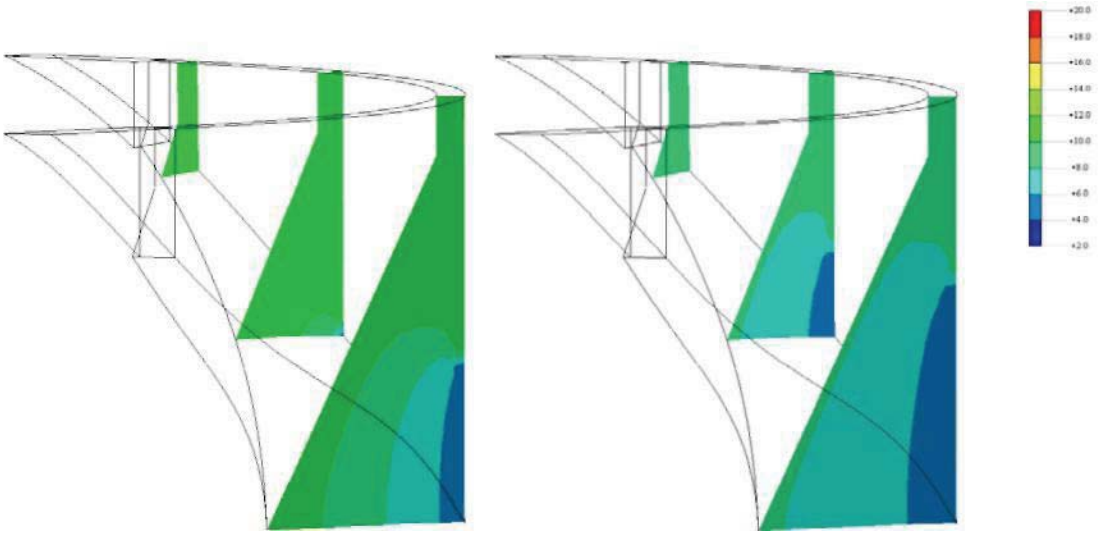

(a) $T_{env} = 11\ ^{o}C$, $H_{water} = 1288$ m (b) $T_{env} = 8.2\ ^{o}C$, $H_{water} = 1300$ m

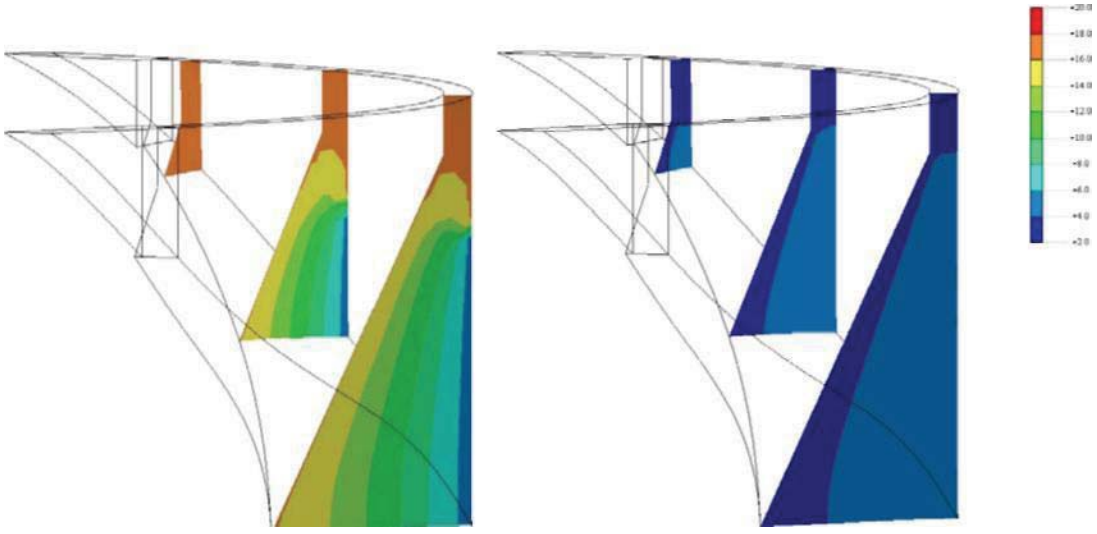

(c) $T_{env} = 16.1\ ^{o}C$, $H_{water} = 1304$ m (d) $T_{env} = 3.7\ ^{o}C$, $H_{water} = 1316$ m

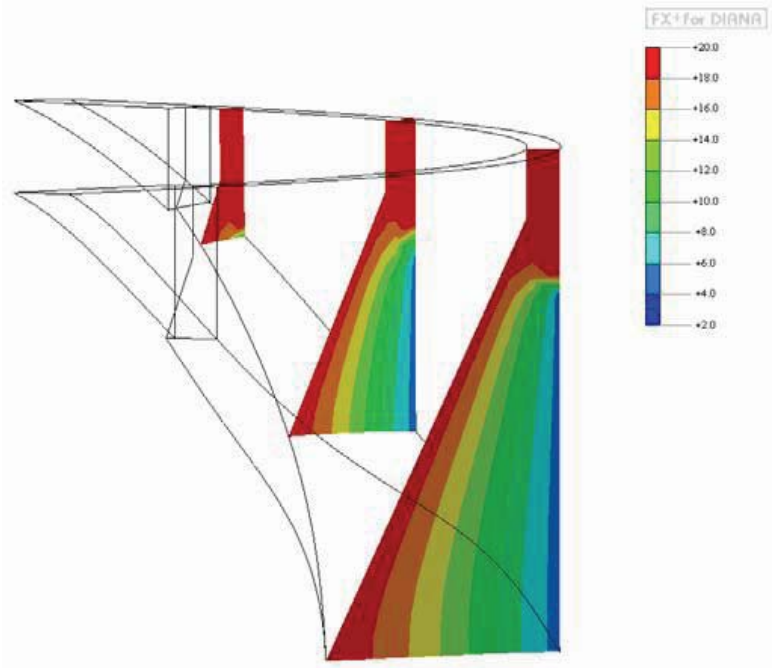

(e) T_{env} = 19.6 ^{o}C, H_{water} = 1310 m

Figure 9: Temperature contours in different cross sections of the dam for different load situations (the colour scale is the same for each load situation)

The contours plots of the total displacements in the deformed model are displayed for each load situation in Figures 10a to 10 e.

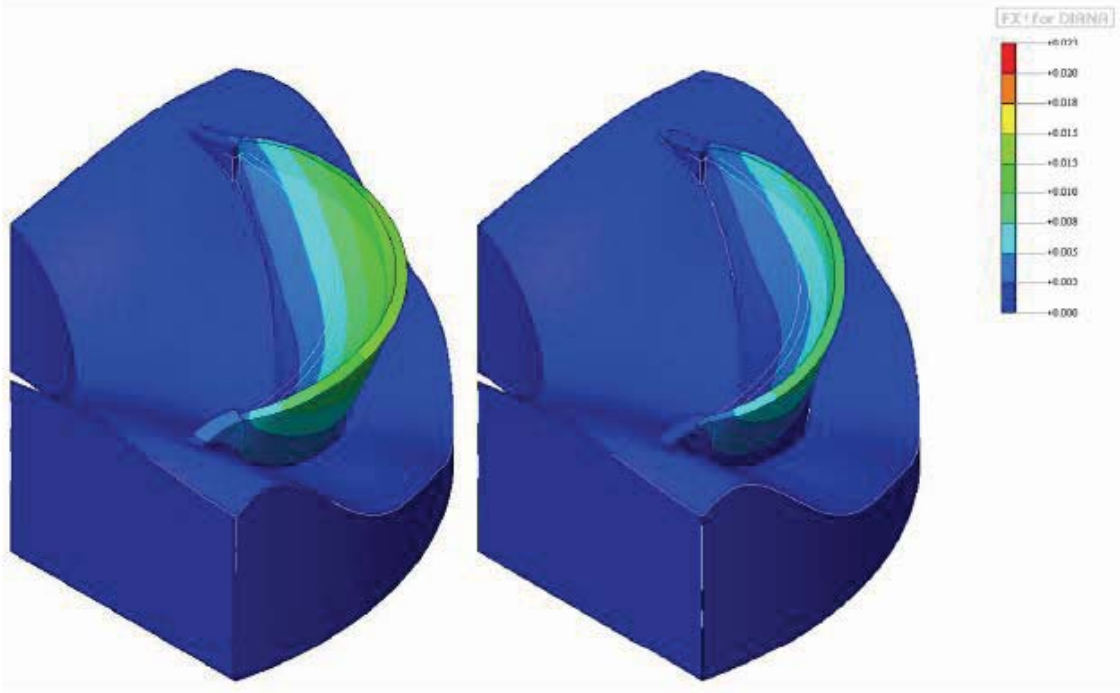

(a) Tenv = 11 oC, Hwater = 1288 m (b) Tenv = 8.2 oC, Hwater = 1300 m

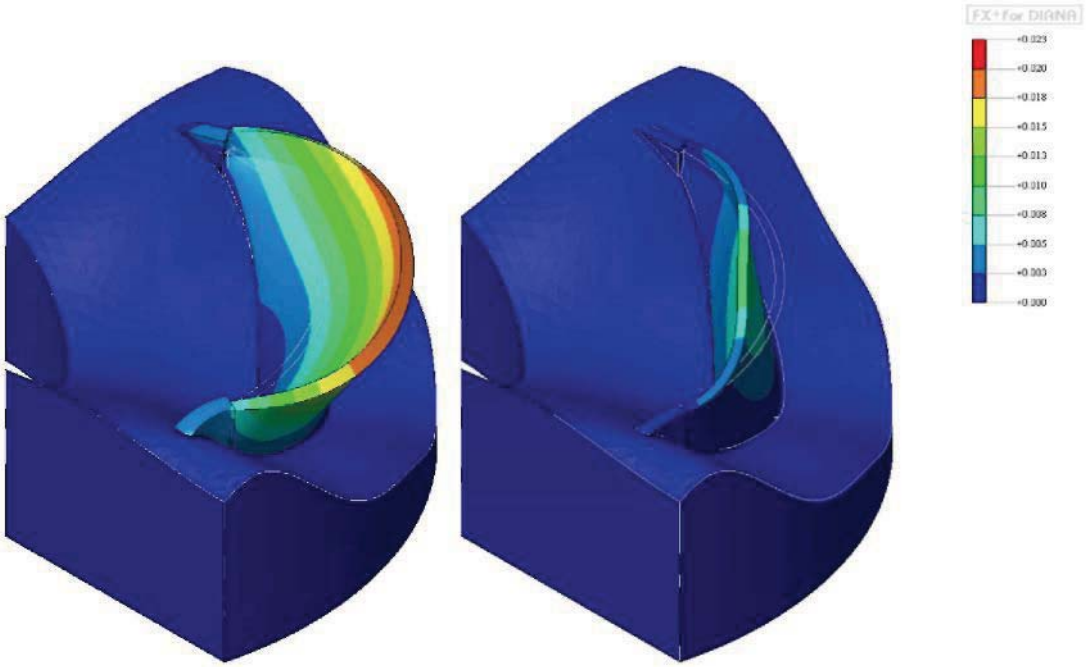

(c) T = 16.1 °C, H_{water} = 1304 m (d) Tenv = 3.7 °C, H_{water} = 1316 m

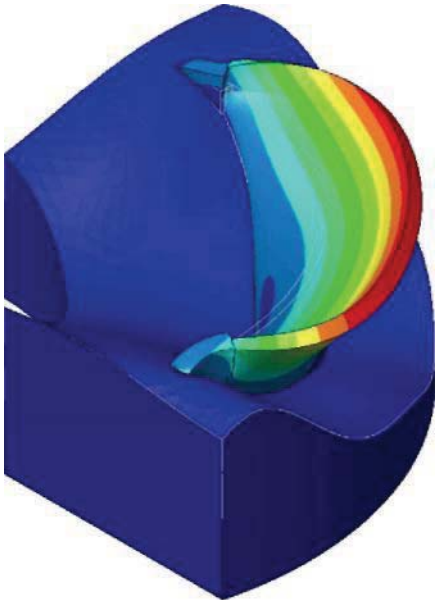

(e) T_{env} = 19.6 °C, H_{water} = 1310 m

Figure 10: Contour plots of the total displacements for different load situations (the colour scale is the same for each load situation)

It is evident from Figure 10 that the crest of the dam moves upstream in some load situations. The relative horizontal displacements at the downstream face of the dam between the bottom gallery and the crest of the dam (D1), and between the bottom and middle gallery (D2) are

summarized in Table 1. The load situation of 06/10/1999 is considered as reference.

Date	Target D1 (mm)	Target D2 (mm)	Analysis D1 (mm)	Analysis D2 (mm)
06/10/1999	0.0	0.0	0.0	0.0
25/04/2000	17.5	6.0	5.8	3.1
22/08/2000	-5.0	3.0	-5.5	0.8
06/02/2001	32.0	13.0	21.9	9.5
14/08/2001	1.0	7.5	-8.2	1.4

Table 1: Relative horizontal displacements: between bottom gallery and crest of the dam (D1); between bottom and middle gallery (D2). The assumptions made for material parameters and load conditions are described in paragraph 3.

For comparison, the same analysis was repeated considering only the hydrostatic pressure and neglecting the thermal load. The corresponding results are summarized in Table 2.

Date	Target D1 (mm)	Target D2 (mm)	Analysis D1 (mm)	Analysis D2 (mm)
06/10/1999	0.0	0.0	0.0	0.0
25/04/2000	17.5	6.0	2.0	1.4
22/08/2000	-5.0	3.0	3.3	2.2
06/02/2001	32.0	13.0	10.9	5.9
14/08/2001	1.0	7.5	6.3	3.8

Table 2: Relative horizontal displacements: between bottom gallery and crest of the dam (D1); between bottom and middle gallery (D2). The assumptions made for material parameters are as in the analyses whose results are summarized in Table 1. In the load conditions the thermal load is neglected.

When the thermal expansion is neglected, the upstream movement of the crest of the dam cannot be captured. For this reason it is possible to conclude that thermal expansion dominates the behaviour of this dam.

5. ANALYSIS RESULTS FOR PART 2

The results reported in the previous paragraph still show large differences with the measured horizontal displacements. In order to achieve a better fitting of the measured displacements, some parameters of the model were varied as follows:

- A lower stiffness of the foundation is considered
- The temperature of the dam is considered constant over the year in the core of the dam
- The water temperature is varied over the year

The corresponding results are summarized in this paragraph.

5.1 Lower stiffness of the foundation

The stiffness of the foundation is assumed equal to 0.2 GPa (realistic stiffness value for a clay-type foundation) instead of 10 GPa. This strong reduction may account for different effects: 1) in the numerical model dam and foundation are rigidly connected, which may be not sufficiently realistic; 2) the boundaries of the foundation are relatively close to the dam, which contributes to further increase the stiffness of the foundation; 3) 10 GPa is the stiffness of a very hard and intact rock, whereas the foundation of this dam may be fractured.

The corresponding calculated horizontal displacements are summarized in the following table.

Date	Target D1 (mm)	Target D2 (mm)	Analysis D1 (mm)	Analysis D2 (mm)
06/10/1999	0.0	0.0	0.0	0.0
25/04/2000	17.5	6.0	6.7	3.8
22/08/2000	-5.0	3.0	-3.2	2.3
06/02/2001	32.0	13.0	28.4	13.7
14/08/2001	1.0	7.5	-3.1	4.2

Table 3: Relative horizontal displacements: between bottom gallery and crest of the dam (D1); between bottom and middle gallery (D2). The stiffness of the foundation is assumed 0.2 GPa.

In this case the calculated relative horizontal displacements show reasonable agreement with the measured target displacements. The largest differences occur at the load situation corresponding to 25/04/2000. Such differences may be caused by an erroneous assumption concerning water or environment temperature. For example, the month of April in 2000 may have been colder than the average over the years, as it is considered in the analysis.

5.2 Constant temperature in the core of the dam body

The temperature in the core of the dam body is assumed constant and equal to 11 ^{o}C during the whole year. The core of the dam body is defined as the portion of the volume at a distance larger than 3 m from the outer surfaces of the dam. In this case the temperature is assigned to all nodes that fall in the core of the dam body, while the temperature at the nodes that fall outside are determined from the steady-state thermal analysis. The corresponding temperature profiles for the different load situations are displayed in Figures 11a to 11e.

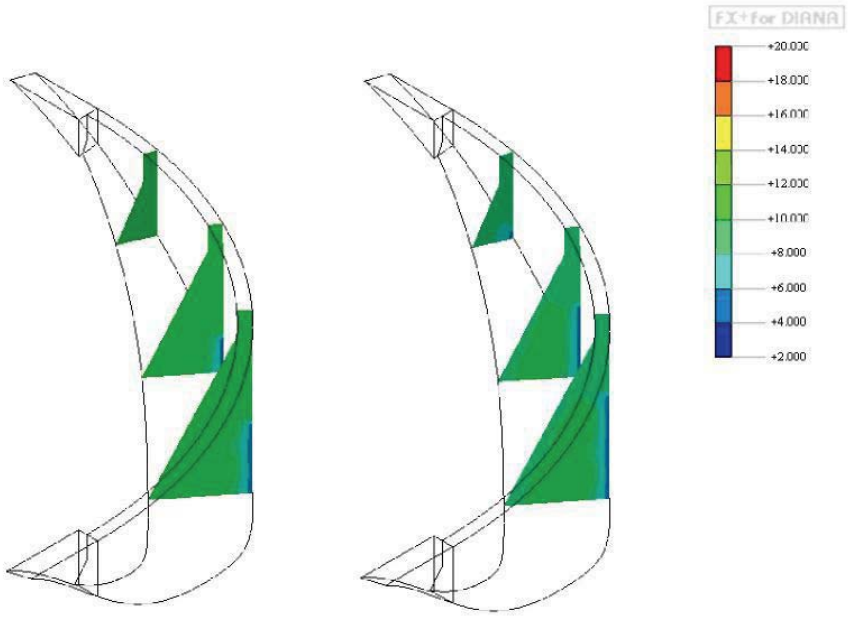

(a) T_{env}= 11 ^{o}C, H $_{water}$ = 1288 m (b) T_{env} = 8.2 ^{o}C, H $_{water}$ = 1300 m

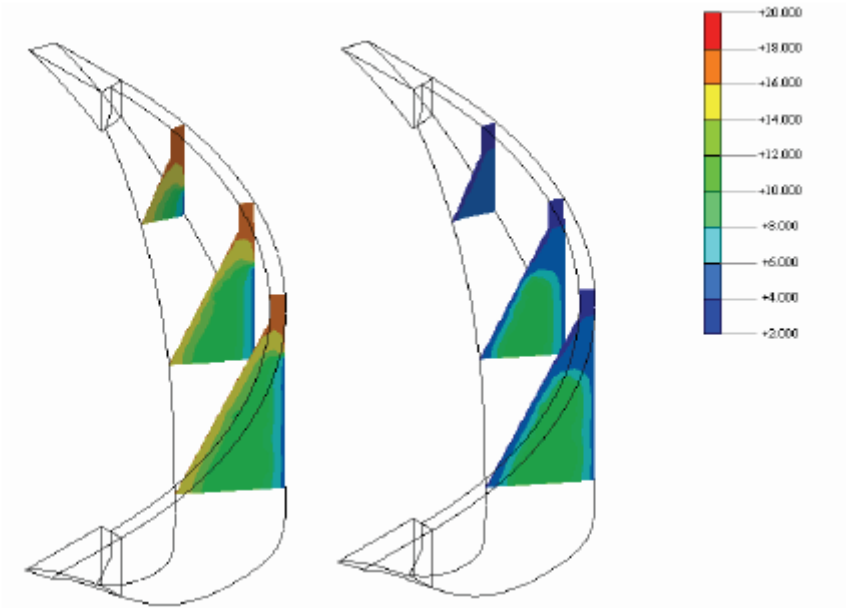

(c) T_{env} = 16.1 ^{o}C, H $_{water}$ = 1304 m (d) T_{env} = 3.7 ^{o}C, H_{water} = 1316 m

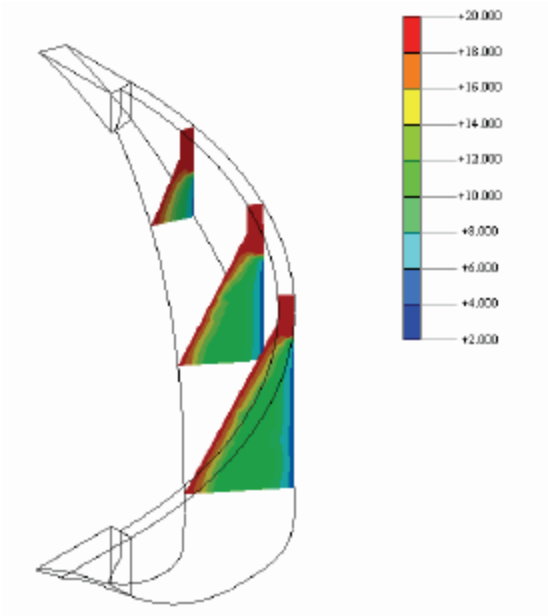

(e) T_{env} = 19.6 °C, H_{water} = 1310 m

Figure 11: Temperature contours in different cross sections of the dam for different load situations (the colour scale is the same for each load situation). The temperature in the core of the dam body is constant over the year (11 °C).

The corresponding results are summarized in the table below.

Date	Target D1 (mm)	Target D2 (mm)	Analysis D1 (mm)	Analysis D2 (mm)
06/10/1999	0.0	0.0	0.0	0.0
25/04/2000	17.5	6.0	5.6	2.8
22/08/2000	-5.0	3.0	-5.4	1.1
06/02/2001	32.0	13.0	21.3	9.0
14/08/2001	1.0	7.5	-7.7	1.9

Table 4: Relative horizontal displacements: between bottom gallery and crest of the dam (D1); between the bottom and middle gallery (D2). The temperature in the core of the dam body is constant over the year (11 °C).

The differences between these results and the results obtained with the original model (PART I) are small, especially for the relative displacement between bottom gallery and crest of the dam.

5.3 Variable water temperature over the year

The water temperature is considered equal to 14 °C at the load situations 06/10/1999, 22/08/2000 and 14/08/2001 (in the summer or close to the summer), and equal to 5 °C at the load situations 25/04/2000 and 06/02/2001 (in the spring or in the winter). The calculated displacements are as follows:

Date	Target D1 (mm)	Target D2 (mm)	Analysis D1 (mm)	Analysis D2 (mm)
06/10/1999	0.0	0.0	0.0	0.0
25/04/2000	17.5	6.0	2.7	2.5
22/08/2000	-5.0	3.0	-4.6	0.3
06/02/2001	32.0	13.0	18.7	9.0
14/08/2001	1.0	7.5	-7.2	0.1

Table 5: Relative horizontal displacements: between bottom gallery and crest of the dam (D1); between bottom and middle gallery (D2).The water temperature is considered equal to 14 ^{o}C in the summer or close to the summer, and to 5 ^{o}C in the winter or close to the winter.

The differences with the results obtained in PART I are in this case larger than in the case of constant temperature in the core of the dam body. Nevertheless, the assumption of variable water temperature over the year does not lead to a better fitting of the measured displacements.

6. CONCLUSIONS

- Advanced Finite Element software makes possible to take into account complex geometries and loadings of dams and their foundation.

With respect to the displacements measured in the La Aceca dam:

- The major role is played by the effect of thermal expansion, which dominates the effect of the hydrostatic loading.
- Temperature distribution in the core of the dam body has a relative minor effect.
- A reduced stiffness of the foundation (in the order of 0.2 GPa rather than 10 GPa) results in a better fit of the measured displacements. .
- When reduced foundation stiffness (0.2 GPa) is assumed, displacements of the dam under hydrostatic loading and thermal expansion can be reasonably well predicted even under the simplistic assumptions of linear elastic material behaviour.
- Better results may be expected when more detailed information concerning the input parameters are known: real profile of the ground surface, foundation stiffness, development of water temperature and environment temperature.

NUMERICAL SIMULATION OF AN ARCH – GRAVITY DAM BEHAVIOUR DURING OPERATION

Adrian Popovici
Professor, Head of Department,
Technical University of Civil Engineering of Bucharest, e-email: popovici@utcb.ro
Radu Sarghiuta
Associate Professor,
Technical University of Civil Engineering of Bucharest, e-mail: sarghiut@utcb.ro.

Summary. The back-analysis of some displacements recorded at a pendulum installed in the body of La Acena arch-gravity dam (H = 61 m) is carried out using ANSYS computer code. The displacements are computed in 3D and, respectively 2D finite element models using material characteristics recommended by formulator. New mechanical characteristics of materials from the dam-foundation system were considered in order to obtain a better correlation with the recordings. The back-analysis pointed out this dam works probably like a gravity dam for some load combinations.

1. Introduction

La Acena is an arch gravity dam with 61 m maximum height, belonging to the Madrid water supply system. The first impounding of the dam reservoir was performed from February 1999 until May 2001. The maximum radial displacement to downstream during first impounding was 1.8 cm.

During dam operation, after the first reservoir impounding, the recordings at that four pendulums installed in the dam body pointed out an apparently significant and unexpected increase of the dam displacements to downstream. During reference period the maximum radial displacement recorded at pendulums reached around 4.0 cm.

This problem was proposed to be analysed in the framework of the 9th ICOLD Benchmark Workshop on Numerical Analysis of Dams. The formulator asks to explain the dam behaviour based on recorded displacements at the pendulum No. 3 (located in the block No. 3) taking into account reservoir water level and air temperature time history [1].

In this paper La Acena dam behaviour is analysed according to the data supplied by formulator using ANSYS computer code [2].

2. Short description of the computer code and mathematical model

The ANSYS computer code is a commercial program developed by Swanson Analysis System Inc., well-known and frequently applied in U.S.A. and Europe. It is a large-scale general purpose program for the solution of several classes of engineering analysis problems and includes pre-processing, solution and post-processing functions.

ANSYS is used in a wide range of disciplines for solutions to mechanical, thermal and electronic problems. The computer code library consists of over 100 finite element types. Structural analysis capabilities include static and dynamic, plastics, creep and swelling, small and large defections and other applications.

The finite element back-analysis of the La Acena dam behaviour was performed in bi-(2D) and three-dimensional (3D) hypotheses.

The 3D finite element mesh of the dam-foundation system is presented in the Figure 1.

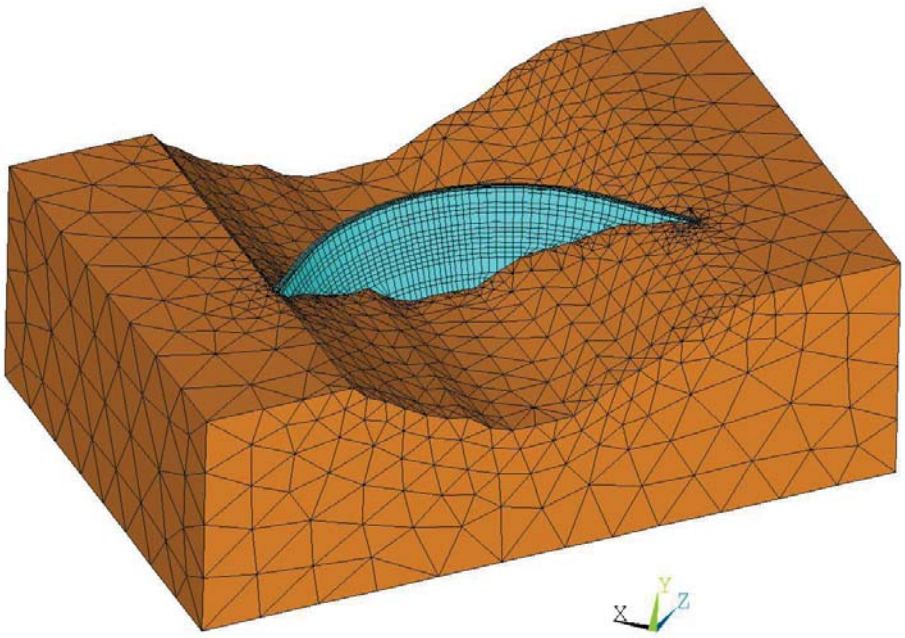

Fig.1 3D finite element mesh of the dam - foundation system

The dam body was discretized with the SOLID 45 element type, using four rows of elements on the dam thickness. This element is defined by 8 nodes and is linear, isoparametric with incompatible modes included. The type of FE mesh employed is highly dependent on the geometry of the dam.

A sufficient volume of the rock foundation extended on upstream, downstream, lateral and down-ward directions of about 1.5 H_d (H_d – dam maximum height) has been meshed with tetrahedral solid element (SOLID45). Its only role herein was to provide an elastic support of the dam.

Three-dimensional heat-flow analysis for the dam body has been performed using the same 3D model developed for the static stress analysis, but replacing the structural element type with thermal one that has a 3D thermal conduction capability. The element has eight nodes with a single degree of freedom, temperature, at each node and it is applicable to 3 D, steady-state thermal analysis.

In the Table 1 are shown some data concerning 3D finite element mesh of the La Acena dam-foundation unitary system.

Table 1

Type of the parameter	Dam body	Foundation	Total
Nodes	3601	3131	6339
Elements SOLID 45	2625	14147	16772
Degrees of freedom	10803	9393	19017

The finite element mesh used in 2D analysis is illustrated in the Figure 2. It was developed on the dam radial direction in the section with the pendulum No. 3 (block No 3).

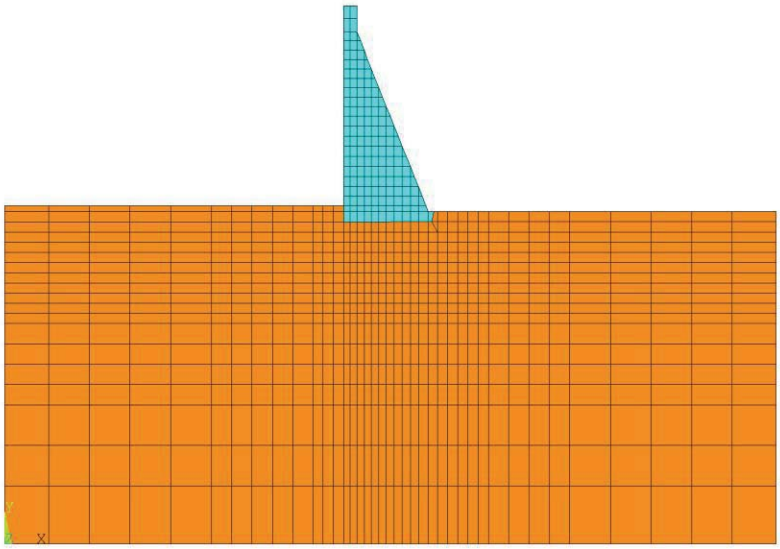

Fig.2 2D finite element mesh of the dam - foundation system for the dam section with pendulum No. 3

The same type of plane element with 4 nodes, named PLANE 42 was used for both dam body and foundation discretization. This element is linear, isoparametric with incompatible modes included.

Some data on 2D finite element mesh can be seen in the Table 2.

Table 2

Type of the parameter	Dam body	Foundation	Total
Nodes	179	765	928
Elements PLANE42	153	705	858
Degrees of freedom	358	1430	1856

3. Input data and results

In the first stage of the analysis, the mechanical/thermal data (Table 3) supplied by formulator were considered in order to compare the computed displacements at the dates proposed by formulator with those registered at the pendulum No. 3.

Table 3

Property	Foundation	Dam body
E (bulk modulus)	10000 MPa	20000 MPA
Poisson's ratio	0.2	0.2
Coefficient of thermal expansion	0	$10^{-5}\ ^{0}C^{-1}$

The monthly average air temperature was applied on the dam faces in contact with the atmosphere. For the interested dates they were extracted from the table showing historical monthly average temperatures in Peguerinos station (near La Acena's dam) and are presented in the Table 4.

Table 4

Date	Monthly average air temperatures °C
06/10/1999	11
25/04/2000	8.2
22/08/2000	19.6
06/02/2001	3.7
14/08/2001	19.6

It is known that reservoir water temperatures follow air temperatures with some delays increasing with depth from the water free surface and with amplitudes decreasing with the water depth. At about 60 m depth the water temperature is constant and equal to 4.5 °C [3].

The deepnesses of the reservoir water in the Block No.3 section and at the interested dates were moderate ones (excepted 58.20 m at 06/02/2001) varying between 29.4 m and 49.73 m. In these conditions in the present application the reservoir water temperature was considered constant one and equal to 8 °C (this means 2 °C less than multiannual average air temperatures).

The same temperature of 8 °C was considered on the contact dam-foundation. In the steady-state thermal analysis was considered only dam body.

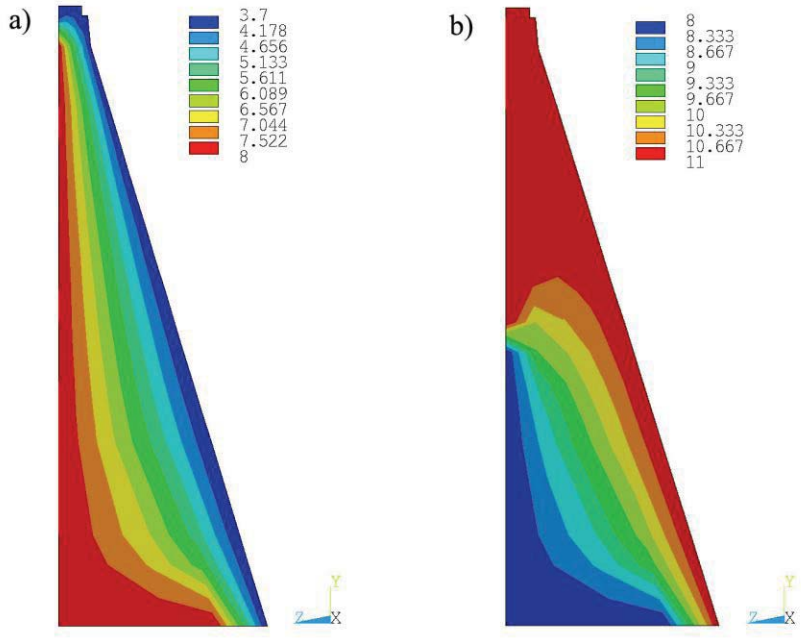

Fig.3 Contours of the dam body temperatures at: a) 06/10/1999 and b) 06/02/2001

The temperature contours in the Block No. 3 for two representative dates can be seen in the Figure 3.

In order to compute the dam-foundation response (displacements, strains, stresses) to the temperature action, the reference temperature (corresponding to dam body temperatures at the contraction joints grouting moment) was needed to consider. Lacking other information, the reference temperature was considered equal to 10 °C.

A general view of the dam displacement contours generated by hydrostatic pressure and temperatures at two requested dates by formulator, respectively 06.10.1999 and

06.02.2001 are illustrated in the Figure 4. It can be remarked that dam structure was considered as monolithic one, meaning that the contraction joints were not modelled. Moreover, the uplift pressure was neglected taking into account the thickness of the dam base is small one. The analysis was performed in the linear elastic hypothesis.

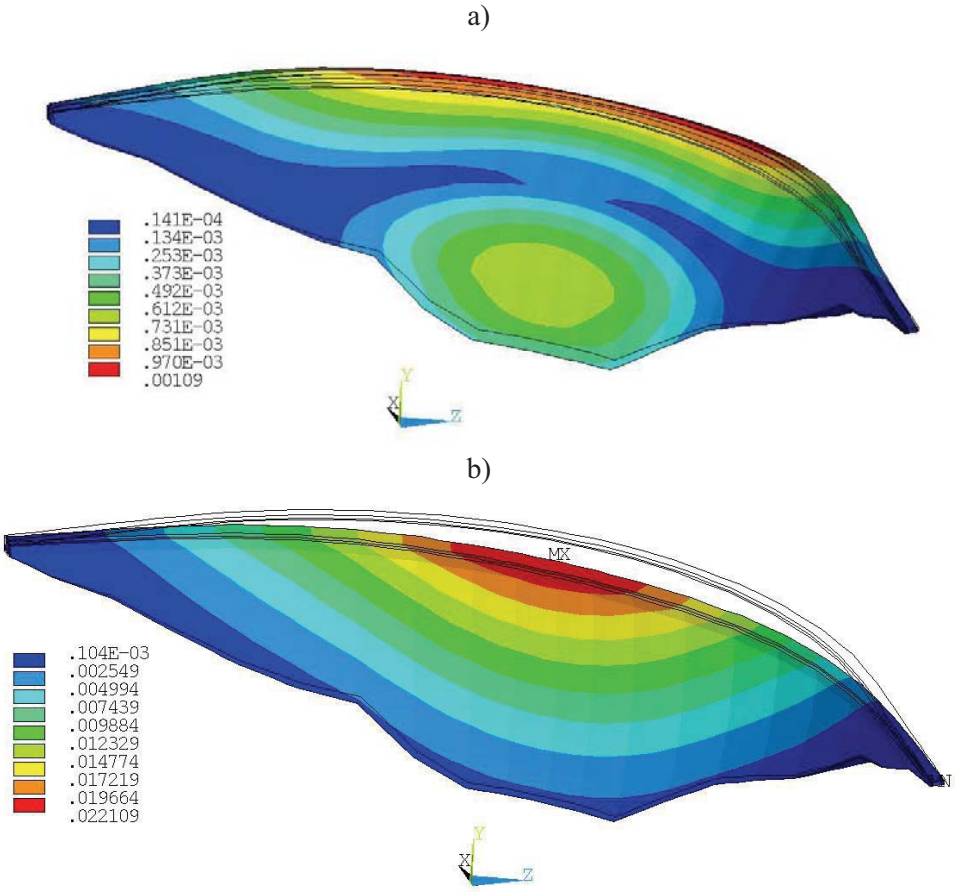

Fig. 4 General view of the dam displacements due to hydrostatic pressure and temperatures: a) 06/10/1999; b) 06/02/2001

For the same dates, the contours of the radial displacements in 2D analysis, in the section including pendulum No. 3, due to hydrostatic pressure and temperatures are presented in the Figure 5.

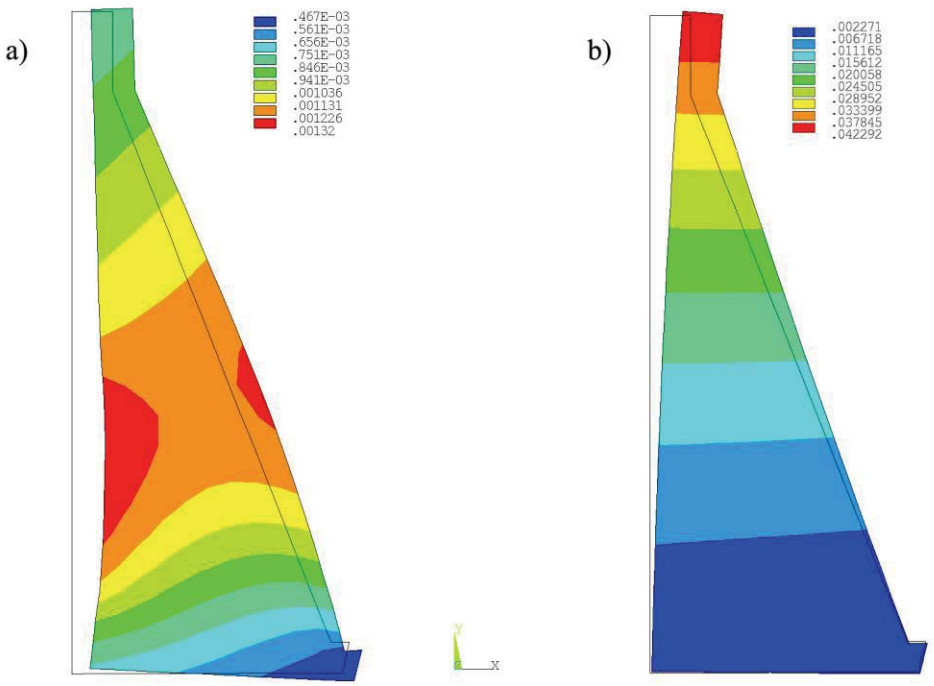

Fig. 5 2D model - Radial displacements due to hydrostatic pressure and temperatures in the dam section with pendulum No. 3 at: a) 06/10/1999; b) 06/02/2001

A synthesis of the horizontal displacements computed/recorded in the section including pendulum No. 3 obtained in the 3D and 2D analyses using the mechanical/thermal data, recommended by formulator is presented in the Table 5 and the Figure 6a,b.

Table 5

Data	Recorded		Computed 3D analysis		Computed 2D analysis	
	Dis 1 (mm)	Dis 2 (mm)	Dis 1 (mm)	Dis 2 (mm)	Dis 1 (mm)	Dis 2 (mm)
06/10/1999	0.	0.	-1.3	0.0	0.0	0.0
25/04/2000	17.5	6.3	4.4	2.2	9.4	4.1
22/08/2000	-6.5	3	-10.1	0.1	-3.3	1.2
06/02/2001	33.3	12.9	17.4	5.7	33.37	11.65
14/08/2001	-4.3	4.6	-9.4	0.9	0.1	-2.8

(+) to downstream direction

Dis 1: incremental horizontal displacements from lower gallery to the dam crest
Dis 2: incremental horizontal displacements from lower to intermediate gallery.

At the first view, it may remark that 2D analysis displacements are closer to recorded displacements than their correspondent from 3D analysis. The displacements computed by 3D analysis are smaller than their corresponding recorded displacements excepting Dis1 in 22.08.2000 and 14.08.2001. The conclusion is that the stiffness of the dam-foundation system considered in 3D analysis was too high.

a)

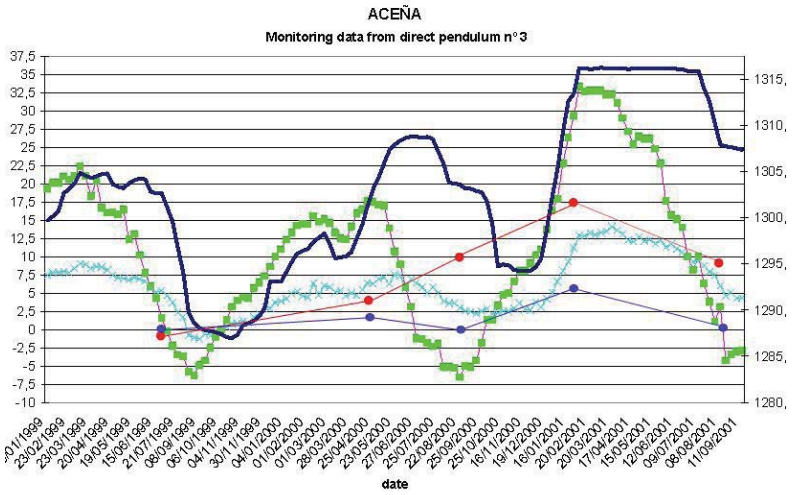

b)

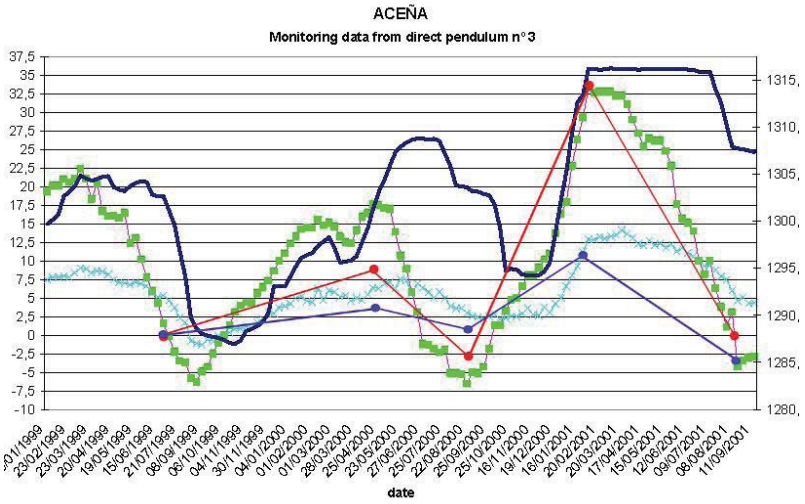

c)

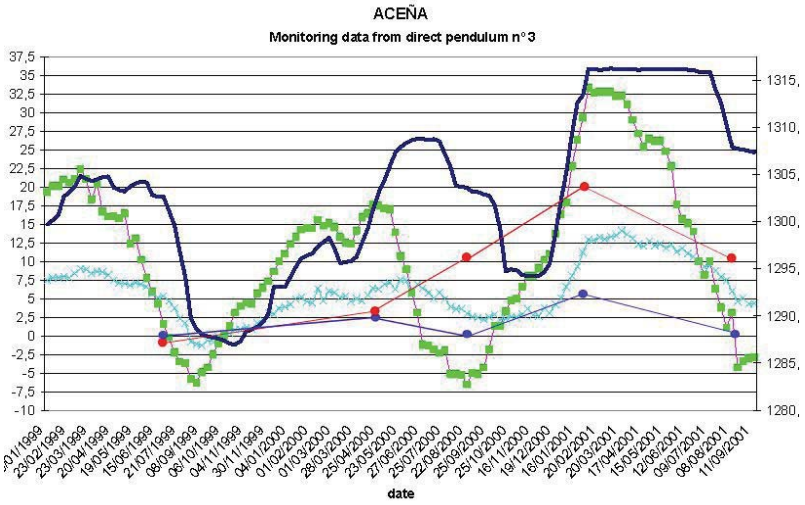

Fig. 6 Comparison between computed and recorded radial displacements in the dam section with pendulum No. 3: a) - 3D model using the dam-foundation mechanical characteristics recommended by formulator; b) - 2D model using the dam-foundation mechanical characteristics recommended by formulator; c) - 3D model using the dam foundation mechanical characteristics proposed by authors.

In order to reduce the difference between recorded/computed displacements, the stiffness of the dam-foundation system was diminished, using new material mechanical characteristics to the inferior limit usually accepted for this type of dam. The new mechanical characteristics are presented in the Table 6.

Table 6

Property	Foundation	Dam body
E (Young modulus)	7000 MPa	18000 MPA
Poisson's ratio	0.2	0.2
Coefficient. of thermal expansion	0	$1.2*10^{-5}\ ^0C^{-1}$

The displacements computed with the new material mechanical characteristics are presented in the Table 7 and the Figure 6c.

Table 7

Date	Computed 3D analysis, new material mechanical characteristics	
	Dis 1(mm)	Dis 2 (mm)
06/10/1999	-1.5	0.0
25/04/2000	5.1	2.6
22/08/2000	-11.6	0.1
06/02/2001	20.0	6.6
14/08/2001	-10.8	0.9

In the new conditions concerning material characteristics the displacements taken into analysis increased with 10…27% versus their correspondents computed with material characteristics recommended by formulator. However, they don't reach the recorded displacements excepting Dis1 in 22.08.2000 and 14.08.2001. The performance of the computed displacements versus recorded ones would be improved taking into account a better evaluation of the dam body temperatures.

4. Concluding remarks

On the basis of above presented data, it may be concluded as follows:

● The increase in time of the gravity or arch dam displacements to downstream in the first years (decades) after reservoir impounding is not an atypical phenomenon.

It has been observed that during first filling the gravity dam crest can move upstream or have downstream displacements conspicuously smaller than expected. This phenomenon can be explained by cooling of the dam upstream face by reservoir water and also by the water load on the bottom of the reservoir causing the upstream shifting of the dam [4].

During operation, the interstitial pressures due to seepages in the reservoir and dam foundation, concrete creep and shrinkage, abutment displacements can generate displacements to downstream [5]. [6].

A statistical analysis performed on 46 arch dams in France has pointed out that 58% from these dams after first reservoir filling have registered increasing irreversible displacements to

downstream which generally stopped after few decades or in few cases they have continued even if 40 years had passed since the first reservoir impounding [5].

● The computed displacements in the 3D finite element model using ANSYS computer code and mechanical/thermal material characteristics recommended by formulator versus corresponding displacements recorded at the pendulum No.3 are generally smaller. The computed displacements in the 2D model are closer to the corresponding displacements recorded at the pendulum No.3, than those computed in the 3D model. These results lead to the conclusion that the contraction joints grouting work was not very efficient one and, the dam blocks work independently one another for some load combinations or with very small interaction.

● In order to improve the performance of the 3D model the stiffness of the dam-foundation system was decreased using new material mechanical characteristics corresponding to the inferior limit usually accepted for dams like La Acena. In this case the displacements taken into account increased with about 15% versus their correspondents computed with characteristics given by formulator, but they continued to be generally smaller than recorded ones. The conclusion is the hypotheses about dam body temperatures considered in this paper are a very coarse approximation of the real temperatures.

References

1. Ignacio Escuder Bueno, Francisco Blazquez Prieto. Analysis of the elastic behaviour of an arch gravity dam. Proceedings IX-th ICOLD Benchmark Workshop on Numerical Analysis of Dams. Theme A, Sankt Petersburg, 2007.
2. *** ANSYS – User's Manual. Swanson Analysis System, Inc., Houston, USA.
3. Popovici, A., Popescu C. Dams for water storage. 1st Volume (in Romanian) Editura Tehnica, Bucharest, 1992.
4. Bonaldi, P., Fanelli, M., Giuseppetti, G., Mazza, G. Pseudo-3D analysis of the effects of basin deformations: comparison with experimental measurements. ISMES Publications, No.74, Bergamo, 1982.
5. Fabre, J.P., Bourdarot, E. Analysis of the long term behaviour of arch dams. Proceedings 21st ICOLD Congress, 2nd Volume, Q82 – R43, Montreal, 2003.
6. Popovici, A., Ilinca, C. Comments upon irreversible displacements from Bradisor arch dam. Scientific Bulletin TUCEB, No.1, Bucharest, 2007.

THEME B

Embankment Dams

International Commission On Large Dams

AD Hoc Committee on Computational Aspects of Analysis and Design of Dams

9th Benchmark Workshop on Numerical Analysis of Dams

22 -24 June, 2007 - St.Petersburg, Russia

THEME B – Embankment Dam

Stress-strain state of high rock-fill dam with a central earth core at large amplitude of operation water level changes in the upstream

Formulator: **Dr S.I.Panov**

Vedeneev VNIIG Inc.
Gzhatskaya Str. 21, St. Petersburg,
195220, Russia
pansta@concrete.vniig.ru

Introduction

Information about the structure

The rock-fill dam of Kolymskaya HPS (Fig.1) with a central earth core has maximum height of 130 m with length of 780 м over the crest. The mean ratio of upstream slope of the dam is 1:1.8, that of the downstream - 1:1.7. Four berms of 7 m wide each are located on the downstream slope higher the elevation of 353 m with intervals 15-30 m over the height of the dam. Layout of the main structures of Kolymskaya HPP is shown on Fig. 2.

The dam is located in the north-eastern extremity of the Asian continent, Magadan district, the Kolyma River. The area belongs to the Far North and is characterized with sharp continental climate with very cold winter and warm-temperate summer. The annual amplitude of air temperature fluctuations reaches 97°C. The average annual air temperature is minus 12°C, the average temperature in January is minus 38°C, in July - +15°C. The absolute minimum of air temperature is minus 61°C, the absolute maximum is +36°C. The territory belongs to the zone of continuous propagation of permafrost.

Fig.1 The dam of Kolymskaya HPS.

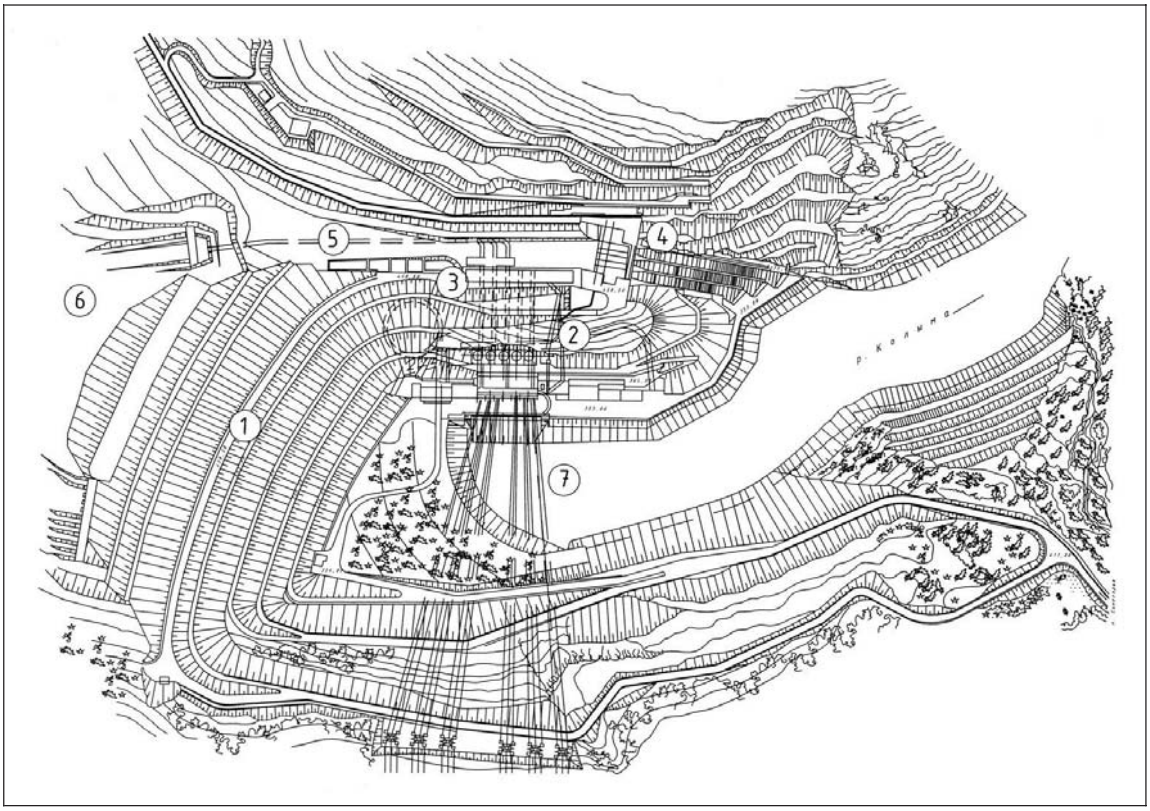

Fig.2. Layout of the main structures of Kolymskaya HPP
1- dam, 2 – underground complex of the powerhouse hall, 3- water inlet, 4 - spillway, 5 – head race, 6 - reservoir, 7 - downstream

The core of the dam is filled with gruss clay loams (Fig.3). The inverse filter from the side of the upstream up to elevation 432 m consists of a single layer and made of sand-gravel mix (SGM), above – it consists of double layer and made of sand and SGM. The downstream filter consists of double-layer and is also made of sand and SGM. The side prisms of the dam are filled with non-sorted rock mass. At the base of the dam along the core axis a grout curtain is arranged.

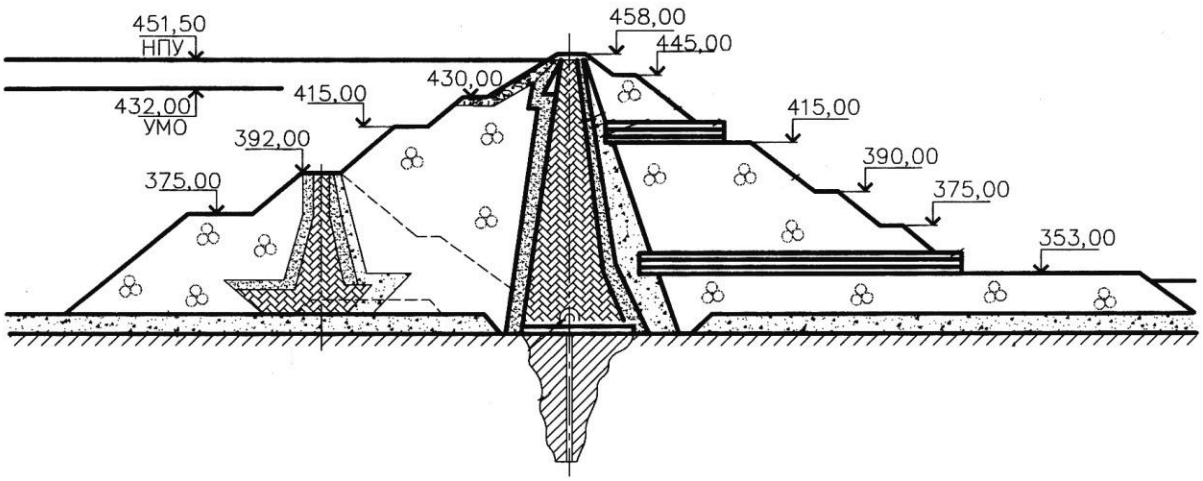

Fig. 3. Structural scheme of the maximum dam cross-section of Kolymskaya HPP
1 – temporary dam, 2 – earth core, 3, 4 – layers of filter, 5 - downstream prism,
6 - control equipment galleries, 7 - grouting gallery, 8 - cutoff curtain

At present the upstream prism, filter, core and the first layer of the downstream filter below the depressive curve are in thawed state, the downstream retaining prism and the second layer of the filter are mainly in permafrost state (Fig.4).

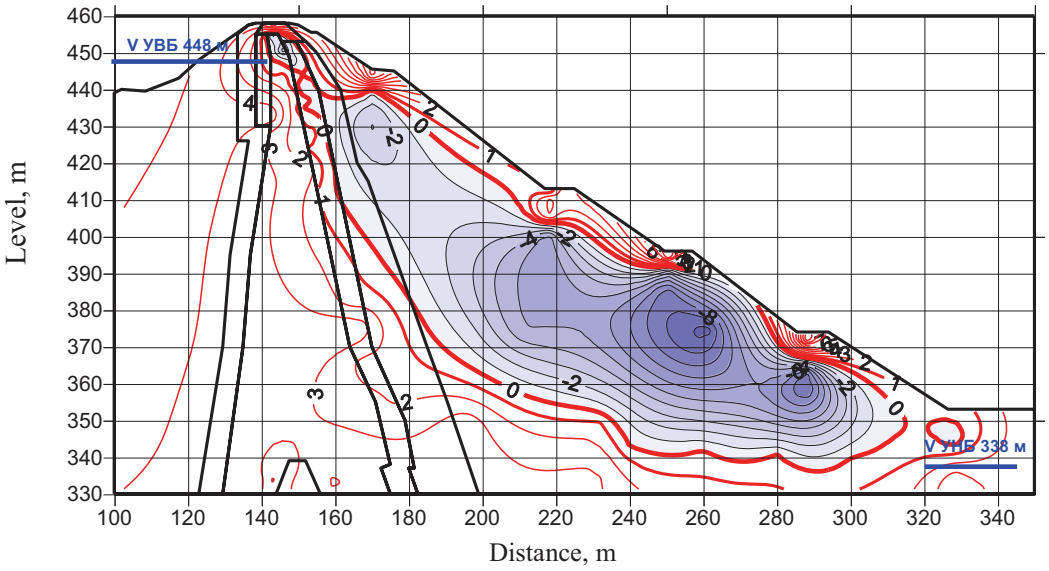

Fig.4. Temperature state of downstream prism.

The foundation of all hydraulic structures of Kolymskaya HPP are represented by powerful massive of granites weathered on the surface and remained intact at depth with relatively high strength properties. The granites are practically watertight in the frozen state. After melting they acquire very high permeability.

The feature of operation of the Kolymskaya HPP that influences on strain behaviour of the dam is large amplitude of seasonal change of upstream level from elevation 432m (minimum drawdown level) to elevation 451.5m (NPL - normal pool level). For the first time the water level in the reservoir was raised to elevation NPL in 1994, therefore the beginning of operation of the hydraulic facilities in the design conditions refers to 1995.

Information of the dam behavior at operation

The system "dam-foundation" is quite well equipped with control instrumentation including soil temperature sensors, piezometric pressure sensors and sensors for deformation processes in the dam body soils.

According to the in-situ observation data (fig. 4) at the present time the dam upstream prism, upstream transition zone, soil core and the first layer of the dam downstream transition zone are permanently in the thawed state. Considerable parts of the downstream retaining prism and the second layer of the downstream transition zone are constantly frozen with low temperature values (up to minus 16-18^{o}C). This can influence on the dam deformation behavior because the sand-gravel soils and rock mass in the frozen state have got considerably higher strength and less deformability in comparison with the similar features of such soils in the thawed state (Table 1).

Comparison results of the settlement measurements and the dam crest horizontal displacements demonstrate that the annual upstream level changes considerably influence on the dam deformation character both in horizontal and vertical directions.

Initial data

It is suggested to use for calculation the dam cross-section maximum by its height that is shown in fig. 3. The outline of the permafrost zone formed by the present time in the downstream retaining prism of the dam is shown in fig. 4. The scheme of the evaluated cross-section division to inhomogeneous soil zones and the finite elements of the first level could be provided to participants.

- Geometry of the dam maximum cross-section over the height is shown in Fig. 3. The layout of the multiyear frost formed in the downstream retaining prism of the dam is shown in Fig. 4.

- It is possible to accept the following physical and mechanical characteristics according to the data of experimental investigations of the soils of the dam body.

- According to the operation data the design filling of the reservoir up to elevation NPL was carried out in 1995. For the next ten years the reservoir is annually being filled by the end of August up to elevation 452 m, then for the winter period it drawdowns up to elevation 432 m. So the amplitude of annual water level changes in the reservoir reaches 20 m that results in corresponding change of hydrostatic head on the dam.

Table 1

Types of soils	γ, t/m^3	Measurement range		C, MPa	tgφ
		E, MPa	ν		
Rock mass of downstream prism, frozen	2.2	20- 100	0.25-0.35	0.5	0.90
Rock mass of downstream prism, melt	2.1	20-60	0.30-0.35	0.05	0.75
Rock mass of upstream prism, melt, weighted	1.1	10	0.30-0.40	~0	0. 65
SGM of transition zones of downstream prism	2.0	35-60	0.30-0.35	0.01	0.70
SGM of transition zones of upstream prism, weighted	1.1	15	0.30-0.40	~0	0.60
Clay loam of the core	1.8	45-60	0.30-0.35	0.02	0.55

- Data of field observations of settlements (S) and horizontal displacements (U) of the dam crest in its maximal cross-section for the last 5 years of operation in the design conditions (1999 is conditionally accepted as time reference):

Table 2

Crest displacement	Years of observations						
	1999	2000	2001	2002	2003	2004	2005
S, mm	0	83	159	228	292	350	?
U, mm	0	69	126	175	217	253	?

- According to the data of field observations, settlement distribution of the berms of the dam downstream slopes is practically proportional to their altitude position.
- The pattern of horizontal displacements distribution of the berms of the dam downstream slopes is shown in Fig. 5.
- For the period passed from the completion of construction (about 20 years ago) the surface of the upper part of the upstream slope (in the zone of water level change) was subjected to settlements exceeding considerably the settlement of the crest; the depth of the cone of maximum declinations from the design position reached 4-4.5 m.

Aim of the theme

Perform static analysis of stress-strain state of cross-section of the dam of Kolymskaya HPP and compile prognosis of changes with time of stresses, settlements and horizontal displacements of the elements of its profile in 2005 during operation of the reservoir in design conditions of impoundment.

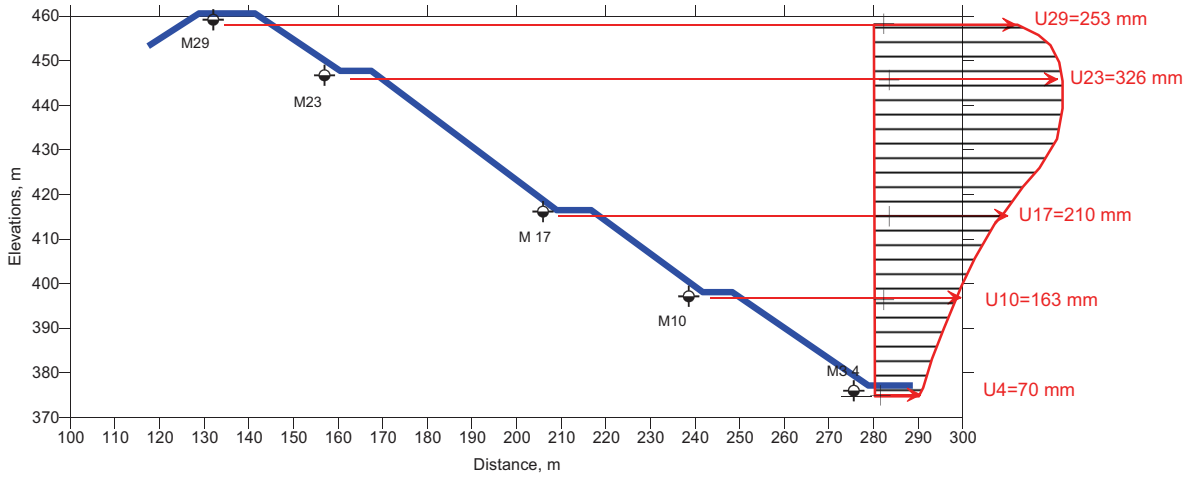

Fig. 5. The pattern of horizontal displacements distribution of dam downstream slope in 2004

Special conditions

At choice of a design model and performing analysis it is necessary to take into account:

- inhomogeneity of properties of soils of design section;
- elastoplastic deformation and creep of soils;
- essential differences in the values of instant and long-term strength and deformability of frozen rock mass of the downstream prism;
- load anisotropy of thawed non-coherent soils of the upstream retaining prism in tension and in compression;
- non-cohesion and looseness of sand and sand-pebble soils of the upstream transition zone (their potential ability for moving downwards with horizontal displacements of the core under action of hydrostatic load changing in seasons).

STRESS-STRAIN STATE OF ROCKFILL-EARTH DAM WITH CENTRAL SOIL CORE AT GREAT AMPLITUDE OF OPERATION UPSTREAM WATER LEVEL CHANGES (BY THE EXAMPLE OF KOLYMSKAYA HPP)

Prof. Stanislav PANOV

(B.E. Vedeneev VNIIG, Saint-Petersburg)

1. INTRODUCTION

The aim of the theme B is to evaluate the stress-strain state of cross-section of the Kolymskaya HPP rockfill-earth dam (H=130 m, Russia) at seasonal changes of the reservoir water level during HPP operation. It was suggested to predict changes of the settlements and horizontal displacements on basis of the results of numerical evaluation and statistical analysis of the in-situ observation data.

The data presented by the theme formulator to solve this problem were received from dam safety monitoring for the last 5 years of the dam operation (1999-2004) include:

- geometrical dimensions of the design cross-section;
- physical and mechanical characteristics of the dam body soils;
- data of the seasonal water level changes in the reservoir;
- data of the annual settlement increments and dam crest displacements for the last 5 year of operation;
- data about abnormal deformations of the dam upstream side surface in the zone of the seasonal water level changes in the reservoir.

Requirements to the choice of design model

The design model of the dam stress-strain state should be chosen taking into account:

- inhomogeneity of properties of soils of design section;
- elastoplastic deformation and creep of soils;
- load anisotropy of soils deformability;
- non-cohesion and looseness of sand and sand-pebble soils of the upstream prism;

Deformations of the dam calculated taking into account the presented in-situ observation data allow to predict the dam deformation behavior and also correspond satisfactorily to the control data observed in 2005.

2. LIST OF PARTICIPANTS

Unfortunately only one participant Mr. Bachir Touileb (Hydro-Québec, Montréal, Québec, Canada) presented the report on the theme B named "Analysis of the long term behaviour of Kolymskaya Dam (Russia) under full design conditions".

As the report of Mr. Bachir Touileb is fully given below, we can comment it briefly here.

Mr. Bachir Touileb was absolutely right when he had emphasized two ways to solve the given task. The first way is a brief forecast of dam deformations, based on the in-situ observation data analysis with the use of the so called "statistical evaluation model". The second one is more detailed and comprehensive and is connected with the development and corresponding calibration of the "phenomenological computation model".

Due to lack of time given for preparation of the report, on this stage Mr. Bachir Touileb realized only the statistical approach to solve the task. This way is quite efficient and gives good results but only for the short prediction period.

Really, the comparison of the predicted settlement values and horizontal dam crest displacements in 2005, obtained by Mr. Bachir Touileb, with the available in-situ observation data demonstrates the satisfactory coincidence of these data. The forecast error is not more than 5-10%. However the predicted values obtained for a longer period have got a greater error.

In particular the actual values of the annual settlement increments and horizontal dam crest displacements based on the in-situ observation data even now exceed the values determined by the forecast of Mr. Bachir Touileb.

3. COMPUTATION MODEL

To clarify the essence of deformation processes in the dam and to predict changes of the dam settlements and horizontal displacements for a long period the most promising way is creating of an adequate "phenomenological computation model". Such model will allow forecasting dam deformation more substantially and help to understand the reasons of the specific deformation behavior of the structure.

According to the in-situ observation data the dam deformation behavior during its operation in the project regime has got the following main peculiarities:

- the seasonal changes of settlements and horizontal displacements have not practically got the elastic component and are of pure plastic character with gradual decay of their annual increment values;
- the dam downstream berm at the height of 445 m have abnormally small values of the annual settlement increments and abnormally great values of the annual horizontal displacement increments at seasonal water level changes in the upstream (upstream level (UL));
- during rise of upstream level the horizontal displacements of the dam crest are actively increasing and the settlement increments at this time have practically zero values; during UL descending this relationship is changing vice versa – the crest settlement is actively increasing whereas the horizontal displacement increments do not practically change;
- after the dam had been constructed the near-crest part of the dam upstream side experienced abnormal great settlements, which were considerably more than the maximum settlement of the structure crest.

The information given above allows to consider that the character of the elements deformation of the dam free surface is determined by complicated kinematics of displacements of the structure top part at seasonal hydro-static load changes.

To prove this suggestion we carried out the numerical solution of the problem on the dam stress and strain changes at cyclic water level variation in the upstream. The peculiar features of the results are discussed below.

3.1 Finite-element mesh of the design section

The dam cross-section maximum by the height was accepted as the design section.. The scheme of design section zoning by soil inhomogeneity and finite elements of the first level is shown in Fig. 1.

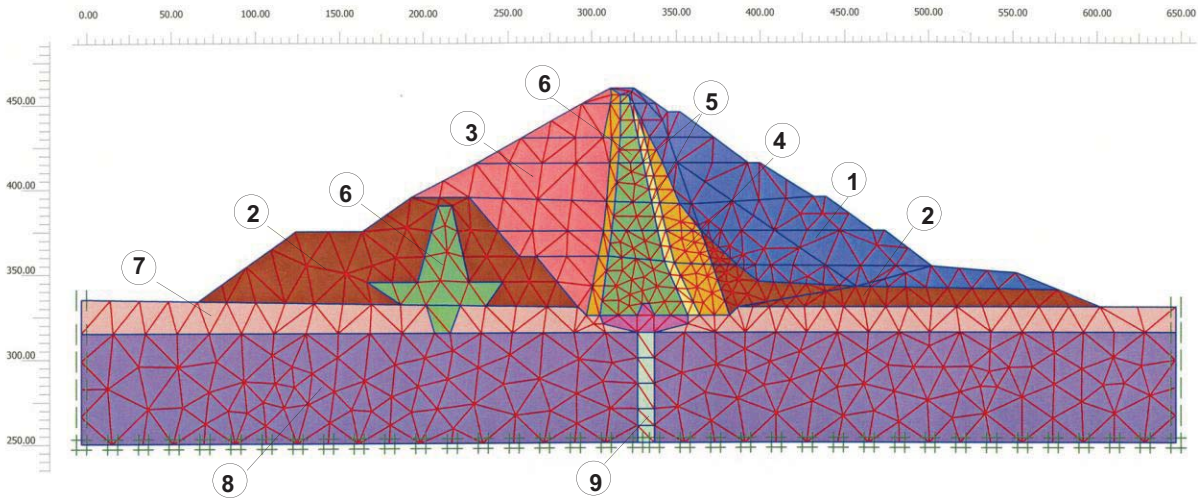

Figure 1. Dam design section zoning by soil inhomogeneity
1 - frozen rock fill, 2 - thawed rock fill, 3 - underwater thawed rock fill, 4 - sand-gravel soil, 5 - sand, 6 - loamy soil, 7 - river alluvium, 8 - foundation rock, 9 - cement-grout curtain

3.2 Material characteristics

The physical and mechanical characteristic values (Fig. 1) of the dam body soils were accepted according to the experimental study data. They are given in Table.

Type of soil		Value change ranges				
№	Name	γ, т/м^3	E, MPa	ν	C, MPa	tgφ
1	Rock mass of downstream prism, frozen	2.2	20-100	0.25-0.35	0.5	0.90
2	Rock mass of downstream prism, thawed	2.1	40-60	0.30-0.35	0.05	0.75
3	Rock mass of upstream prism, thawed, weighted	1.1	20-30	0.30-0.40	~0	0. 65
4	Sand-gravel soil of transition zones	2.0	30-60	0.30-0.35	0.01	0.70
5	Sand of transition zones	1.1	25	0.30-0.40	0.01	0.60
6	Loamy soil of the core	1.8	30-40	0.30-0.35	0.02	0.55

3.3 Loads

According to the operation data the first reservoir impounding up to the headwater level (HWL) height was carried out in 1995. For the next decade the reservoir was impounded annually up to the 452 m height by the end of August and then in winter it was discharged up to the 432 m height (Fig. 2).

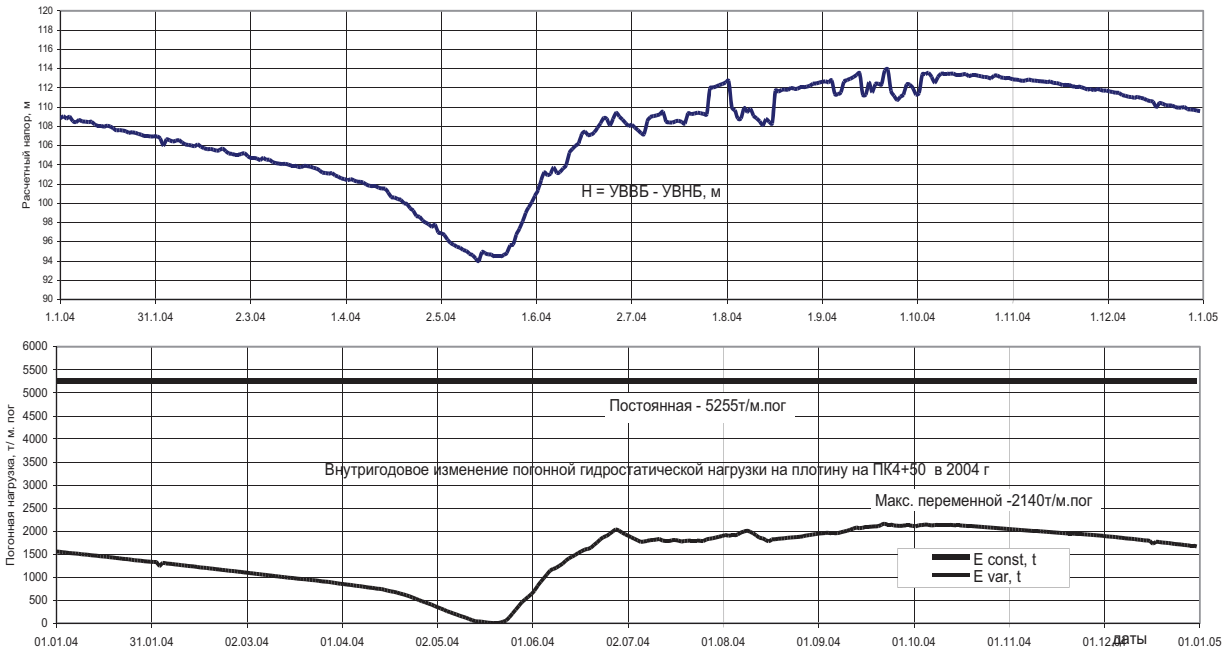

Figure 2. Seasonal changes of the upstream water level and hydro-static load on the dam

Fig. 2 shows that the maximum amplitude of the annual water level changes in the reservoir achieves 20 m.

In in-situ conditions the instrumentation measurements of settlements and horizontal displacements are carried out twice a year – at the minimum and maximum water levels in the reservoir. That is why the dam stress-strain state was calculated for a number of annual cycles of the upstream level changes in the range of "432-453-432".

3.4 The design model and calculation results

The solution was carried out by the program package PLAXIS 8.5 for the elastic-plastic model of the soil. There was used step-by-step decreasing of design values of long-term soil strength characteristics of the downstream retaining prism for every cycle. According to the known literature data the following assumption was accepted in the evaluation: soil strength decrease because of creeping occurs basically due to parameter C changes in time at practically constant values of the parameter $tg\varphi$.

Some main solution results of this task are given further.

The evaluation results demonstrate that distribution of increments of the dam residual (plastic) displacements after the annual cycles of reservoir water level changes is of a complicated character.

Fig. 3 shows that in top part of the cross-section in the zone of conjugation of the upstream retaining prism with the core the vectors of the general displacement increments are directed downward and to the downstream side. Relatively great settlements of the core top part and horizontal displacements of its central part as well as relatively small upward displacement of its low part are dominated in the core. In the body of the downstream retaining prism, in its upper part, the displacement increment vectors are basically directed horizontally to the side of the downstream. In the low part of this prism the displacement vectors are directed down and to the downstream side due to settlements increase.

Comparison of the evaluations results for different years of the structure operation (Fig. 3a, b) showed that decreasing of the absolute values of the annual displacement increments in time does not affect the character of their distribution in the design section.

The identified particularities of the dam deformation behavior at its cyclic loading are clearly reflected on the free surface displacements.

Fig. 4-7 demonstrate that the near crest part of the dam upstream prism experiences abnormal great settlements every season, which exceed the maximum settlement of the dam crest located above. The berm of the dam downstream at the 445 m height has abnormally great values of the annual horizontal displacement increments and abnormally small values of the annual settlement increments.

Undoubtedly the used elastic-plastic soil model, standard for the program PLAXIS, is quite simple and does not reflect all specific features of the behavior of the rockfill-earth dam with central core at cyclic loading by variable hydro-static load. Nevertheless the qualitative compliance of the obtained calculation results with the data of in-situ observations for structure deformations allows to consider further study of stress-strain state for such structures as prospective with the use of the other more complicated soil models.

In general, the problem on the theme B has not been yet solved, that is why it could be discussed at the next similar seminar.

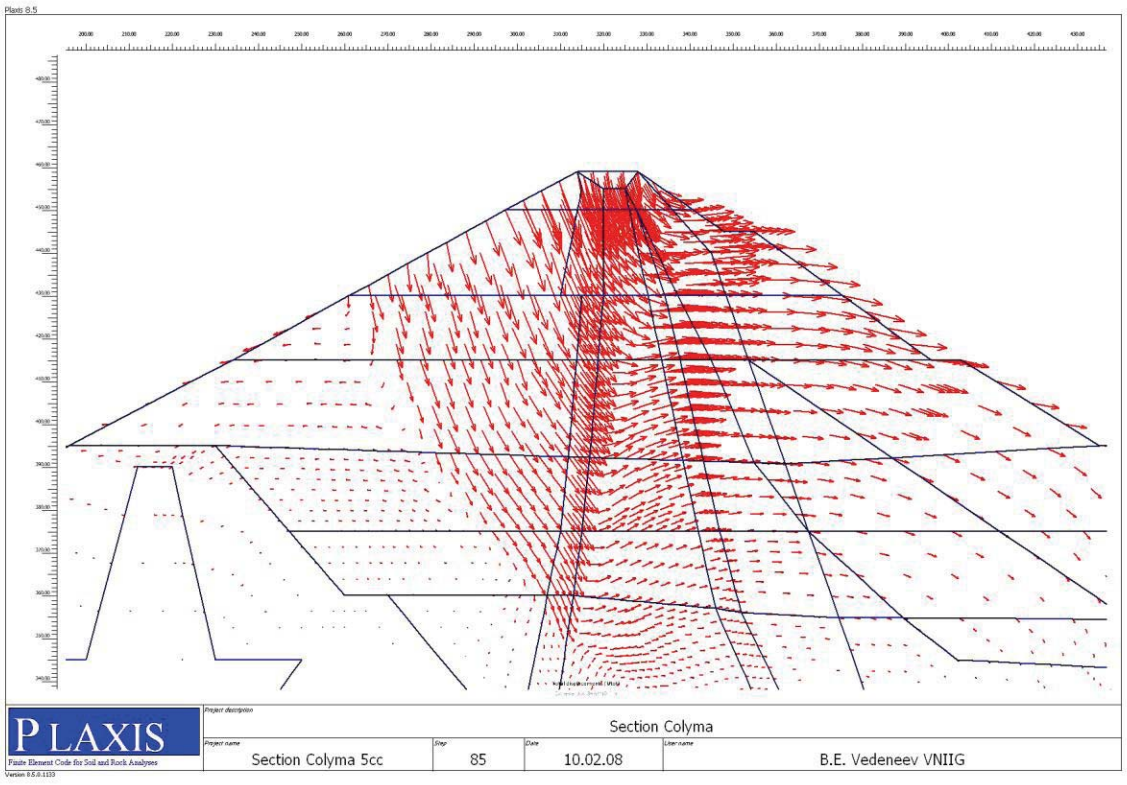

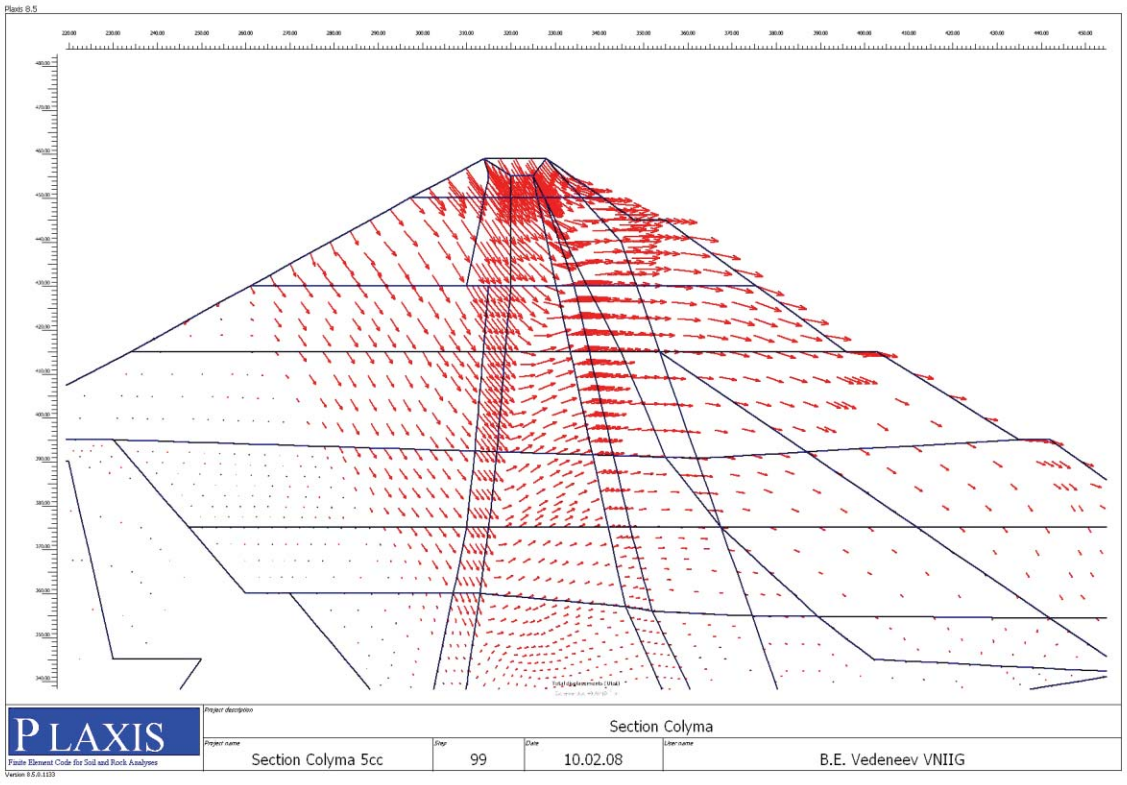

Figure 3. Vectors of the general residual (plastic) displacements of the dam elements after annual cycles of upstream water level changes in the range of "432-452-432 m" in 2001 (a) and 2005 (b).

..

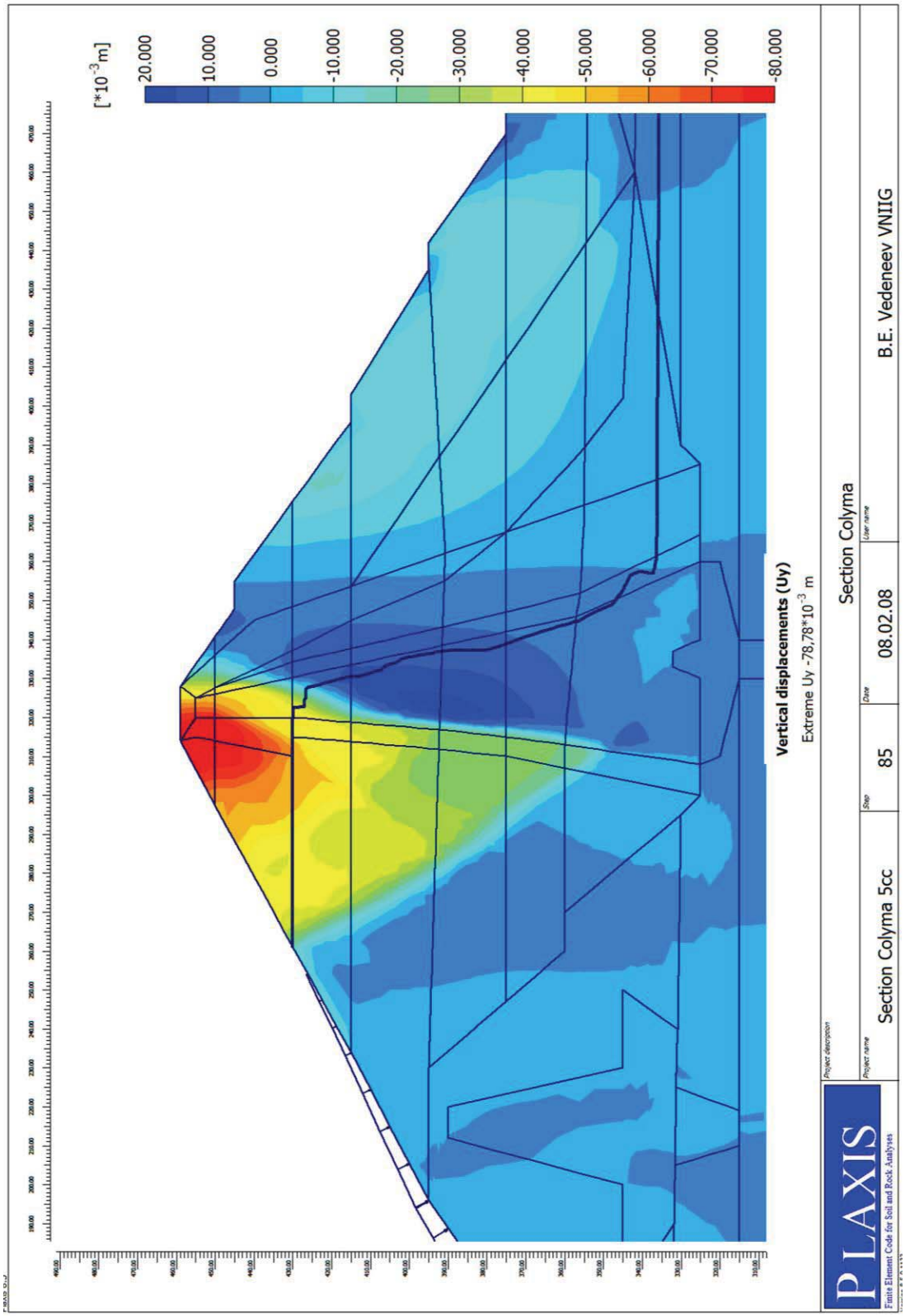

Figure 4. Settlement increments distribution in the dam design section in 2001 after finishing the annual cycle of the upstream level changes "232-252-232".

…

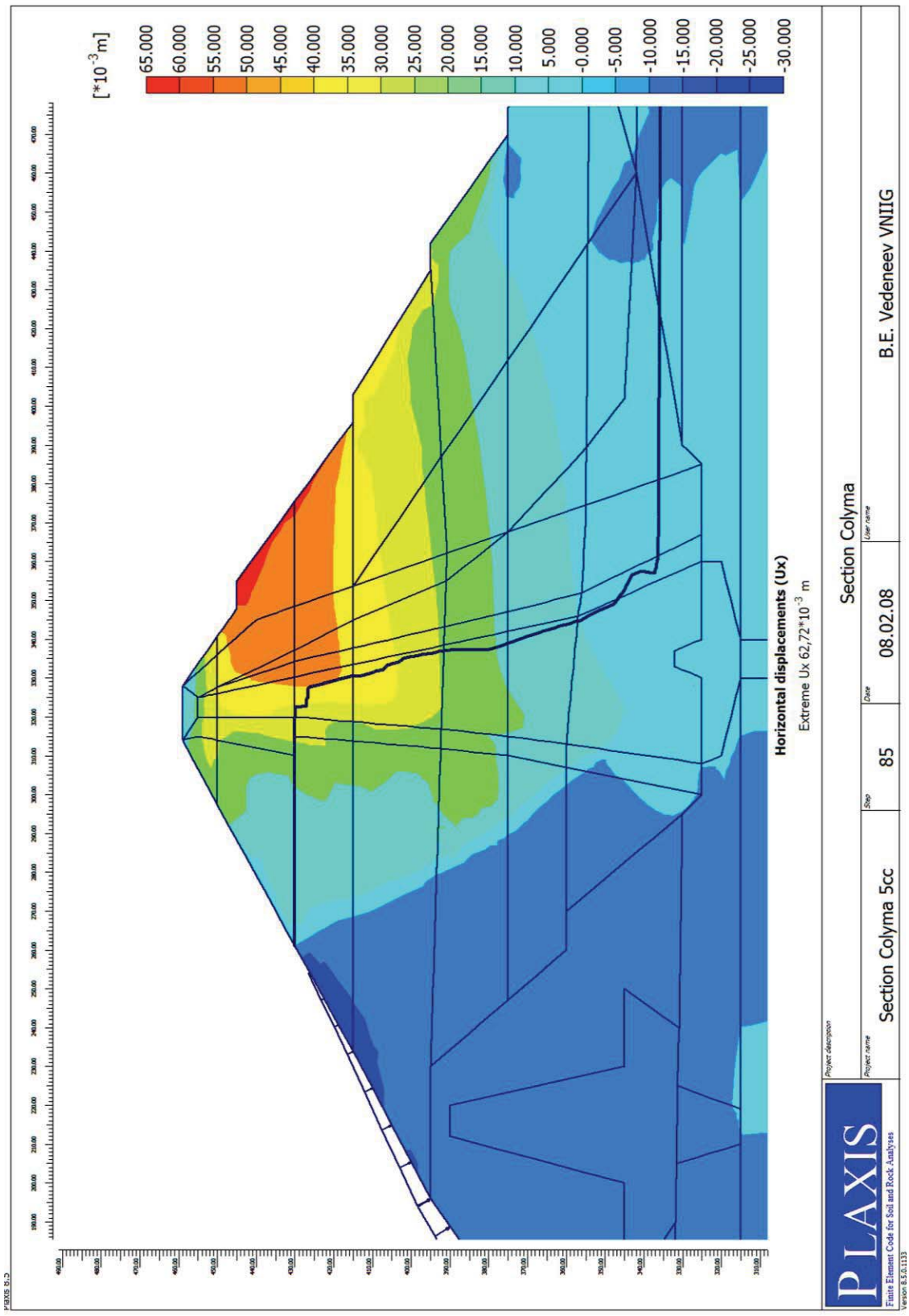

Figure 5. Horizontal displacement increments distribution in the dam design section in 2001 after finishing the annual cycle of the upstream level changes "232-252-232".

…

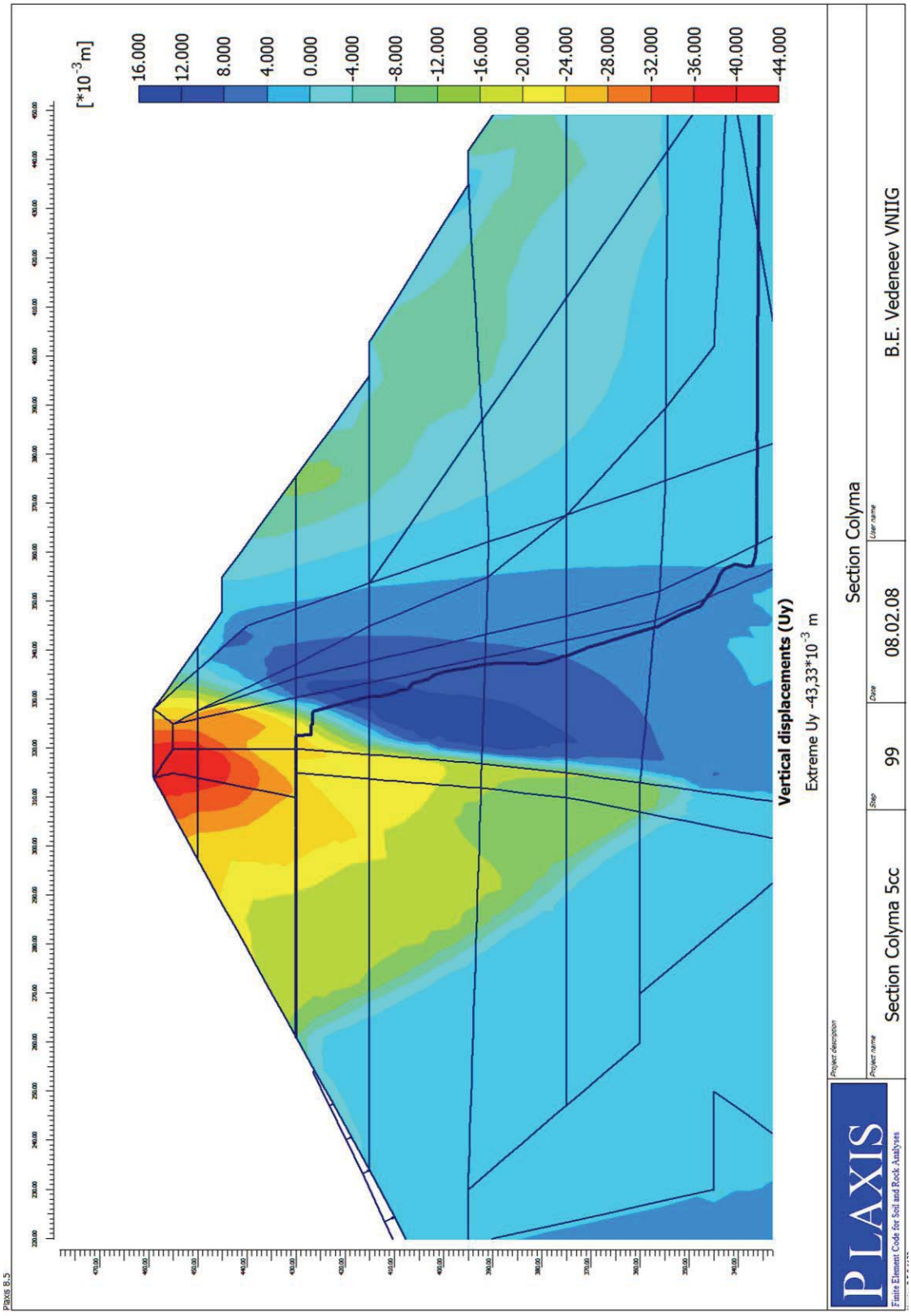

Figure 6. Settlement increments distribution in the dam design section in 2005 after finishing the annual cycle of the upstream level changes "232-252-232"

…

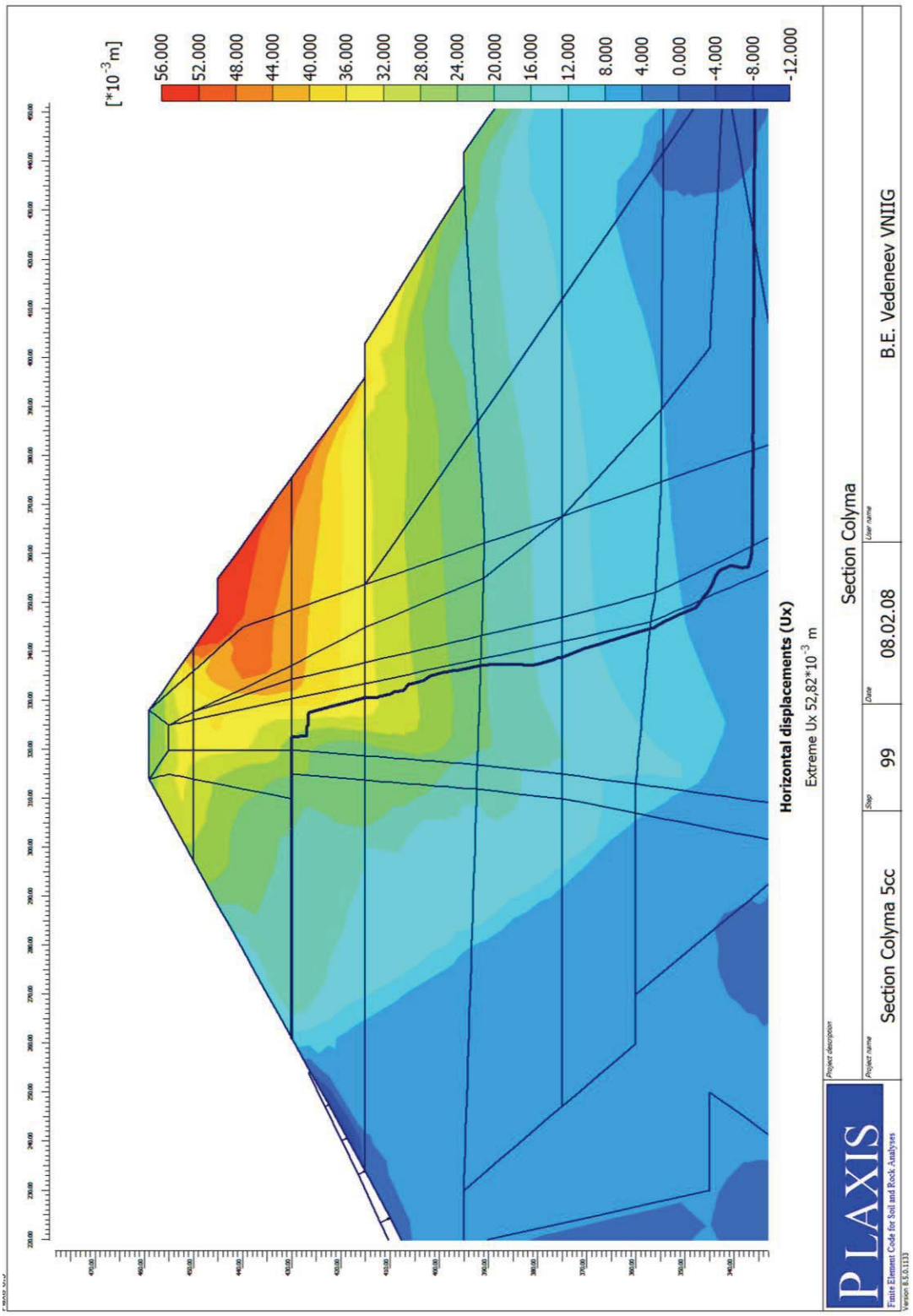

Figure 7. Horizontal displacement increments distribution in the dam design section in 2001 after finishing the annual cycle of the upstream level changes "232-252-232".

…

ANALYSIS OF THE LONG TERM BEHAVIOUR OF KOLYMSKAYA DAM (RUSSIA) UNDER FULL DESIGN CONDITIONS

Bachir Touileb
Hydro-Québec, Montréal, Québec, Canada

1.0 ABSTRACT

Analysis of the long term behaviour of Kolymskaya dam under full design conditions can be performed by means of two different approaches. First, a simplified approach consisting of using the released measurements and actual trends in order to develop a model allowing for the evaluation of future settlements and horizontal displacements (approach #1). Secondly, a more detailed approach consisting of a comprehensive analysis using the released data to calibrate the time dependant stress-strain laws and develop a complete model that can be used for the evaluation of future changes of stresses, settlements and horizontal displacements (approach #2). Both approaches are meant to be able at least to provide prognosis for 2005 - and subsequent years – regarding the settlements and horizontal displacements of the crest and the downstream slope of the dam. In the actual contribution, it is found sufficient due to limited time to use the first approach that turned out to represent a valuable and a necessary step for any more detailed analysis.

2.0 KOLYMSKAYA DAM DESCRIPTION

Description of Kolymskaya dam such as provided by Panov (2007) is recalled hereafter only for completeness of the actual paper.

Kolymskaya dam is located in the north-eastern extremity of the Asian continent, Magadan district, the Kolyma river (Fig. 1). The area belongs to the Far North and is characterized with sharp continental climate with very cold winter and warm-temperate summer. The annual amplitude of air temperature fluctuations reaches 97°C. The average annual air temperature is minus 12°C, the average temperature in January is minus 38°C, and plus 15°C in July. The absolute minimum of air temperature is minus 61°C, the absolute maximum is +36°C. The territory belongs to the zone of continuous propagation of permafrost.

The maximum height of this rockfill dam is 130 m, and its length over the crest is 780 m. The watertightness of the dam is ensured by a central clay core. The mean ratio of the upstream slope of the dam is 1.8H:1,0V, and that of the downstream slope is 1.7H:1,0V. Four berms of 7 m wide each are located on the downstream slope above the elevation of 353 m, at vertical intervals of 15-30 m over the height of the dam (Figs. 2 and 3).

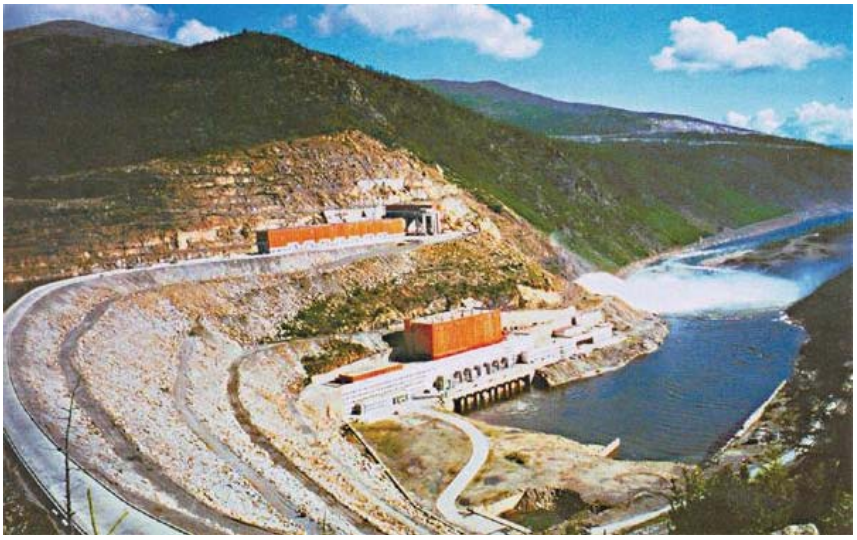

Fig. 1.Kolymskaya dam. Aerial view of downstream shoulder

The core of the dam is constituted of gruss clay loams (Figs. 2 and 3). The upstream filter consists of a single layer and made of sand-gravel mix (SGM) up to elevation 432 m. Above that elevation, it consists of a double layer and made of sand and SGM. The downstream filter consists of double-layer and is also made of sand and SGM. The shoulders of the dam are filled with non-sorted rock mass. At the base of the dam along the core axis a grout curtain is arranged.

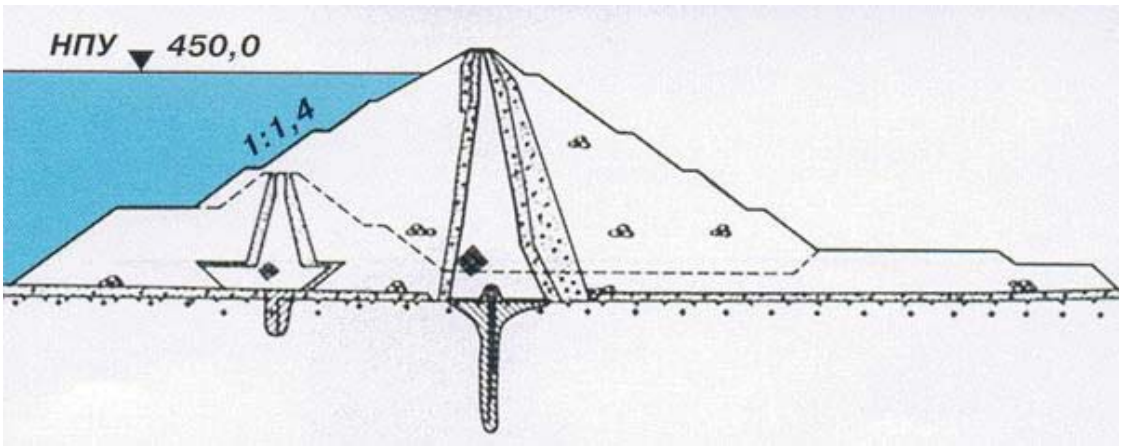

Fig. 2.Kolymskaya dam. Cross section

At present the upstream shoulder, filter, core and the first layer of the downstream filter below the depressive curve are in thawed state. However, the downstream retaining shoulder and the second layer of the filter are mainly in permafrost state (Fig.4).

The foundation of all hydraulic structures of Kolymskaya HPP are constituted by a competent massive granite, that is weathered on the surface, but remains intact at depth with relatively high strength properties. The granites are practically watertight in the frozen state, but after thawing they acquire very high permeability.

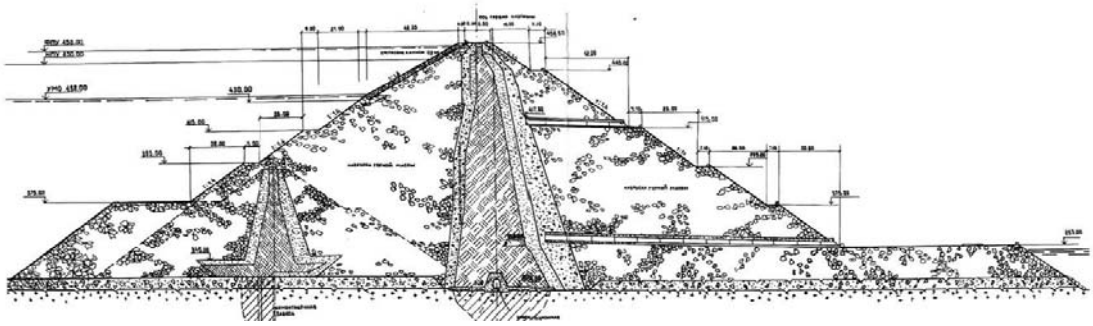

Fig. 3.Kolymskaya dam. Cross section – details

The feature of operation of the Kolymskaya HPP that influences the strain behaviour of the dam is the large amplitude of seasonal change of reservoir water level from elevation 432m (minimum drawdown level) to elevation 451.5m (NPL - normal pool level). For the first time the water level in the reservoir was raised to elevation NPL in 1994, therefore the beginning of operation of the hydraulic facilities in the design conditions refers to 1995 (Fig. 5).

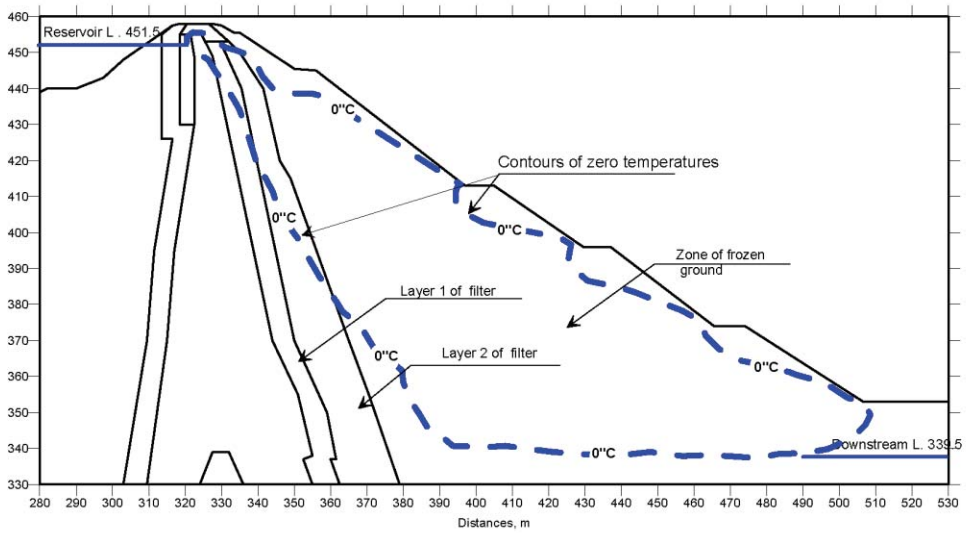

Fig. 4. Extend of freezing in the downstream shoulder

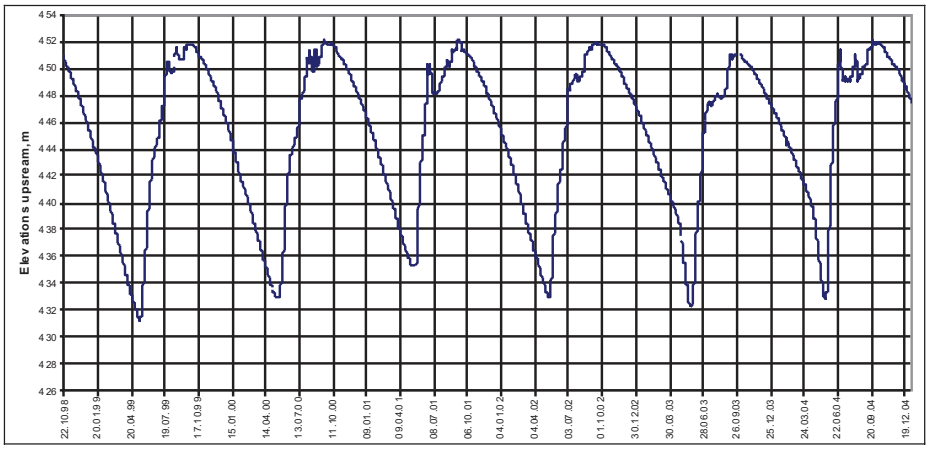

Fig. 5. Water level management under full design conditions

3.0 CREST DISPLACEMENTS

3.1 Observed crest deformation trends under full design conditions

Preliminary analysis of observed settlements (S) and horizontal displacements (U) at the crest of dam (relatively to a reference year taken as 1999) shows that the rate of both displacements (ΔS) and (ΔU) are in a steady decrease (Table 1 and Figs. 6 and 7). This observation allows for the determination of the approximate date at which S and U will reach a quasi-constant value. Such a situation corresponds to a rate of displacement almost equal to zero. This is clearly shown in Figs. 6 and 7 by means of the dates corresponding to the intersection of the rate linear curve and the horizontal line of rate=0. In the case of the representation by means of a Log-Log scale, a very small rate such as 0,001 provides the quasi-end of creep as well.

In the case of U, it is believed that end of creep will occur during 2008. However, in the case of S, a longer period is needed with a zero rate expected for the year 2013 (Figs. 6 and 7).

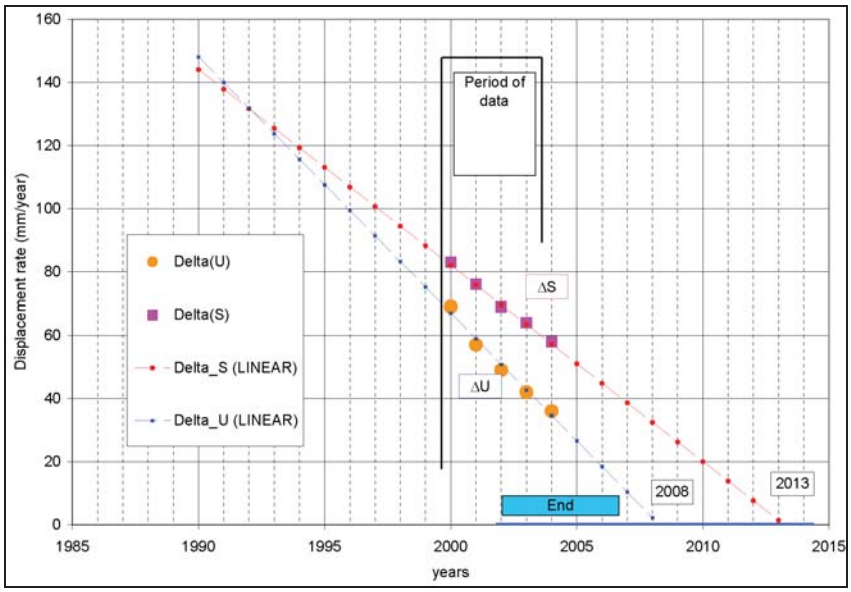

Fig.6. Decreasing rates of displacement (U and S at crest of the dam)

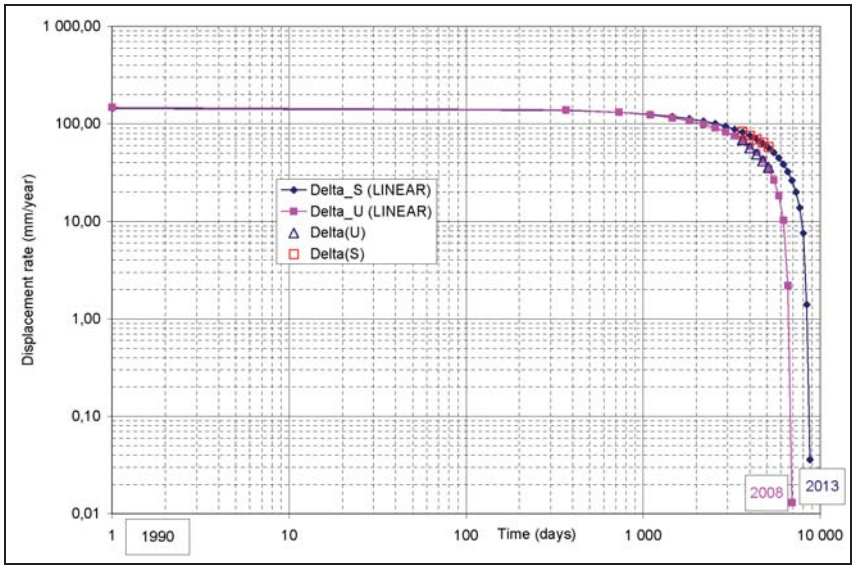

Fig.7. Observed decreasing rates of displacement (U and S at crest of the dam) (Log-Log scale)

3.2 Model for long term crest displacements (S and U)

Given that the rate of S and U, that is (ΔS) and (ΔU) respectively, at the crest of the dam is fairly well represented by means of a linear curve, then both S and U can be represented by a polynomial of the second order.

In the case of S at the crest, this is illustrated in Fig. 8, and corresponding very low residuals are shown in Fig. 9. In parallel, Figs. 10 and 11 show the model used for U and its corresponding very low residuals.

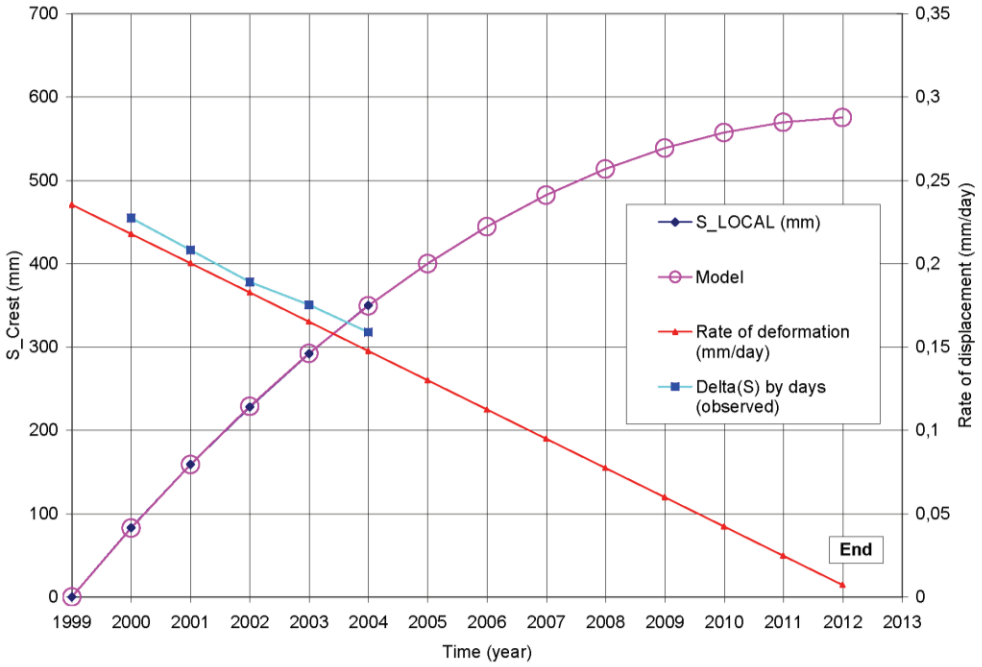

Fig.8. Model for S and its rate (crest of the dam)

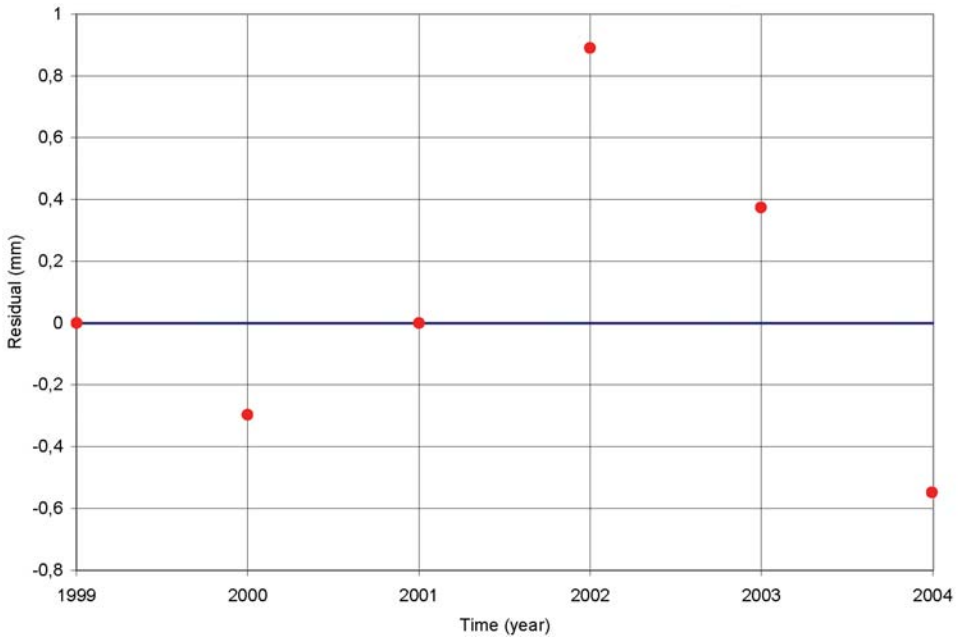

Fig.9. Residuals obtained from the model (S at crest of the dam)

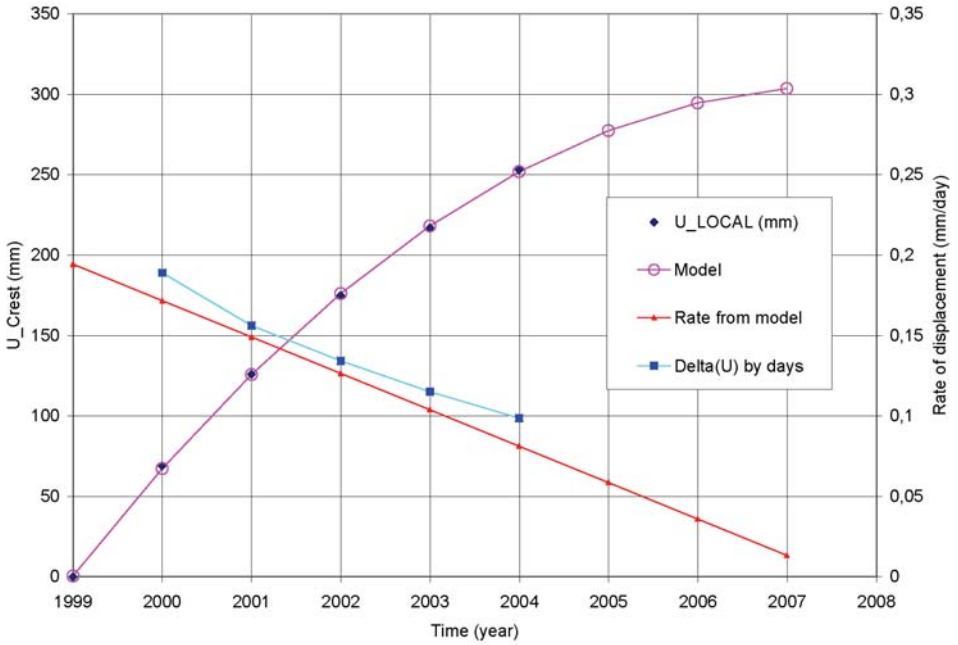

Fig.10. Model for U and its rate (crest of the dam)

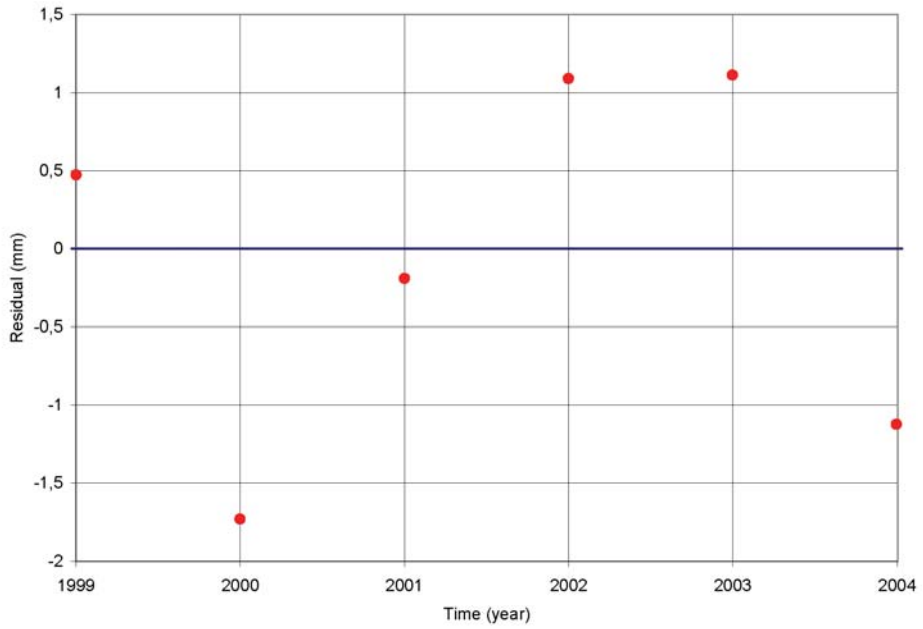

Fig.11. Residuals obtained from the model (U at crest of the dam)

Table 1 shows the expected settlements and horizontal displacements at the crest of the dam for 2005 and beyond relatively to the 1999 reference year.

Table 1. Displacements S and U at the crest of the dam. Observations and released data (1999-2004), estimated rates and prognosis for 2005 and beyond

Year	1999	2000	2001	2002	2003	2004
Released data (S and U)						
S (mm)	0	83	159	228	292	350
Delta(S) (mm/year)	-	83	76	69	64	58
U (mm)	0	69	126	175	217	253
Delta(U) (mm/year)	-	69	57	49	42	36
Computed unreleased results (S and U)						
Year	**2005**	**2006**	**2007**	**2008**	**2009**	**2010**
S (mm)	400,1	444,4	482,3	513,7	538,7	557,4
Delta(S) (mm/year)	50,7	44,3	37,9	31,5	25,1	18,6
U (mm)	277,4	294,6	303,6	304,4		
Delta(U) (mm/year)	25,5	17,3	9,0	0,7		
Computed unreleased results (S and U)						
Year	**2011**	**2012**				
S (mm)	569,6	575,5				
Delta(S) (mm/year)	12,2	5,8				

4.0 SETTLEMENT PROFILES VERSUS TIME ALONG THE DOWNSTREAM BERMS AND SLOPE

4.1 Observations Model for settlements (U)

It is reported that settlement profiles along the downstream slope of the dam present a linear shape, with settlements being proportional to the height of the dam since the early stage of operation (Panov 2007). That means a settlement zero at the base of the downstream slope (boundary condition), and a maximum being reached at the crest. Knowing this, and having already developed a model for the crest, it is possible to determine the settlement profiles for the period 2000 and beyond (see Fig. 12). The rates of annual settlements (mm/year) at each elevation along the downstream slope, including the instrumented berms, might also be evaluated such as shown in Fig. 13.

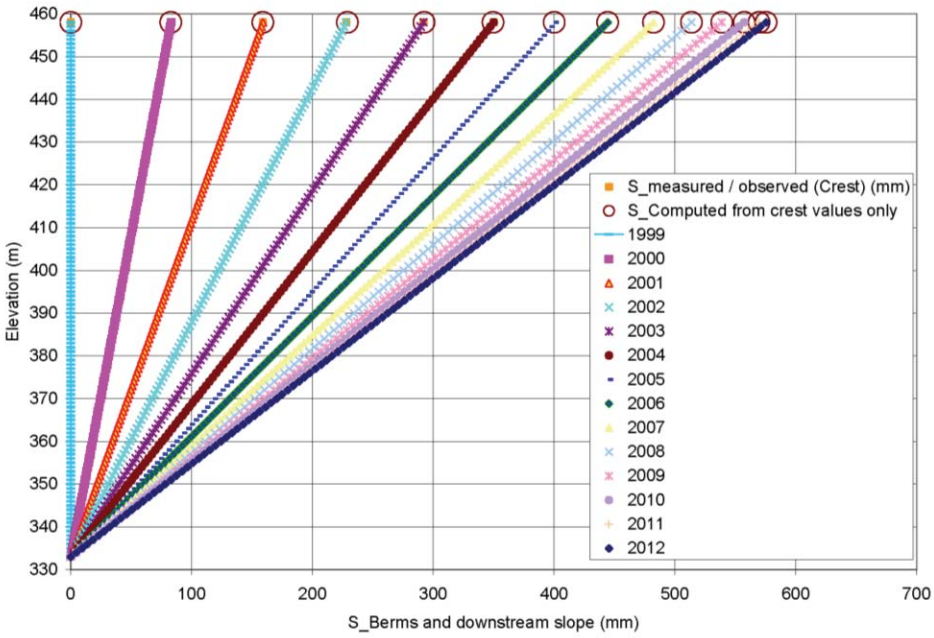

Fig.12. Prognosis of S (2000 and beyond) along the downstream slope

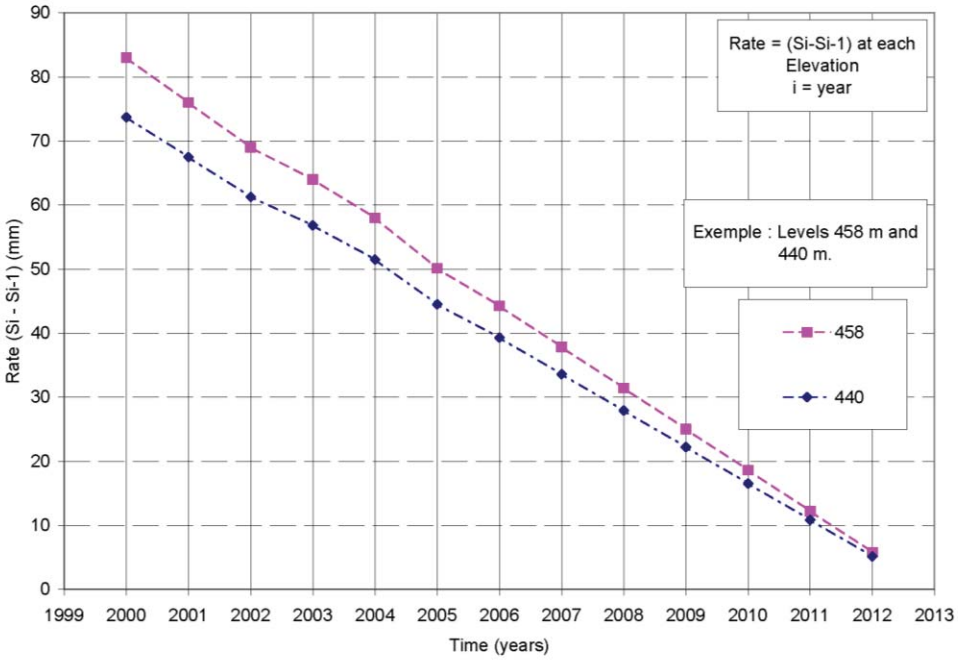

Fig.13. Rates of S at each elevation with respect to time

5.0 HORIZONTAL DISPLACEMENTS PROFILES VERSUS TIME ALONG THE DOWNSTREAM SLOPE

5.1 Observed horizontal displacements along the downstream slope for 2004 under full design conditions

Preliminary analysis of observed horizontal displacements U along the downstream slope of the dam (Table 2 and Fig. 14) allows a fairly well representation of this profile by means of a polynomial of the fourth order (Fig. 15). Corresponding very low residuals are shown in Fig. 16.

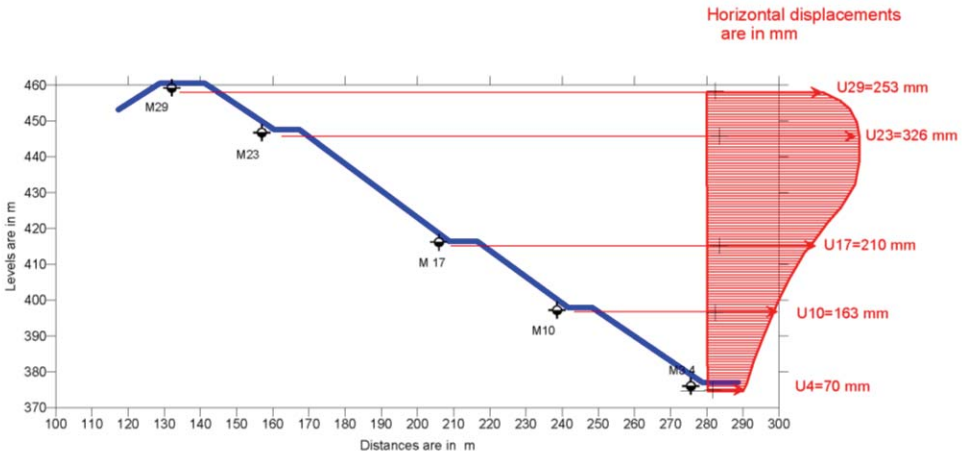

Fig.14. Observed U on crest and downstream berms for 2004

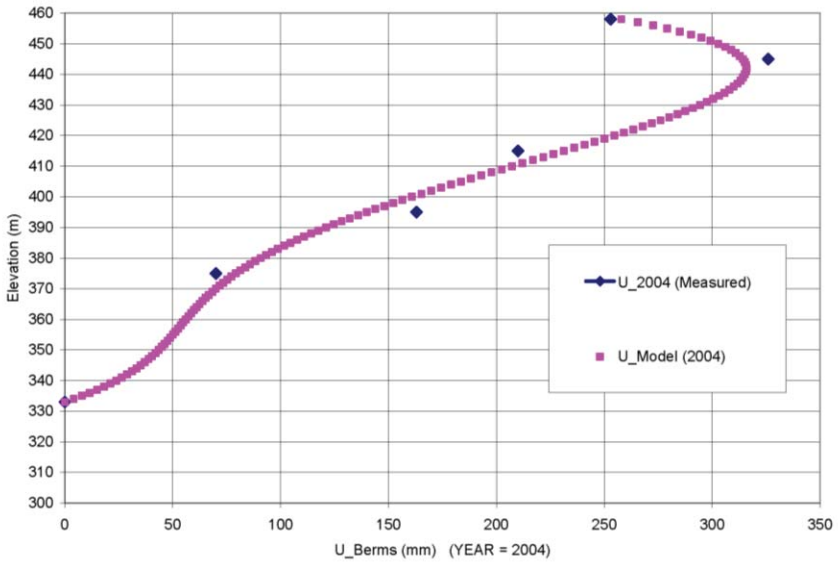

Fig. 15. Model for U(2004) along the downstream berms

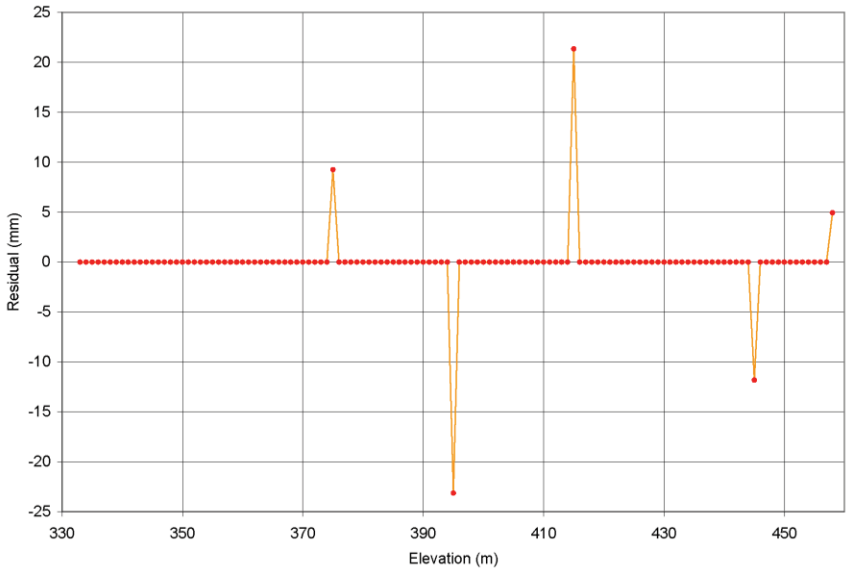

Fig.16. Residuals from the model U(2004) along the downstream berms

In parallel, one can assume, such as done previously in the case of crest displacements, that 1999 is considered as a reference year, with all horizontal displacements set to zero. Therefore, the computed horizontal displacements along the downstream slope for the year 2000 and beyond are relative to 1999.

Table 2. Observed horizontal displacements along the downstream berms of the dam.

Benchmark Number	Elevation (m)	Horizontal displacement (U) (mm) Year = 2004
M29	458	253
M23	445	326
M17	415	210
M10	395	163
M34	375	70
Base	333	-[1]

[1] Horizontal displacement at the base of the downstream slope of the dam is assumed to be zero, at the contact dam/bedrock.

5.2 Model for downstream horizontal displacements (U)

Variation of the horizontal displacements profile along the downstream slope is believed to develop from a linear curve (corresponding to the reference year 1999) to a polynomial of order 4 for the long term, such as in 2004.

Assuming that the creep is likely to stop, or at least to vanish drastically, near the year 2008, and that the rate of horizontal displacement is linear with respect to time (Fig. 17), then it is possible to determine the displacement profiles for the periods before and after 2004 (i.e. 2000-2003, and 2005-2012). The profiles for 2000-20012 are shown in Fig. 18.

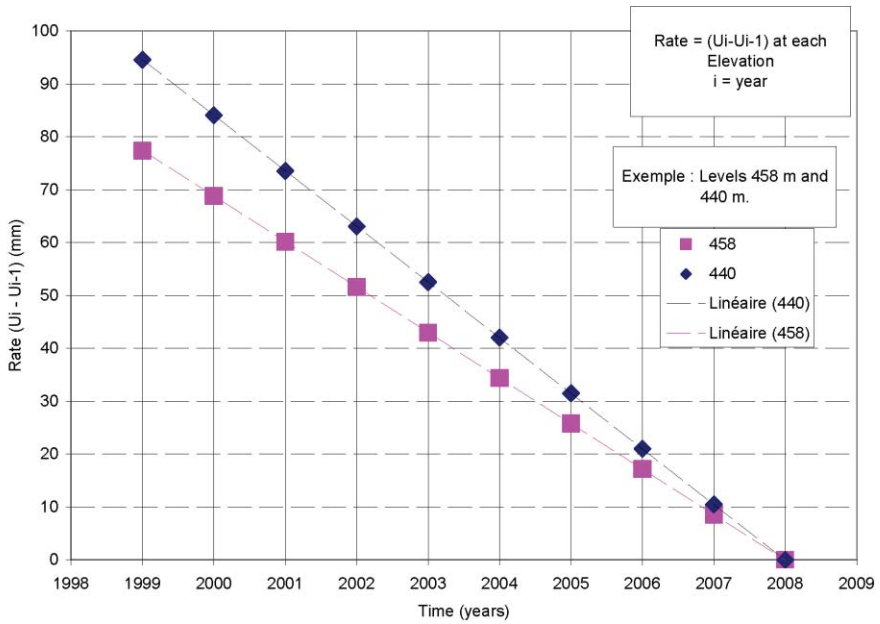

Fig.17. Rates of U at each elevation with respect to time

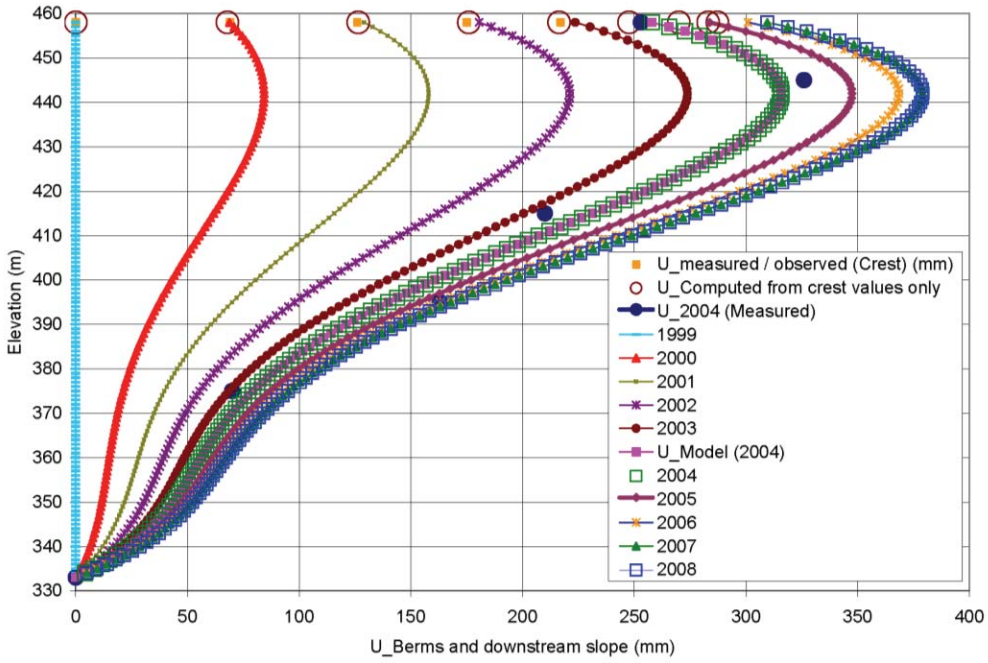

Fig.18. Prognosis of U (2000 and beyond) along the downstream slope

6.0 CONCLUSION

Based on actual data of settlements (S) and horizontal displacements (U) at the crest of the dam, the rates of displacements (ΔS) and (ΔU) are in a steady decrease with time. Displacements seem to be near their end: Settlements (S) are expected to stabilize in 2012/2013, and horizontal displacements (U) in 2007/2008).

Also based on available data and this simplified analysis, it is believed that Kolymskaya dam is about to reach its steady state under the design conditions which started in 1994, with the reservoir water level reaching the maximum elevation of 452 m for the first time, and a 20 m annual change of water/level with a frozen downstream shoulder.

The period of stabilization of the behaviour seems to be about 15 to 18 years (1994 – 2013).

ACKNOWLDGEMENTS

The author of this contribution would like to thank Dr. Panov (Vedeneev VNIIG Inc.) for the preparation of this theme and for answering some other questions, and to the organizers of the actual Benchmark : Dr. Galogovsky (Vedeneev VNIIG Inc.) and Dr. Alain Carrère (Coyne et Bellier, France) for providing numerous and valuable assistance in reference to the ICOLD Ad-Hoc Committee on Computational Aspects of Analysis and Design of Dams.

The author would like also to thank Mr. Phuong Huu Nguyen, Head of Dams and Hydraulics (Hydro-Québec), and Mr. Gérard Verzeni, Director of Dams and Environment (Hydro-Québec) for supporting the actual contribution.

REFERENCES

Panov, D.I. – Theme B Formulator. Vedeneev VNIIG Inc. 9th ICOLD Benchmark workshop on numerical analysis of dams. Theme B – Embankment dams. Stress-strain state of high rock-fill dam with a central earth core at large amplitude of operation water level changes in the upstream. St.Petersburg, Russia. 2007.

THEME C

Open Theme

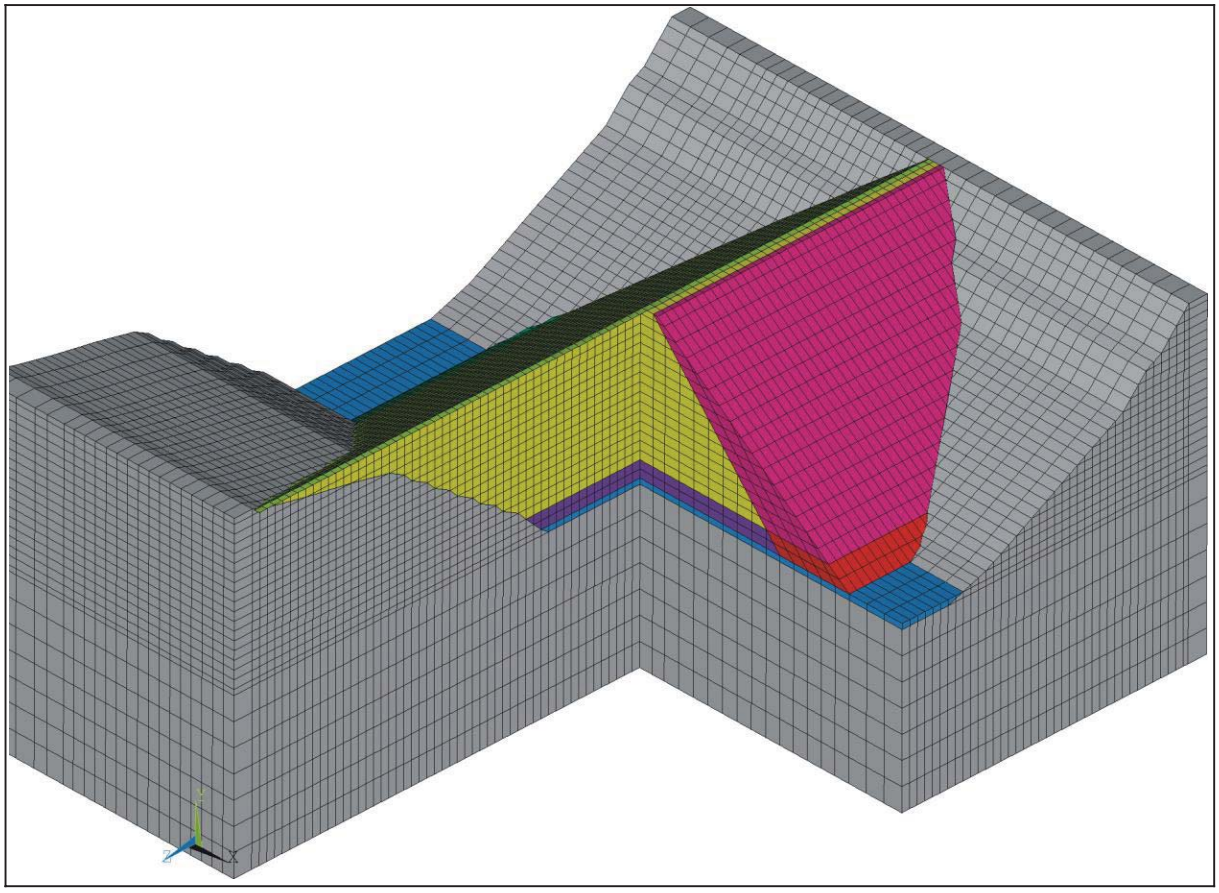

International Commission On Large Dams

Committee on Computational Aspects of Analysis and Design of Dams

9th Benchmark Workshop on Numerical Analysis of Dams

22 -24 June, 2007 - St.Petersburg, Russia

THEME C – Open Theme

ADVANCED NUMERICAL MODELLING FOR DAMS

Formulator: **Alain Carrère**
Alain.carrere@coyne-et-bellier.fr
Coyne et Bellier, Bureau d'Ingénieurs Conseils,
9 allée des Barbanniers 92632 Gennevilliers Cedex, France

In this open theme, participants are invited to propose a solution to a problem which is left free to their choice, provided it gives a valuable experience on recent advances in the field of numerical modelling.

In this respect, preference should be given:

- either to problems which could not be fully adequately analysed by numerical models in the recent past (e.g. influence of ageing of concrete, internal erosion in embankments, etc); reference should be made to the classification of modelling capability presented in Section 4 of ICOLD Bulletin n°122 '*Computational procedures for dam engineering*',
- or to problems raised by the actual behaviour of prototype dams, which give concern to professionals in their practical activity, and for which the present experience in modelling is not well established; a good example is that of the behaviour of concrete faces of high CFRD, some of which have shown severe defects during construction or impounding; to date the effects of rockfill high compressibility, valley shape, sequence of slab construction, nature of slab support, etc. have not been adequately modelled.

In both cases, preference shall be given to problems for which a physical reference solution exists.

Participants will include in their paper

- a full description of the practical problem to be solved,
- all necessary clarifications on the method, assumptions and tools they use,
- results of analyses obtained,
- a conclusion on the validity of the process.

PARAMETRIC STUDY CONCERNING THE EFFICIENCY OF THE SEISMIC-ENERGY ABSORBENT LAYERS FOR THE EARTHQUAKE PROTECTION OF THE EMBANKMENT DAMS

Adrian Popovici
Professor, Head of Department,
Technical University of Civil Engineering, Bucharest, E-mail: popovici@utcb.ro
Radu Sarghiuta
Associate Professor,
Technical University of Civil Engineering, Bucharest, E-mail: sarghiuta@ utcb.ro

Abstract

In some previous papers [3], [4] the concept of the seismic-energy absorbent layers as defensive aseismic provision for embankment dams was developed.

In this paper the efficiency of the thickness of the absorbent layer and of the ratio between shear modulus of the absorbent layer (G_l) and maximum shear modulus of the dam body (G_{md}) on the decrease of the dam seismic response is analyzed by parametric study.

The results of the study may be applied for the seismic protection of embankment dams having their body of permeable coarse alluvium, gravel or rockfill which do not present risk of liquefaction because of earthquake shaking.

1. Introduction

The statistical data concerning the performance of the embankment dams which have been subjected to strong earthquake shaking have pointed out some aspects of major importance [1]:

- the dams built on foundation or having in their body saturated sandy cohesionless materials with high risk of liquefaction have suffered the most damage and failure;
- the dams having their body composed of clay soils or permeable coarse alluvium, gravel and rockfill, this means materials which do not build up large pore pressures or change their strength during earthquake shaking, generally have suffered more or less large settlement and cracks; the seismic performance of these dams has been strongly influenced by inertia forces developed during earthquake shaking.

The seismic response of the embankment dams is strongly dependent of the dam body materials property and setting. Based on this remark, A. Popovici developed a defensive measure of the embankment dams against earthquake shaking negative effects including in the dam body some layers or braces with function to absorb as much as possible from earthquake energy [2] [3] [4]. This defensive measure can be applied for embankment dams of permeable coarse alluvium, gravel or rockfill, meaning materials which do not present risk of liquefaction because of the earthquake shaking.

The seismic-energy absorbent layers (braces) must screen the seismic waves with periods like lowest natural periods of the dam body, absorbing and transferring their energy to seismic waves with periods much different from those of lowest dam natural periods.

In a dam site the seismic response is mainly generated due to vertical propagation of the shear waves (S) from the base rock (Fig 1).

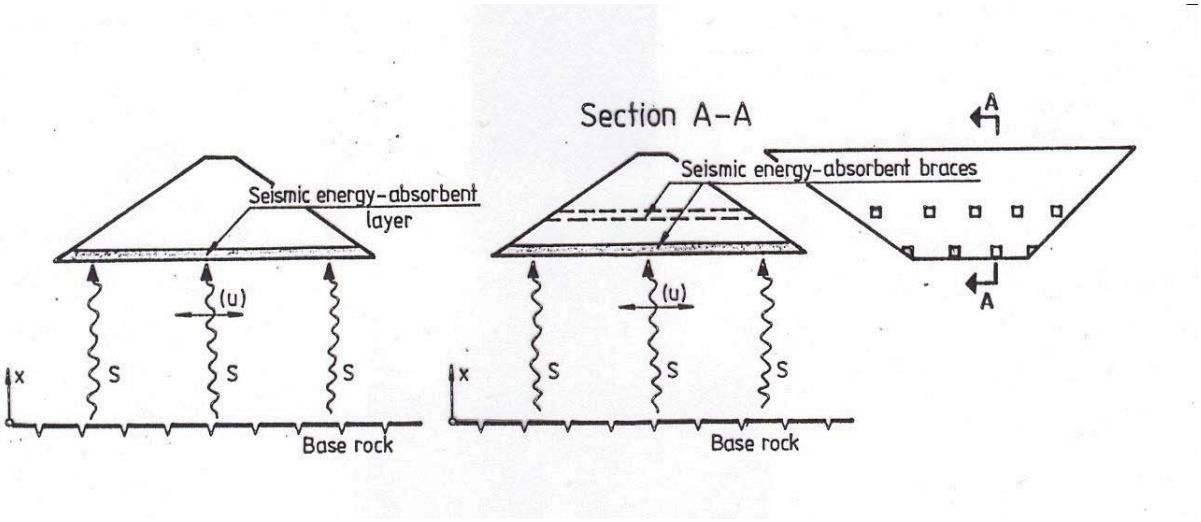

Fig. 1. General concept of the seismic absorbent layers (braces).

Certainly, the inertia forces generated by earthquake shaking in the dam body will decrease proportional to the absorption degree of the earthquake energy performed by above mentioned layers or braces. As a direct consequence of the inertia forces decrease, the dam seismic response in displacements and stresses will be diminished and the dam will be better protected against earthquakes negative effects (large settlements with loss of free board and danger of uncontrolled release of water from reservoir, cracks and slopes sliding).

The seismic absorbent layers or braces may be considered as seismic isolators from buildings or bridges. They must to filter as much as possible only the seismic waves which are not dangerous for dam, having periods much different from dam's lowest natural periods and to screen the seismic waves with periods corresponding dam's lowest natural periods zone. Particularly, is was remarked that natural alluvial layers from river bed which were not removed from earth dam foundation had significant effects in diminishing dam seismic response in equivalent condition versus an earth dam founded on sound rock foundation [1].

Generally, the stiffness of the seismic energy absorbent layers (braces) is recommended to be softer than dam foundation and dam body stiffnesses. The layers must keep constantly their stiffness during dam life. A possible solution for the material used for a seismic energy absorbent layer can be a monogranular coarse alluvium (coarse sand, gravel) put in work in layers free of compaction. Additionally, these layers can have a drainage function of the dam body if the dam shells could not perform this role.

The variant of seismic energy absorbent braces can present some advantages versus layers variant being better protected against compaction (and increase of their stiffness) by arch effect of the adjacent compacted layers. The solution presents also technological advantages. Initially, the layer is put in work with vibrocompaction as usually. In the next stage, some trenches for braces are dug in the vibrocompacted layer and they are filled with specific material. The material resulted from trench excavation is used in the next vibrocompacted layer. However, some analyses have shown that the efficiency of the braces in diminishing the earth dam seismic response is smaller in equivalent condition versus layers one [4].

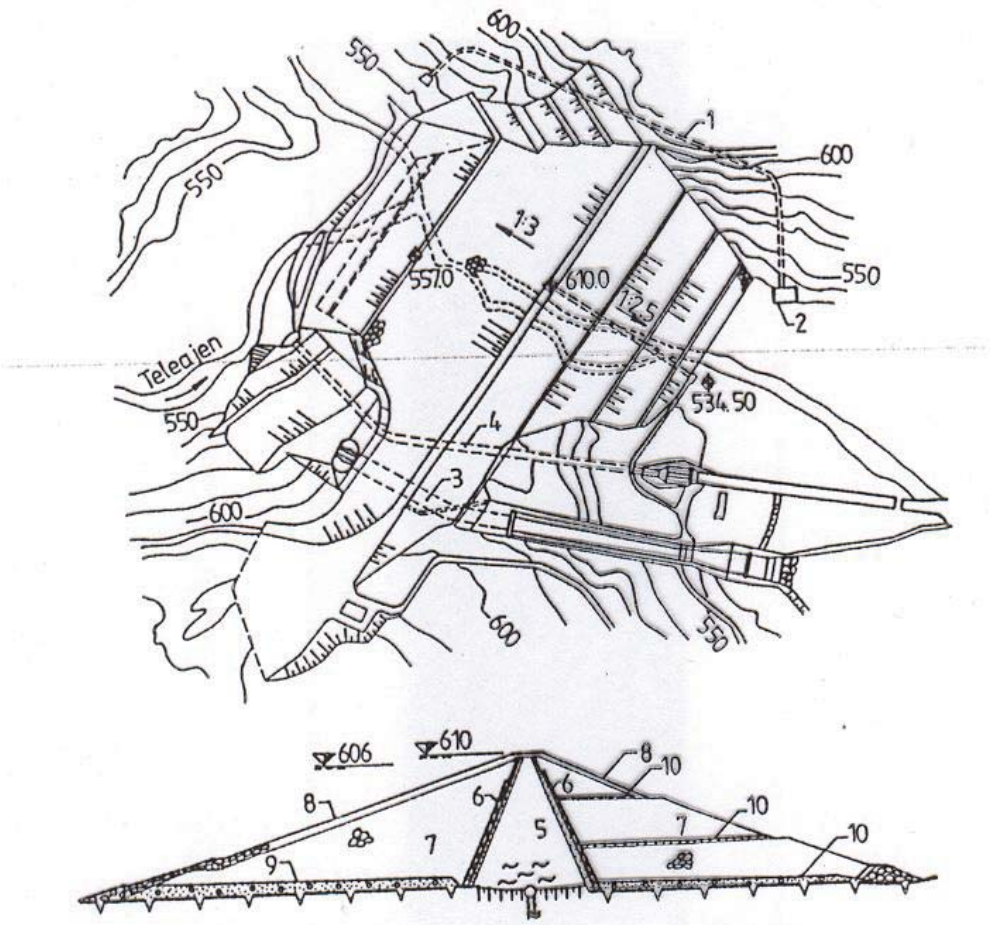

Fig. 2. Maneciu dam: a - layout, b - typical cross-section; 1 - headrace tunnel, 2 - hydropower station, 3 - morning glory spillway, 4 - water outlet, 5 - clay core, 6 - inverse filters, 7 - alluvial vibrocompacted shells, 8 - rockfill protection, 9 - natural alluvial layer, 10 - seismic energy absorbent braces.

In a previous paper [4] the defensive measures against seismic shaking for an important earth dam with 75 m maximum height from Romania were carefully analyzed. This dam named Maneciu is an earth dam with clay core (Fig. 2) located in a high seismic area. The dam was commissioned in 1990 year and the main aseismic provisions applied were the followings:

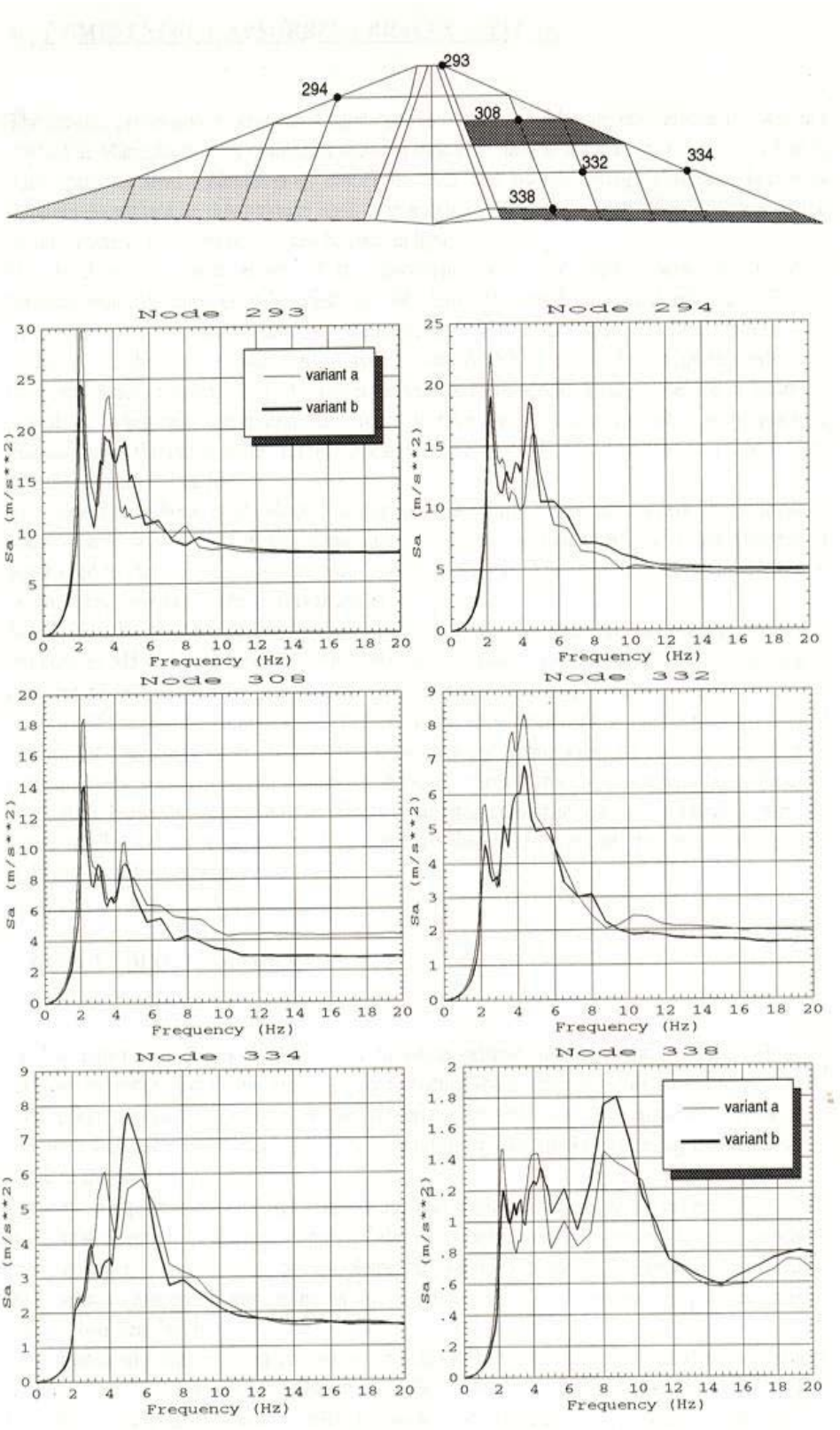

Fig. 3. Maneciu dam-response spectra in variant with seismic energy absorbent layer/braces (b) versus standard variant (a) free of seismic protection.

- thick core consisting of clays with high plasticity in order to reduce the risk of core break by eventually cracks;

- higher freeboard at the crest (4 m difference between normal retention level and crest level);

- incorporating of the upstream and downstream cofferdams in the dam body;
- provision of large filtering zones with drainage properties;
- lining of the entire upstream face and partially of the downstream face with rockfill thick layer (rip-rap);
- lining of the dam left abutment with concrete plates and post-tensioned cable anchors;
- the uses of the natural alluvial layer from river bed as seismic energy absorbent layer at the base of the dam upstream shell (see Fig. 2);
- the uses of the seismic energy absorbent braces at three dam elevations in the downstream shell (see Fig. 2).

In the Figure 3 are presented comparatively in different nodes from the body of Maneciu dam the response spectra in variant with seismic absorbent layer/braces versus standard variant free of seismic protection. The analysis was performed in the three-dimensional finite element mesh applying ANSYS computer code. First three natural mode shapes of the dam can be seen in the Figure 4. It can be remarked that in the frequency field corresponding to the lowest natural periods of the dam the amplitudes of the spectral accelerations in the variant with seismic absorbent layers/braces are 5...10% smaller than in the variant free of seismic protection.

In the present paper a comprehensive parametric study on the efficiency of the seismic energy absorbent layers is performed. The analysis is performed with FLUSH computer code. The influence of the ratio between G_l/G_{md} (G_l - shear modulus of the seismic energy absorbent layer, G_{md} - maximum shear modulus of the dam body) and of the relative thickness of the seismic energy absorbent layers on the dam seismic response is analyzed for a standard profile of an embankment dam.

The result of the study can be useful in the selection of the seismic energy absorbent layers characteristics.

2. Computational model

The assumption often made on the propagation mechanism of the seismic waves is that soil motions are primarily generated by the vertically propagation of shear waves (S) and compressional waves (P).

The differential equation of the P waves propagation into a linear elastic field has the form:

$$(\lambda + 2\,G)\,\nabla^2\,\varepsilon_v = \rho \frac{\partial^2\,\varepsilon_v}{\partial\,t^2} \tag{1}$$

where ∇^2 is Laplace operator second degree $\nabla^2 = \frac{\partial^2}{\partial x^2} + \frac{\partial^2}{\partial y^2} + \frac{\partial^2}{\partial z^2}$ (2)

ρ -material field density; ε_v - volumic specific strain and λ, G - Lame constants:

$$\lambda = \frac{\mu\, E}{(1-2\,\mu)\,(1+\mu)}; \qquad G = \frac{E}{2\,(1+\mu)} \tag{3}$$

with E - elasticity modulus, μ - Poisson coefficient.

The differential equations of the S waves propagation into linear elastic field are as follows:

$$\begin{aligned} G\ \nabla^2 \mu &= \rho \frac{\partial^2}{\partial\, t^2} \\ G\ \nabla^2\ v &= \rho \frac{\partial^2\ v}{\partial\, t^2} \\ G\ \nabla^2\ w &= \rho \frac{\partial^2\ w}{\partial\, t^2} \end{aligned} \tag{4}$$

where u, v and w are the displacements of a point along axes O_x, O_y and respectively O_z in a three-dimensional orthogonal system.

The present application is based on the finite element computational model implemented in FLUSH computer code [5]. The nonlinear and hysteretic behavior of materials from the dam-foundation unitary system was modeled by Seed-Idriss equivalent linear procedure.

According to complex response method, the equation of dam-foundation motion system takes the form:

$$[M]\{\ddot{u}\} + [K]\{u\} = -[M]\{r\}\ddot{y}\,(t) \tag{5}$$

when $\{u\}$ is the nodal displacement vector relative to the rigid base, $[M]$ and $[K]$ are plain-strain mass and complex stiffness matrices and $\{r\}$ is a vector related to the direction of rigid motion at the base rock.

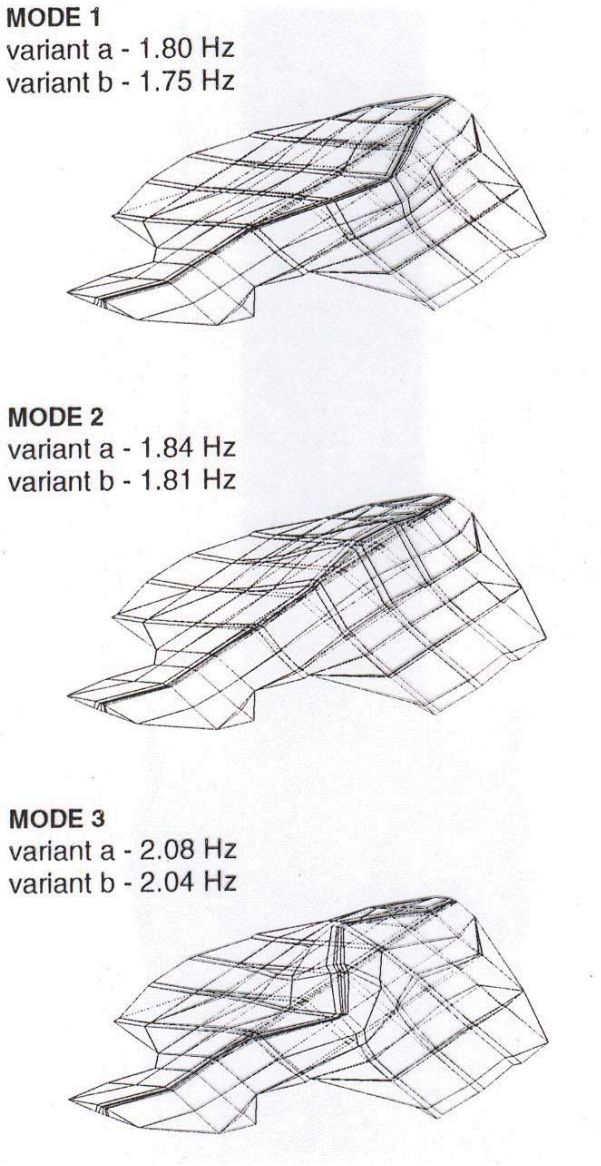

Fig. 4. Maneciu dam - three lowest natural periods of the dam resulted in three-dimensional analysis.

The viscous damping of the dam-foundation system is included in the complex stiffness matrix [K]. The complex shear modules are expressed by the relation:

$$G^* = G\ (1 - 2\beta^2 + 2\,i\ \beta\ \sqrt{1-\beta^2}) = G\ e^{2\,i\,\beta} \qquad (6)$$

where G is the real shear modulus of the material and β is the critical damping ratio.

The system of motion equations included in FLUSH code has a similar form with relation (5):

$$[M]\{\ddot{u}\} + [K]\{u\} = -[M]\{r\}\,\ddot{y}(t) - \{V\} + \{F\} - \{T\} \qquad (7)$$

The forces $\{V\}$ act along the planar slice sides and correspond to viscous forces produced by the relative motion of the dam-foundation system with the free field motion:

$$\{V\} = \frac{1}{L}[C]\,(\{u\} - \{u\}_f) \tag{8}$$

in which L is the thickness of the slice and $[C]$ is the simple diagonal damping matrix depending of the properties of the free field. The forces $\{F\}$ act upon the lateral edges of the slice and correspond to spring forces in vertical plane involving no horizontal transmission of wave energy:

$$\{F\} = \{G\}\{u_f\} \tag{9}$$

where $\{G\}$ is the frequency - independent shear complex stiffness matrix of the foundation soil in the free field. The forces $\{T\}$ depend on the motion of the dam-foundation system relative to the free field and correspond to the forces generated by the horizontal energy transmission at the lateral edges of the system:

$$\{T\} = ([R] + [L])(\{u\} - \{u_f\}) \tag{10}$$

where $[R]$ and $[L]$ are the frequency-dependent boundary stiffness matrices [5].

FLUSH code is developed on the assumption of rigid baserock at the lower boundary of the foundation-structure system, the seismic action being generated by vertically propagating of S and P waves. Field observations confirmed that this assumption is acceptable for engineering computations.

3. Parametric study

The parametric study concerning the efficiency of the solution based on seismic-energy absorbent layers was performed in the cross-profile of an embankment dam with 50 m maximum height (Fig. 5 a). The seismic-energy absorbent layers were placed at the base of the dam, adjacent to the foundation consisting of sound rock.

The analyses were performed with a package of computer codes including: SIMEX code for sequential bidimensional dam erection and FLUSH code for bidimensional nonlinear seismic analysis [2].

The dam erection was simulated in 7 steps (layers), the hyperbolic Duncan-Chang model was used for dam body material behavior modeling. In the Figure 5 b, the dam body shear modules (G in MPa) variation at the end of the dam construction is presented. They were considered as the initially material characteristics in the nonlinear seismic analyses. The characteristics of the seismic-energy absorbent layer were successively varied as relative shear modules (G_l/G_{md}) and thickness.

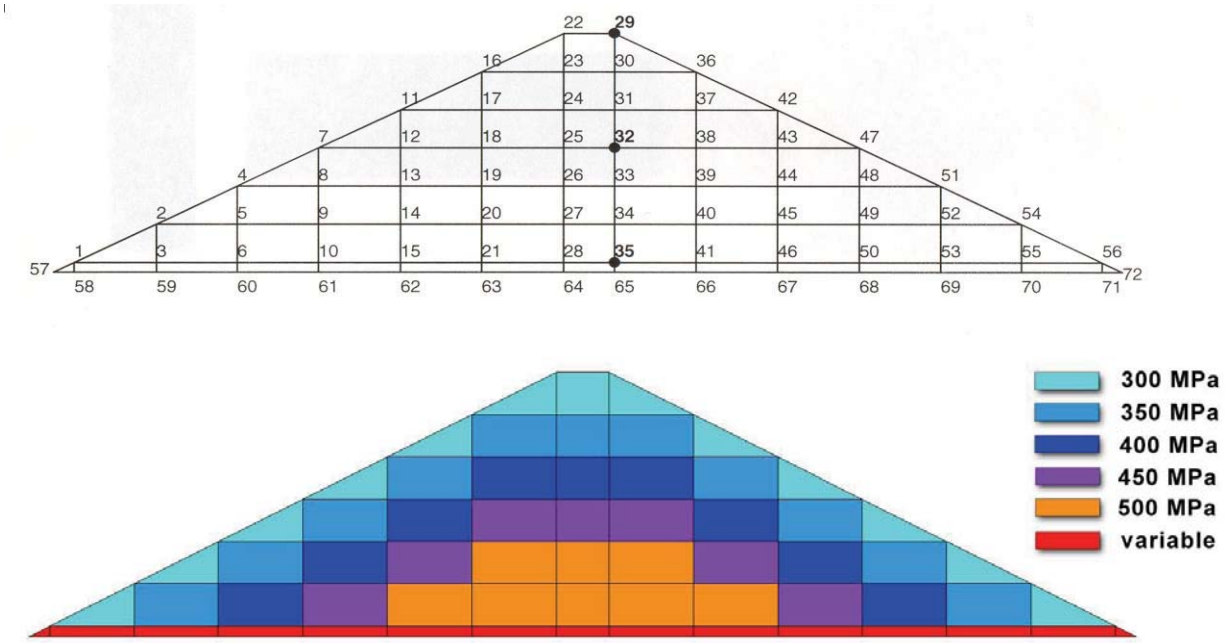

Fig. 5. The finite element mesh of the standard profile used for parametric study and the contours of the shear modules (G) at the end of the dam erection.

Two different seismic inputs on the dam profile were considered, both scaled at 0.5 g (g-gravity) and acting on horizontal direction. One of the inputs was a sinusoidal accelerogram with constant period of 0.33 seconds and 20 seconds duration. Secondly was a typical Vrancea accelerogram for mountain zones with prevailing periods between 0.15 s and 0.50 s and 20 seconds duration.

The nonlinear behavior of the dam body materials under seismic actions was modeled according to linear equivalent method elaborated by Seed and Idriss. Diagrams concerning strains (γ%) compatible with relative shear modules (G/G_{max}) and rates of the critical damping (υ%) for alluvial materials were taken into account [5].

The efficiency of the seismic energy absorbent layer in different constructive variants, as was above mentioned, was evaluated versus standard variant of the dam profile free of seismic energy absorbent layer.

Some results concerning the parametric study carried out with the input data above mentioned are presented in the Figures 6...12.

The contours of horizontally maximum acceleration response in the dam body at the action of the typical Vrancea accelerogram show important decrease of the acceleration response field for thicknesses of the absorbent layer varying from 2 to 4 m. (relative thickness versus height of the profile 0.04...0.08). For thicknesses of the absorbent layer higher than 4 m the efficiency in the relative decreasing of the seismic response is lower. (Fig 6). The same conclusions resulted at the action of the sinusoidal accelerogram.

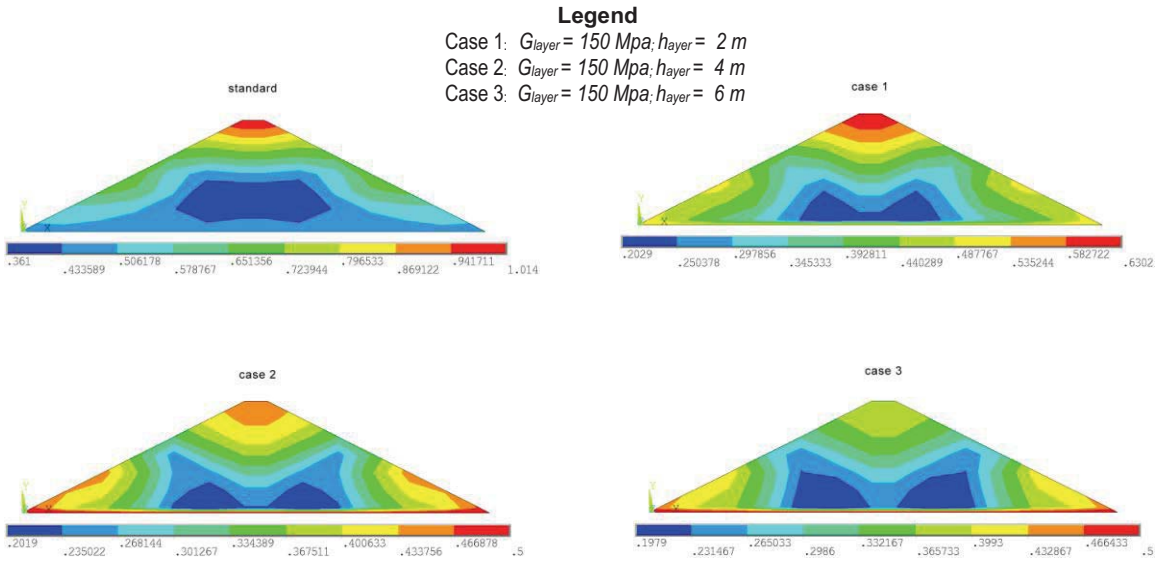

Fig. 6. The contours of the horizontally maximum accelerations generated by a typical Vrancea accelerogram, 0.5 g maximum acceleration applied horizontally.

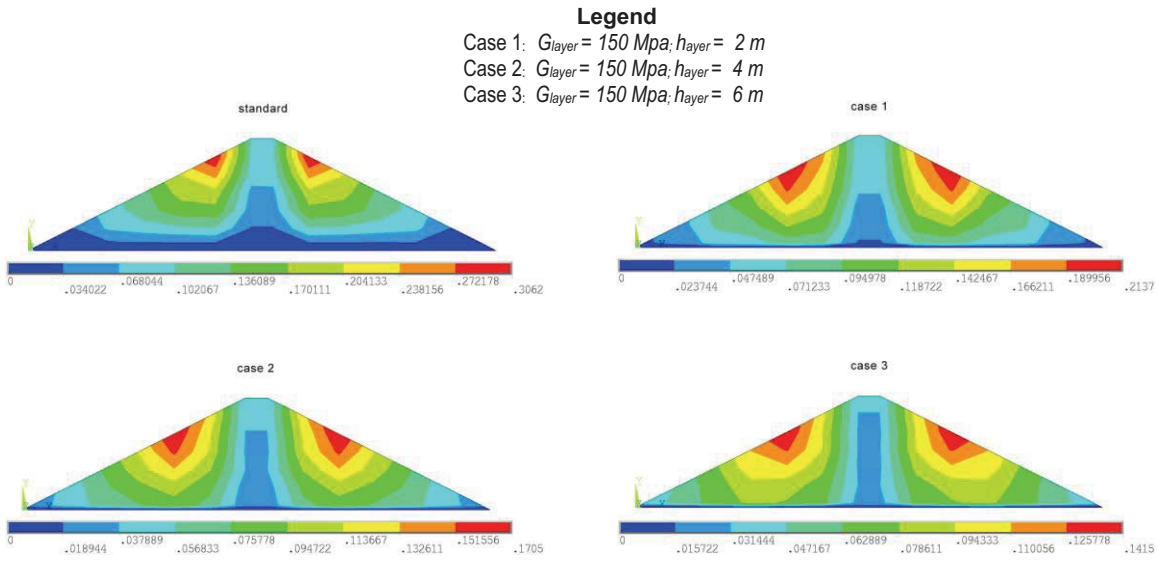

Fig. 7. The contours of the vertically maximum accelerations generated by a typical Vrancea accelerogram, 0.5 g maximum acceleration applied horizontally.

The contours of vertically maximum acceleration response in the dam body have values between 0...0.38*g* for standard variant and 0...0.21 g for variants with absorbent layers (Fig 7). In compliance with these results it may remark that absorbent layers have efficiency also on dam acceleration response on vertical direction. However the seismic response on vertical direction is less important for the dam seismic safety.

The acceleration response spectra in the node 29 from the crest of the profile point out that higher relative amplification is in the case of sinusoidal accelerogram action. In the standard variant the maximum response amplification reach 4.7 g on the sinusoidal accelerogram frequency (3 Hz) at its action and, respectively 3 g on 2 Hz frequency at the action of the typical Vrancea accelerogram. In the variants with absorbent layers the peaks of

the acceleration response spectra decrease successively in ratio with the increase of the absorbent layer thickness for both accelerograms (sinusoidal and typical Vrancea). The decreases are more important for thicknesses of the absorbent layer varying between 2 m to 4 m. (Fig. 8).

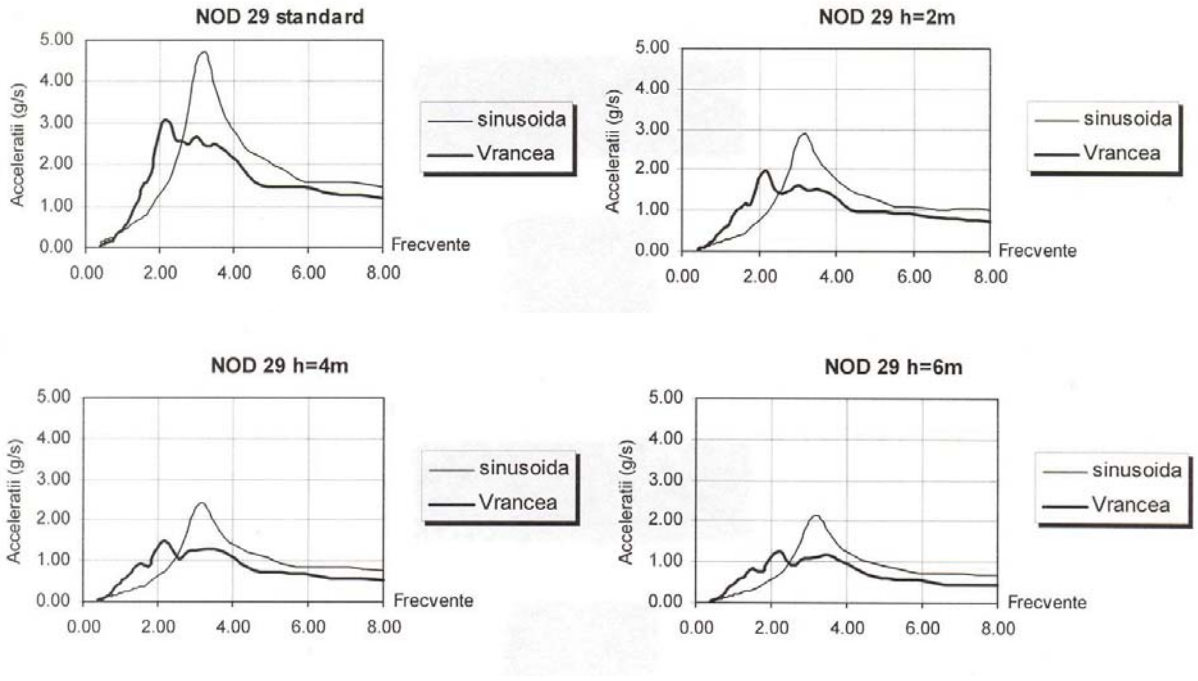

Fig. 8. The acceleration response spectra on horizontal direction at the dam crest in four variants of the dam profile at the action of a sinusoidal accelerogram of 3 Hz frequency and of a typical Vrancea accelerogram, both applied horizontally and scaled to 0.5 g maximum acceleration (g - gravity).

The conclusion above formulated that absorbent layers having 2...4 m thickness (relative thickness versus dam height 0.04...0.08) have maximum efficiency is supported with the data illustrated in the Figures 9, 11 and 12. Especially, from the Figure 9, it results very clear that increasing of the thickness of the absorbent layer over 4 m the decrease of the dam body inertia forces for both directions, horizontally and vertically, is insignificant one.

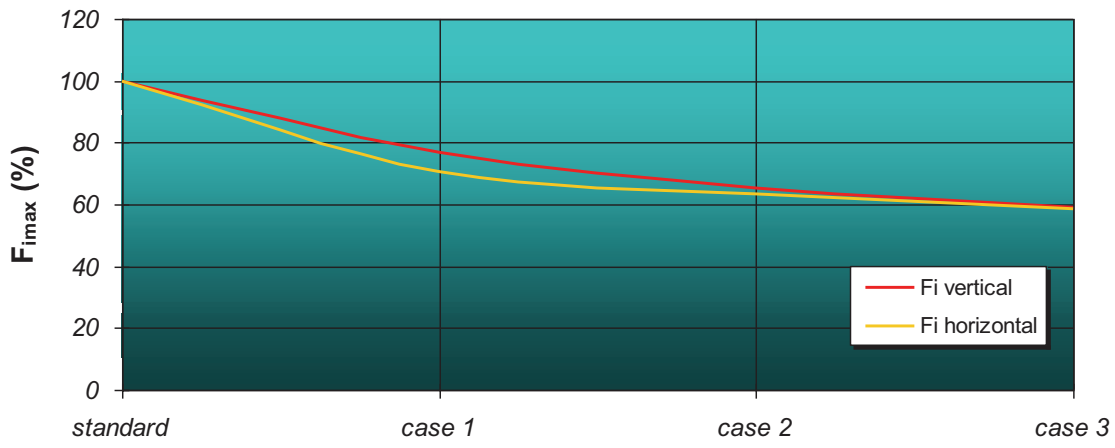

Fig. 9. The variation of the inertia forces versus the thickness of the seismic-absorbent layer at the action of the typical Vrancea accelerogram 0.5 g applied horizontally.

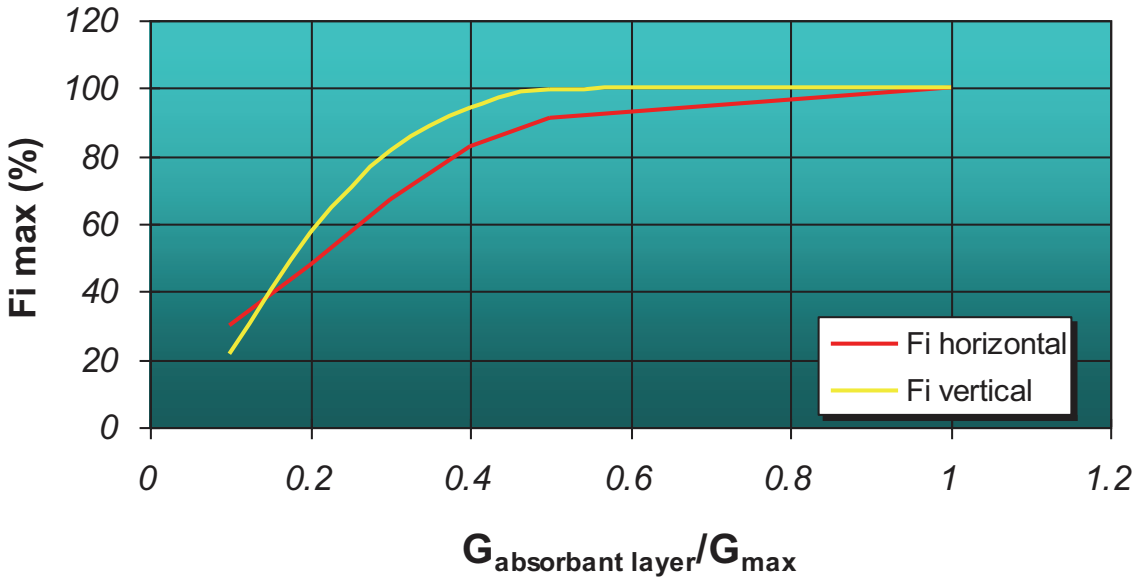

Fig. 10. The variation of the inertia forces versus the ratio G_l/G_{md}, in the profile variant 2 at the action of a sinusoidal accelerogram 3 Hz, 0.5 g applied horizontally.

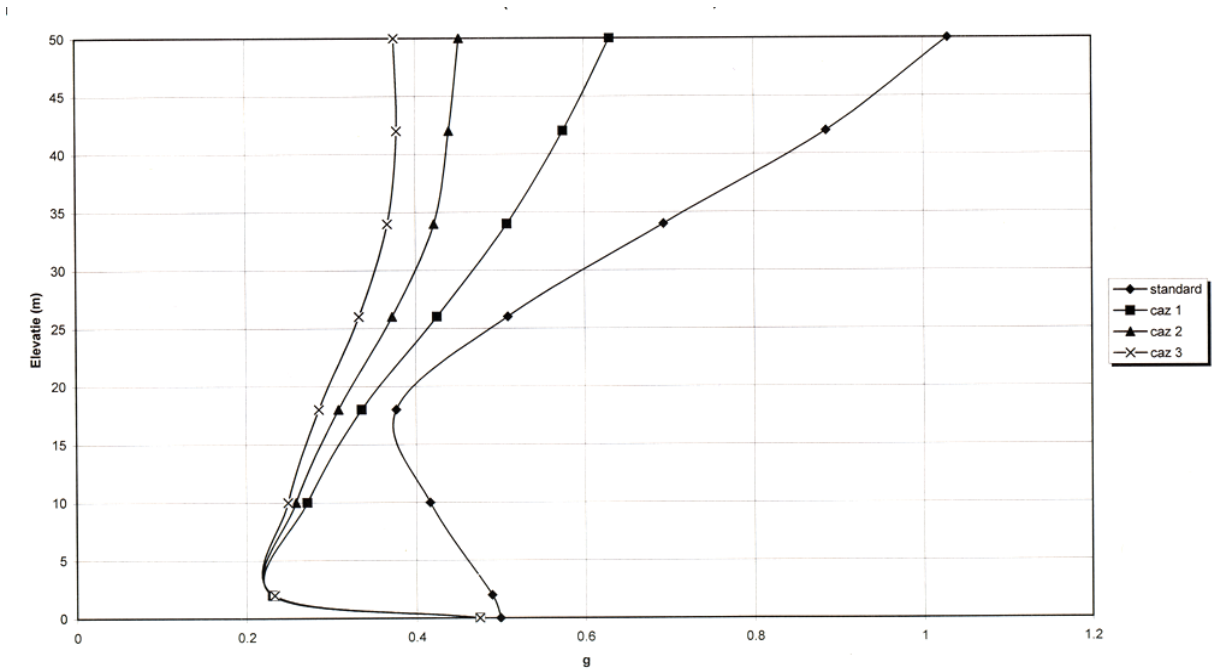

Fig. 11. Variation of the horizontally maximum accelerations response on elevation in the central section of the dam profile in four variants, at the action of the typical Vrancea earthquake 0.5 g, applied horizontally. (G_l/G_{md} = 0.5).

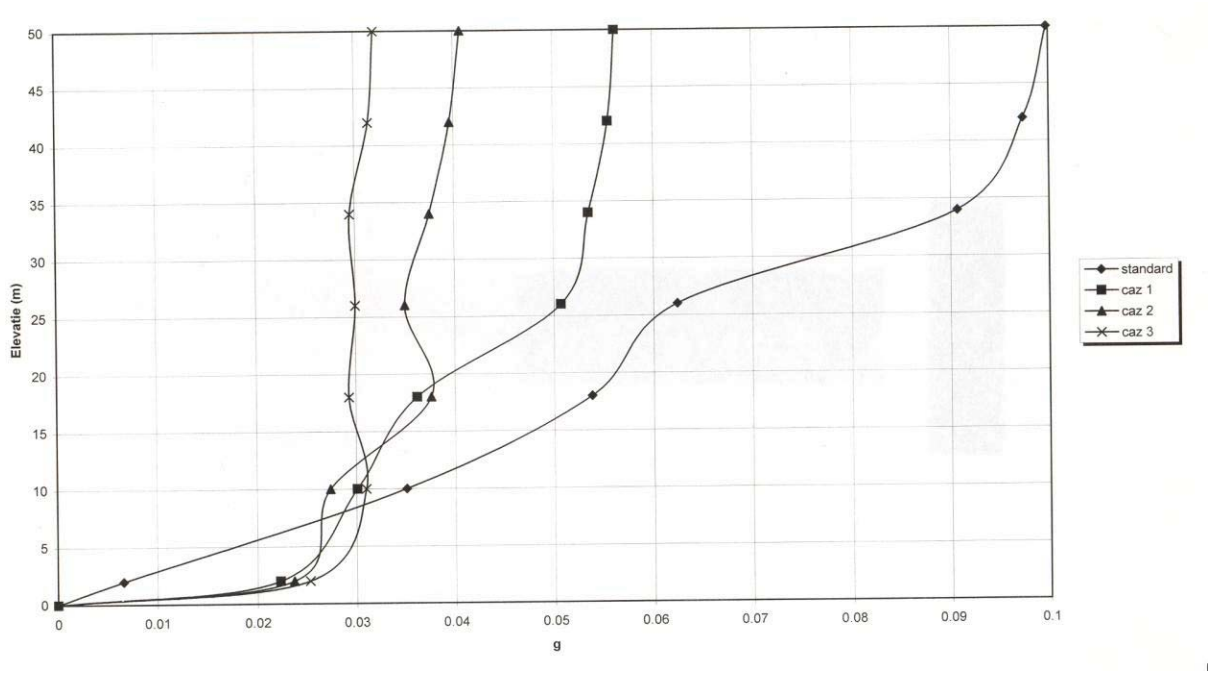

Fig. 12. Variation of the vertically maximum acceleration response on elevation in the central section of the dam profile in four variants, at the action of the typical Vrancea earthquake 0.5 g, applied horizontally. (G_l/G_{md} = 0.5).

In the Figure 10 is illustrated the variation of the dam body inertia forces versus the ratio between the shear modulus of the absorbent layer (G_l) and the maximum shear modulus of the dam body (G_{md}). The diagrams correspond to the case of an absorbent layer with 4 m thickness and at the action of the sinusoidal accelerogram, 3 Hz frequency, 0.5 g acceleration amplitude applied horizontally upstream-downstream. It can be remarked from diagrams that a ratio G_l/G_{md} = 0.5 is practically optimum one for the point of view of the efficiency of the absorbent layers.

4. Concluding remarks

● In some previous papers [3], [4] the concept of the seismic energy absorbent layers for the earthquake protection of the embankment dams was developed. As a matter of fact they are seismic isolators placed on the contact dam-foundation consisting of the granular natural material (coarse sand, gravel) with the function to screen as much as possible the seismic waves dangerous for the dam safety.

● In this paper the influence of the absorbent layers thickness and of the ratio G_l/G_{md} (G_l - shear modulus of the absorbent layer, G_{md} - maximum shear modulus of the dam body) on the decrease of the dam seismic response is analyzed by parametric study.

● Based on the results of the parametric study, could be recommended as optimum absorbent layers, those with 2...4 m thickness (relative thickness versus dam height 0.04...0.08) and with ratio G_l/G_{md} = 0.5

References:

[1] HANS BOLTON SEED Considerations in the earthquake-resistant design of earth and rockfill dams. Geotechnique 29, No.3, 1979.

[2] ADRIAN POPOVICI Dams for water storage 2nd. Volume (in Romanian). Editura Tehnica, Bucharest, 2002.

[3] ADRIAN POPOVICI Seismic absorbent layer for embankment dams aseismic protection. Proceedings 9-th European Conference on Earthquake Engineering, Moscow, September, 1990.

[4] ADRIAN POPOVICI, RADU SARGHIUTA, ION TOMA. Seismic protection of a large earth dam by seismic energy absorbent braces. Proceedings Symposium on Research and Developments in the Field of Dams. Crans-Montana, Switzerland, September, 1995.

[5] JOHN LYSMER, TAKEHAZU UDAKA, CHAN-FENG TSAI, HANS BOLTON SEED "FLUSH-A computer program for approximate 3-D analysis of soil-structure interaction problems. Report No. EERC 75-30, University of California, Berkeley, 1975.

MONITORING OF THE STRUCTURES WITH STOCHASTIC IRREVERSIBLE FLEXIBILITY

Ivan I. Zagryadskiy

Head of Laboratory, Vedeneev VNIIG, St. Petersburg, Russia

The method of monitoring of structures which include elements with stochastic irreversible flexibility (hereinafter SSIF) is considered. Behavior and accordingly methods of SSIF monitoring based on in-situ measurements processing have its peculiarities and differ essentially from those ones used for structures working in elastic or elasto-plastic range (Zagryadskiy I.I., 2001, 2001, 2005). The stress-strain properties common for all SSIF are shown below, and the problem of composing the resolving system of the method is elucidated. Algorithm for continuous SSIF monitoring is described.

SSIF behavior is investigated under influence of relatively slowly varying loads (so called quasi-static problem) therefore dynamical effects being not taken into account. The aforementioned loads are: point or distributed forces and temperature exposure, which also results to changes in SSIF mode of deformation. Commonly used SSIF diagnostic parameters dependent on loads are: displacements, deformation and stress. The set of building structures which can be considered as SSIF is relatively wide. Some of them are shown at fig.1:

a beam with two pin hinges on the edges leant on the pile (right support). The right pile is sinking into the ground stochastically, step-wise and irreversibly in consequence of slippage on contact with the ground or of ice smelting (fig.1*a*);

a beam with rigid attachment of the left edge and with cross-crack progressing in it stochastically, step-wise and irreversibly. Forces $F_1(t)$ and $F_2(t)$ are applied to the elastic working stretch of the beam on the left of the crack. Force $F_3(t)$ is applied to the stretch on the right of the crack (fig.1*b*);

a bearer concrete fundament beginning to crush unpredictably (fig.1*c*);

a guy bridge span or a guy covering span, some guys of which begin to rip stochastically (fig.1*d*);

a lattice girder with central post failing by buckling due to overload (fig.1*e*);

a concrete dam with cross-cracks on upstream face progressing stochastically, step-wise and irreversibly (fig.1*f*).

The distinguishing feature of SSIF is as follows: all of them include elements with unpredictable load-carrying ability (the so called stochastic flexibility). The transformation of common structure to SSIF is often connected with its simultaneous passage to emergency stage and may be provoked by extremely load combinations. The elements with stochastic flexibility differ from elastic or elasto-plastic ones, thus they have various progressing crip-

plings such as: cracks in material, rips of ropes, unsafe slipping contacts, support bearing failures, failures by buckling and so on. In elements with stochastic flexibility the irreversible destructive processes can continue for years, and they should be under control in most important structures, agreeable to the safety standards.

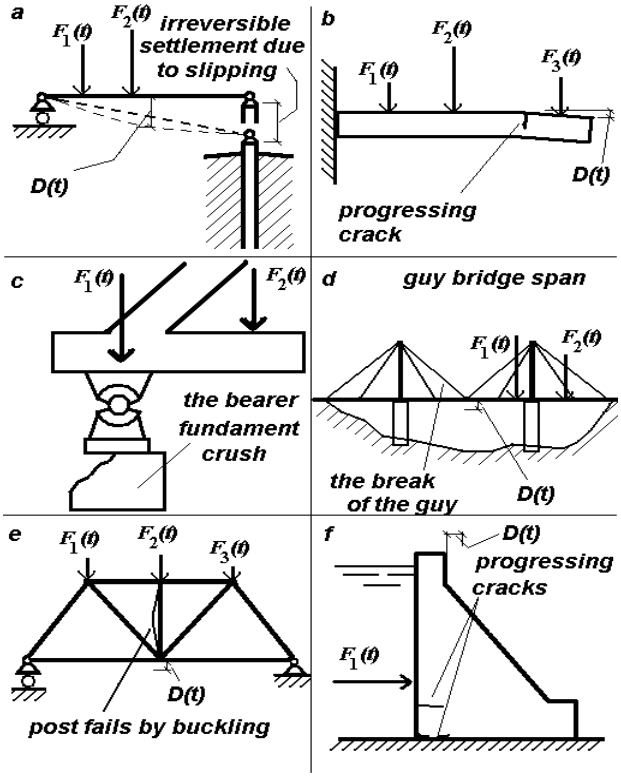

Fig. 1 Examples of Building Structures with Stochastic Irreversible Flexibility (SSIF)

Two problems are examined below to demonstrate procedure of composing the resolving system of discussed method. First problem is simple and well known. The second one is more complicated and requires applying of new methodology for its solving. In the first simple case monitoring of the beam working in elastic range is considered (fig.2). Let the values of forces $F_1(t)$, $F_2(t)$ and the flexing of the beam in the middle of its span $D(t)$ be measured, and let $D(t)$ be viewed as diagnostic parameter. The relationship between forces, mechanical properties of the beam, of its supports and its flexing may be obtained according to the rules of the structural mechanics. This relationship will also be the resolving system of the problem:

$$D(t_j) = \delta_1 + \delta_2/2 = F_1(t_j)[L^3/(48E_1J_1) + 1/(4E_2A_2)] + F_2(t_j)/(2E_2A_2), \qquad j = 1..n \qquad (1)$$

where t is the time; $E_1 J_1$ is bending rigidity of the beam; $E_2 A_2$ is rigidity of the left elastic support; j=1…n is the number of measurement run of loads and of diagnostic parameter. The values $E_1 J_1$ and $E_2 A_2$ are unknown.

By in-situ measurements processing it is usually recommended to transform the system (1) accurate to unknown scalars x_0, x_1, x_2

$$D(t_j) = x_0 + x_1 F_1(t_j) + x_2 F_2(t_j), \qquad j = 1..n, \qquad (2)$$

and to estimate three unknowns solving system (2) by means of the *least-squares* method. Then equation (2) with estimated parameters x_0, x_1, x_2 characterizing the bending rigidity of the beam and the rigidity of the elastic support may be used for forecast of $D(t)$ values by any combinations of forces and for comparison of measured $D(t)$ values with predicted ones.

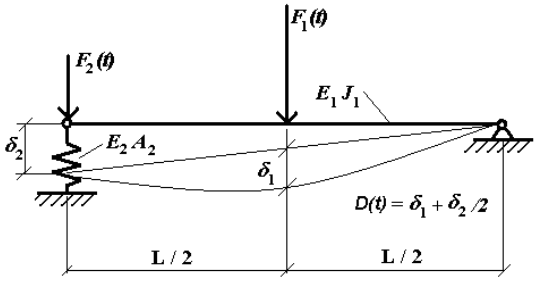

Fig.2 Example of the Simple Building Unit Working in Elastic Range: the Elastic Beam under Influence of Two Forces

In the second and more complicated case monitoring of the beams shown at fig.1*a*,*b* is considered. Suppose, the values of forces and the beam flexing in the middle of its span (fig.1*a*), or the beam right edge flexing (fig.1*b*), are measured. Beam flexing is viewed as diagnostic parameter $D(t)$. The beams being discussed in this case belong to SSIF class of structures, and therefore their diagnostic parameters will have not only elastic (as in the first simple case) but also stochastic irreversible part. The resolving system will be as follows:

$$Ir(t_j) + \sum_{k=1}^{n_f} x_{k+n_i} F_k(t_j) = D(t_j), \qquad j = 1..n_e, \tag{3}$$

where t is the time; n_e is total number of measurement runs of forces and of diagnostic parameter; n_f is total number of forces; $Ir(t)$ is irreversible stochastic component which describes irreversible and inelastic effects in elements with stochastic flexibility and is the resultant value of such effects; n_i is total number of unknown scalars assigning the form of $Ir(t)$.

Suppose SSIF at fig.1*a*,*b* satisfy the following conditions:

the bad investigated load-carrying ability of the pile (fig.1*a*), as well as of the beam cross-section with the crack (fig.1*b*), is defined by stochastic values depending on space coordinates, on loads values and on the time;

the average load-carrying ability of the pile (fig.1*a*) varies with its deepening into the ground step-wisely and unpredictably;

the beam (fig.1*b*) has fibrous structure, e.g. strongly reinforced concrete, and the crack progresses step-wisely and unpredictably.

Both processes (fig.1*a,b*) of the step-wise, irreversible and unpredictable increasing of diagnostic parameters may be described by assigning recursively their stochastic irreversible components:

$$Ir(t_1) = const_1; \qquad Ir(t_{j+1}) = Ir(t_j) \pm \zeta_{j+1}, \qquad j = 1..n_e - 1, \tag{4}$$

where ζ_j is nonnegative stochastic value. Its distribution in frequency depends on properties of the investigated SSIF and, as a rule, is unknown when processing the in-situ measurements. At that the type of distribution in frequency of ζ_j is not important. In equation (4) there must be put the sign «plus» before ζ_{j+1} for non-decreasing component $Ir(t)$ and the sign «minus» –

for non-increasing component $Ir(t)$. The resolving systems for SSIF at fig.1*a,b* have not significant difference, though they can be reduced to the unit form. For SSIF at fig.1*a* the equation (3) is quite correct. For SSIF at fig.1*b* the resolving system will be:

$$Ir(t_j)F_3(t_j) + \sum_{k=1}^{2} x_{k_i} F_k(t_j) = D(t_j), \qquad j = 1..n_e. \tag{5}$$

It can be transformed to (3) by the change of variables: $F_1^*(t) = F_1(t)/ F_3(t)$; $F_2^*(t) = F_2(t)/ F_3(t)$; $F_3^*(t) = F_3(t)/ F_3(t) = 1$; $D^*(t) = D(t)/ F_3(t)$.

It is not efficient to put the irreversible component defined by (4) in (3), because in that case the resolving system (3) has not standard decidable form. Therefore, when processing in-situ measurements got on SSIF, it was suggested (Zagryadskiy I.I., 2001) to approximate the stochastic irreversible component $Ir(t)$ with a linear combination of piece-linear basis functions (like in *finite-element* method) multiplied by unknown scalars:

$$Ir(t_j) = \sum_{k=1}^{n_i} x_k S_k(t_j), \qquad j = 1..n_e, \tag{6}$$

where $S_k(t)$, $k=1\ldots n_i$, are given piece-linear basis functions, a demonstrational set of which is shown at fig.3. This set includes 6 basis functions with the knots placed in every 5 measurement runs. In other words, the distance between the knots is equal to 5 in this case. The value of each basis function can vary from 0 to 1 and vice versa. In numerical tests carried out the distance between the knots was usually lying in the numerical interval from 2 to 6, and the quantity of basis functions in a set was up to 1500.

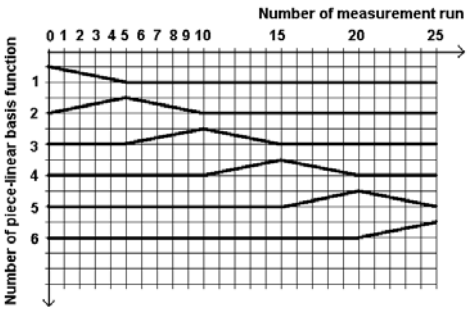

Fig. 3 A Demonstrational Set of Piece-linear Basis Functions
Which Defines the Irreversible Component

To obtain strictly irreversible component the values of unknown scalars x_k, $k=1\ldots n_i$, in (6) must be bounded with inequality constraints:

for non-decreasing irreversible component

$$x_{k+1} - x_k \geq 0, \qquad k = 1..n_i - 1; \tag{7-1}$$

for non-increasing irreversible component

$$x_{k+1} - x_k \leq 0, \qquad k = 1..n_i - 1. \tag{7-2}$$

So, to find all unknowns and $Ir(t)$ one should substitute $Ir(t)$ defined by (6) in (3), and thereafter solve (3) subject to inequality constraints (7-1) or (7-2), using *quadratic programming* or *constrained least-squares* method. In any case the total number of unknowns ($n_i + n_f$) should not exceed the total number of equations n_e. The distance between the knots of piece-linear basis functions must be defined so as to satisfy this condition.

Before discussing the next accompanying problem it is necessary to describe the resolving system of the standard *quadratic programming* method or of the similar to it *constrained least-squares* method (Gill P.E., Hammarling S, 1984), (Gill P.E., Hammarling S, 1986), (Coleman, T.F. and Y. Li, 1996):

$$\textit{find} \quad x \quad \textit{in} \quad \textit{the} \quad \textit{space} \quad R^n \quad ,$$

$$\textit{which} \quad \text{minimizes } f(x), \quad \textit{subject} \quad \textit{to} \quad \text{constraints} \quad l \le \begin{Bmatrix} x \\ Cx \end{Bmatrix} \le u, \tag{8}$$

$$\textit{where} \quad f(x) = \frac{1}{2} \| b - Ax \|^2 \quad \textit{or} \quad f(x) = c^T x + \frac{1}{2} x^T Mx, \tag{9}$$

where $\boldsymbol{C}$ is n_c by n matrix which contains coefficients of *general* constraints on unknowns $\boldsymbol{x}$ (e.g. *general* constraint is: $\boldsymbol{l}_{30} \le 4\,\boldsymbol{x}_1 + 6\,\boldsymbol{x}_5 \le \boldsymbol{u}_{30}$; *bound* constraint is: $\boldsymbol{l}_5 \le \boldsymbol{x}_5 \le \boldsymbol{u}_5$); n_c is the total number of *general* constraints; n is the total number of unknowns; $\boldsymbol{l}$ is (n+n_c)-element vector containing lower bounds of all constraints; $\boldsymbol{u}$ is (n+n_c)-element vector containing upper bounds of all constraints; $\boldsymbol{b}$ is n_e-element vector ($n_e \ge n$) containing known scalars (*vector of observations*); $\boldsymbol{A}$ is n_e by n matrix containing known scalars (*matrix of observations*); $\boldsymbol{M}=\boldsymbol{A}^T\boldsymbol{A}$ is n by n matrix containing known scalars (*matrix of the normal equations*); $\boldsymbol{c} = -\boldsymbol{A}^T\boldsymbol{b}$ is the working n-element vector containing known scalars. Both equalities in (9) are very similar as follows from the given description of values in (9).

As was shown above, procedure of in-situ measurements processing for SSIF (second example) is more complicated, than for the structures, working in elastic range (first example). It was solved for the first time in (Zagryadskiy I.I., 2001) and hereinafter it will be noted as *one-step algorithm for SSIF*. The next accompanying problem consists in adapting of *one-step algorithm for SSIF* for continuous uninterruptable SSIF monitoring. Hereinafter the last one will be noted as *continuous data processing algorithm for SSIF* or *multi-step algorithm for SSIF*. Its developing is actual taking into account the following circumstances.

It is very important to fix with high precision the moment of irreversible component $Ir(t)$ step-wise varying during SSIF monitoring. Such a step in $Ir(t)$ may indicate transfer of structure to emergency stage. The less will be time intervals between the knots of piece-linear basis functions $S_k(t)$, k=1…n_i, in (6), the more precise the moment of such a step can be estimated by means of in-situ measurements processing. But such time intervals decreasing leads to the measurement runs quantity increasing, which embarrasses data processing. Inevitable the moment will come, after which the data processing algorithm will not be able to operate fast with all accumulated data at one go.

Thus, there arouse the necessity to process time series on separate time intervals (time windows) solving (3) subject to constraints (7-1) or (7-2) with coupling and co-ordination of results in neighboring intervals. Such coupling and co-ordination may be provided by adding a set of equality constraints into *one-step algorithm for SSIF* (Zagryadskiy I.I., 2005). Illustrations at fig.4,5 help to understand better the procedure under discussion. At fig.4 is given the

time diagram of irreversible component *Ir*(*t*) varying step-wise and the shifted time window in various positions. Fig.5 interprets the logical schema of the *multi-step algorithm for SSIF*.

The problem of continuous data processing for SSIF was solved in the following consecution (fig.4). The time window was put in position 1 at the beginning of the data series. Then the *one-step algorithm for SSIF* was applied (system (3) taking into account (6) with constraints (7-1)). After getting estimates of unknowns x_k in (3) and in (6) for window position 1, the time window was shifted to the right along the time axis to position 2.

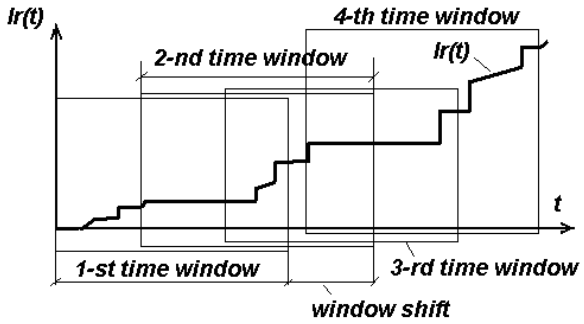

Fig.4 The Time Diagram of the Irreversible Component *Ir*(*t*)
and the Shifted Time Window in Various Positions

In position 2 the *one-step algorithm for SSIF* was repeated with a significant difference: constraints (7-1) or (7-2) were augmented with a set of equality constraints by modifying matrix *C* and vectors *l* and *u* in (8). These equality constraints had to provide the identity of the irreversible component *Ir*(*t*) values estimated in positions 1 and 2 on the time interval lying within the intersection of time windows 1 and 2. This requirement was quite essential: the stretch of the irreversible component *Ir*(*t*) already estimated in the first window had to remain unchanged.

In all the following shifted time windows the *one-step algorithm for SSIF* supplemented with a set of equality constraints was repeated by analogy with that one for the second window.

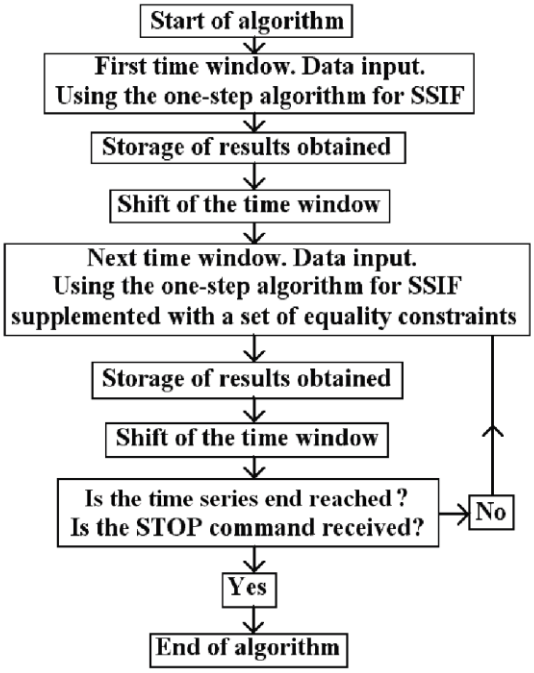

Fig.5 Logical Schema of the Algorithm for Continuous SSIF Monitoring (*Multi-step Algorithm for SSIF*)

Both *one-step algorithm for SSIF* and *multi-step algorithm for SSIF* were tested on imitated and on in-situ measured data with good results. The quality of estimates in the case of imitated data and step-wise varying irreversible component $Ir(t)$ was appreciably better than by applying the standard *least-squares* method. Both aforementioned algorithms for SSIF monitoring work robust including the case, when the irreversible component $Ir(t)$ is defined by any simple and smooth function (e.g. logarithmic, power, exponential function) because it may be defined correctly with a set of piece-linear basis functions.

Described algorithms can be applied for research of more complicated SSIF than that ones shown at fig.1. Irreversible component $Ir(t)$ in complicated SSIF may be viewed as an integral characteristic, accumulated in consequence of the presence of unpredictable flexibility of many small elements. Two examples of estimation of irreversible component $Ir(t)$ of diagnostic parameters of Sayano-Shushenskaya arch-gravity dam are shown below. Displacements of the dam crest (first case) and arch stress in the dam body near the crest (second case) were investigated in (Zagryadskiy I.I., 2001). Empirical model of both processes was given in the form (3). The first load $F_1(t)$ was set equal to hydrostatic head $H(t)$, the second load $F_2(t)$ was set equal to $H(t)^2$. The third load $F_3(t)$ was represented by water temperature measured in reservoir in the point deepened by 10 meters under water level near the upstream dam face, and the fourth load $F_4(t)$ – by smoothed and shifted by 30 days air temperature. Irreversible component $Ir(t)$ was given in form (6), and constraints (7-1) and (7-2) were applied. The *one-step algorithm for SSIF* was used to solve both problems.

Results are illustrated at fig. 6. It was shown that the growth of irreversible component $Ir(t)$ of dam displacements was proceeding step-wise mainly in Spring and in Summer during intensive reservoir impounding. Two noticeable steps were timed to repair works of the dam upstream face and to its rock foundation artificial strengthening (fig.6*a*). The same tendencies were present in behavior of irreversible component of normal arch compression stress (with the sign "minus"). It was also varying step-wise in the similar manner (fig.6*b*). One can interpret such results in the following way. Steps in $Ir(t)$ diagrams indicated moments of defects

in the dam body and rock foundation (cracks, opening joints etc.) arising or progressing. Then the structure worked in elastic stage some time up to the next adverse and extreme load combination, which lead to the next step in $Ir(t)$ diagram and so on. Repair works could also have the same consequences. Thus each step in $Ir(t)$ diagram of diagnostic parameter could indicate changes in monitoring subject. Diagrams of residuals $Res(t)$, which are equal to the differences between measured diagnostic parameters and estimated ones, confirm a good quality of estimation.

In many successfully solved test problems the ideal situation was imitated: the so called in-situ measurements were supposed to be free of noise. Moreover, the structure of system (3) and accordingly the set of loads were supposed to be known exactly. Some other tests carried out elicited a fact that the addition of noise to the data processed reduces the results quality. Though, described methods of SSIF monitoring had advantage over the other ones even in the presence of noise and uncertainty of the structure of resolving system.

One of such tests is discussed below. The non-decreasing irreversible component $Ir(t)$ was specified according to (4) with the sign "plus" in it. First ten loads were represented by a set of first ten Chebyshev orthogonal polynomials, and the eleventh one – by the white noise. Then $Ir(t)$ and eleven loads multiplied by given scalars were summed to obtain the diagnostic parameter $D(t)$. Diagrams of all loads except the last one, of $Ir(t)$ and of $D(t)$ are shown at fig.7*a*,*b*,*c*. All series included 1000 values. Up to that moment all calculations were carried out with 14 significant digits. After that only four significant digits were left in all series to imitate a real metering process with limited precision. Correct values of $Ir(t)$ and of multipliers by loads were "forgotten" and then estimated by means of least squares method and by means of *one-step algorithm for SSIF*.

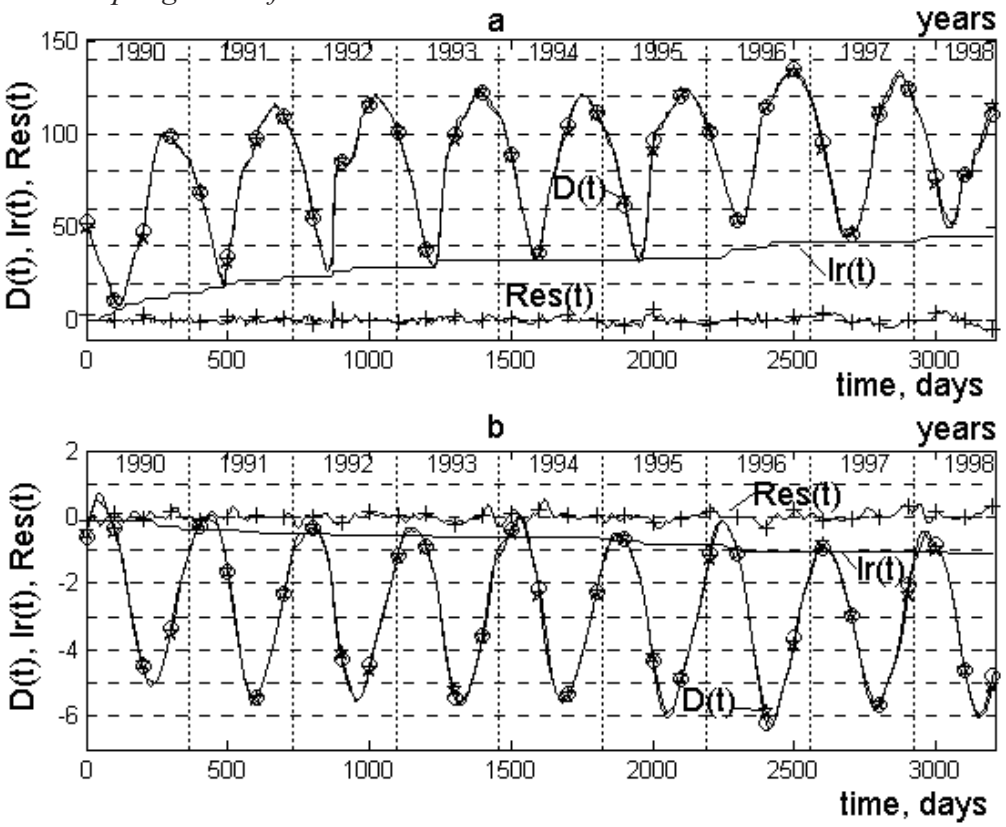

Fig.6 Results of Processing of Diagnostic Parameters of Sayano-Shushenskaya Arch-gravity Dam. *a* – Displacements of the Crest in Millimeters;
b – Normal Arch Compression Stress in MPa.

Values of multipliers by loads are given in table 1 below. Diagrams of estimated $Ir(t)$ and of $D(t)$ are shown at fig.7*c*.

Table 1
Correct and Estimated Multipliers by Loads in test example

Loads	Correct Multipliers by Loads	Multipliers Estimated by One-step Algorithm for SSIF	Multipliers Estimated by Least Squares
Absolute term	408.108	468.935	-31591.101
$F_1(t)$	231.672	170.333	53692.509
$F_2(t)$	0.719	115.940	-25911.620
$F_3(t)$	8.314	-57.920	-3204.325
$F_4(t)$	2.467	-21.123	21708.678
$F_5(t)$	7.520	128.717	-25522.044
$F_6(t)$	-8.722	-183.282	19053.612
$F_7(t)$	-1.679	161.585	-9952.833
$F_8(t)$	3.620	-104.134	3483.313
$F_9(t)$	0.645	48.761	-662.134
$F_{10}(t)$	-5.316	-16.530	14.733
$F_{11}(t)$	0.777	0.777	0.768

This relatively complicated test problem was solved in both cases very approximately. Correct and estimated values of multipliers by loads differ essentially (see table 1 above). But the estimation made by means of *one-step algorithm for SSIF* is more realistic.

The difference between correct $Ir(t)$ and its estimation made by means of *one-step algorithm for SSIF* is not big (about 15% of its magnitude) and is quite acceptable taking into account complexity of the problem. Interpretation of least squares method results is more complicated. When analyzing the residuals diagram $Res(t)$ at fig.7*c*, got by Least Squares method one can pick out moments of its step-wise increasing. But we cannot suggest any reliable method to transform such saw-tooth oscillations of $Res(t)$ to non-decreasing $Ir(t)$ described by (4).

Thus *one-step algorithm for SSIF* had advantages in the test example above as well as in many other tests. But it is reasonable to use both methods when solving ill-posed problems. Such way permits to avoid errors provoked by numerical instability. In the abovementioned test example the values of steps of $Ir(t)$ at fig.7*c* are comparable with steps of $Res(t)$ at fig.7*c*. It instills confidence in getting results of acceptable quality.

Besides optimal determining of the complicated step-wise varying form of the irreversible component, the described method of continuous SSIF monitoring (*multi-step algorithm for SSIF*) allows to detect the changing of unknowns x_k by loads $F_k(t)$ in (3) if it really occurs with time, e.g. due to beam rigidity decreasing as a result of cracks progressing (fig.1*a,b*).

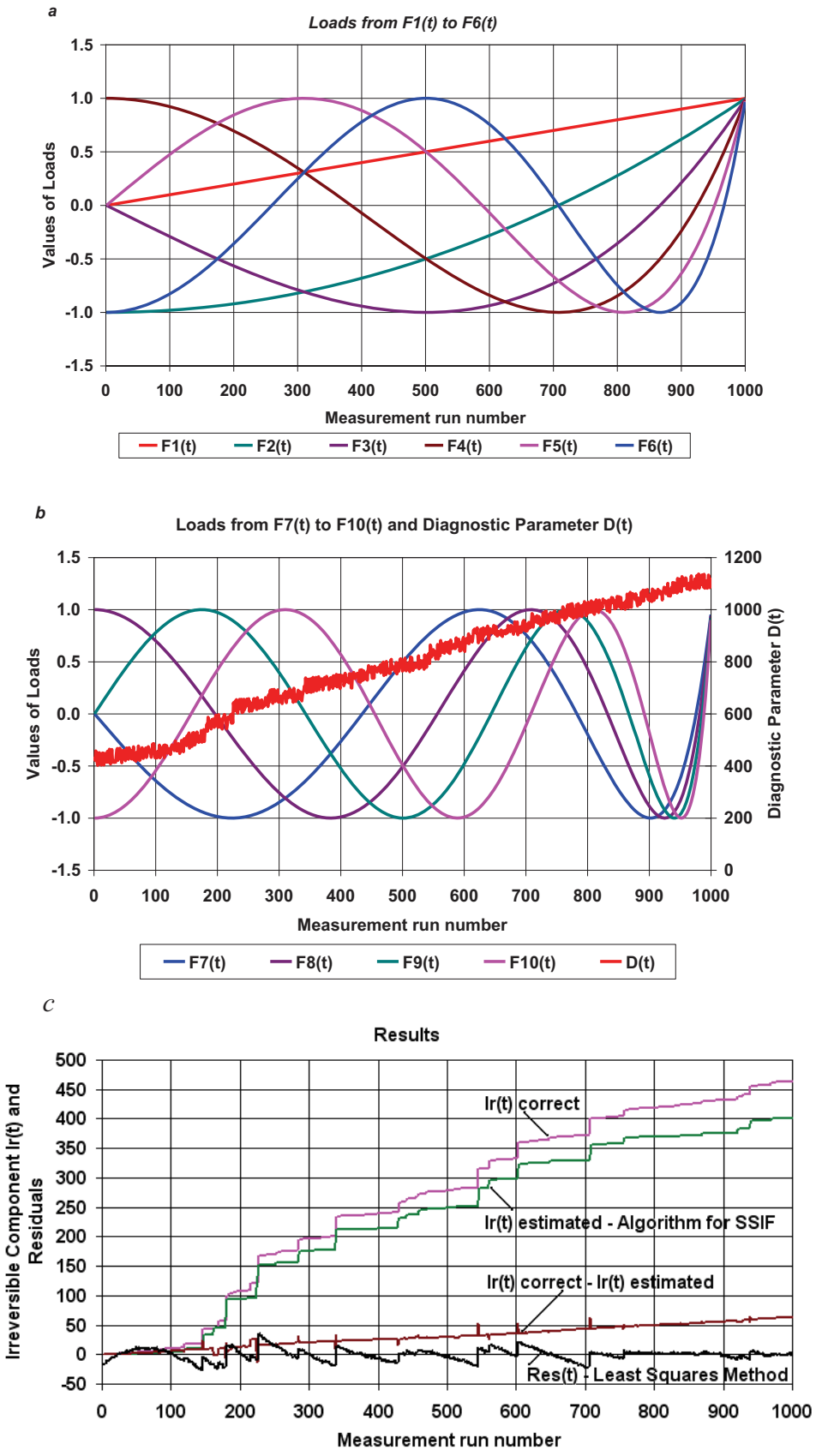

Fig.7 Results of Test Example Solving. *a,b* – Loads and Diagnostic Parameter; *c* – Irreversible Component *Ir*(*t*) Correct and Estimated and Residuals

The described *one-step* and *multi-step* algorithms may be recommended for research and monitoring of simple and complicated SSIF. They require precise input data, as well, as other algorithms for data processing and structures monitoring. The area of application of considered methods is sufficiently wide, because every elastic structure can change over to emergency stage and simultaneously to the SSIF class, being provoked by extremely load combinations.

REFERENCES

Coleman, T.F. and Y. Li, "A Reflective Newton Method for Minimizing a Quadratic Function Subject to Bounds on some of the Variables," SIAM Journal on Optimization, Vol. 6, Number 4. (1996). 1040-1058

Gill P.E., Hammarling S, Murray W, Saunders M.A. and Wright M.H. Procedures for optimizations problems with a mixture of bounds and general linear constraints. ASM Trans. Math. Software 10. (1984). 282-298.

Gill P.E., Hammarling S, Murray W, Saunders M.A. and Wright M.H. Users guide for LSSOL (Version 1.0). Report SOL 86-1. Department of Operations Research, Stanford University. (1986)

Zagryadskiy I.I. Use of the quadratic programming method for solving the problem of control of concrete dams. Scientific and technical news. Saint-Petersburg Technical University. № 1 (23). Saint-Petersburg. (2001) 85-90 (in Russian)

Zagryadskiy I.I. Exposure of irreversible changes in construction behavior, accumulating with varying velocity and step-wise, based on processing of in-situ measurements. Collected articles of the 4-th International Conference «Scientific and technical problem − the forecast of safety and durability of building structures − and methods of its solving». Saint-Petersburg Technical University. Saint-Petersburg. (2001) 127-131 (in Russian)

Zagryadskiy I.I. Method of continuous monitoring of building structures, including elements with stochastic flexibility. Scientific and technical news. Saint-Petersburg Technical University. № 1 (34). Saint-Petersburg. (2005) 158-165 (in Russian)

Abstract

Monitoring method of structures, which include elements with stochastic irreversible flexibility (hereinafter SSIF) is described. Behavior and, accordingly, SSIF monitoring numerical algorithms based on in-situ measurements processing using quadratic programming or constrained least-squares method have appreciable peculiarities and differ from those ones intended for structures working in elastic or elasto-plastic range. Properties which are common for all SSIF are shown, and the problem of composing of the resolving system of the method is considered. The discussed algorithm is adopted for continuous SSIF monitoring.

ENGURI DAM, REHABILITATION'S PROJECT*

Claude Bossoney

STUCKY SA Ltd, Renens, Switzerland

CHARACTERISTICS OF THE DAM

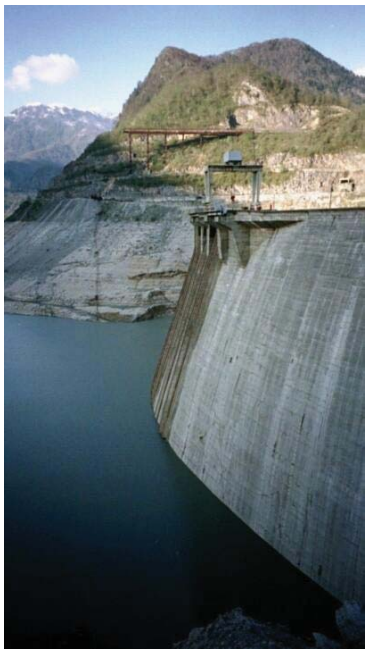

- Crest Elevation	511.5 m.a.s.l.
- Drawdown reservoir elevation (bottom outlet)	329 m.a.s.l.
- Normal minimum reservoir elevation	410 m.a.s.l.
- Normal maximum reservoir elevation	510 m.a.s.l.
- PMF level	510.5 m
- Max. height above foundation	271.5 m
- Crest length	728 m
- Volume of the dam	3.9 mio m^3
- Lombardi Boldness Coefficient	12.5
- Ratio between crest length and height	2.7
- Catchment area	4'060 km^2
- Total storage volume	1'100 mio m^3

STARTING CONDITIONS

- The stoplogs were lying into the reservoir.
- Only two bottom outlets were operable.
- The spillways were out of use.
- Only two turbines were operable.
    - The control of the reservoir operation was lost.
- Rumors about abutments displacements.
- Impressive leakage passing through the dam.
- VI Horizon was flooded.
- Evidence of piping into some galleries.
- Monitoring system severely damage.
- Dam archives were practically non-existent.
- Budget available.

* The publication is based on the author's presentation at 9th Benchmark Workshop

THE PROBLEMS POSED

Hierarchy of the Problems.

- Check the behaviour of the dam.
- Refurbish the monitoring system
  - Compare magnitude of displacements with those of a numerical model.
  - Evolution of measurements with the time.
- Reduce the high seepage.
- Refurbish powerhouse and pressure tunnel
- Other problems of the second priority.

THE SOLUTIONS IN PROGRESS

1. The monitoring system is working.
2. Repair of the grout curtain in progress.
3. Refurbishment of the Powerhouse in progress.
4. Refurbishment of the Power tunnel: first refurbishing step accomplished.
5. Behaviour of the dam checked by monthly monitoring and back analysis.

BACK ANALYSIS

Aims of this work:

- To obtain a reasonable picture of displacements for the normal load cases.
- To evaluate the change brought by exceptional load cases.
- To make a tentative safety analysis for seismic loads with available data.

Dam Layout and Geometric Model Development

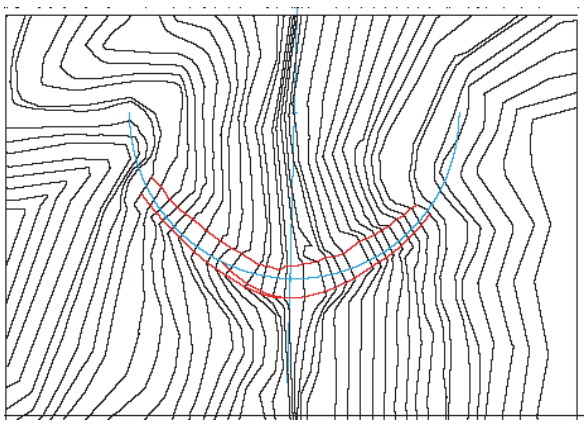

Topography and Dam footprint Dam

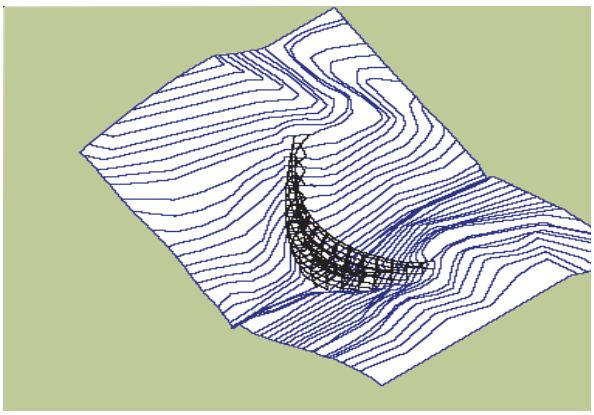

Super Element and Topography

Sources:

- Topography & dam drawing: Fax sketch without scale.
- Dam, blue copies of the horizontal sections for the dam at levels 265, 315, 360,402, 450.5, 511.5 masl. GIDROPROEKT. Drawing numbers: from 4297-1013012 to 4297-1013015, Scale 1:500
- Discreet Mesh from a former computation (supplied by Prof.Kalabegishvili) Russian-Georgian FE Model , in term of txt and excel files.

Basic Modelling Approach and Available Control Data

FE Geometry Comparison at Levels:

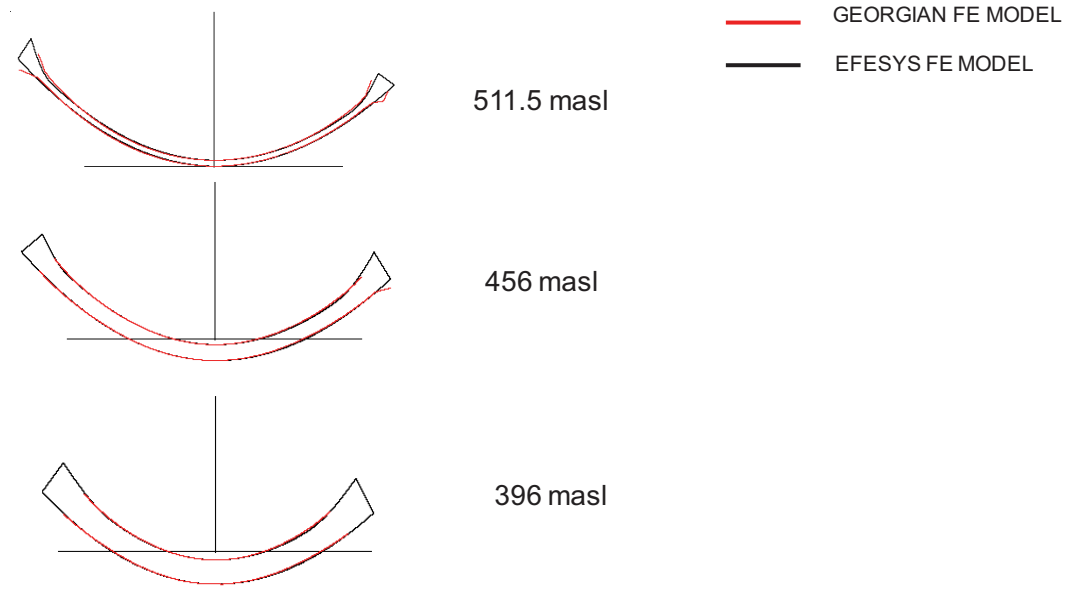

Geology

Foundation-Rock Properties and FE Zoning System

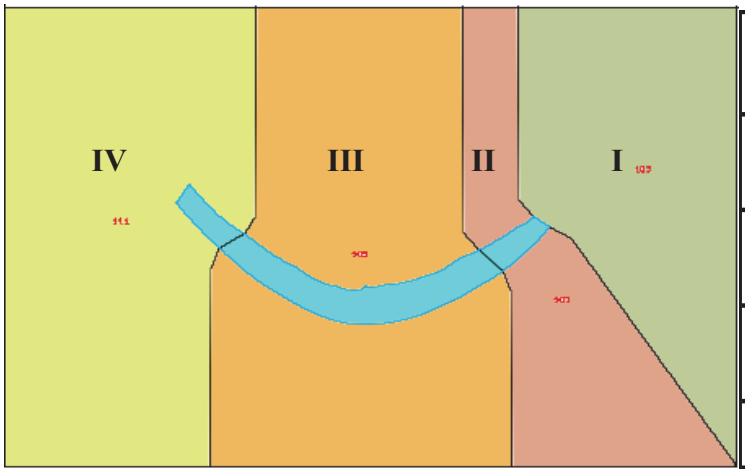

Zone Name	Geological Zone	Elasticity Modulus [GPa]
Outer Right Bank	I	2 3
Inner Right Bank	II	3.5 4.5
Valley Bottom	III	13 16
Left Bank	IV	7 9

Source:

1. The Enguri Power Station, Book in Russian by ChogovadzaG., Megabrushwilli E. and Lomov., Edited by Energotommizdat, Moscow, 1987, pages 23-26

2. Data by supplied by Prof.Kalabegishvili (in terms of word.file)

Concrete Specifications

Determined Dam Concrete Zones

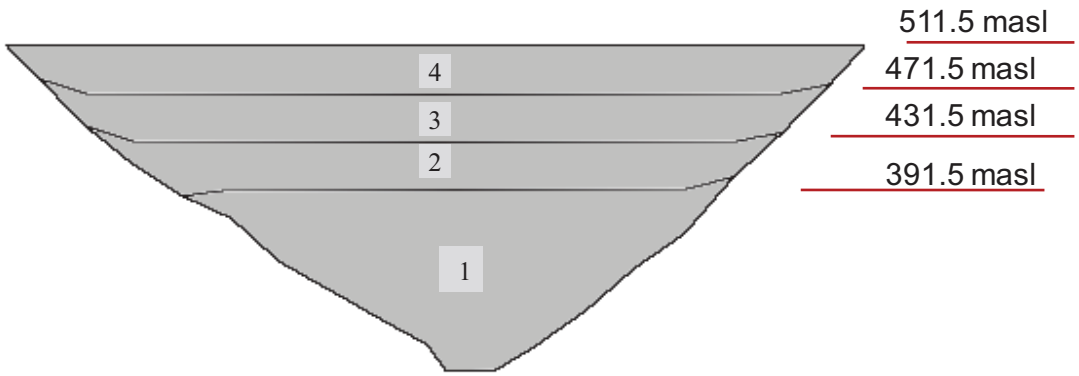

Zone Name	Elasticity Modulus [GPa]	Stage
1	32	I
		Until levels 416 or 370 masl according to the upper and lower levels of the blocs
2	32	I
3	40	II
4	51	II
		Until level 511.5 masl incl. anti-seismic belt

Steel Reinforcement

Location	Concrete Volume 10*3 m3	Monolith concrete Total Reinforcement t	Monolith & pre-cast concrete Reinforcement kg/m3 Concrete	Total Reinforcement t	Reinforcement kg/m3 Concrete
I Stage	2150	19588	9.1	22 738	-
II Stage, inc. anti-seismic	1670	33 821	20,2	36 646	-
Anti-seismic	-	22 000	13.2	-	-
Total for the dam	3820	53 409	14.4	59 384	15.5

Source:

The Enguri Power Station, Book in Russian by ChogovadzaG., Megabrushwilli E. and Lomov., Edited by Energotommizdat, Moscow, 1987, page 41

Reinforced Mass Concrete

Quantity	Stage 1	Stage 2 lower	Stage 2 upper		
	general	general	general	belt only	total horizontal
Total Concrete Volume [m3 x 1000]	2150	918.50	751.5	751.5	751.5
General reinforcement [t x 1000]	19.59	11.27	22.55		
Reinforcement assumed for each direction [t x 1000]	9.79	5.64	11.27		
Reinforcement for seismic belt [t x 1000]				22.00	33.27
Density of steel [t/m3]	7.85	7.85			7.85
Volume of steel / volume of concrete	0.058%	0.078%			0.564%
Assumed Concrete elasticity modulus [GPa]	31.00	39.00			44.25
Elasticity modulus for steel [GPa]	200.00	200.00			200.00
Total modulus in direct tension/compression [GPa]	31.10	39.13			45.13
Total modulus in bending [GPa]	31.68	39.91			50.77

Static and Dynamic Loads

Combinations of Basic Static Loads

Load Combination	Basic Loads								Safety Factor	
	Self Weight	Hydrostatic [m a.s.l.]					Temperature		Zones Compression & Tensions	
		Reservoir Water				Silt				
	Single Grouting Stage	Draw-down	Normal Min.	Normal Max.	PMF	Max	Max	Min		
	329	410	510	512	320	Summer	Winter	C-C	T-T	
Self Weight	1									
Drawndown Summer	1	1				1	1		3	1
Drawndown Winter	1	1				1		1	3	1
Min. Operating Level Summer	1		1			1	1		3	1
Min. Operating Level Winter	1		1			1		1	3	1
Max. Operating Level Summer	1			1		1	1		3	1
Max. Operating Level Winter	1			1		1		1	3	1
PMF Summer	1				1	1	1		2	1
PMF Winter	1				1	1		1	2	1

Combinations of Dynamic Loads

Load Combination	Basic Loads								
	Self Weight	Hydrostatic [m a.s.l.]				Temperature		Seismic	
		Reservoir Water			Silt				
	Single Grouting Stage	Draw-down	Normal Min.	Normal Max.	Max	Max	Min		
	329	410	510	320		Summer	Winter	OBE	MCE
Drawndown Summer + OBE	1	1			1	1		1	
Drawndown Winter + OBE	1	1			1		1	1	
Min. Operating Level Summer + OBE	1		1		1	1		1	
Min. Operating Level Winter + OBE	1		1		1		1	1	
Max. Operating Level Summer + OBE	1			1	1	1		1	
Max. Operating Level Winter + OBE	1			1	1		1	1	
Max. Operating Level Summer + MCE	1			1	1	1			1
Max. Operating Level Winter + MCE	1			1	1		1		1

Correlation Studies

- Thermal Calibration
- Displacements Correlation

Back-Analysis of Thermo-Couple Data

Approximation of Ambient and Reservoir Water Temperatures using Stucky-Derron Method

$$\theta_a(t) = \overline{\theta_a} + A_a \cos(\omega t - t_{a,0})$$

$$\theta_w(t) = \overline{\theta_w} + A_w \cos(\omega t - t_{w,0})$$

The ambient temperature of the air and reservoir water at elevations 343 and 485 masl were measured during a given year (in our case 2000).

Variation of Ambient Air Temperature for Year 2000

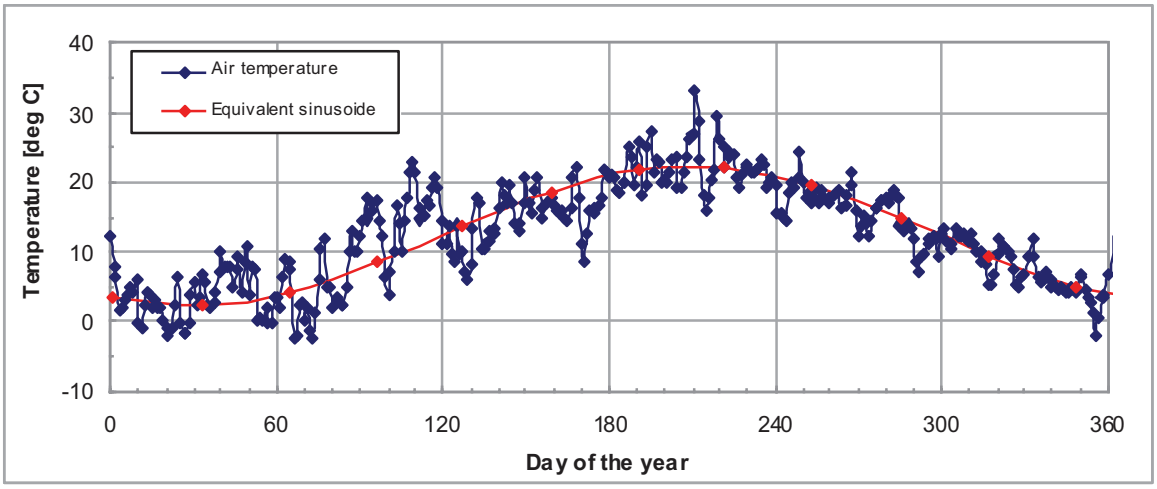

Showing the equivalent cosine function of time.

Variation of Water Temperature at Elevation 485 masl for Year 2000

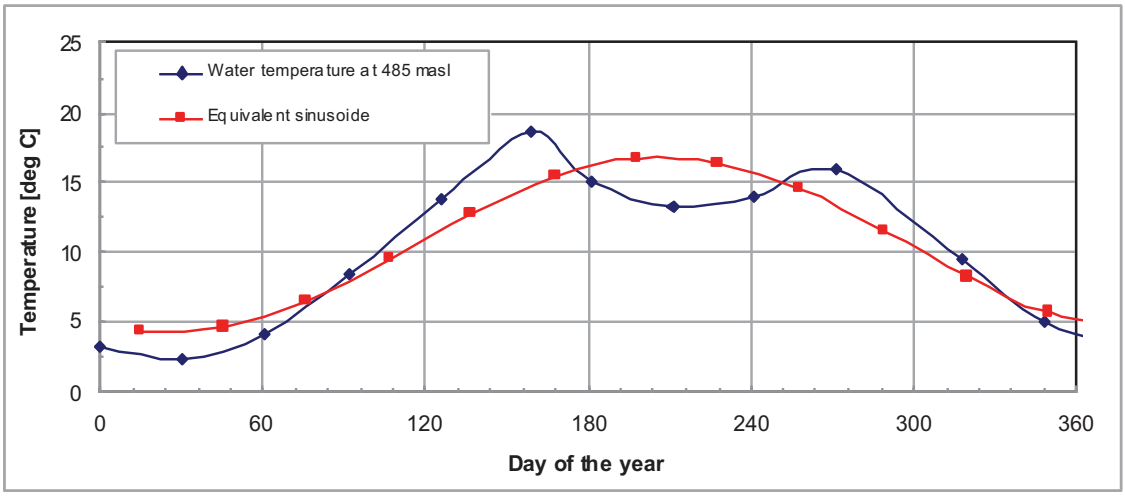

Showing the measured temperature when the lake level is over the measurement point as well showing the equivalent cosine function of time

Correlation of Measured with Computed Temperatures

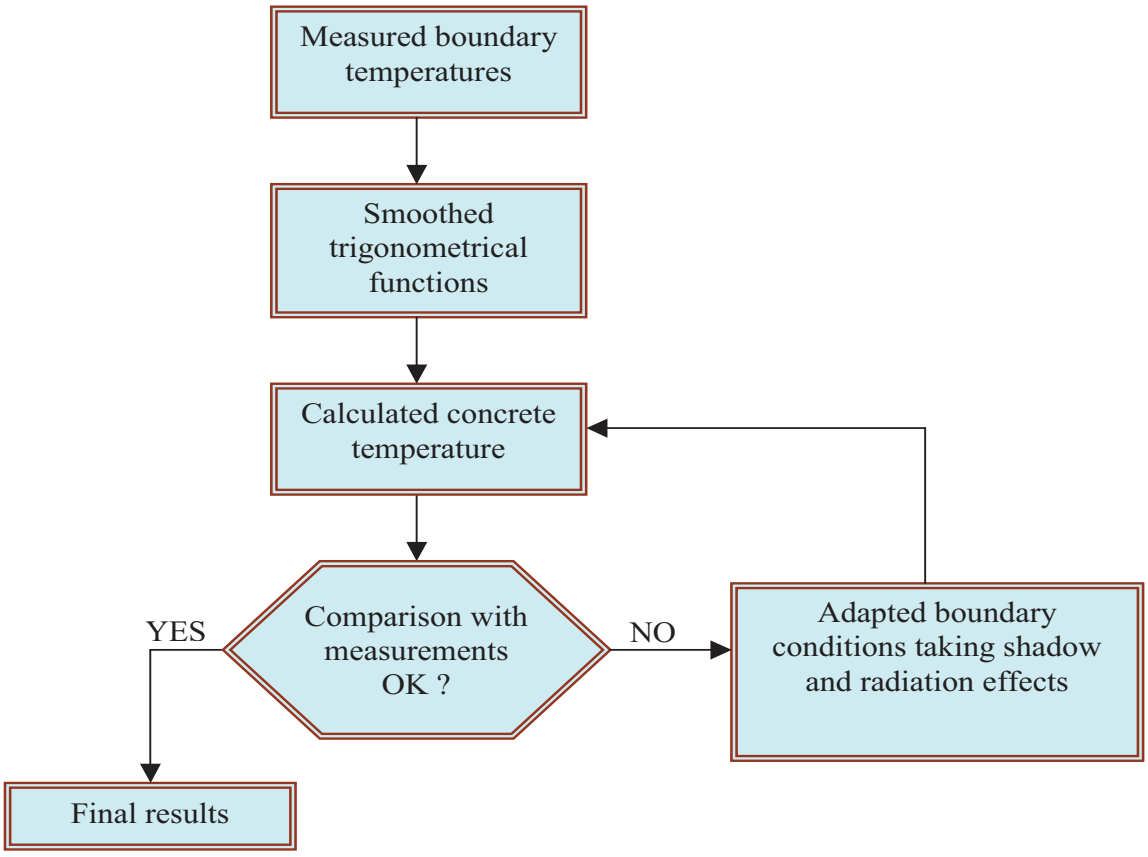

Temperature Calibration (year 2000) at level 485 masl

Block 12 | Block 18 | Block 26

US

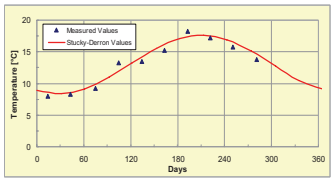

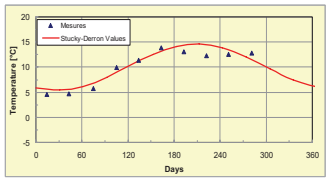

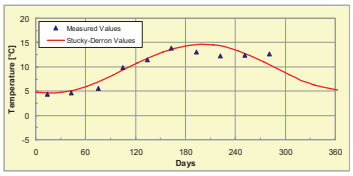

C

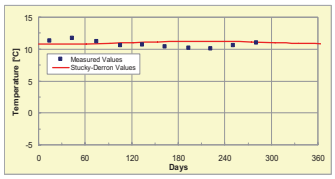

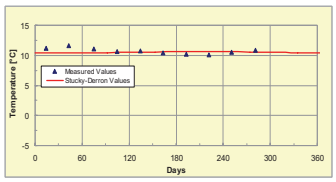

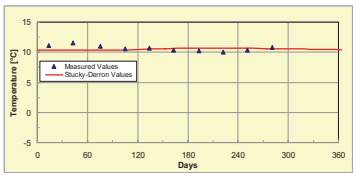

DS

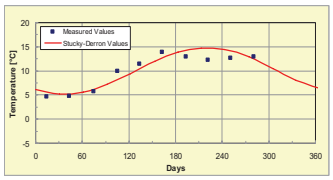

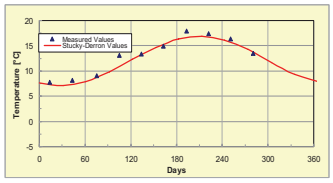

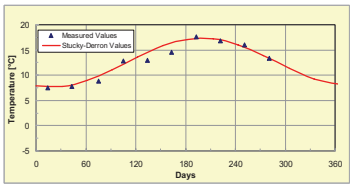

Temperature Calibration (year 2000) at Level 343 masl

Block 12 | Block 18 | Block 26

US

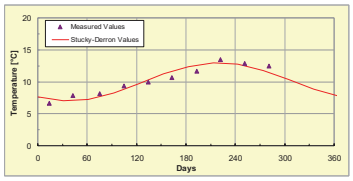

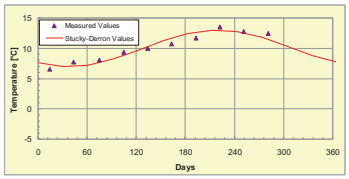

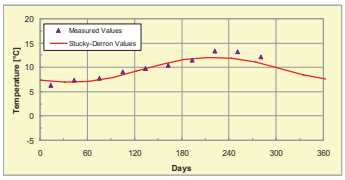

C

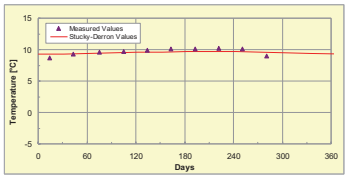

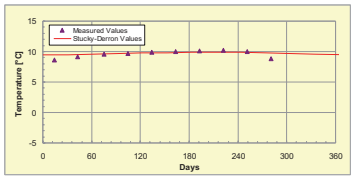

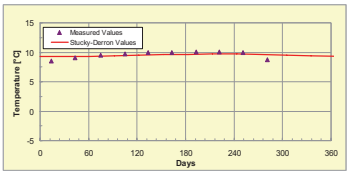

DS

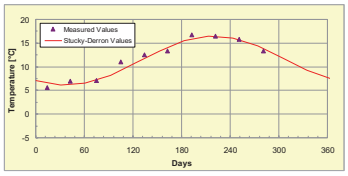

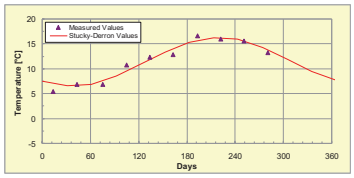

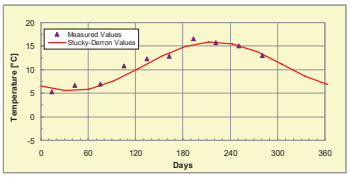

Face Temperatures Correlated from the Stucky-Derron Formulation in Comparison with the Temperatures Correlated from Ambient Conditions

Face	Mean or Amplitude	Elevation [masl]	S-D Correlated Temperature [°C]	Ambient Correlated Temperature [°C]	Difference Temperature [°C]
Upstream	Mean	485	10.5	10.5	0
		343	9.5	8.7	0.8
	Amplitude	485	6.3	6.3	0
		343	4.1	3.5	0.6
Downstream	Mean	485	12	12.5	-0.5
		343	11.5	12.5	-1
	Amplitude	485	6.8	10	-3.2
		343	7.2	10	-2.8

Face temperatures correlated from the Stucky-Derron formulation in comparison with temperatures correlated from ambient conditions

Difference [c°] obtained between the Stucky-Derron calculated and the correlated mean and amplitude values for the various thermocouple locations for Blocks 12, 18 and 26

Measurement Location	Mean or Amplitude	Elevation [masl]	Block 12	Block 18	Block 26
Upstream	Mean	485	-2.4	0.6	1
		343	-0.5	-0.5	0
	Amplitude	485	0	0	-0.4
		343	-0.2	-0.2	0.2
Centre	Mean	485	0.3	0.8	0.8
		343	1.7	1.5	1.7
	Amplitude	485	0	-0.1	0
		343	-0.3	-0.5	-0.3
Downstream	Mean	485	1.9	-0.1	-0.6
		343	0.2	0.1	0.8
	Amplitude	485	0.2	0.1	0.2
		343	-0.2	0.1	-0.2

Displacement Correlation

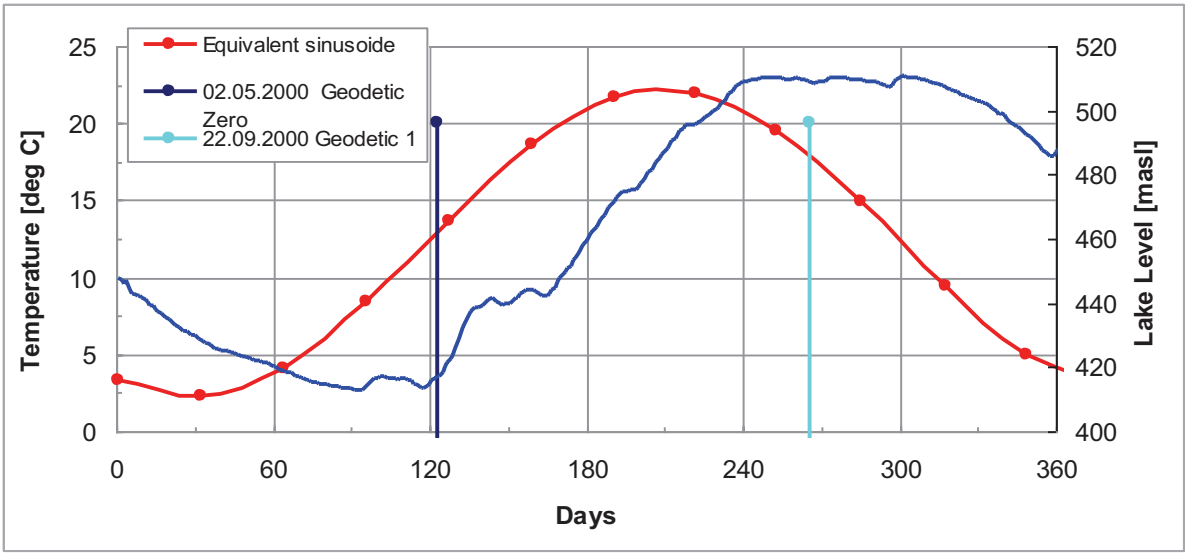

Equivalent sinusoid ambient temperature variations showing also the dates for the zero and the first geodetic surveys

Geodetic Measurement Comparisons

Displaced Section at Elev. 511.5 masl

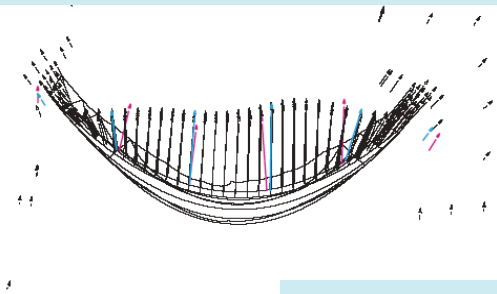

Displaced Section at Elev. 450 masl

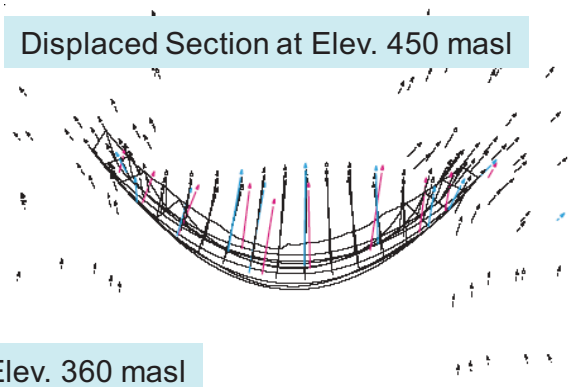

Displaced Section at Elev. 360 masl

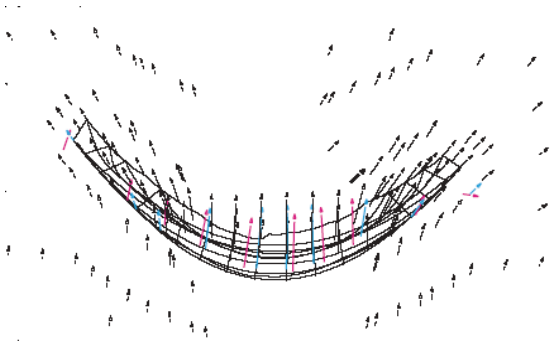

PLUMB-LINE DATA

Thermal and Hydrostatic Effects

Case 1 Thermal Effect

Date:	Lake level
29.01.1996	430.26 m a.s.l.
10.05.1996	427.08 m a.s.l.

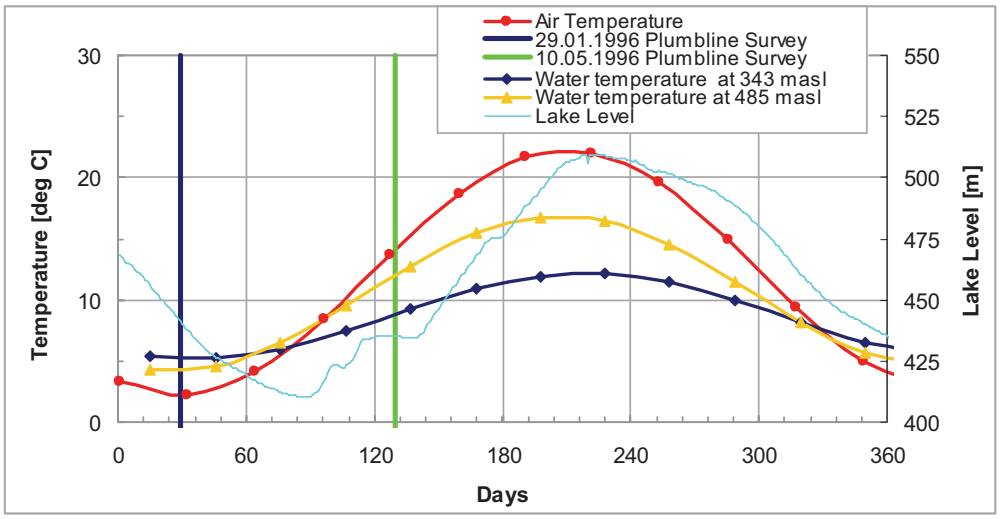

Temperature and Hydrostatic Effects

Case 2 Hydrostatic Effects & Temperature

Date:	Lake level
11.03.2001	403.50 m a.s.l.
05.08.2001	509.83 m a.s.l.

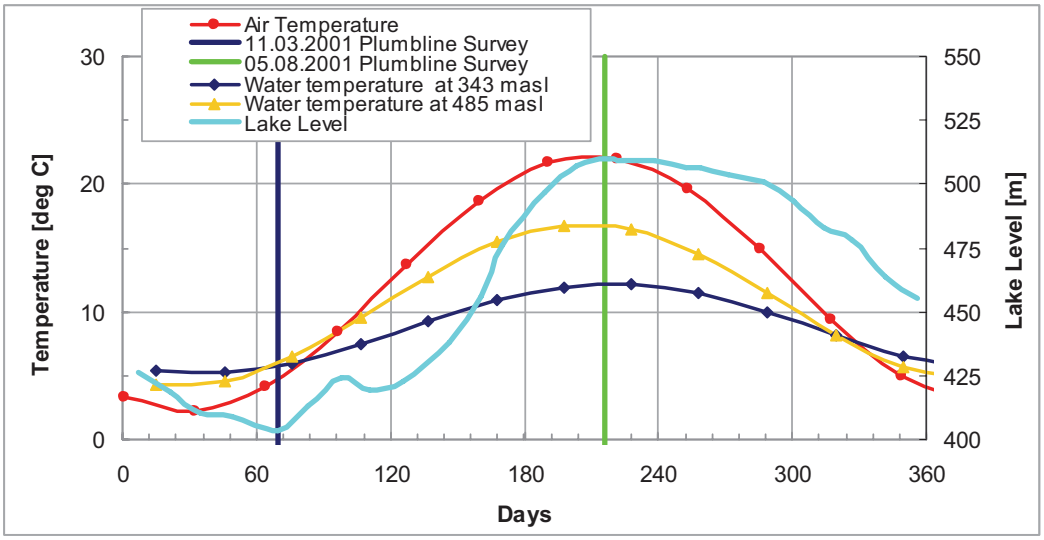

Plumbline Correlation

Displacement Vector Length for Blocks 12, 18 and 26

	Case 1	Case 2
Block 12 Left Bank	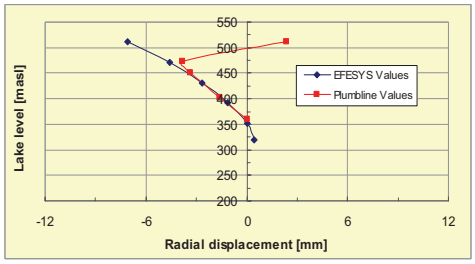	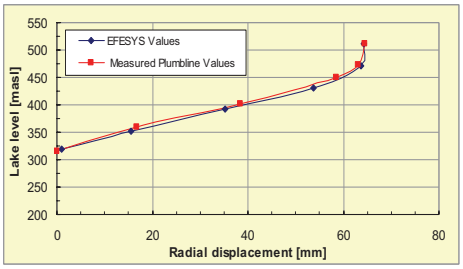
Block 18	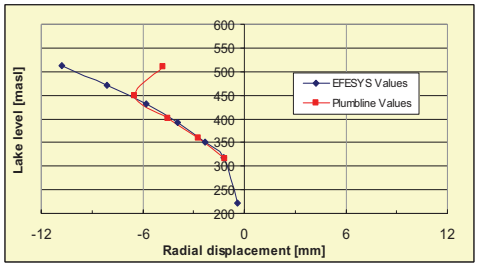	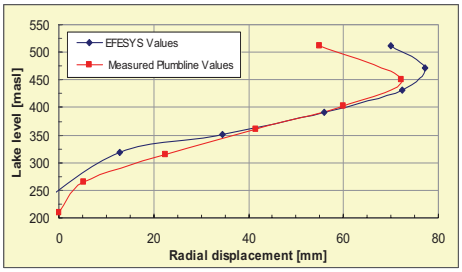
Block 26 Right Bank	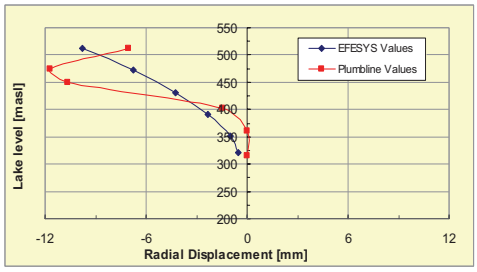	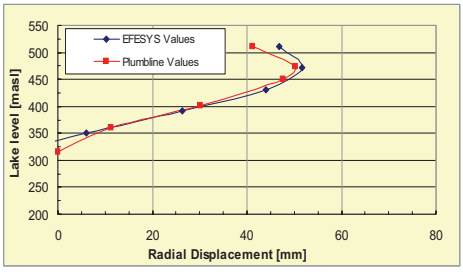

The numerical model

Geometrical Model of the Dam and Perspective View of the Foundation

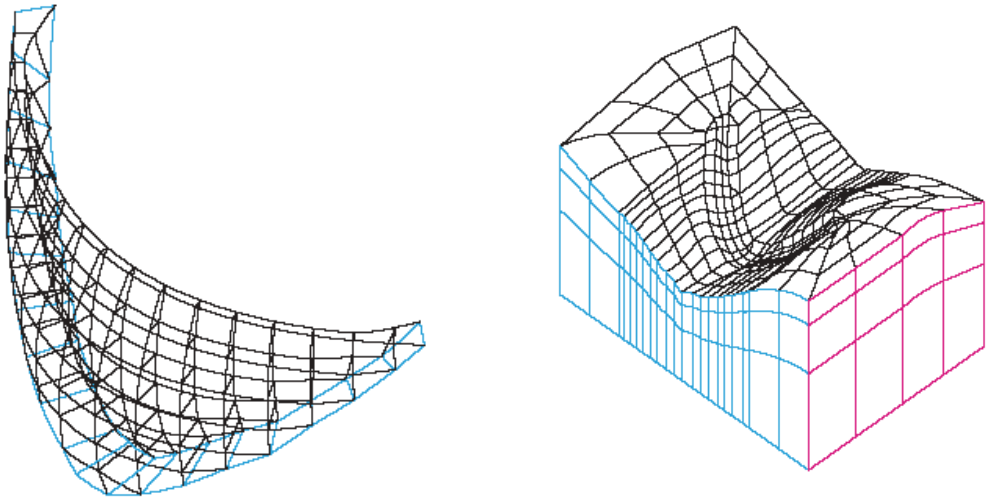

Super Elements of the Dam

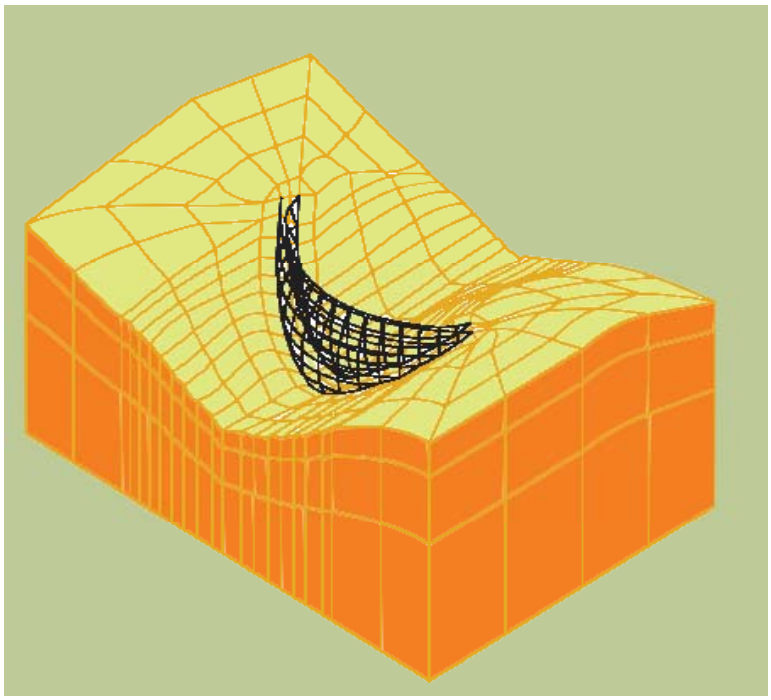

A total of 6'160 nodes resulted from the model, each with three degrees of freedom.

Earthquake Time History

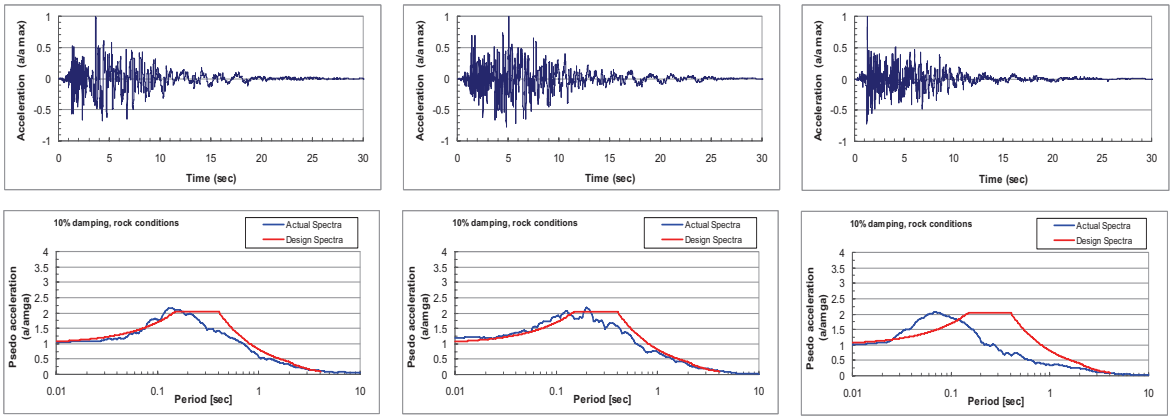

Cross Valley motion | Upstream – Downstream motion | Vertical Motion

Earthquake: 1984 year, event at Morgan Hill, California.

The magnitude of the earthquake was 6.2

The total earthquake duration was 30 seconds

Scaled at a max = 0.54 g for MCE

Scaled at a max = 0.23 g for OBE

Safety Evaluation

Resonant frequences [Hz] for the first eight modes of vibration for reservoir empty and full

Lake Level	Frequency for the given mode number [Hz]							
	1	2	3	4	5	6	7	8
Empty	1.58	1.82	2.34	2.89	3.41	3.45	3.69	4.04
Full	1.23	1.40	1.78	2.31	2.73	2.99	3.10	3.61

Maximal Principal Stresses and Required Strengths [Mpa] for Various Static Load Combinations

Annex	Load Combination	Maximum Stress [MPa]				Maximum Required Strength [MPa]	
		Compression		Tension			
		water face	air face	water face	air face	water face	air face
6.1	End of Construction	6.3	3	0.7	1	<15	15
6.2	Drawdown at level 329 masl - Summer	7.2	4.8	0.1	0.8	<25	<25
6.3	Drawdown at level 329 masl -Winter	6.2	3.8	3	2.7	28	<25
6.4	Min. Operating Level - Summer	6.1	6.3	0	0	<25	<25
6.5	Min. Operating Level - Winter	5.1	5.7	2.9	2.9	32	<25
6.6	Max. Operating Level - Summer	11.5	13.6	0.3	0	<33	40
6.7	Max. Operating Level - Winter	7.4	14	1.9	3.2	32	45
6.8	PMF - Summer	11.8	13.9	0.3	0	<25	26
6.9	PMF - Winter	7.5	14.2	2	3.2	31	45

Maximal Principal Stresses and Required Strengths [Mpa] for Various Static & Dynamic Load Combinations

Annex	Load combination	Maximum Stress [MPa]			
		Water Face		Air Face	
		Tension	Compression	Tension	Compression
7.1 - 7.2	Drawdown Level at level 329 masl - Summer + OBE	4.3	9.9	3.7	11.2
7.3 - 7.4	Drawdown Level at level 329 masl - Winter + OBE	9.4	8.5	9.3	5.1
7.5 - 7.6	Min. Operating Level - Summer + OBE	4.2	10.1	4.1	12.1
7.7 - 7.8	Min. Operating Level - Winter + OBE	9.3	7.7	9.6	7.5
7.9 - 7.10	Max. Operating Level - Summer + OBE	3.6	22.9	2.2	25.1
7.11 - 7.12	Max. Operatingl Level - Winter + OBE	4.6	17.7	3.9	18.2
8.1 - 8.2	Max. Operatingl Level - Summer + MCE	4.8	30.2	7.6	32.6
8.3 - 8.4	Max. Operating Level - Winter + MCE	8.5	25.1	13.0	25.7

Block Stability Analysis

The 10 following cantilevers have been checked:

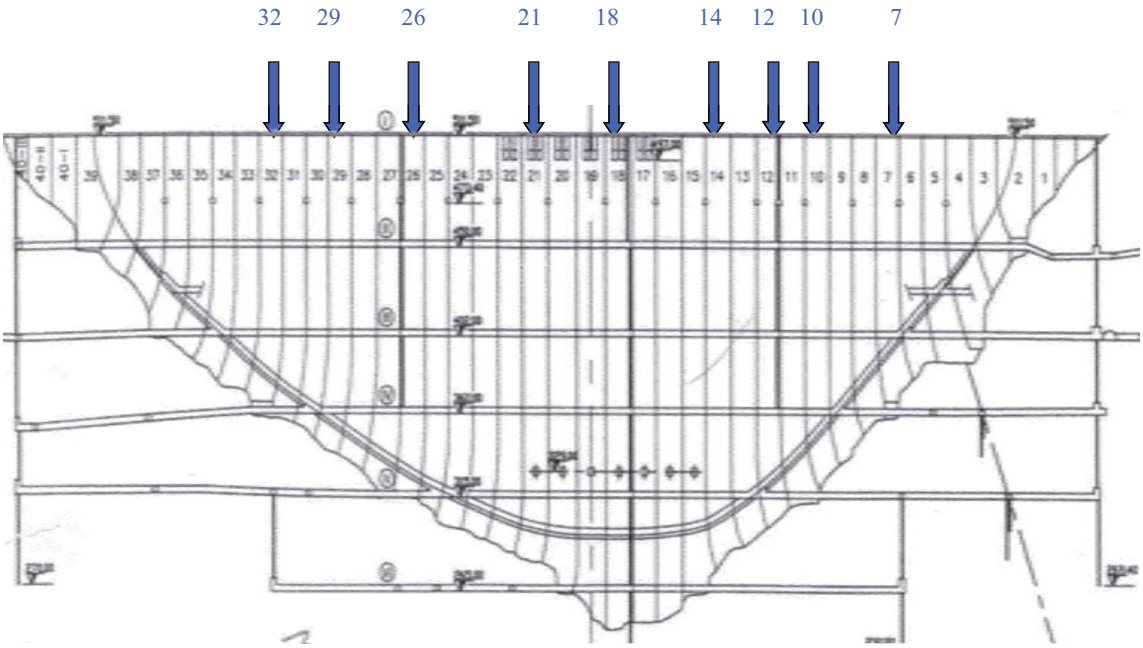

As an example, the geometry of the crown cross-section:

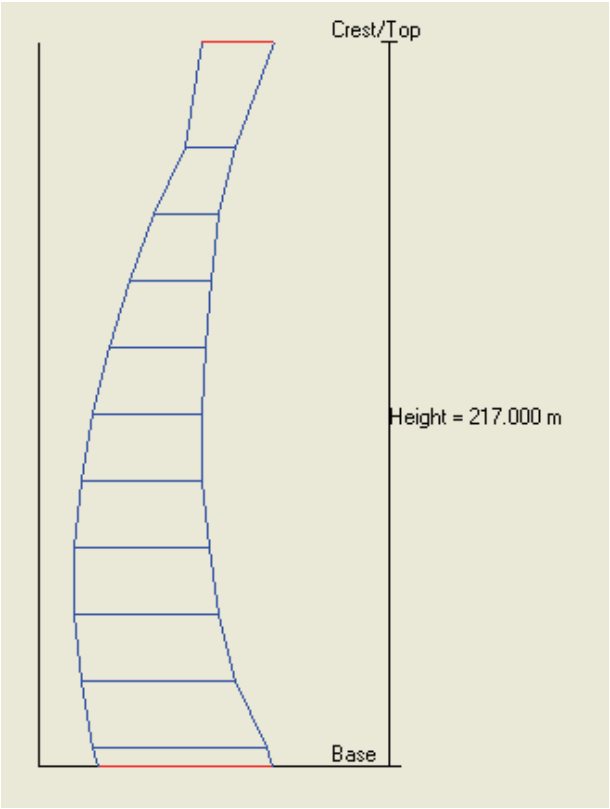

As example, the stresses along the faces for the crown block:

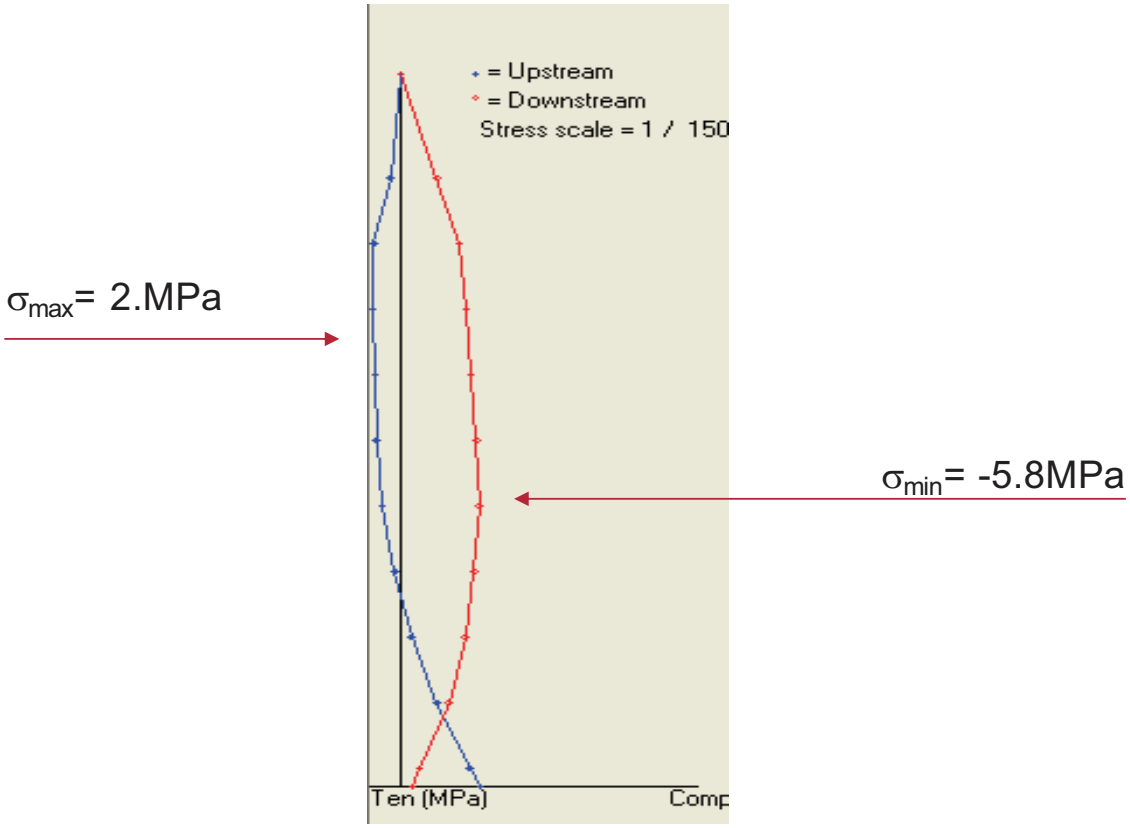

The geometry of the "most critical" block (block 14):

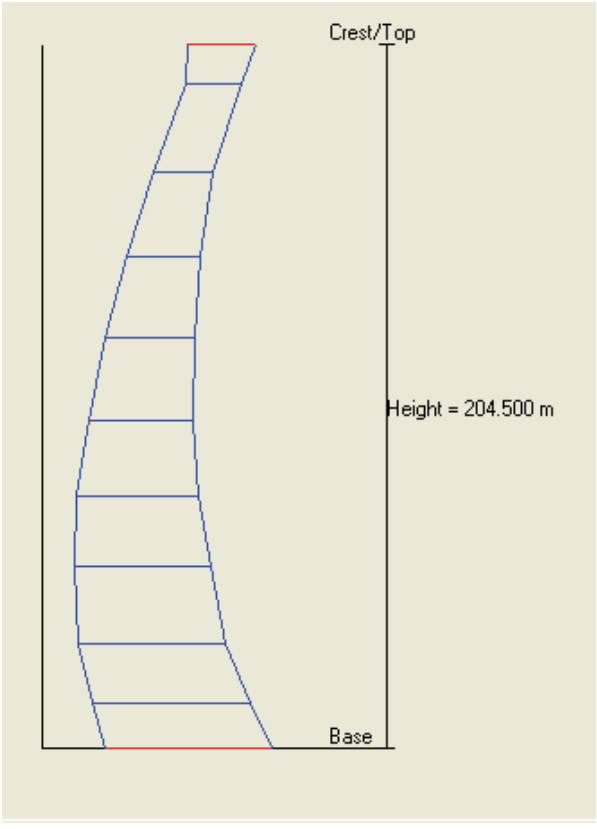

The stresses along the faces for the "most critical" block:

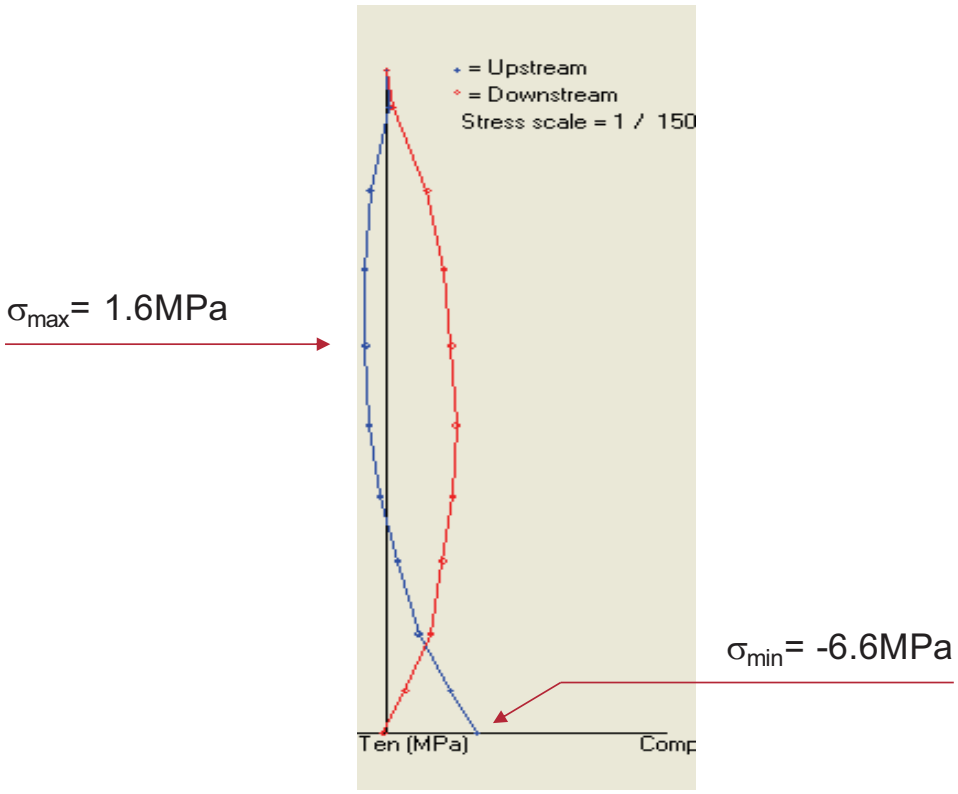

The definition of the Flexural Stability Index:

$$FSI = \frac{-\sigma_{opposite}}{2.\sigma_{tensile}}$$

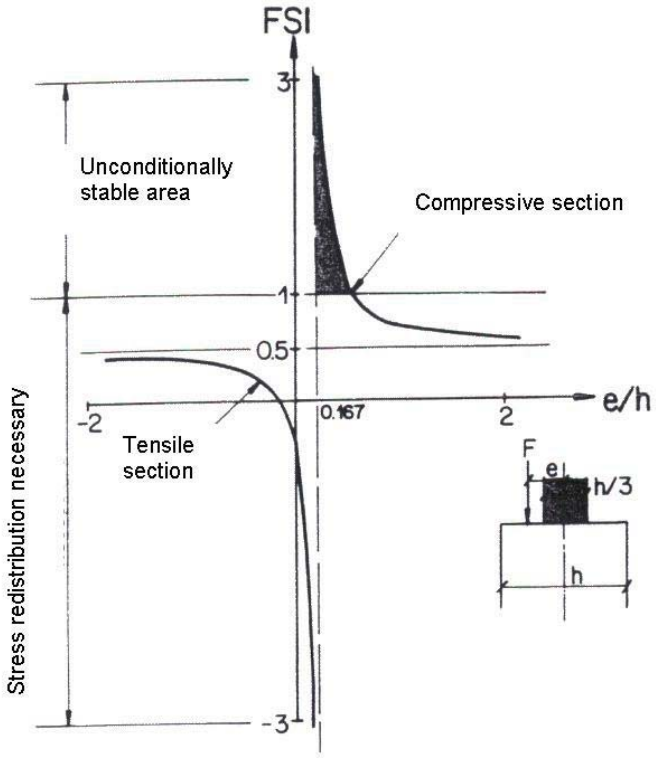

Summary of the results for the maximum drawdown level reservoir load case :

Blocks	Absolute maximum stress*		Maximum stress at pulvino level**	Minimum stress at pulvino level	FSI at pulvino level
	(MPa)	Elevation (masl)	(MPa)	(MPa)	
7	0.08	500.0	-0.85	-2.60	-
10	0.86	475.5	-1.54	-3.27	-
12	1.22	450.0	0.04	-5.70	71
14	1.59	450.0	0.25	-6.58	13
16	2.09	417.5	-1.45	-5.32	-
18	1.99	440.0	-0.90	-5.75	-
21	2.21	426.5	-1.02	-5.78	-
26	0.91	440.0	-1.09	-4.17	-
29	0.56	474.5	-0.65	-3.70	-
32	0.013	480.0	-0.15	-3.48	-

* All occur at upstream face
** At downstream face

The maximum pseudo-static earthquake that blocks can withstand without need of any stress redistribution:

Block	Tensile stress at pulvino level (MPa)	Compression stress at pulvino level (MPa)	α (g)
12	5.67	-11.3	0.22
14	6.33	-12.7	0.19
18	6.65	-13.3	0.23
21	6.81	-13.6	0.21

THE RESULTS

1 Satisfactory matching between calculated and measured displacements by calibration. (geodetic and plumb-line)

2 The state of stresses under static loading indicates that the dam is safe for these conditions.

3 Even under seismic events, at least up to OBE level, no catastrophic release is expected.

COMMENTS & CRITICISMS:

The main objections:

1. We ignore the enormous works made before.
2. The input data is too rough.
3. The numerical model is too coarse.
4. The mathematical model is too simple.

The objections

1.The works made	➡	Lack and dispersion of archives.
2.Input data	➡	Adapt input to the aims and data at disposal.
3.Numerical model	➡	Conform to known data and required degree of accuracy.
4.Mathematical model	➡	Corresponds to the range of normal load cases.

EVOLUTION OF MEASUREMENTS WITH TIME

Displacements: Plumb-line, crown cantilever

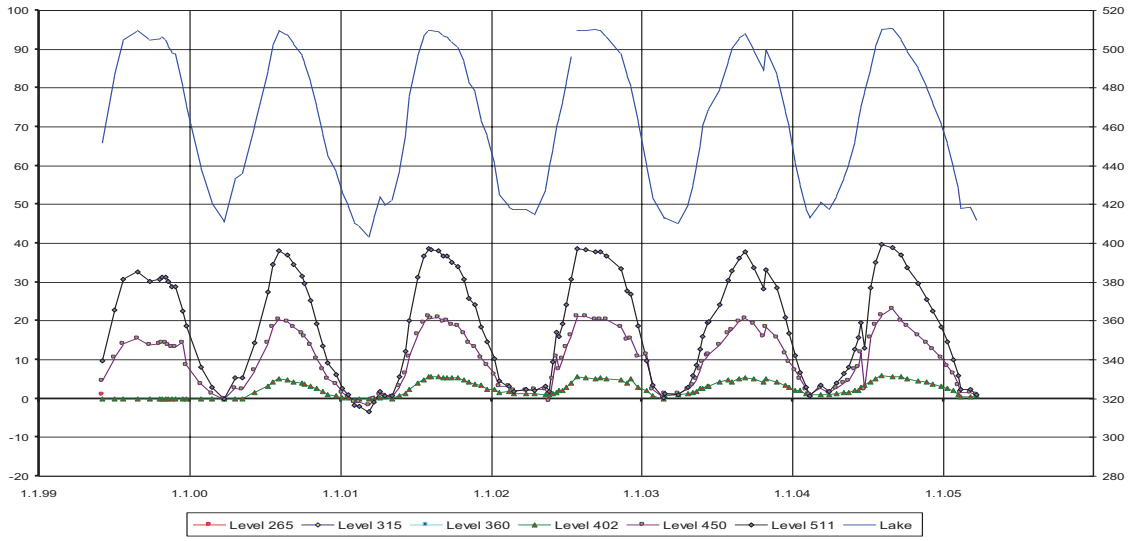

Total measured leakage:

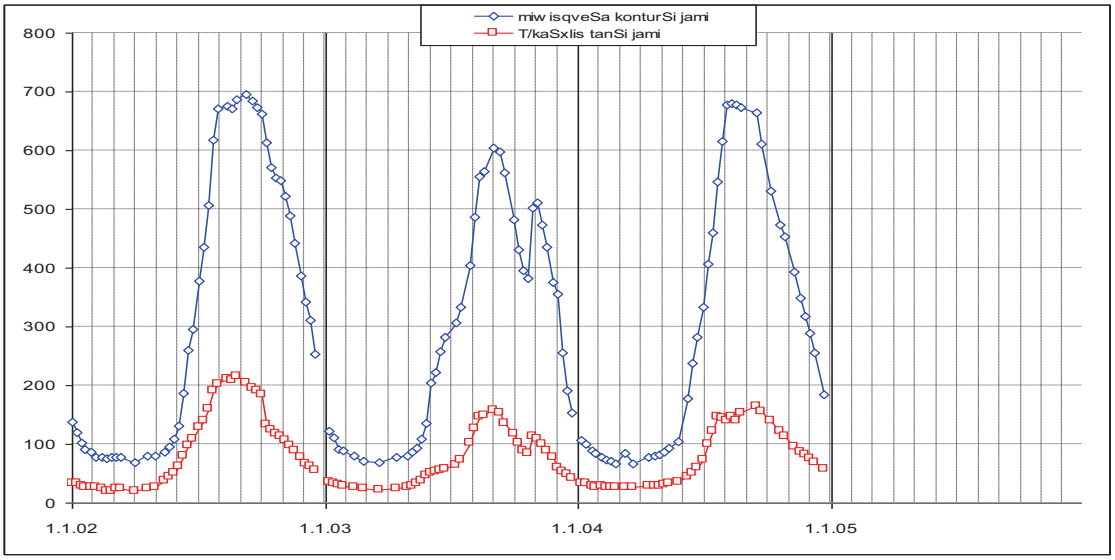

Example of uplift pressures:

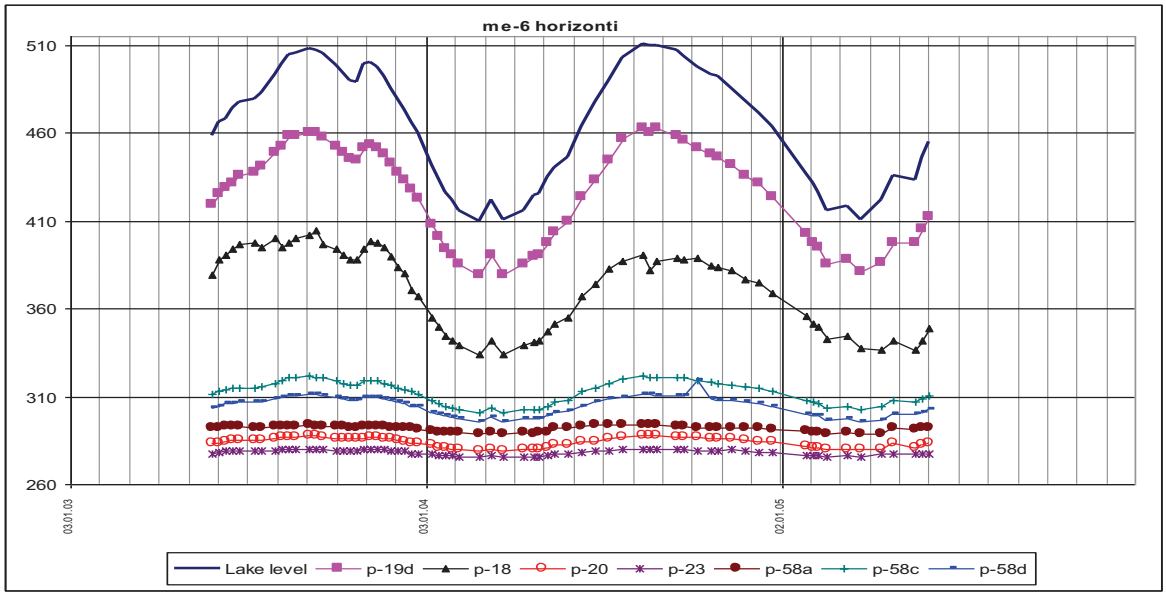

RESERVOIR OPERATION MODE

The former regulation was made with concern about foundation degradation. But up to now we have no clear evidence of such a phenomenon.

The dam behaves elastically and we didn't record any abutment movement.

On the other hand, the rules (minimum water level and speed of filling) were never observed!

Minimum water level

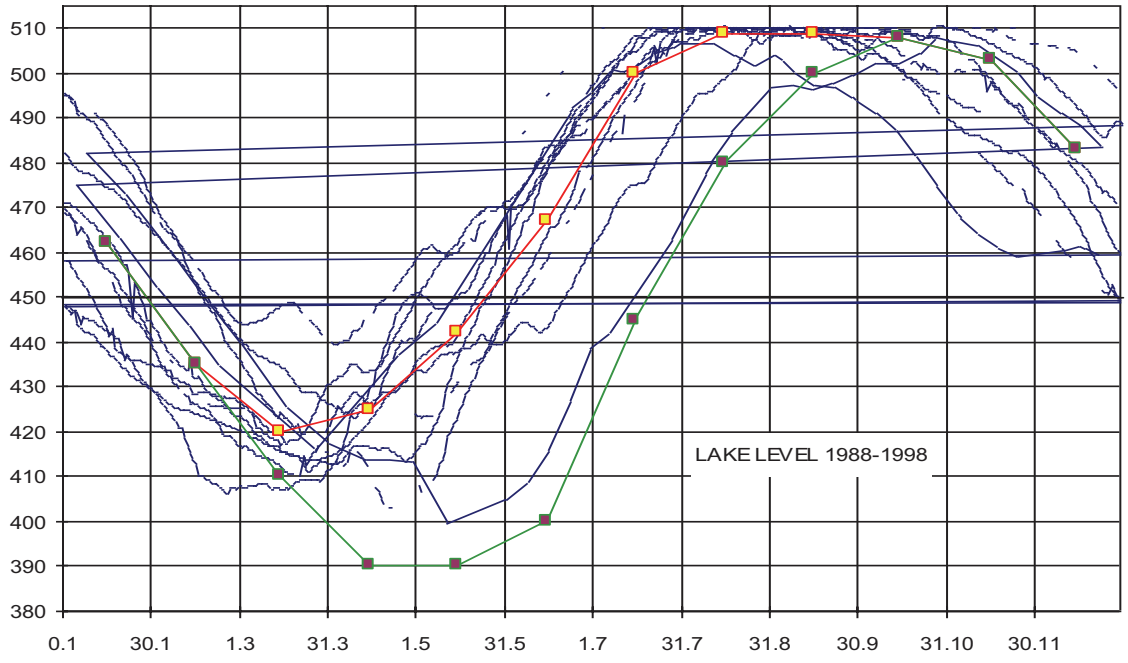

Water rate during filling – emptying

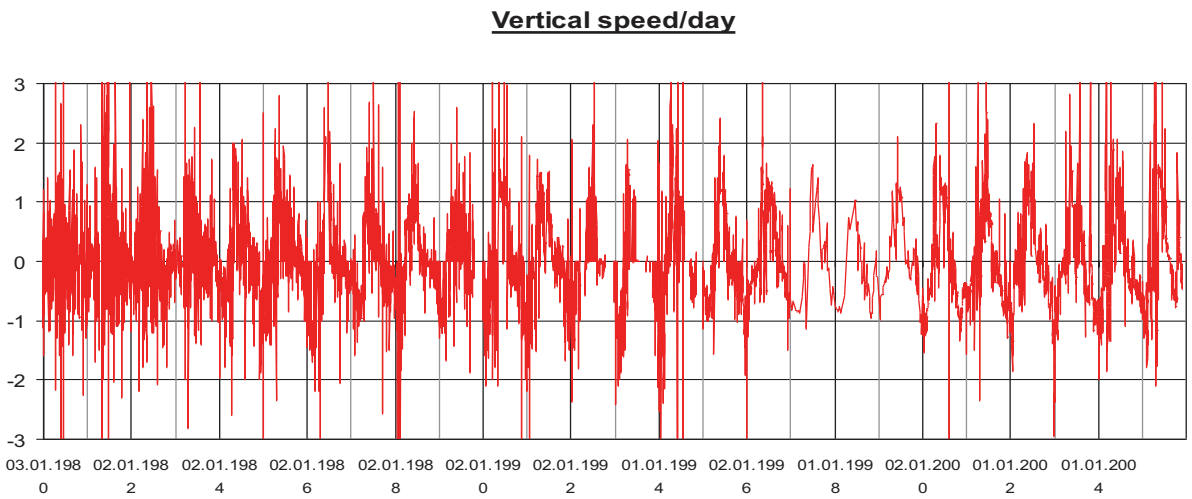

Speed of filling or emptying the reservoir

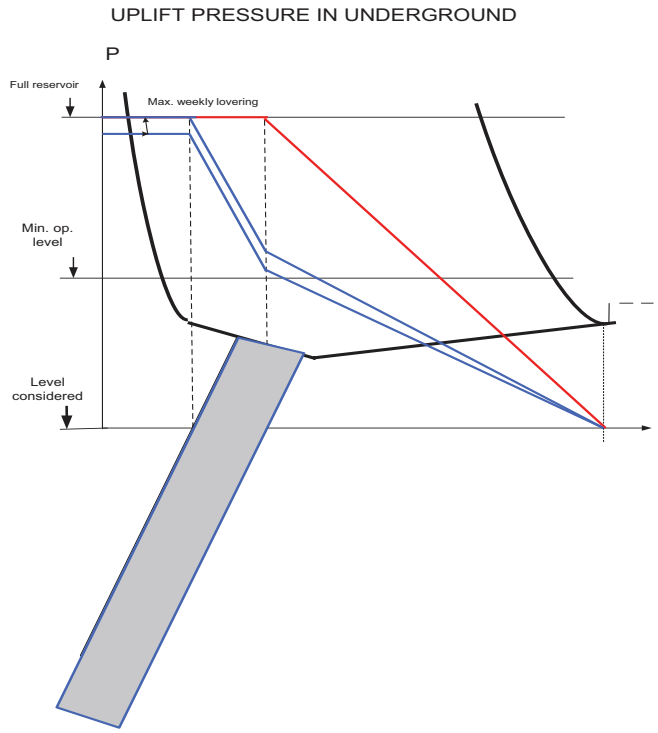

If the grout curtain is not working:

High changes in flow and gradient.

By changing the speed of water level changes:

Only few changes in flow and gradient.

MONITORING DURING DRAWDOWN

Plumb lines

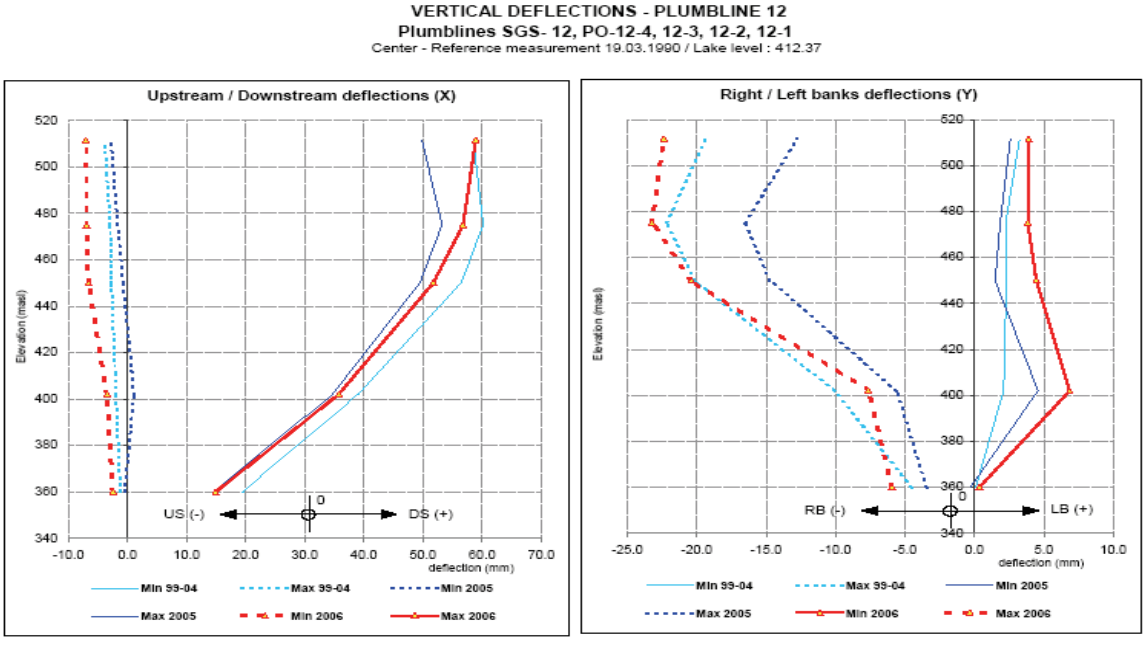

Piezometers

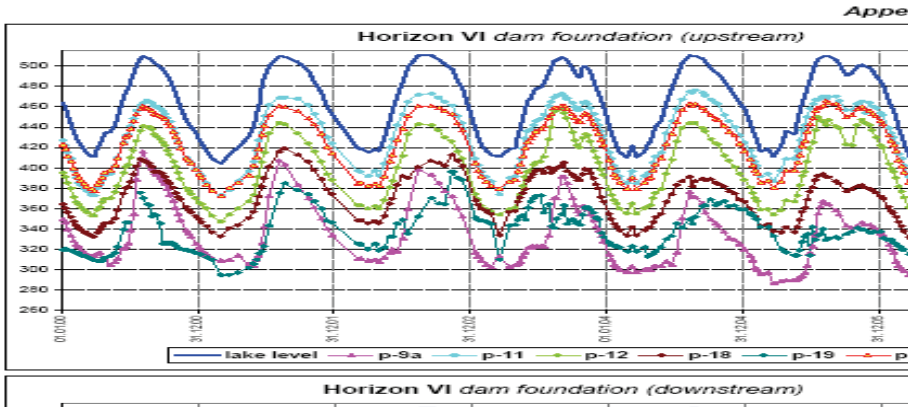

CONCLUSIONS

- The steady behavior of the dam:
    - The structure works strongly.
    - No drift of the displacements the last years.
- The rock foundation behaves well:
    - No apparent disturbing except some risks of piping.
- On a purely technical basis, the regulations could be less severe than at present.
- Further refinements of the model are very interesting but the results will not fundamentally change.
- For the scheme as a whole, the present main problems are the following:
    - Reduce the high seepage.
    - Replace the bottom outlet gates.
    - Finish the refurbishment of the tunnel and powerhouse.
    - The need to handle the sediment problem.
    - Make an emergency plan for the safety of the people downstream.

INVESTIGATION OF CONFINED SEEEPAGE UNDER TRANSIENT OVERTOPPING OF THE CORE*

Bachir Touileb,
Eng., Hydro-Quebec, Montreal, Canada

AIM OF THE PRESENTATION

I. Major increase worldwide of the Design Inflow Flood during the life cycle of an earthdam

II. Increasing trend for using advanced numerical approaches in order to evaluate/justify the impact of each given flood

III. Heightening of dams for extreme floods is not always automatic (see for instance P.H.Nguyen, ICOLD, Barcelona, 2006, Question 86 : "Overtopping and Failure – New Challenges for Dam safety engineers")

Most influencing parameters are :

- Maximum height of the overtopping
- Duration and shape of the transient overtopping
- Internal geometry of the D/S part of the dam
- Hydraulic conductivity contrasts

* The publication is based on the author's presentation at 9th Benchmark Workshop

OVERTOPPING THE CORE (confined flow) VERSUS OVERTOPPING OF THE CREST (unconfined flow):

TWO DIFFERENT SITUATIONS

Wiory earth cofferdam (July 2001). Crest overtopped by 0,65 m of water.[1)]

The picture shows water seeping above the top of the core.

Wiory earth cofferdam (July 2001).[1)]

Note : During a transient flow, and due to the contrast of permeability of different materials in presence, a sand (this case) may behave just like an impervious layer. No water seeping through the D/S shoulder.

[1)] In : "Riprap on earth cofferdam prolongs its durability by overtopping". By Krzysztof Fiedler (Dams Monitoring Centre, Warsaw, Poland). (Photo W.Mielniczuk)

Wiory cofferdam Cross section[2)]

Wiory earth cofferdam (July 2001).

The highest section of the definitive earth dam is presented on the fig. 2.

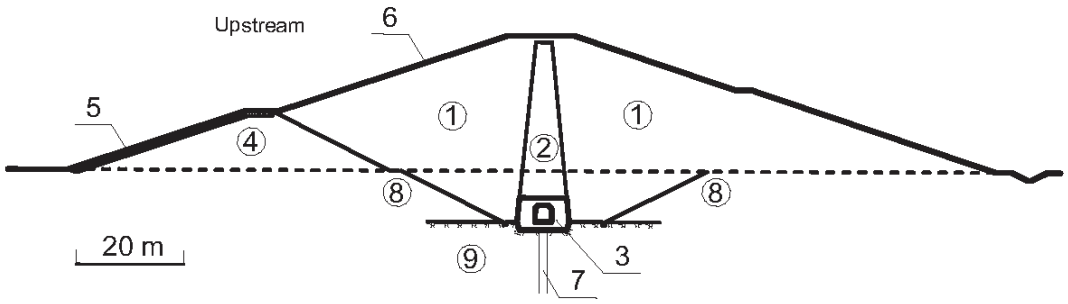

Fig. 2 The highest section of the Wiory dam according to primary design:
1 – main embankment (sand); 2 – clay core; 3 – grouting and inspection gallery; 4 – lower part of the dam fulfilling the temporary task of upstream cofferdam during the third stage of construction; 5- riprap layer (thickness 70 cm) protecting the slope and the crest of the cofferdam; 6 – reinforced concrete slabs; 7 – grouting curtain; 8 – alluvium; 9 - rock

Various preponderant flow paths are possible = f(D/S Geometry)

1-D Horizontal flow in the upper gravel layer (1)

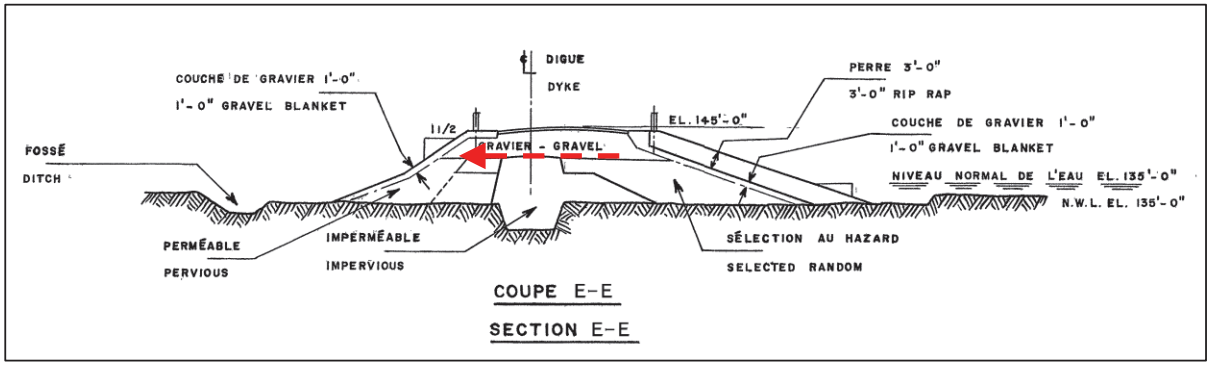

Seepage path

Upper Gravel Layer is usually a Natural Granular Material of Max. Grain Size = 75 mm (3 in.)

[2)] In : "Riprap on earth cofferdam prolongs its durability by overtopping". By Krzysztof Fiedler (Dams Monitoring Centre, Warsaw, Poland).

2-D Flow in all the downstream shoulder (2)

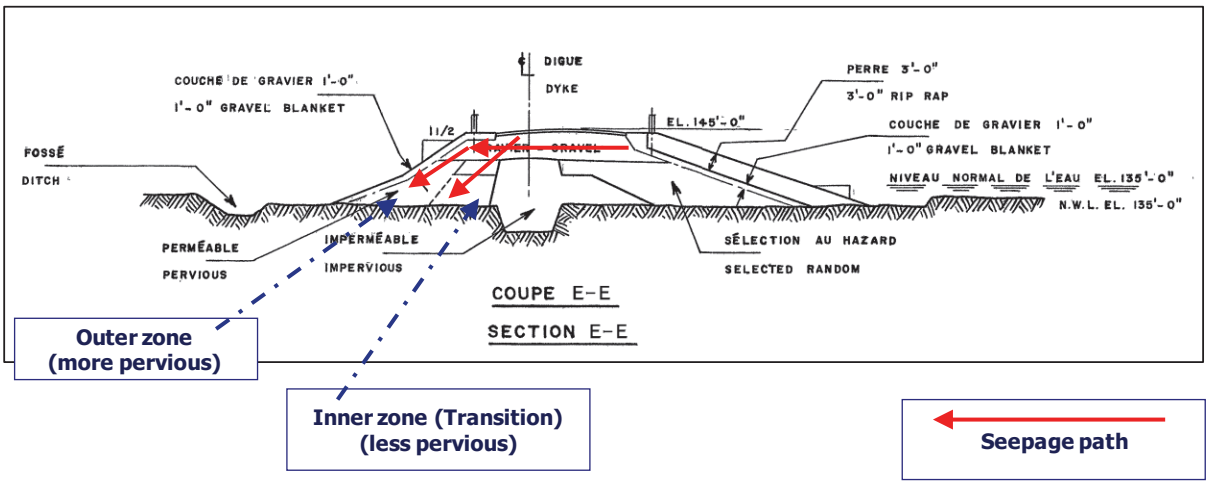

The downstream shoulder is made of 2 zones : Outer zone more pervious than inner zone.

2-D Flow in external layers only (upper gravel layer and external D/S shoulder (3)

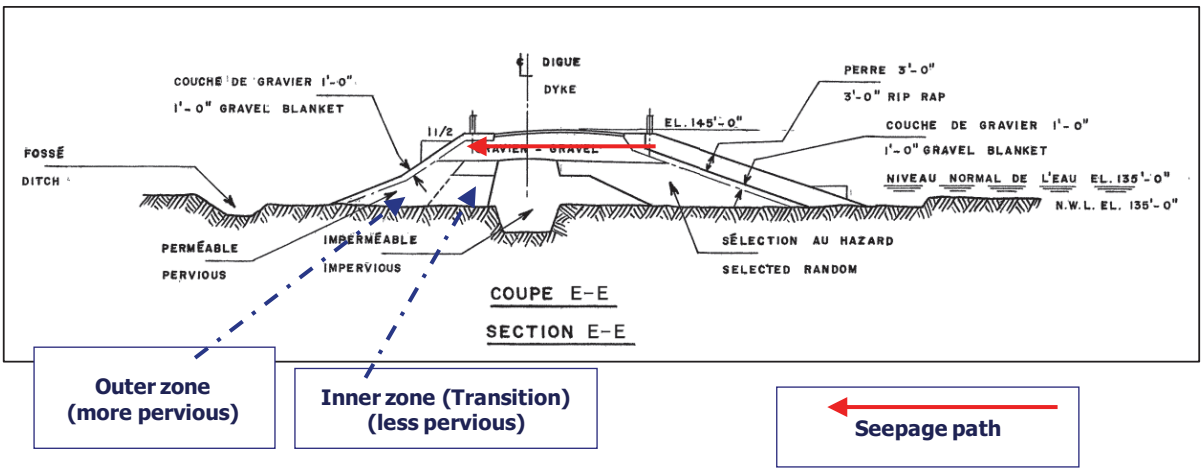

The downstream shoulder is made of 2 zones : Outer zone more pervious than inner zone.

Soil-water characteristic functions

Hydraulic conductivity : K = f(ψ)

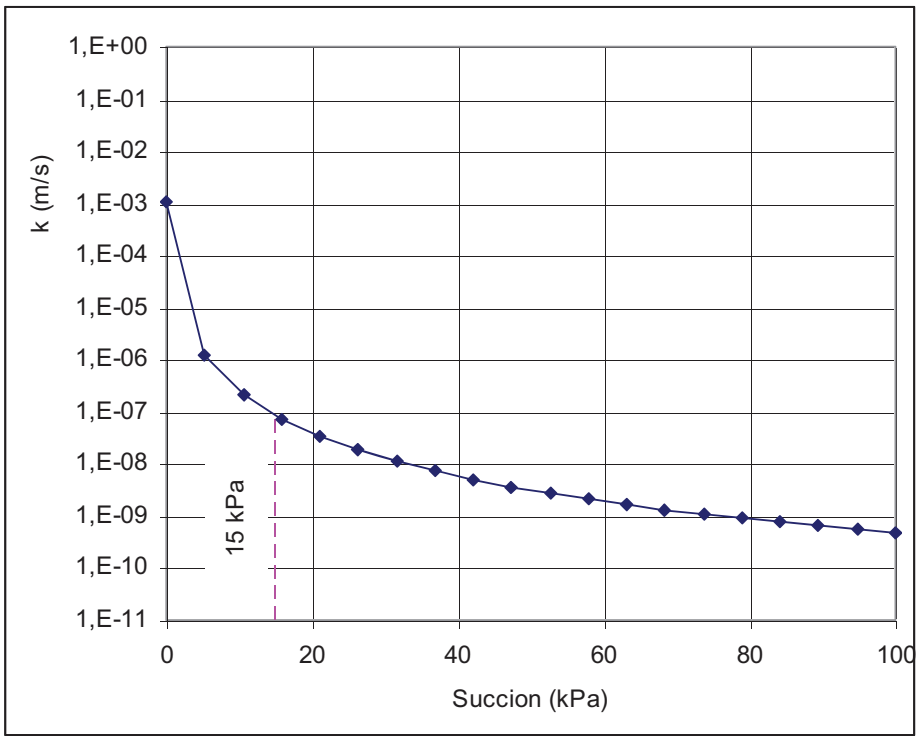

Volumetric water content : θ = f(ψ)

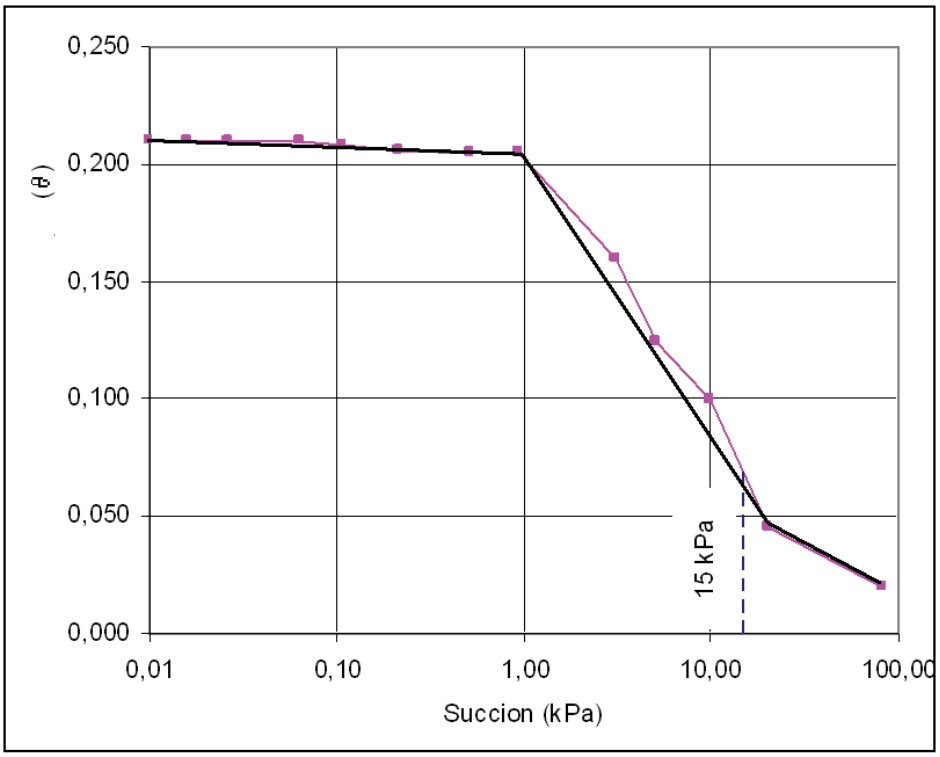

Extreme floods characteristics PMF and 10,000 years floods

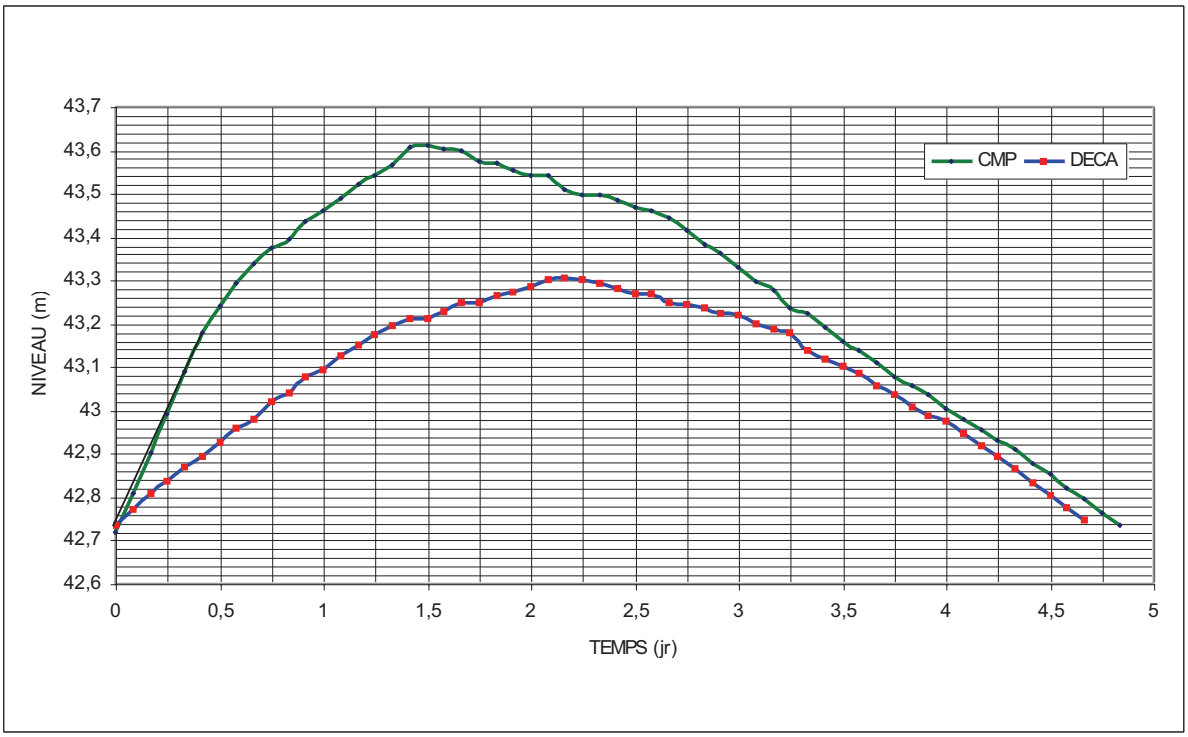

Type of preponderant flow in a more pervious upper gravel layer.
Effect of the contrast of hydraulic conductivities.

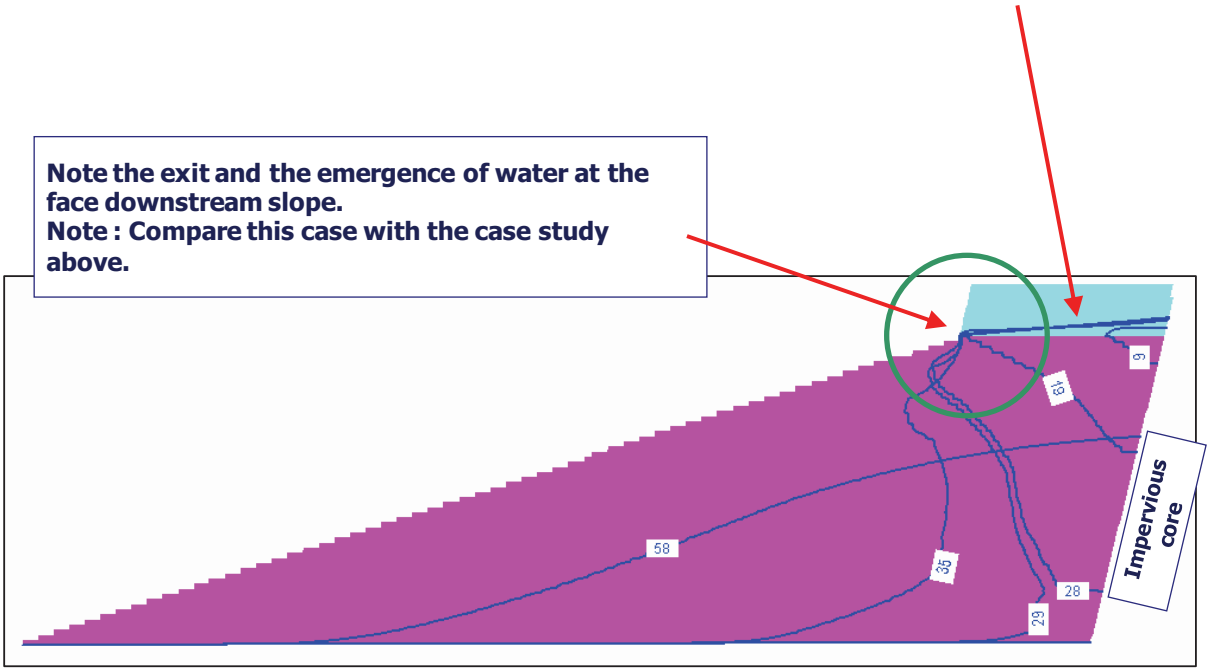

Note :
For a zoned rockfill dam, overtopping the crest is quiet different from overtopping the core. Water seeping is possible through the D/S shoulder.

CASE STUDY:

PMF Flood

+ 0,85 m above the core ; 0,55 m below the crest;

T = max of 5 days ; k = 1 x 10^{-3} m/s = 1 x 10^{-1} cm/s

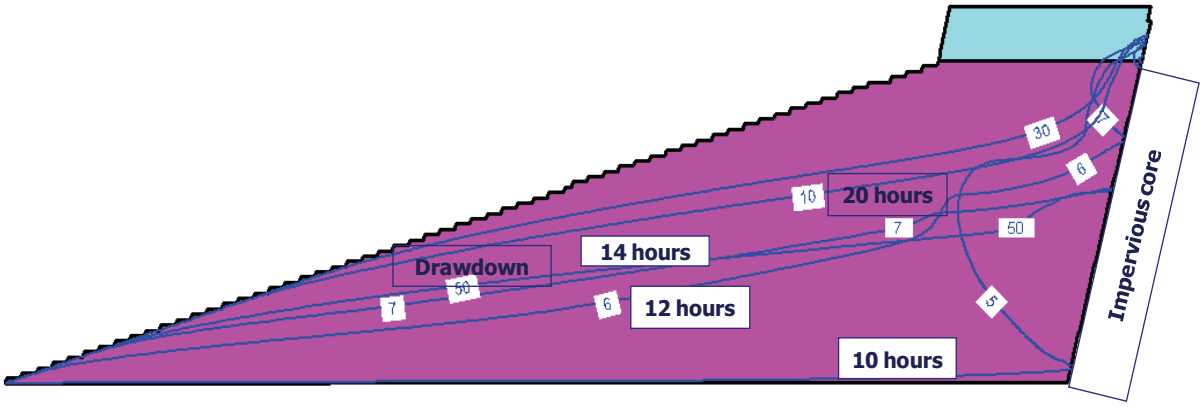

Note:

Label 7 (14 hours since start of the PMF) in this case and its position on the next figure (14 hours since start of the 10,000 years floood)

10,000 years Flood

+ 0,50 m above the core; 0,90 m below crest;

T = max of 5 days; k = 1 x 10^{-3} m/s = 1 x 10^{-1} cm/s

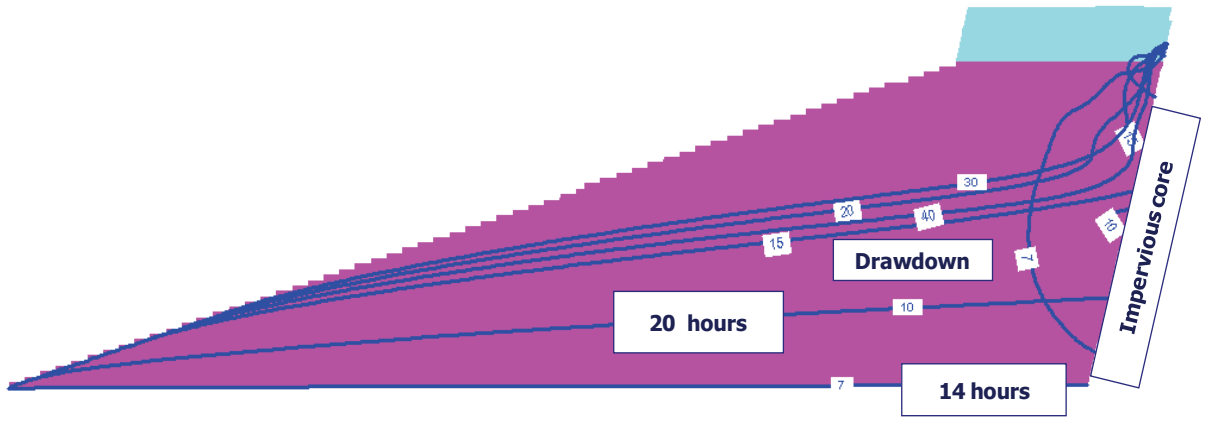

Note:

Label 7 (14 hours since start of the 10,000 years floood) in this case and its position on the figure above (14 hours since start of the PMF)

Previous work in the case of permanent flowthrough rockfill dams :

H. Chanson (Australia), D. Hansen and V. Garga (Canada)

Fig. 1 - Examples of seepage flows through rockfill dams

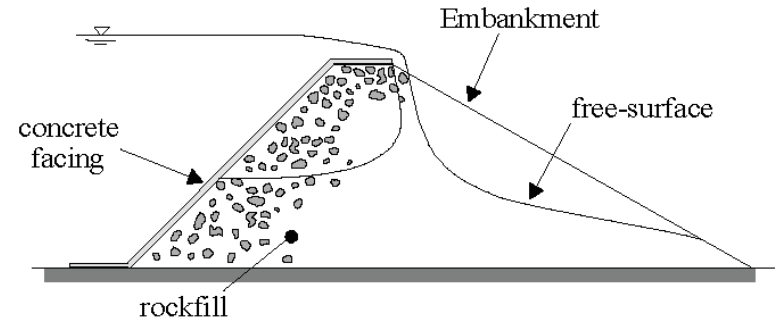

Concrete-faced rockfill dam

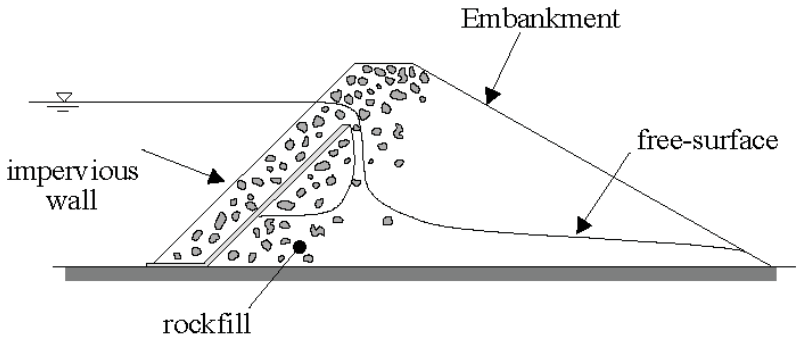

In-built spillway rockfill dam

CONCLUSION

I. Heitening of embankment dams to face extreme floods is not automatic

II. Extreme floods impacts are investigated case by case using advanced numerical methods (Darcy vs Non-Darcy flow)

III. Allowance/Tolerance of partial overtopping of the core during extreme floods is gaining interest (i.e. Arid region with use of unsaturated initial state of upper dry layers, etc.)

IV. In Scandinavia, open discussions on allowing and/or considering partial overtopping of the core were reported (in Carleston, Johansson and Worman 1995)

V. Heitening solutions are TEMPORARY SMALL DAMS BUILT ON TOP OF PERMANENT STRUCTURES

VI. Solutions other than heitening are considered knowing the very low probability of an extreme flood : Refurbish/Reinforce the downstream slope face, Fuse dykes, Decelaration of the damage build-up, etc.

MATHEMATICAL MODEL FOR ROCK FOUNDATION AND CONCRETE DAM OF BUREISKAYA HPS DYNAMIC INTERACTION

A. Khrapkov, B. Tseitlin, A. Skvortsova,

Russia, Saint-Petersburg, B.E. Vedeneev VNIIG,

A.Vasilyev

Russia, Saint-Petersburg,
the Branch of "EES Engineering Center" – "Lenhydroproject Institute"

The basic tasks of the works on development of the mathematical model of the main structures and rock foundation of Bureiskaya HPS are:

- Possibility of fulfilling retrospective calculations modeling step-by-step building up and loading of the structures.
- Definition of eigenfrequencies and eigenmodes of the structures at different stages of readiness of the hydraulic engineering complex and the reservoir filling up.
- Investigation of interaction of structures with rock foundation during propagating of seismic wave.
- Comparison of the received numerical results with the data of engineering seismological observations at the main structures of the hydraulic engineering complex and seismological observations at the construction site of Bureiskaya HPS

Location of apparatus for engineering seismometric observations

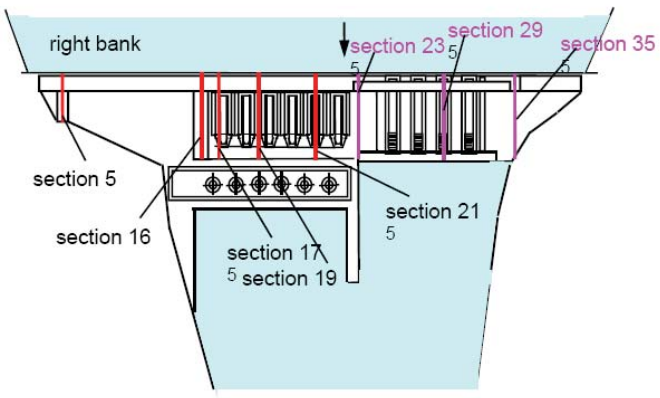

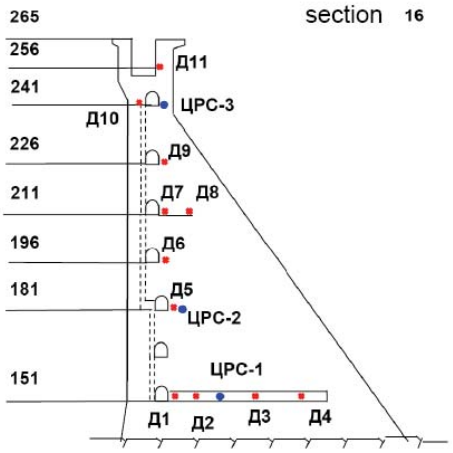

1. GEOLOGICAL ENGINEERING CONDITIONS

The authors of the report give thanks to the specialists of B.E. Vedeneev VNIIG

Senior scientific worker O.K. Voronkova, D.Sc (eng).

Head of the laboratory N.F. Krivonogova., Cand.Sc (eng).

Leading scientific worker A.A. Kagan, D.Sc (eng).

Scientific worker L.F. Ushakova

Engineer of I category V.Yu. Malkova

for the presented data on engineering-geological conditions and physical and mechanical properties of the foundation of Bureiskaya HPS

An engineering-geological scheme of granite mass at the level control mark 125 m with selected elements of inhomogeneity in deformation properties is shown below:

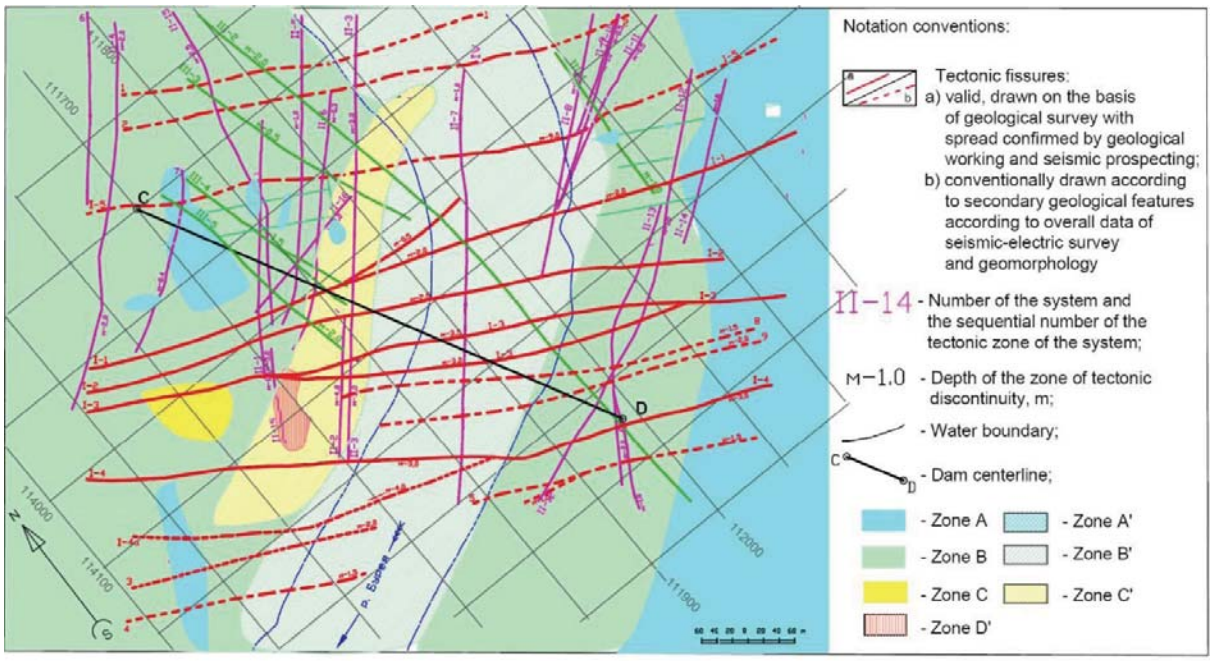

PHYSICAL AND MECHANICAL PROPERTIES OF THE GRANITES OF BUREISKAYA HPS FOUNDATION

Geological Engineering Element	Density, kg/m^3	Modulus of total deformation E_0, MPa	Internal friction factor	Cohesion, MPa	Poisson's ratio, ν		Dynamic modulus of elasticity (seismic survey) $E_{д(с/р)}$, MPa	Dynamic modulus of elasticity (design) E_{seism_pr}, MPa	Logarithmic attenuation decrement Δ
					Static, ν_{st}	Dynamic, ν_d			
Granite relieve zone									
Comparatively «integrity» granite in the relieve zone									
E′	2550	<2000	0,60	0,05	0,32	0,32	6000	3100	0.3
D′	2550	3000	0,65	0,075	0,30	0,30	9500	5400	0,3
C′	2550	6000	0,70	0,25	0,28	0,28	17000	10900	0,3
B′	2550	9000	0,75	0,30	0,26	0,26	26000	18300	0,3
A′	2550	13000	0,80	0,40	0,25	0,25	38000	28900	0,3
Zones of tectonic faults in the relieve zone									
E′	2450	1600	d		0,33	0,33	5000	2500	0,4
D′	2450	1650	d		0,33	0,33	5200	2600	0,4
C′	2450	3300	d		0,33	0,33	11000	6500	0,4
B′	2450	5000	d		0,33	0,33	15000	9400	0,4
A′	2450	7000	r		0,33	0,33	20000	13300	0,4
Rocks deeper than the relieve zone									
«Integrity» granite									
E	2640	3500	-	-	0,29	0,29	12000	7200	0,1
D	2640	5500	-	-	0,28	0,28	17000	10900	0,1
C	2640	8000	-	-	0,27	0,27	21000	14100	0,1
B	2640	12000	-	-	0,26	0,26	35000	26100	0,1
A	2650	17000	-	-	0,24	0,24	48000	38300	0,1
Zones of tectonic faults deeper than the relieve zone									
E	2500	2100	-	-	0.33	0.33	6500	3400	0,2
D	2500	3300	-	-	0.33	0.33	11000	6500	0,2
C	2500	4800	-	-	0.33	0.33	14500	9000	0,2
B	2500	7200	-	-	0.33	0.33	20000	13300	0,2
A	2500	10200	-	-	0.33	0.33	29000	20800	0,2

Relationship of velocity values of Rayleigh (VR) and longitudinal (VP) waves in granite specimens of Bureiskaya HPS foundation

V_R= 0,555 V_p = 0,126 R_2 = 0,97

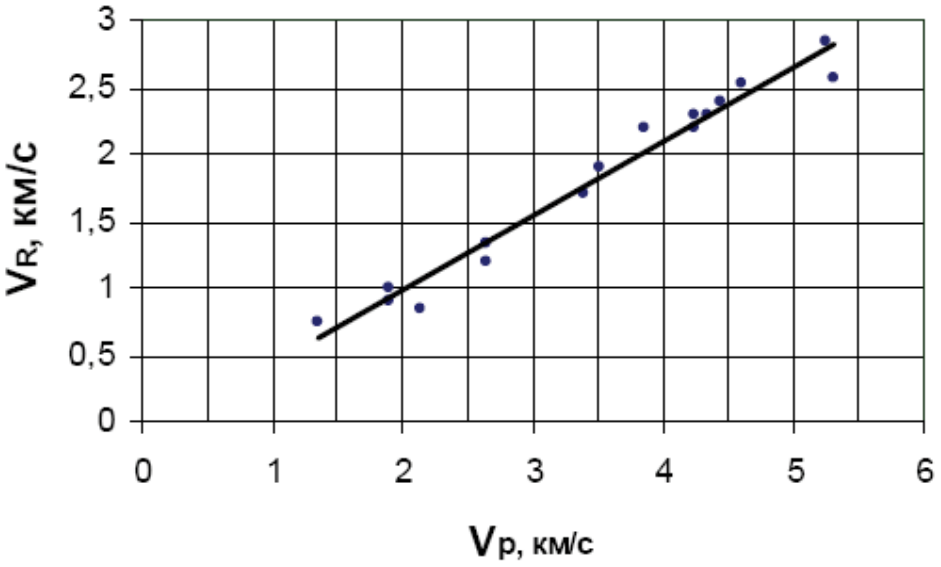

Variations of values V_P, E_d, E_{def} with depth **h** in granite mass of Bureiskaya HPS foundation according to the data of seismic prospecting

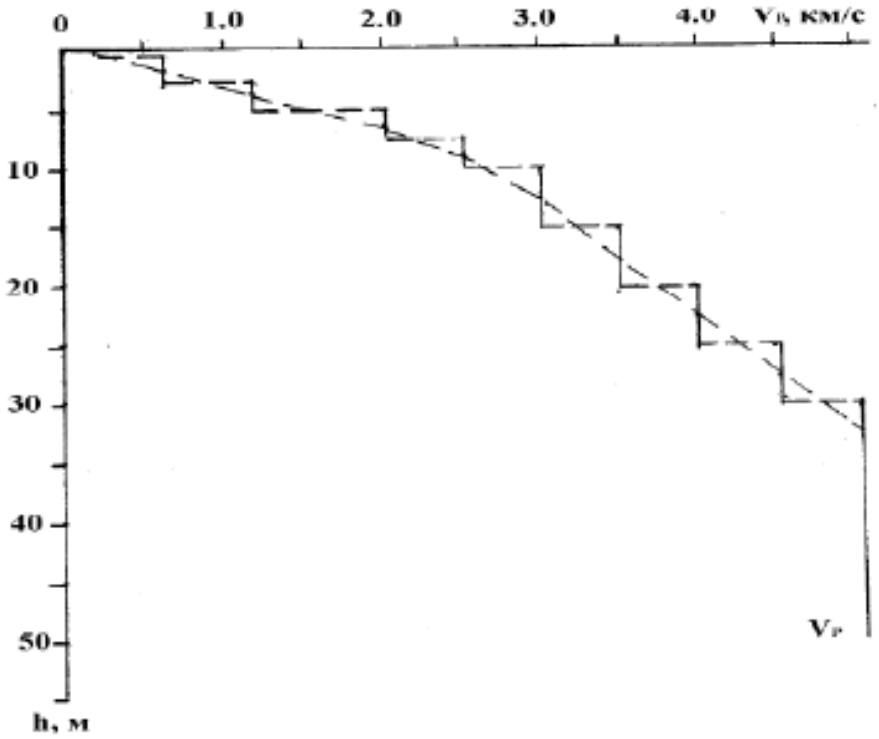

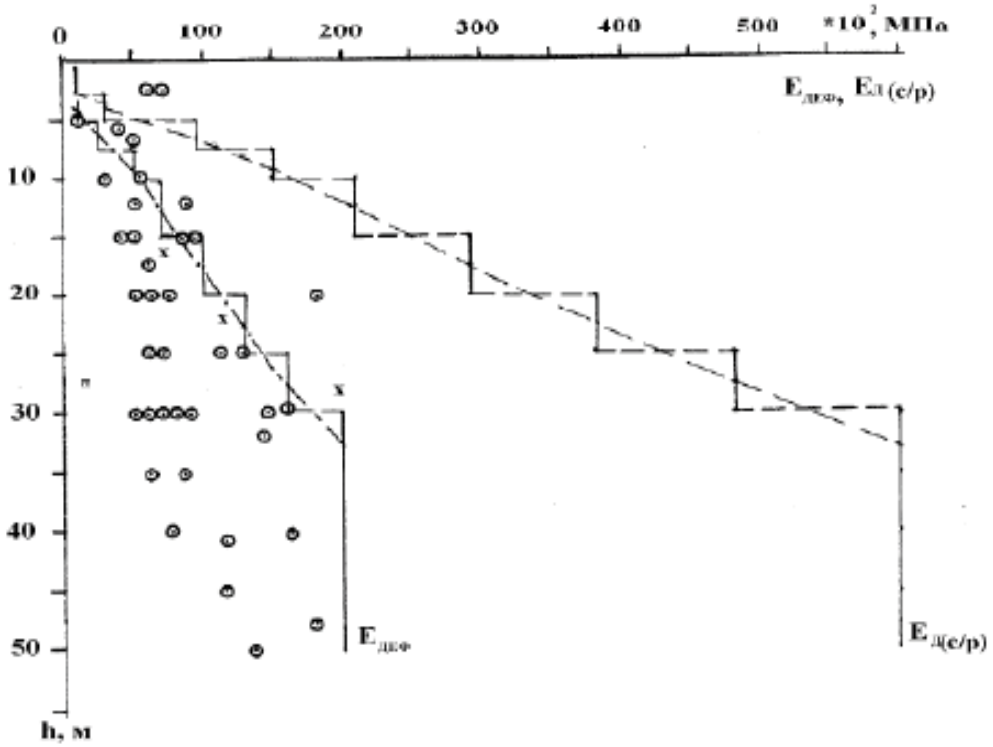

2. MATHEMATICAL MODEL OF THE ROCK FOUNDATION

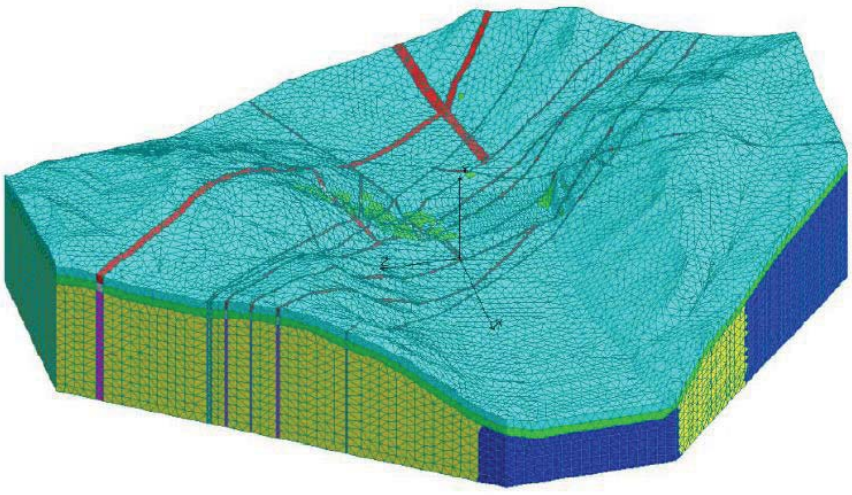

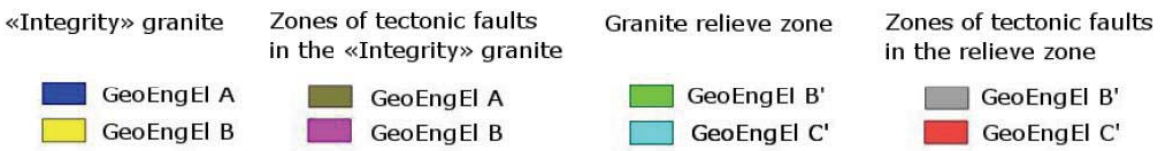

- Number of degrees of freedom 191043
- Average size of finite element 20м
- Wave length λ_s = 135 м
- Tectonic faults are schematized in the form of vertical prisms from 2.0 m up to 22.5 m in width

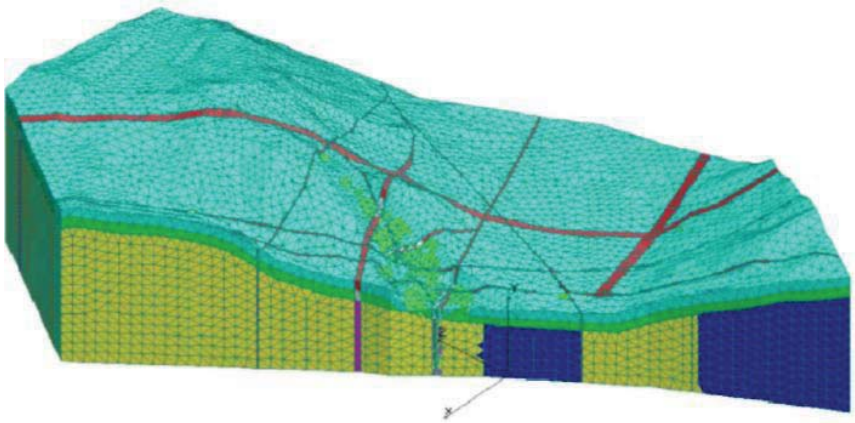

Section along fracture 1-3

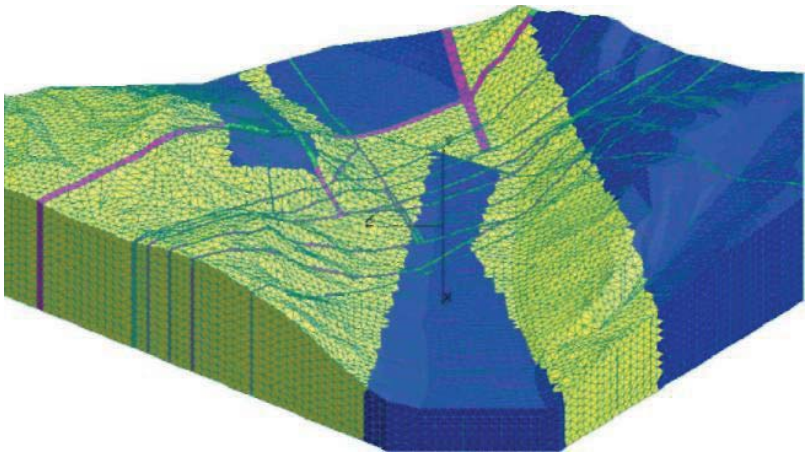

Area of integrity granite

Values of physical and mechanical properties outside the zones of tectonic faults

GEE	Dynamic modulus of elasticity (design) $E_{seism\ pr}$ MPa	Dynamic Poisson's ratio, ν	Density, ρ, kg/m^3	λ, $\times 10^{-3}$ МПа	μ, $\times 10^{-3}$ МПа	V_p, м/с	V_s, м/с
A	38300	0,3	2,65	22,10	14,73	4410	2357
B	26100	0,3	2,65	15,06	10,04	3642	1946
B′	18300	0,4	2,55	26,14	6,53	3920	1600
C′	10900	0,4	2,55	15,57	3,89	3026	1235

Values of physical and mechanical properties for the zones of tectonic faults

GEE	Dynamic modulus of elasticity (design) E_{seism_pr} MPa	Dynamic Poisson's ratio, ν	Density , ρ, kg/m^3
A	20800	0,4	2,50
B	13300	0,4	2,50
B′	9400	0,4	2,45
C′	6500	0,4	2,45

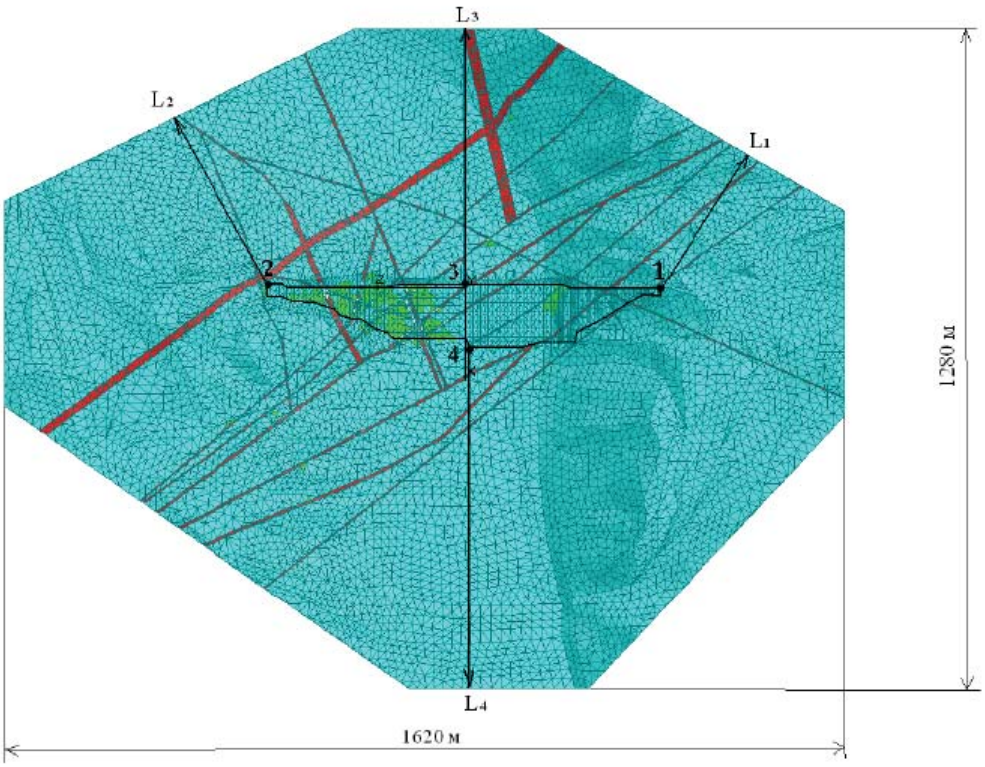

Point number	Distance to the boundary of the design area *L*, m	Time of observation until coming back of *P*-wave *t*, s	Time of observation until coming back of *S*-wave *t*, s
1	323	0,15	0,27
2	371	0,17	0,31
3	495	0,22	0,42
4	670	0,30	0,57

$$V_p = \sqrt{\frac{\lambda + 2\mu}{\rho}} \qquad V_s = \sqrt{\frac{\mu}{\rho}} \qquad \lambda = \frac{E\,\nu}{(1+\nu)(1-2\nu)} \qquad \mu = \frac{E}{2(1+\nu)} \qquad t < \frac{2L}{V_p}$$

TESTING OF THE MATHEMATICAL MODEL OF THE ROCK FOUNDATION

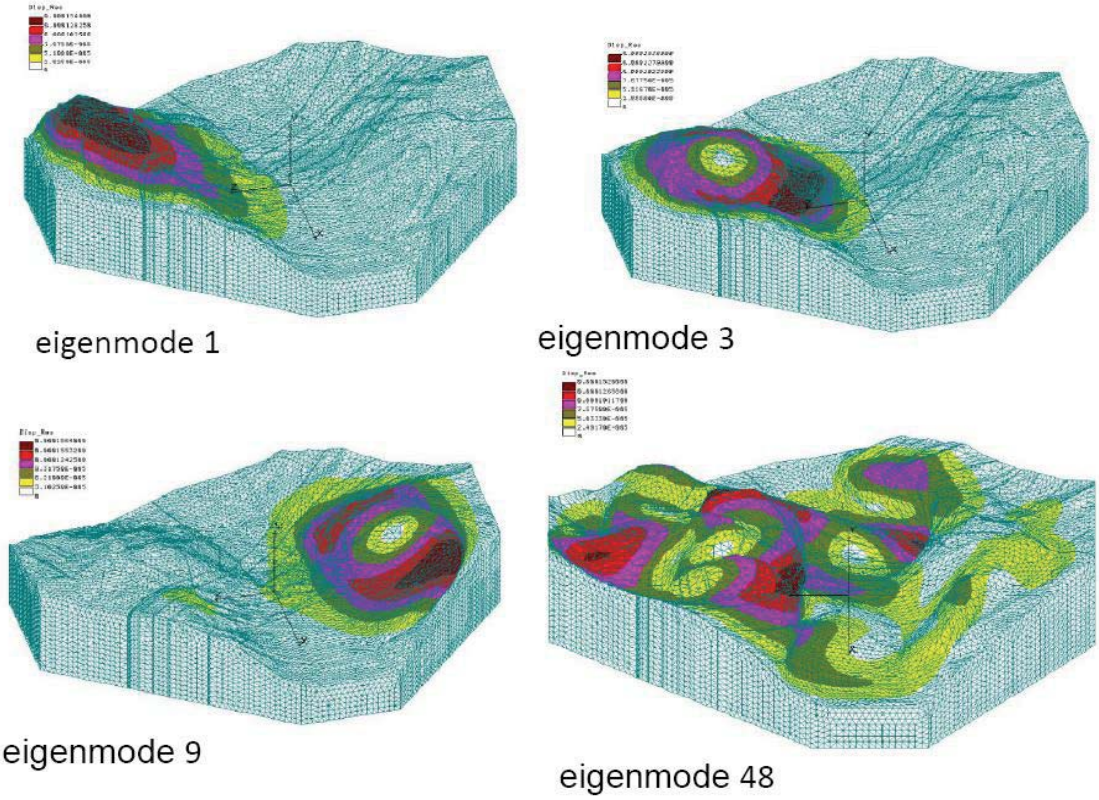

DEPENDENCE OF VERTICAL DISPLACEMENTS ON TIME UNDER ACTION OF IMPULSE LOADS

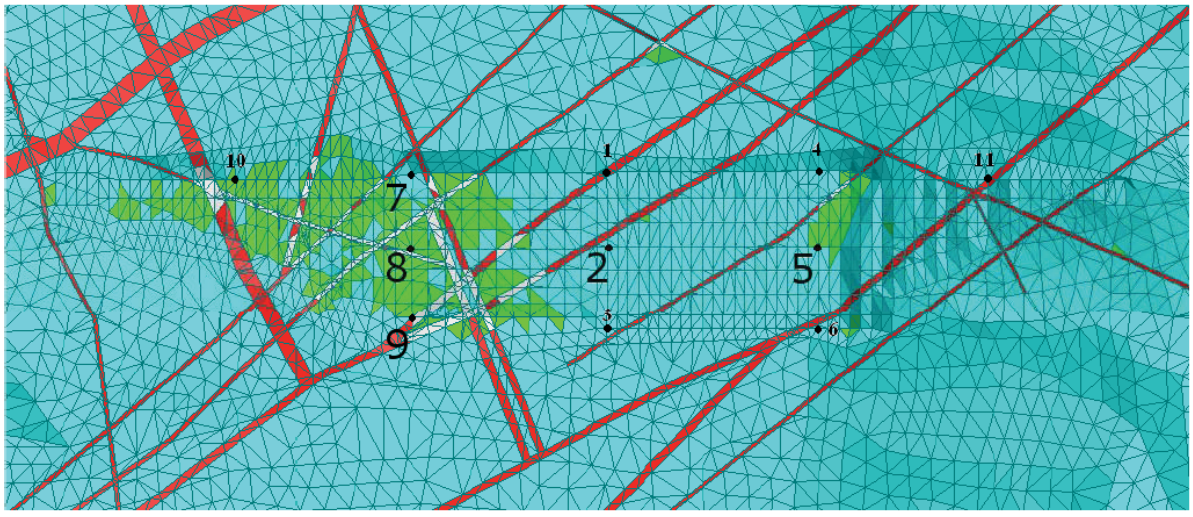

Position of loaded nodes on the day surface of the foundation design area

Triangular pulse

$$\lambda_1(t) = \begin{cases} 0 & , \quad t\Delta t^{-1} \le 0, \\ t\Delta t^{-1} & , \quad 0 \le t\Delta t^{-1} \le 1, \\ 2 - t\Delta t^{-1} & , \quad 1 \le t\Delta t^{-1} \le 2, \\ 0 & , \quad t\Delta t^{-1} \ge 2, \end{cases}$$

Triangular tripolar pulse

$$\lambda_3(t) = \begin{cases} 0 & , \quad t\Delta t^{-1} \le 0, \\ t\Delta t^{-1} & , \quad 0 \le t\Delta t^{-1} \le 1, \\ 2 - t\Delta t^{-1} & , \quad 1 \le t\Delta t^{-1} \le 2, \\ 2(2 - t\Delta t^{-1}), & \quad 2 \le t\Delta t^{-1} \le 3, \\ 2(t\Delta t^{-1} - 4), & \quad 3 \le t\Delta t^{-1} \le 4, \\ t\Delta t^{-1} - 4 & , \quad 4 \le t\Delta t^{-1} \le 5, \\ 8 - t\Delta t^{-1} & , \quad 5 \le t\Delta t^{-1} \le 6, \\ 0 & , \quad t\Delta t^{-1} \ge 6. \end{cases}$$

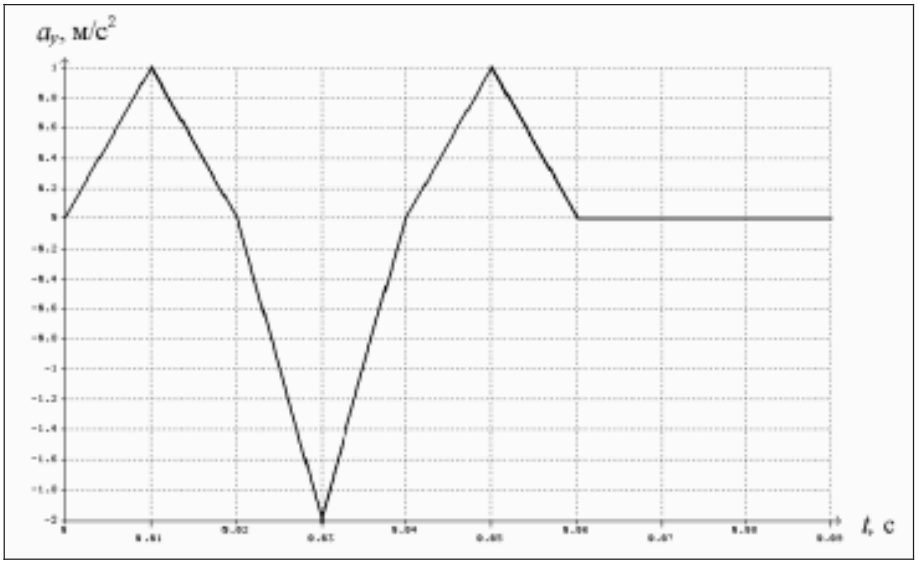

Accelerations (tripolar pulse)

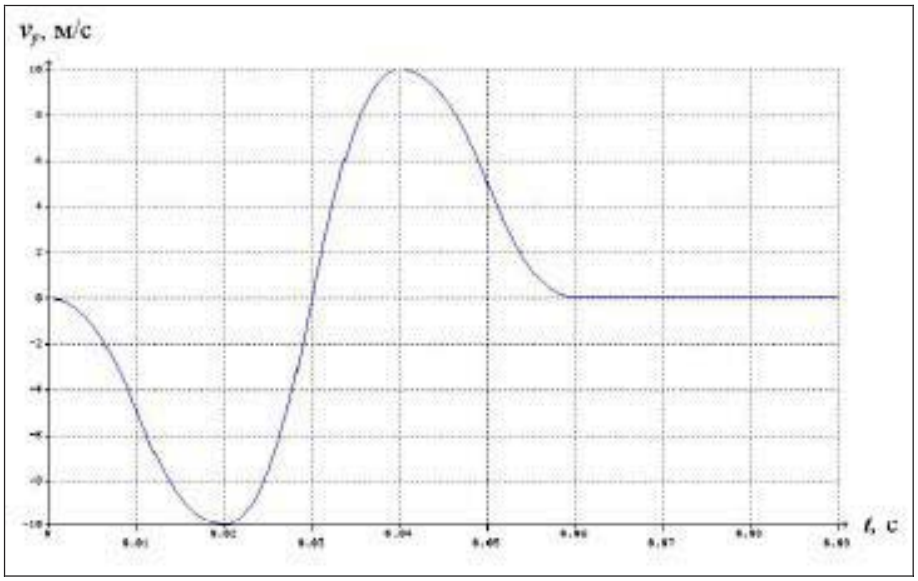

Velocities (tripolar pulse)

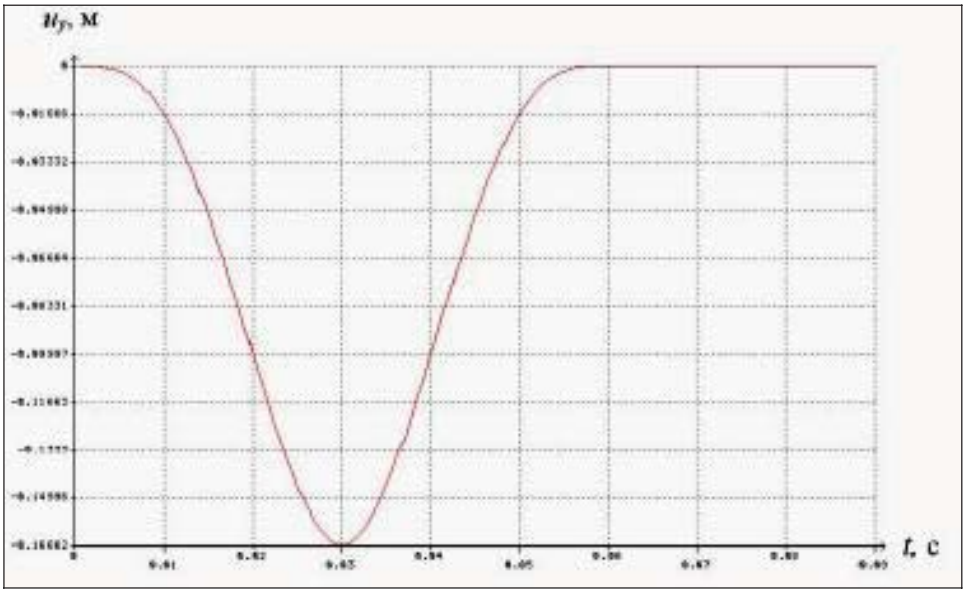

Displacements (tripolar pulse)

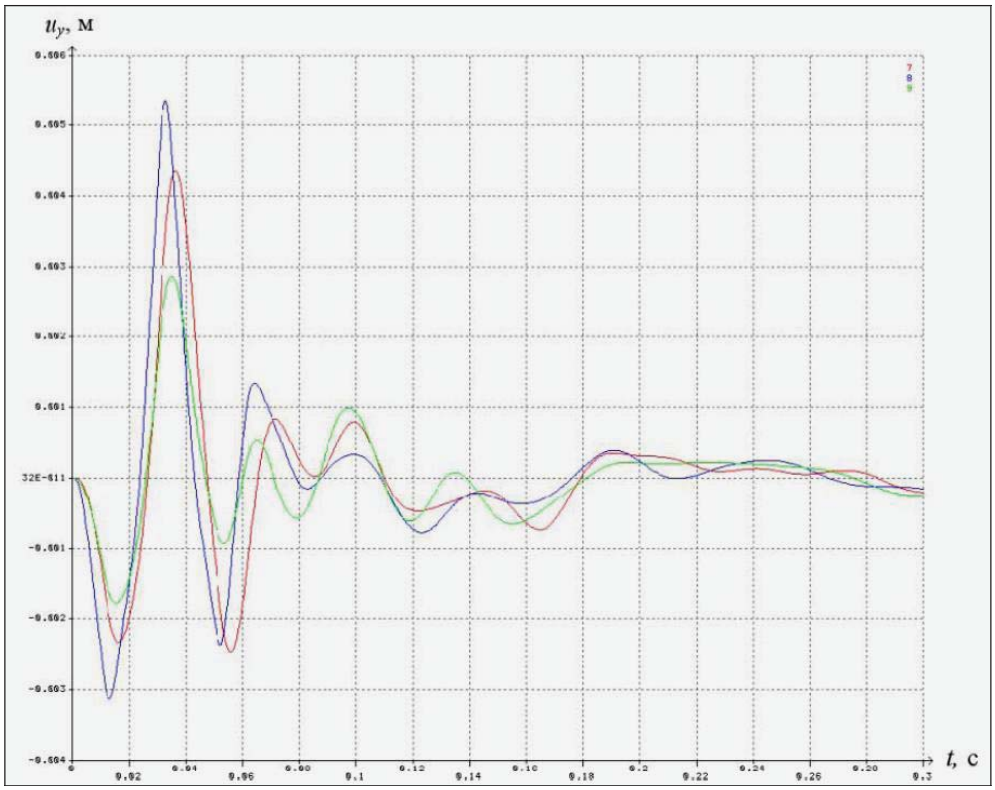

Chronograms of vertical displacements *uy* in points No 7, 8, 9

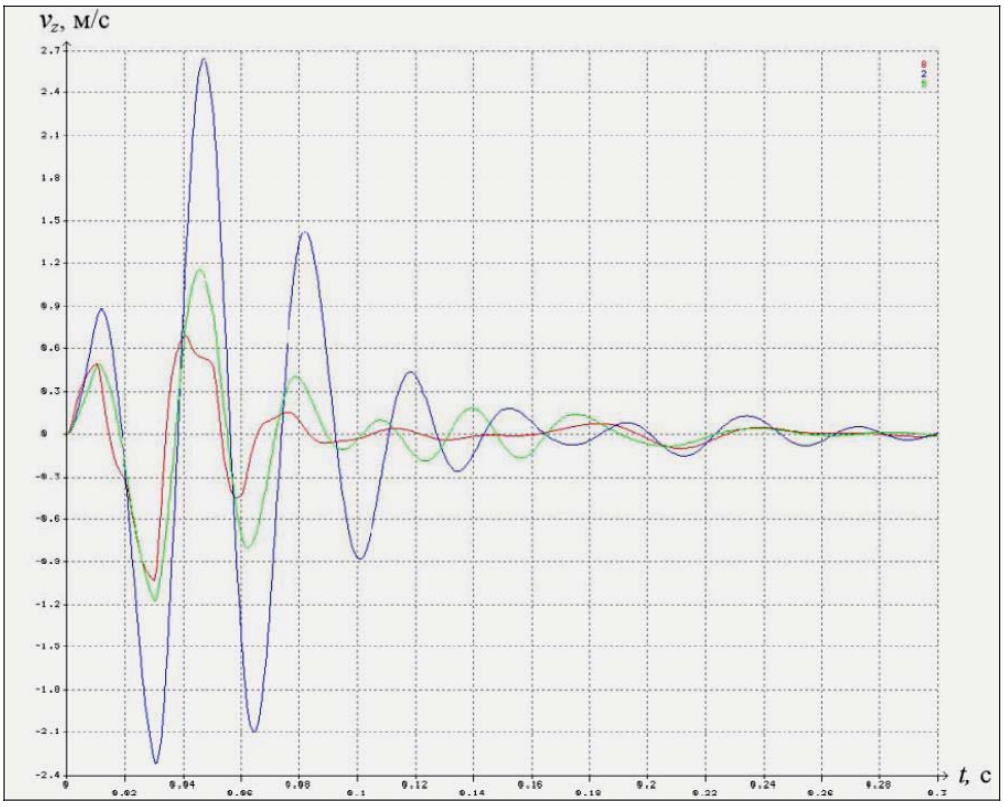

Chronograms of horizontal velocities *vz* oriented across the flow in points No 8, 2, 5

Dam on the flexible foundation

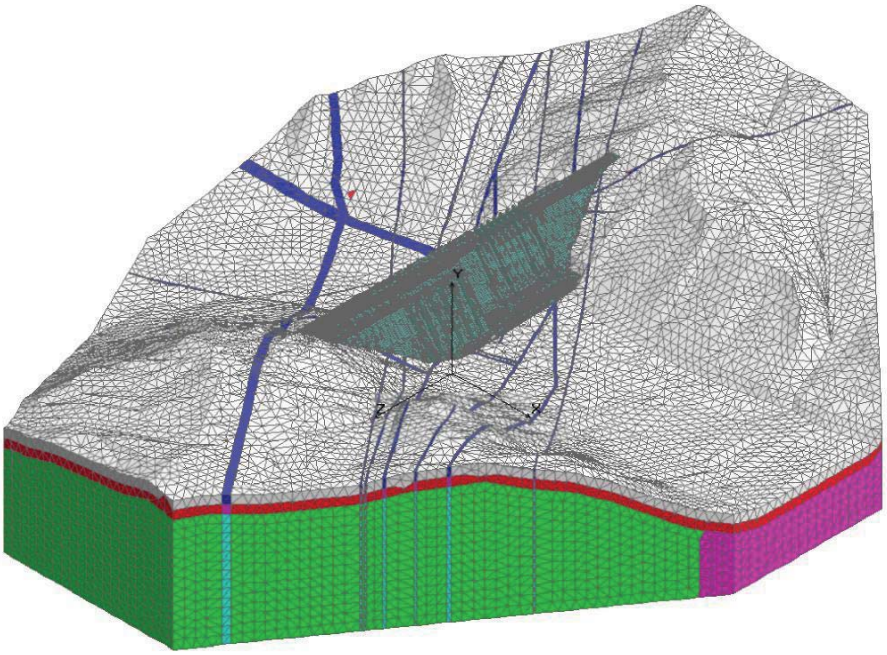

- Number of elements 936849
- Number of nodes 187383
- Number of degrees of freedom 537621

Eigen pairs of the dam on the flexible foundation

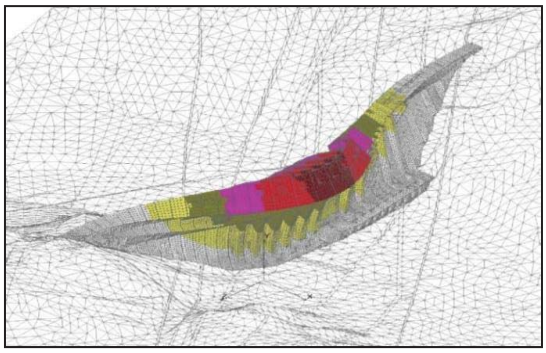

Eigenmode 1

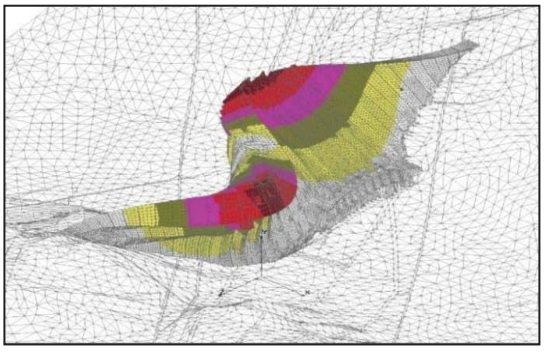

Eigenmode 2

№	Eigenfrequency, Hz
1	2.36363
2	2.97863
3	3.64903
4	4.46176
5	4.67067
6	4.94915
7	5.27794
8	5.66011
9	5.90950
10	6.14251

- Eigenfrequencies of the dam with added masses of water.
- First eigenfrequency without added masses of water is 2.6029 Hz

Mathematical model of the dam (first stage) (Starter complex: hydraulic unit No 1, upstream level 189 m)

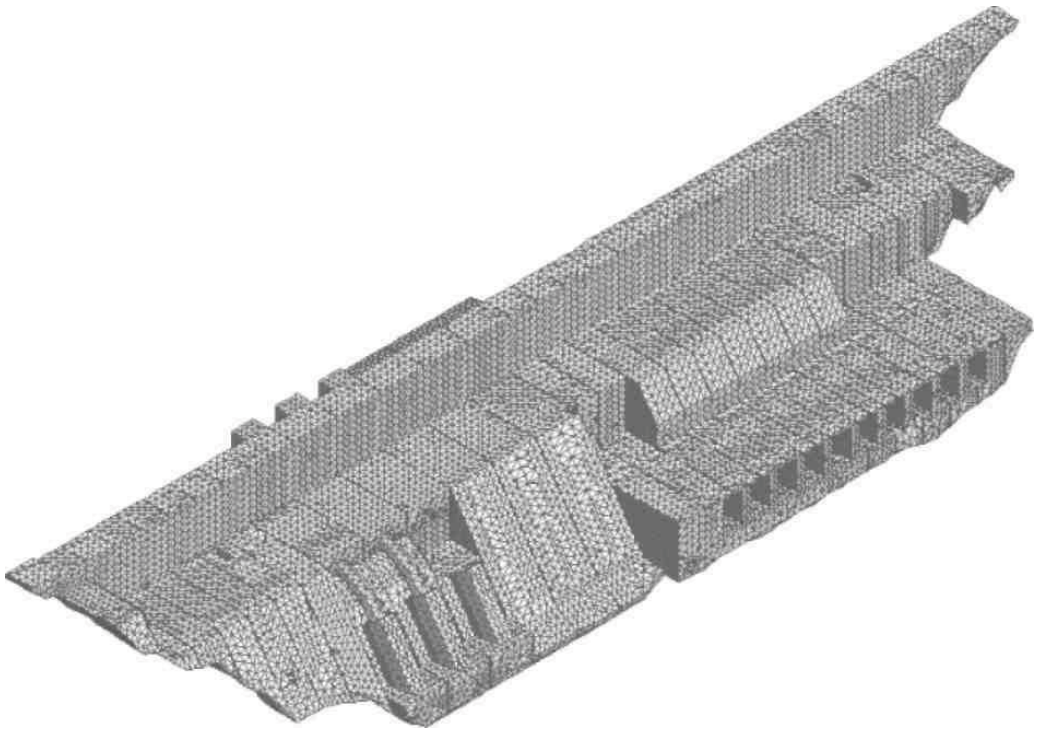

General view

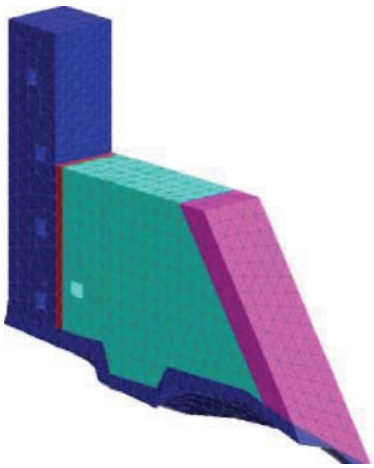

Section with rolled concrete

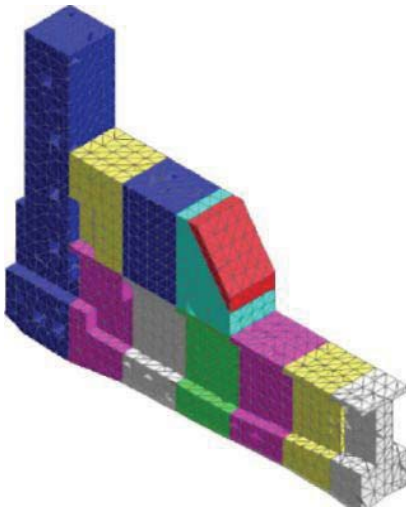

Section of columnar cutting

Eigenpairs of the first stage of the dam

(Starter complex: hydraulic unit No 1, upstream level 189 m)

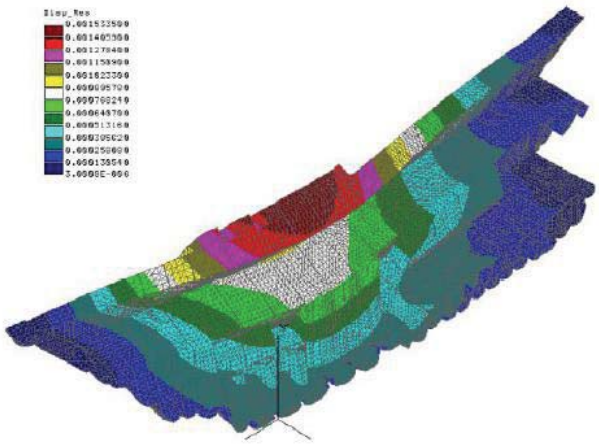

First eigenmode. General view

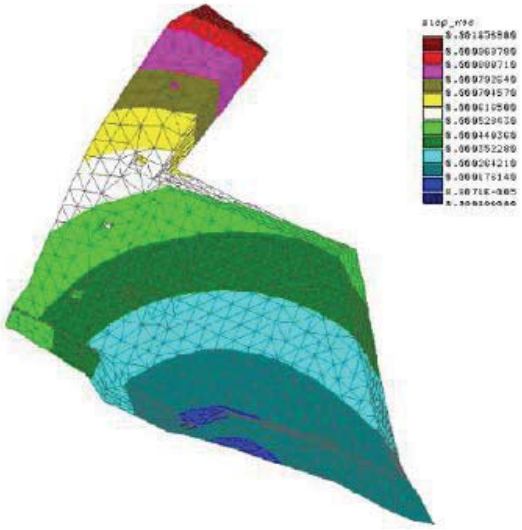

First eigenmode for section 16

Eigenfrequencies of the dam

№	f, Hz, reservoir is free from water	f, Hz, the water masses are taken into account
1	3.14578	2.96743
2	3.93255	3.71777
3	3.97752	3.91784
4	4.23837	4.19916
5	4.80707	4.57176
6	5.08849	4.99630
7	5.33173	5.10247
8	5.55601	5.48627
9	6.10052	5.83656
10	6.53034	6.22719

Completely built up dam

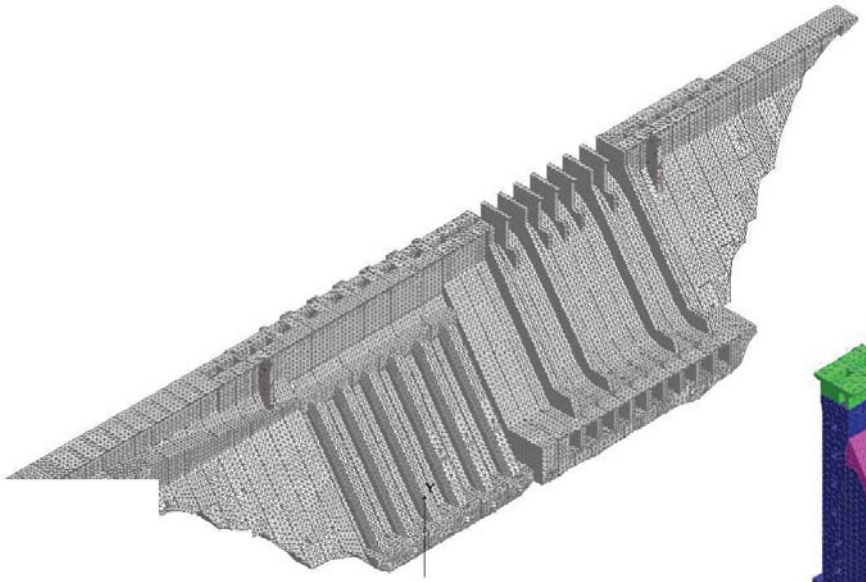

General view

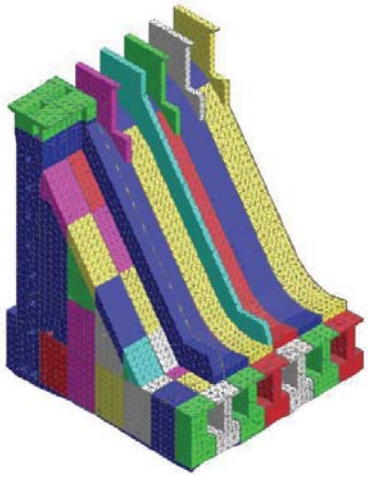

Spillway sections 24-30

- Numberofelements 602871
- Numberofnodes 124259
- Number of degrees of freedom of 372723

First Eigenmode

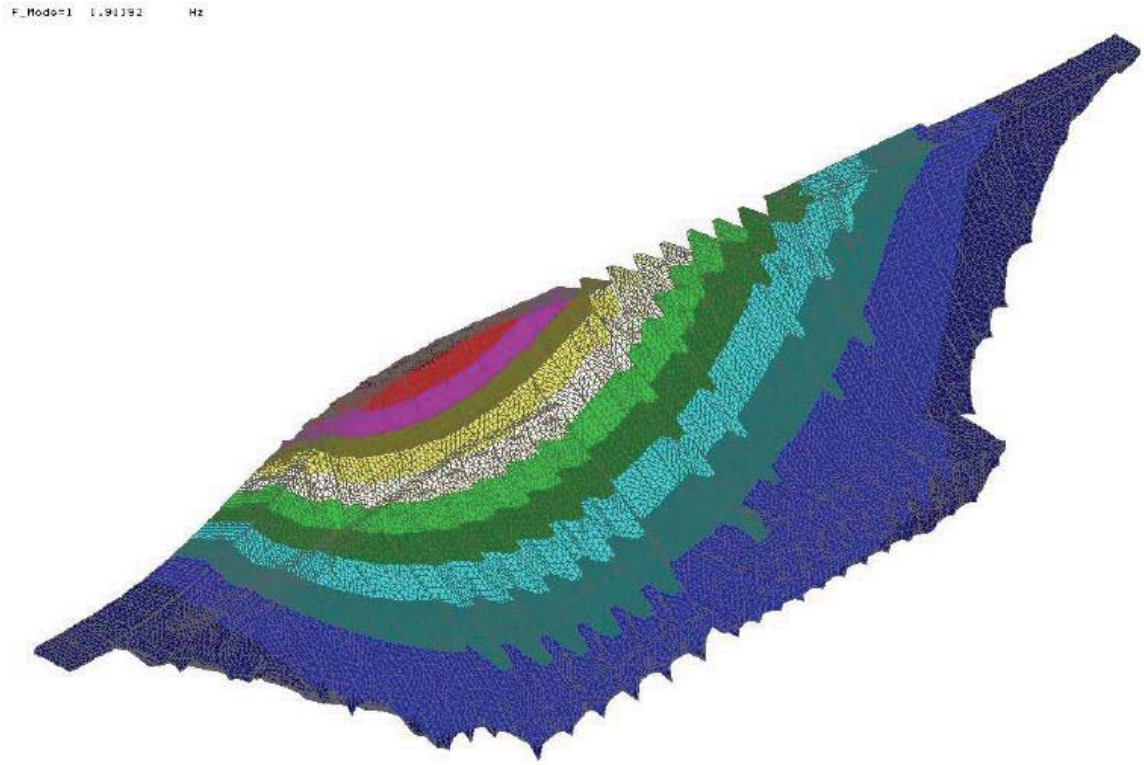

Eigenmodes 2, 3

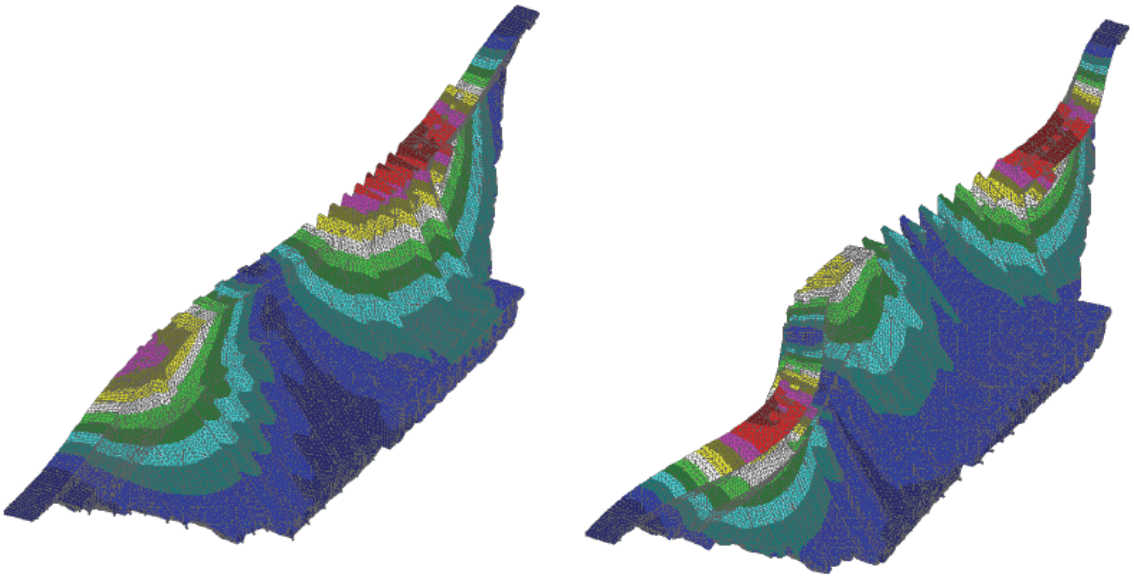

3. DYNAMIC ANALYSIS IN THE SYSTEM STRUCTURE – FOUNDATION IN PROPAGATION OF SEISMIC WAVE

$$M\ddot{q} + B\dot{q} + Kq = F = Q + R \tag{3.1}$$

$$q_s^b = q_g^b \qquad R_s(t) = -R_g(t) \tag{3.2}$$

$$v_s^b = v_g^b \quad w_s^b = w_g^b \tag{3.3}$$

$$\begin{aligned} q_g^b &= q_{0,g}^b + \Pi_{g,q}(R_g(t)) \\ v_g^b &= v_{0,g}^b + \Pi_{g,v}(R_g(t)) \\ w_g^b &= w_{0,g}^b + \Pi_{g,w}(R_g(t)) \end{aligned} \tag{3.4}$$

$$\Pi_{s,q}(R_s(t)) = -\Pi_{s,q}(R_g(t)) = -\Pi_{s,q}(R(t)) \tag{3.6}$$

$$\Pi_{s,v}(R_s(t)) = -\Pi_{s,v}(R(t)) \qquad \Pi_{s,w}(R_s(t)) = -\Pi_{s,w}(R(t)) \tag{3.7}$$

$$q_s^b = q_{0,s}^b - \Pi_{s,q}(R(t)) \qquad v_s^b = v_{0,s}^b - \Pi_{s,v}(R(t)) \qquad w_s^b = w_{0,s}^b - \Pi_{s,w}(R(t)) \tag{3.8}$$

$$\Pi_{g,q}(R(t)) + \Pi_{s,q}(R(t)) = q_{0,s}^b(t) - q_{0,g}^b(t) \tag{3.9}$$

$$\Pi_{g,v}(R(t)) + \Pi_{s,v}(R(t)) = v_{0,s}^b(t) - v_{0,g}^b(t) \tag{3.10}$$

$$\Pi_{g,w}(R(t)) + \Pi_{s,w}(R(t)) = w_{0,s}^b(t) - w_{0,g}^b(t) \tag{3.11}$$

$$\begin{aligned} R(t) &= \sum_{i=1}^{n} p_i(t) s_i = SP \\ P &= (p_1, p_2, ..., p_n)^T \qquad S = [s_1, s_2, s_3, ..., s_n] \qquad S : n_d^b \times n \end{aligned} \tag{3.12}$$

$$\begin{aligned} &q_s(t) = q_g(t) = 0 \quad v_s(t) = v_g(t) = 0 \\ &w_s(t) = w_g(t) = 0 \quad R(t) = 0 \qquad\qquad if \quad t \geq T \end{aligned} \tag{3.13}$$

$$\int_0^T R(t)\,dt = 0 \qquad \int_0^T R(t)\,t\,dt = 0 \tag{3.14}$$

$$p_i(t) = \sum_{j=0}^{N-l} \pi_{ij} \lambda(t - j\Delta t) \qquad P = \Pi\Lambda \tag{3.15}$$

$$\Pi : n \times (N - l + 1) \quad \Lambda = (\lambda_0, \lambda_1, \lambda_2, ..., \lambda_{N-l})^T \quad \lambda_j = \lambda(t - j\Delta t) \tag{3.16}$$

$$R(t)=\sum_{i=1}^{n}p_i(t)s_i \;=SP=S\Pi\Lambda=\sum_{i=1}^{n}\sum_{j=0}^{N-l}\pi_{ij}s_i\lambda(t-j\Delta t) \tag{3.17}$$

$$R(t_k)=\sum_{i=1}^{n}p_i(t_k)s_i \;=SP_k=S\Pi_k\Lambda=\sum_{i=1}^{n}\sum_{j=0,\,j\le N-l}^{k-1}\pi_{ij}s_i\lambda(t_k-j\Delta t) \tag{3.18}$$

$$k=0,1,2,...,N$$

$$Q(t)=s_i\lambda(t)\qquad \xi^b_{s,i}(t)\qquad \xi^b_{g,i}(t)\qquad \xi^b_{s,i}(t)=\xi^b_{g,i}(t)=0,\quad if\quad t\le 0 \tag{3.19}$$

$$q^b_{s,k}=-\sum_{i=1}^{n}\sum_{j=0,\,j\le N-l}^{k\;\;1}\pi_{ij}\xi^b_{s,i,k-j}+q^b_{0,s,j} \tag{3.20}$$

$$q^b_{g,k}=\sum_{i=1}^{n}\sum_{j=0,\,j\le N-l}^{k-1}\pi_{ij}\xi^b_{g,i,k-j}+q^b_{0,g,j} \tag{3.21}$$

$$\xi^b_{s,i,0}=\xi^b_{g,i,0}=0 \tag{3.22}$$

$$S^T[q^b_{s,k}-q^b_{g,k}]=0\quad k=0,1,2,...,N \tag{3.23}$$

$$q^b_{0,s,0}=q^b_{0,g,0}=0 \tag{3.24}$$

$$S^T[\sum_{j=0,\,j\le N-l}^{k-1}(\Xi^b_{g,k-j}+\Xi^b_{s,k-j})\Pi_j+(q^b_{o,g,k}-q^b_{o,s,k})]=0\qquad k=1,2,...,N \tag{3.25}$$

$$\Xi^b_{g,k}=[\xi^b_{g,1,k},\xi^b_{g,2,k},\xi^b_{g,3,k},....,\xi^b_{g,n,k}],$$
$$\Xi^b_{s,k}=[\xi^b_{s,1,k},\xi^b_{s,2,k},\xi^b_{s,3,k},....,\xi^b_{s,n,k}]:\quad n^b_d\times n$$

$$\Pi^T_j=(\pi_{1,j},\pi_{2,j},\pi_{3,j},...,\pi_{n,j})^T \tag{3.26}$$

$$A_k=S^T(\Xi^b_{g,k}+\Xi^b_{s,k})\qquad B_k=S^T(q^b_{o,g,k}-q^b_{o,s,k})\qquad A_k:n\times n \tag{3.27}$$

$$\sum_{j=0,\,j\le N-l}^{k-1}A_{k-j}\Pi_j=B_k\quad k=1,2,...,N \tag{3.28}$$

$$R(t)=\sum_{i=1}^{n}p_i(t)s_i \;=SP=S\Pi\Lambda=\sum_{i=1}^{n}\sum_{j=0}^{N-l}\pi_{ij}s_i\lambda(t-j\Delta t) \tag{3.29}$$

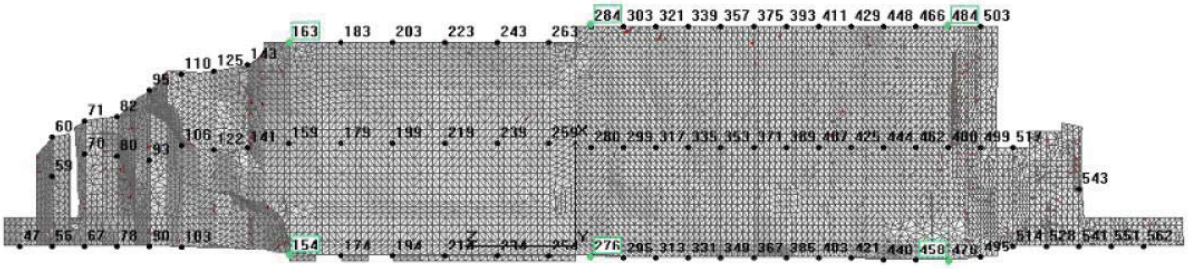

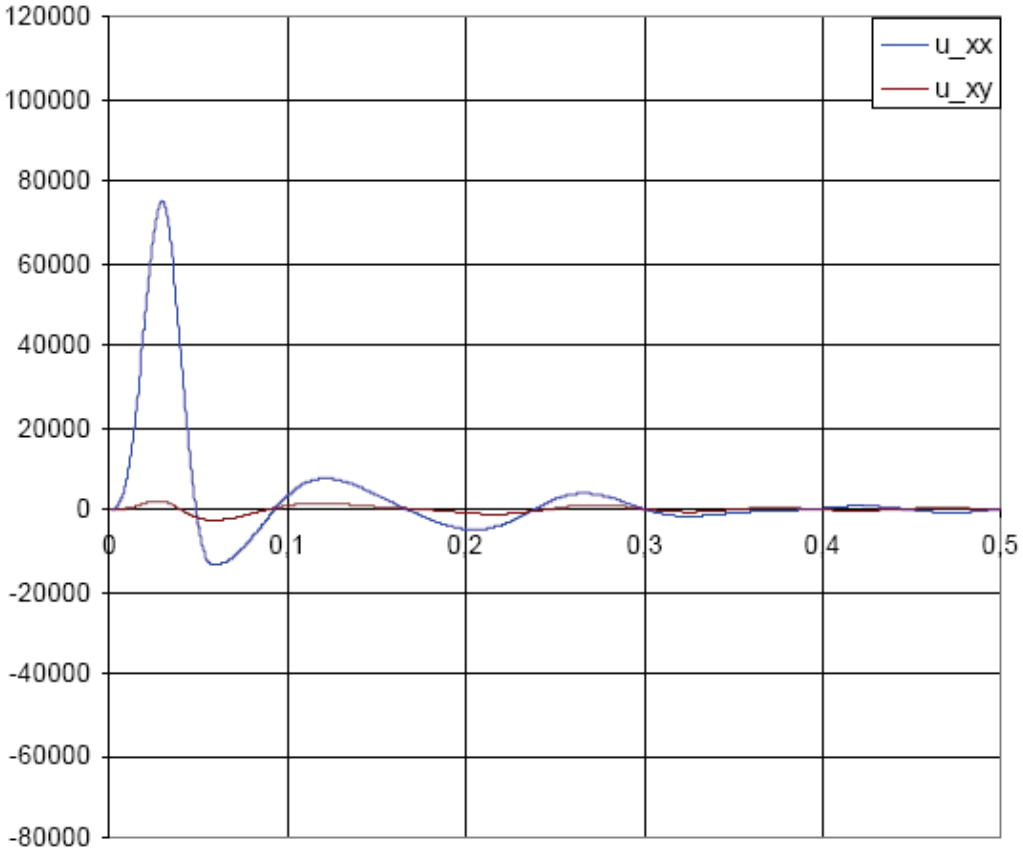

Dependencies on time of diagonal $u_{xx}(t)$ and collateral $u_{xy}(t)$ elements of the matrix of coefficients $A(t)$

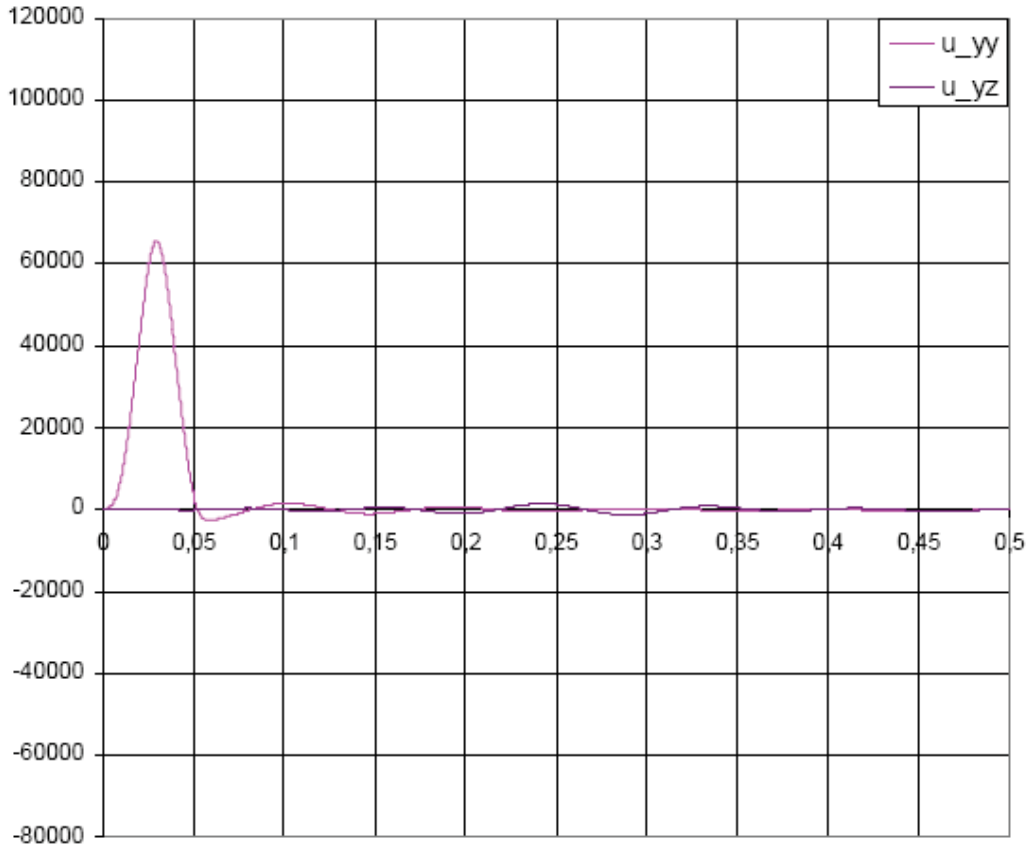

Dependencies on time of diagonal $u_{yy}(t)$ and collateral $u_{yz}(t)$ elements of the matrix of coefficients $A(t)$

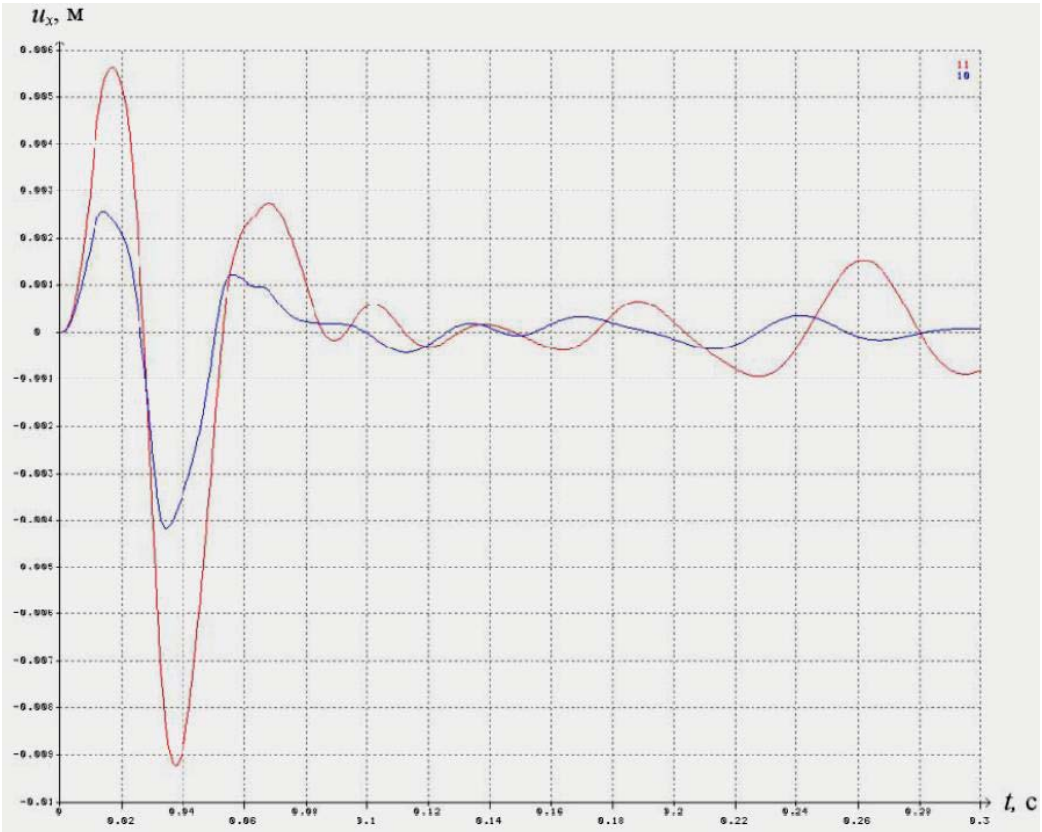

Chronograms of horizontal displacements *ux* oriented along the flow in points No 10, 11

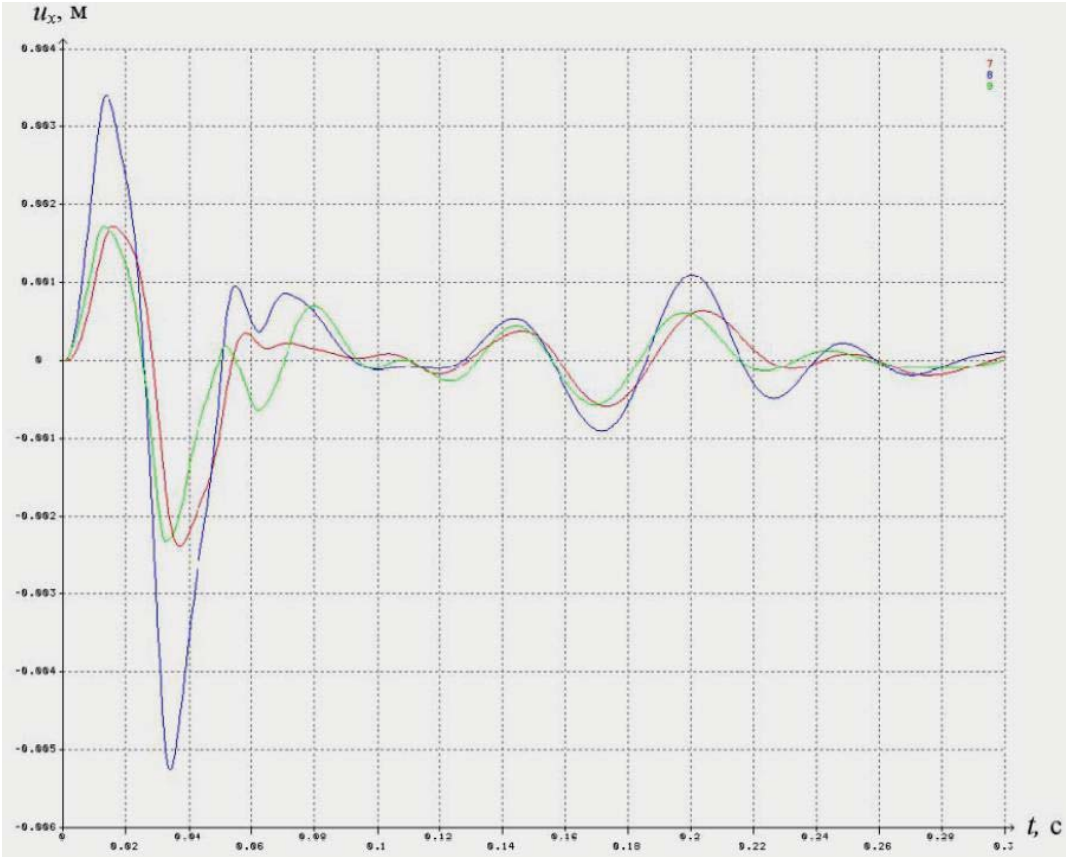

Chronograms of horizontal displacements *ux* oriented along the flow in points No 7,8,9

NUMERICAL MODELING OF CFRD BEHAVIOR

Vyacheslav Glagovsky
Deputy Director, Vedeneev VNIIG, Russia
Elena Kourneva
Engineer, Vedeneev VNIIG, Russia

ABSTRACT

Many of the constructing concrete faced rockfill dams (CFRD) are located in the regions with high seismicity. The properties of the rockfill materials, zoning of the dam body and modeling of the true soil structures behavior at various loads are important questions to assess safe operation of such dams being under the impact of strong earthquakes.

This paper presents the forecast assessment of rockfill elastic modulus influence on reinforced concrete face and dam body displacements at seismic impacts. The studies were carried using the 3D system model "dam – foundation" with applying the finite elements method (FEM). Computations were fulfilled by the programs ANSYS and LS-DYNA.

The obtained results are only of qualitative character because the analysis has been carried out for a hypothetical rockfill dam and the considered material properties have been taken by the similar ones.

INTRODUCTION

The most important questions on CFRD dam safety are needed to be solved even on the designing stage. One of the basic problems is how the reinforced face provides its reliable anti-seepage functions especially at such dams building up in the active seismic regions.

Recently some designers use the numerical analysis to predict mainly the dam displacements and as a consequence possible cracks occurrence on the face during the first reservoir impounding and to observe its behavior in the course of time [1,2]. Many authors confirmed the necessity of CFRD dams 3D analysis when it is needed to predict the concrete face and rockfill embankment deformations because at the usage of 2D analysis one can not take into consideration the 3D character of the structure behavior (load redistribution) [3].

Therefore, the multi-factor numerical 3D analysis of the soil dam behavior under seismic impacts is extremely important for the optimal selection of rockfill material characteristics to predict the values of the concrete face and dam body settlements and displacements to prevent possible crack formation.

Basing on the mentioned above the publication presents the numerical study results of the 3D system model ("dam – soil foundation") under the seismic load. The results demonstrate the influence of the local material property changes in the downstream zone of the dam body rockfill on the dam and face displacements field.

DAM MODEL

The studied variant of the 150 m high dam located on the rock foundation with the slopes of 1:1.5 and the crest width of 12 m is related to the Urgalsk HPP (the Far East of Russia) (Fig. 1). The dam body is consisted of the central (3A) and outer (3B) prisms rockfill, under-slab laying and the reinforced concrete face from the reservoir side. The dam foundation and bank slopes consist of weathered and non-weathered rocks (siltstone). The reinforced concrete slab is of variable width from 0.80 m up to 0.30 m. The slab plates are cut by vertical deformation junction in every 16 m. A perimeter joint was suggested to be on the contact of the dam with the banks.

Fig. 2 shows the 3D "dam – foundation" model and its discretization by finite elements. Totally there were about 150 thousand of the finite elements. Basically they were 8-node 3D elements and partially – 4-6-node 3D elements in the zones of the dam abutment. The slab has been simulated by the 3D shell elements.

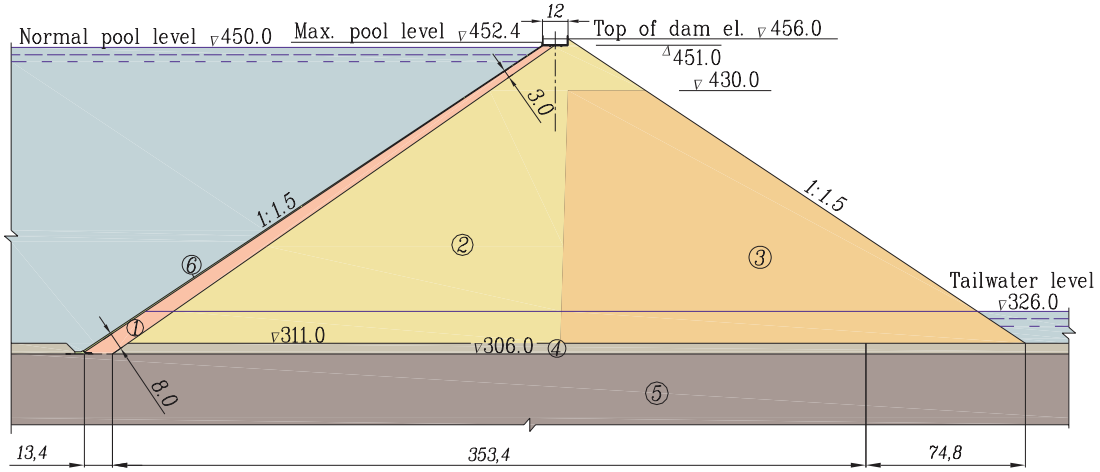

Notation: 1 – filter zone (chipping); 2 – rockfill (central embankment), zone 3A; 3 – rockfill (downstream embankment), zone 3B; 4 – weak rock; 5 – rock foundation; 6 – concrete slab.

Fig.1. Concrete faced rockfill dam cross-section

The degree of certainty of the investigation results significantly depend on plausibility of the stated conditions for the system element joints. Unilateral connections were organized on the slab and dam contacts, in reinforced concrete slab deformation joints, on the dam and banks contacts.

Boundaries of the dam foundation design area were chosen from the condition of quite long distance from the dam not to influence significantly on the structure behavior. Conditions "not to reflect" the seismic waves were stipulated for the boundaries of foundation model [4, 5].

Seismic danger of the dam area was taken as 9 according MSK - scale of earthquake intensity. The accelerogram of 40 s long was used to model such impact on the dam.

The seismic impact was simultaneously assigned by three-component accelerogram applied to the design area foundation (in original rocks). The accelerogram of "Whittier Narrows, CA, 1987" earthquake were taken as the initial ones. It was normalized conformably to the given soil conditions and was evaluated to the depth corresponding to the design model foundation (see Fig. 3). According to the recommendations of the Russian Construction Norms

the reservoir pressure on the dam was taken into account by the added water mass on the area corresponding to wetted slab surface.

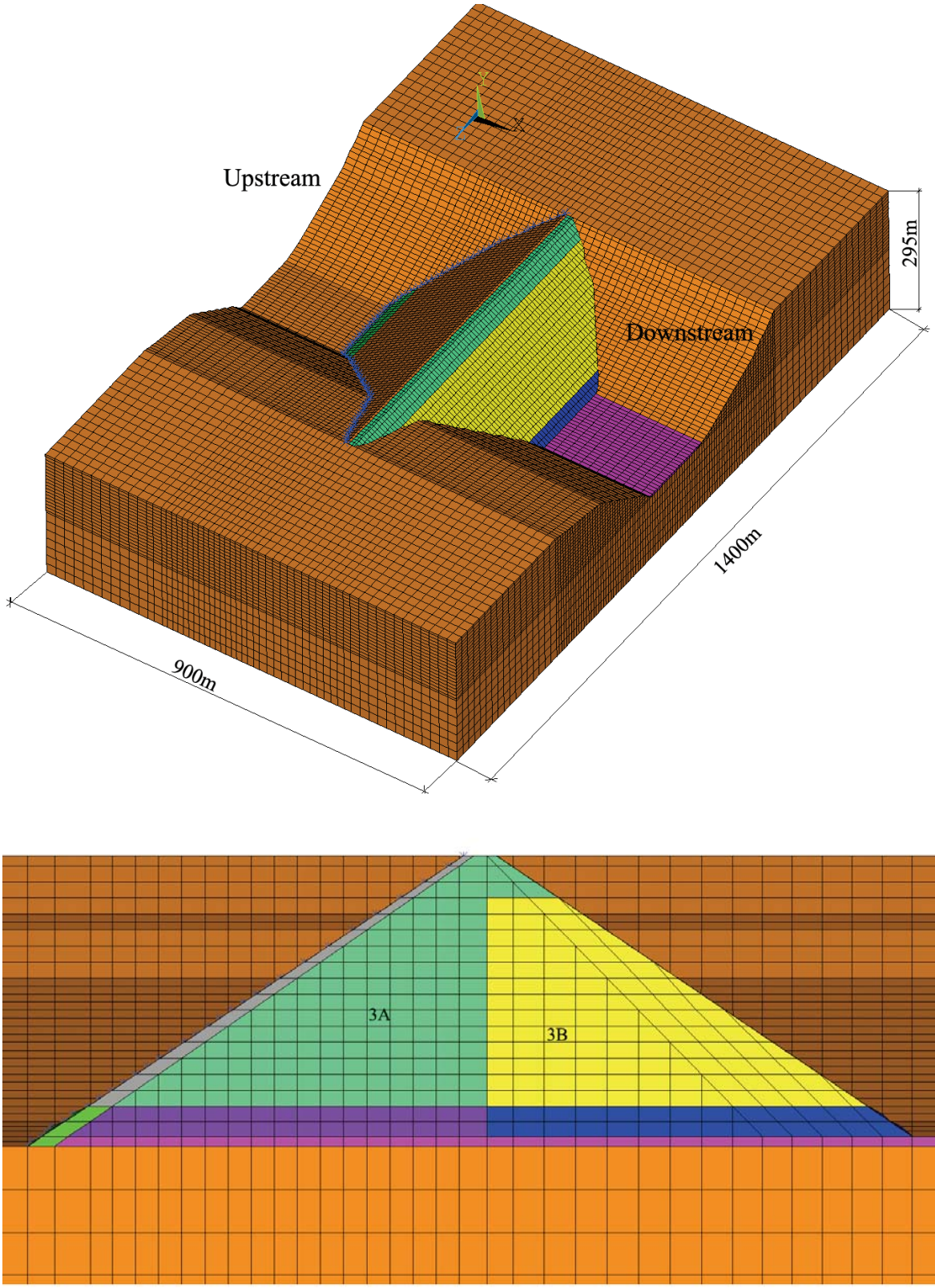

Fig.2. Three-dimension dam model

a)

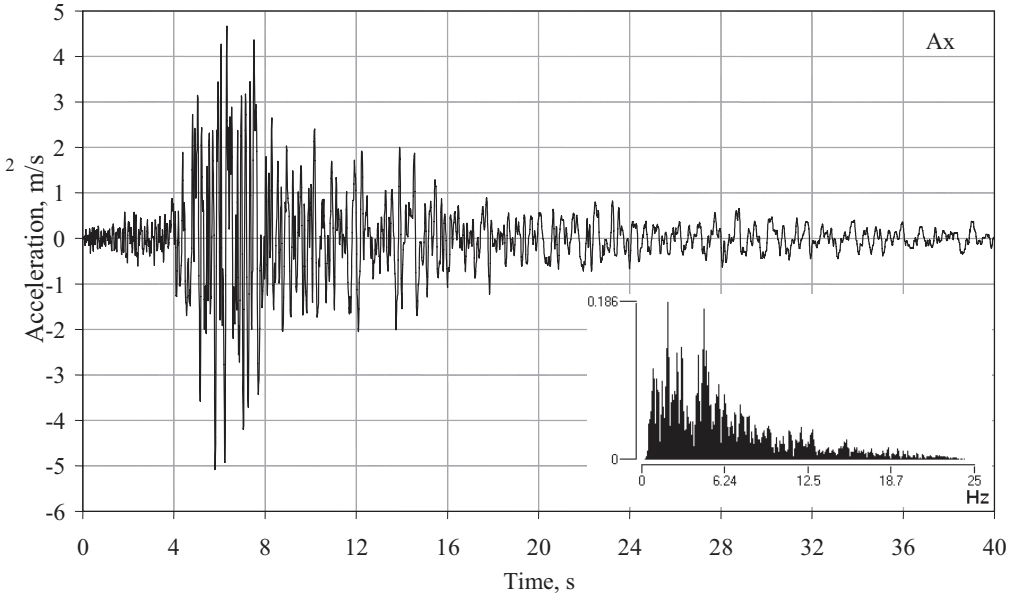

b)

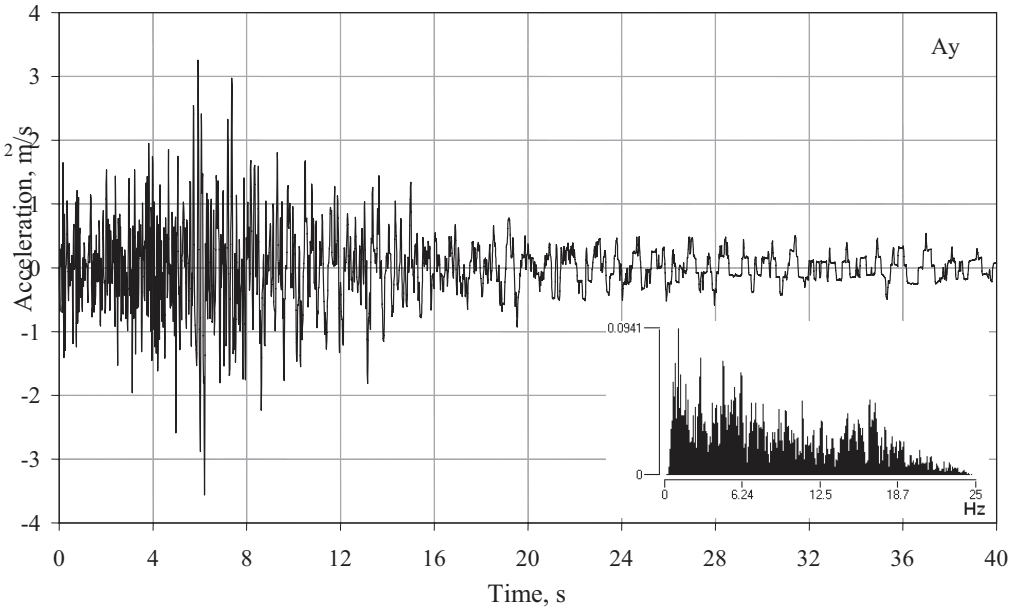

Fig. 3. Input base accelerogram and spectrum:
a) - horizontal component; b) - vertical component

PROPERTIES OF ROCKFILL

The accepted material properties of the dam are presented in table 1. The deformation moduli to be evaluated were accepted by the analogous data. For the studies there were

evaluated three variants of the dynamic problem where the different deformation modulus of the dam downstream rockffill was taken for every variant. For the first variant the modulus was accepted as equal to 40 MPa, for the second – 44 MPa and for the third – 53 MPa where the relationship of the deformation modulus were 2.0, 1.8 and 1.5 correspondingly.

Table 1

	Static			Dynamic
Material	E, MN/m^2	ν	ρ, kg/m^3	E, MN/m^2
Concrete slab	33750	0.3	2300	
Transition	120	0.2	2210	1800
Rockfill central embankment	80	0.2	2160	1200
Rockfill downstream embankment	40	0.2	2120	600
	44	0.2	2120	660
	53	0.2	2120	795
Weak rock	1000	0.3	2740	5000
Rock foundation	6500	0.3	2820	19500

ANALYTICAL PROCEDURES

The analyses were performed by finite element method using the ANSYS software for the static analysis, and LS-DYNA software for the seismic analysis. First, static loading of dam weight and hydrostatic pressure were taken into account. Then the calculation at seismic action was carried out by the method of solving the system of differential dynamic equilibrium equations using direct step-by-step integration by LS-DYNA.

RESULTS AND DISCUSSION

The accelerations used in the evaluation have got the peak values of 0.5 g for the horizontal component and 0.35 g for the vertical one. Fig. 4 and 5 demonstrate the horizontal acceleration component on the dam crest (point A) and foot (point B) for three variants of the evaluated problems. The maximum acceleration on the crest for the horizontal and vertical component is 3-4 times more in comparison with the acceleration along the dam foot.

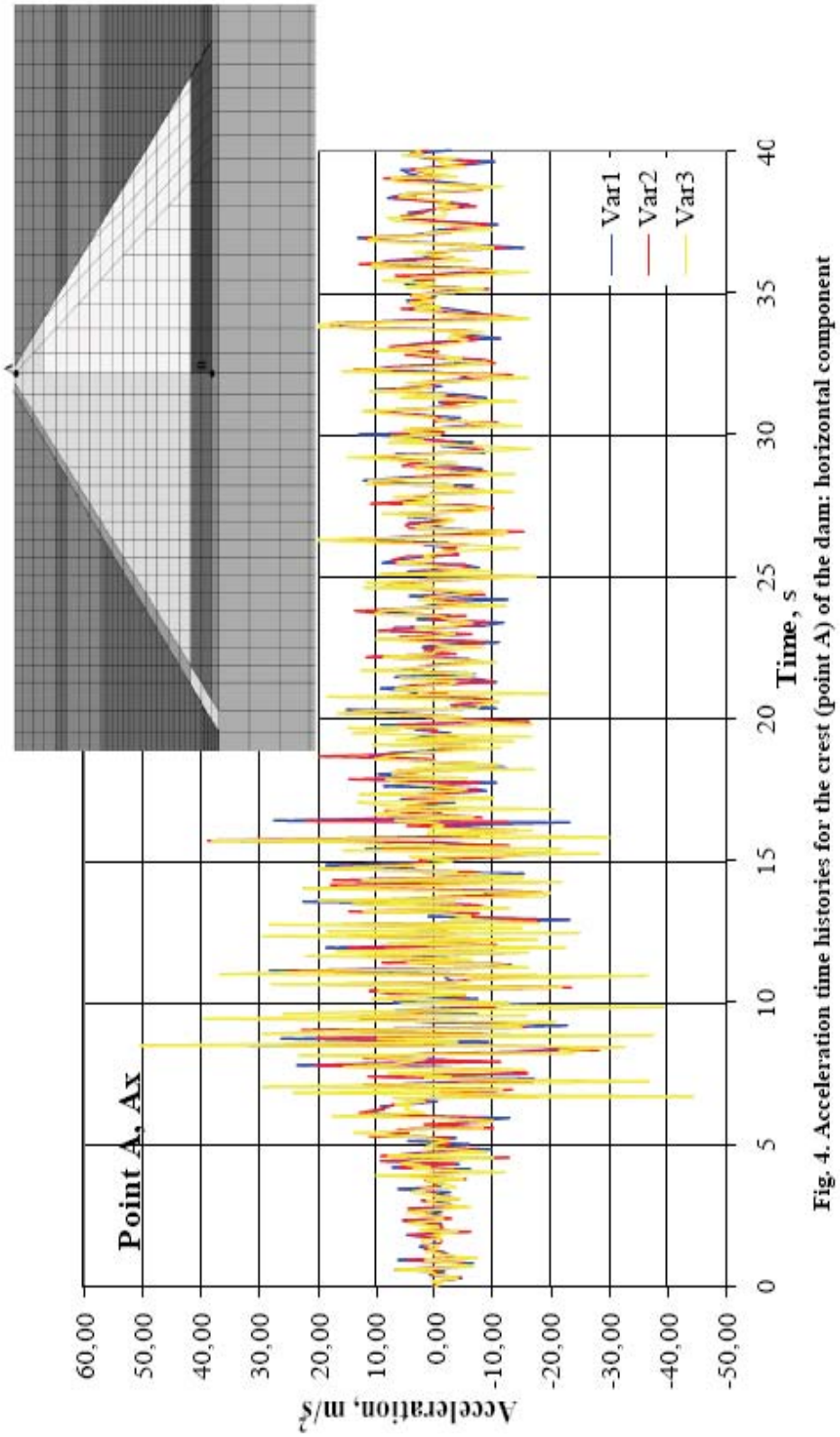

Fig. 4. Acceleration time histories for the crest (point A) of the dam: horizontal component

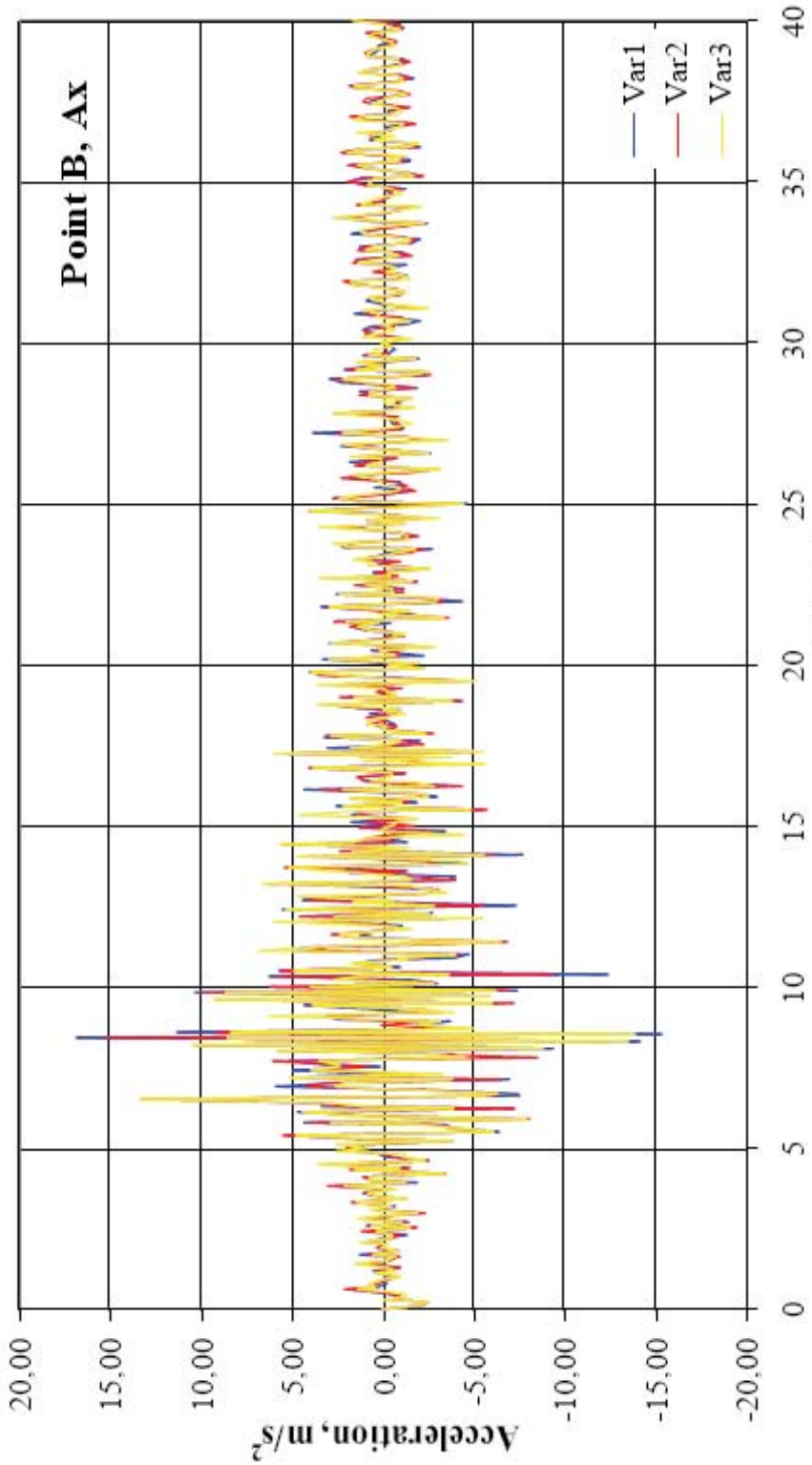

Fig. 5. Acceleration time histories for the foot (point B) of the dam: horizontal component

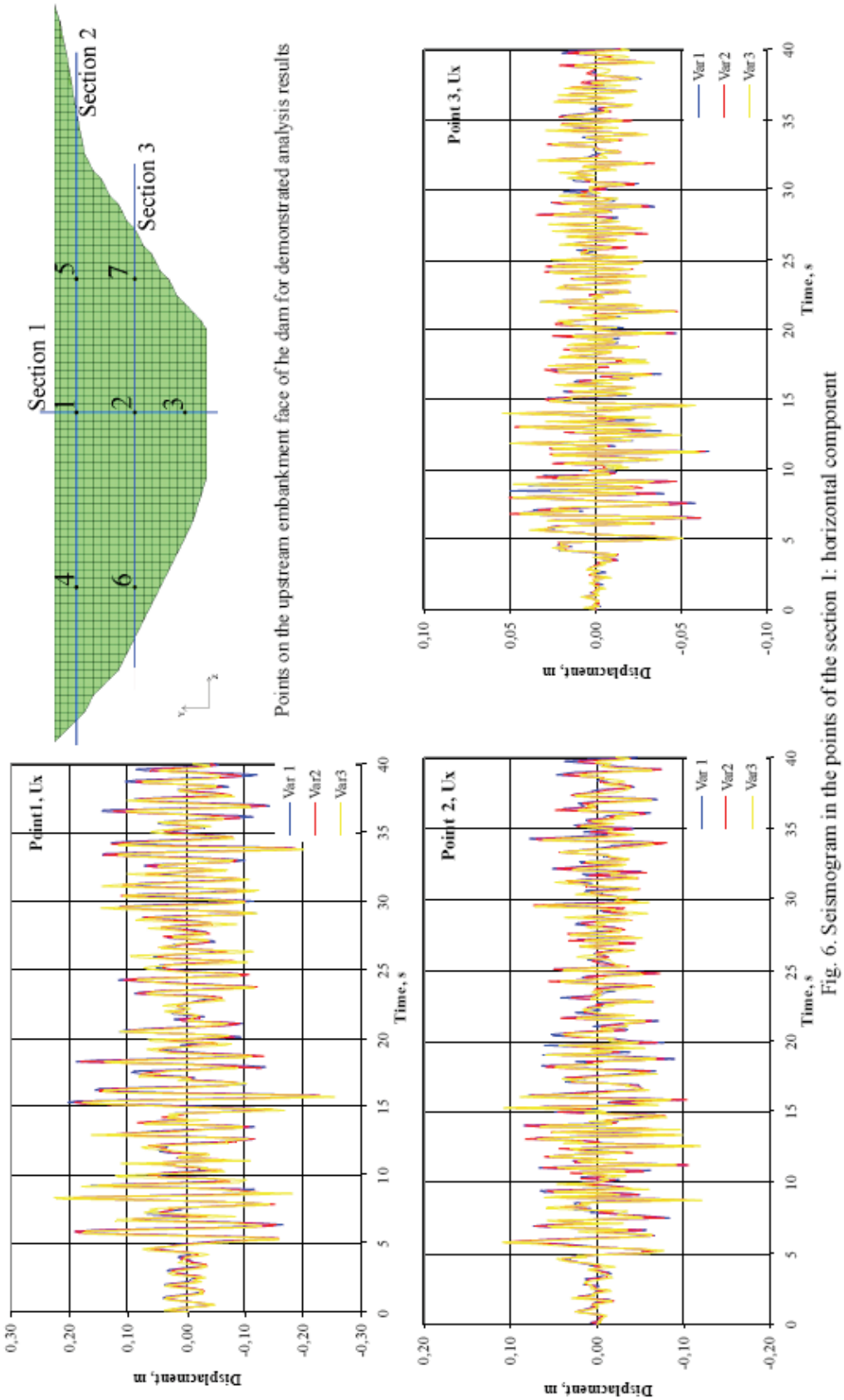

Fig. 6. Seismogram in the points of the section 1: horizontal component

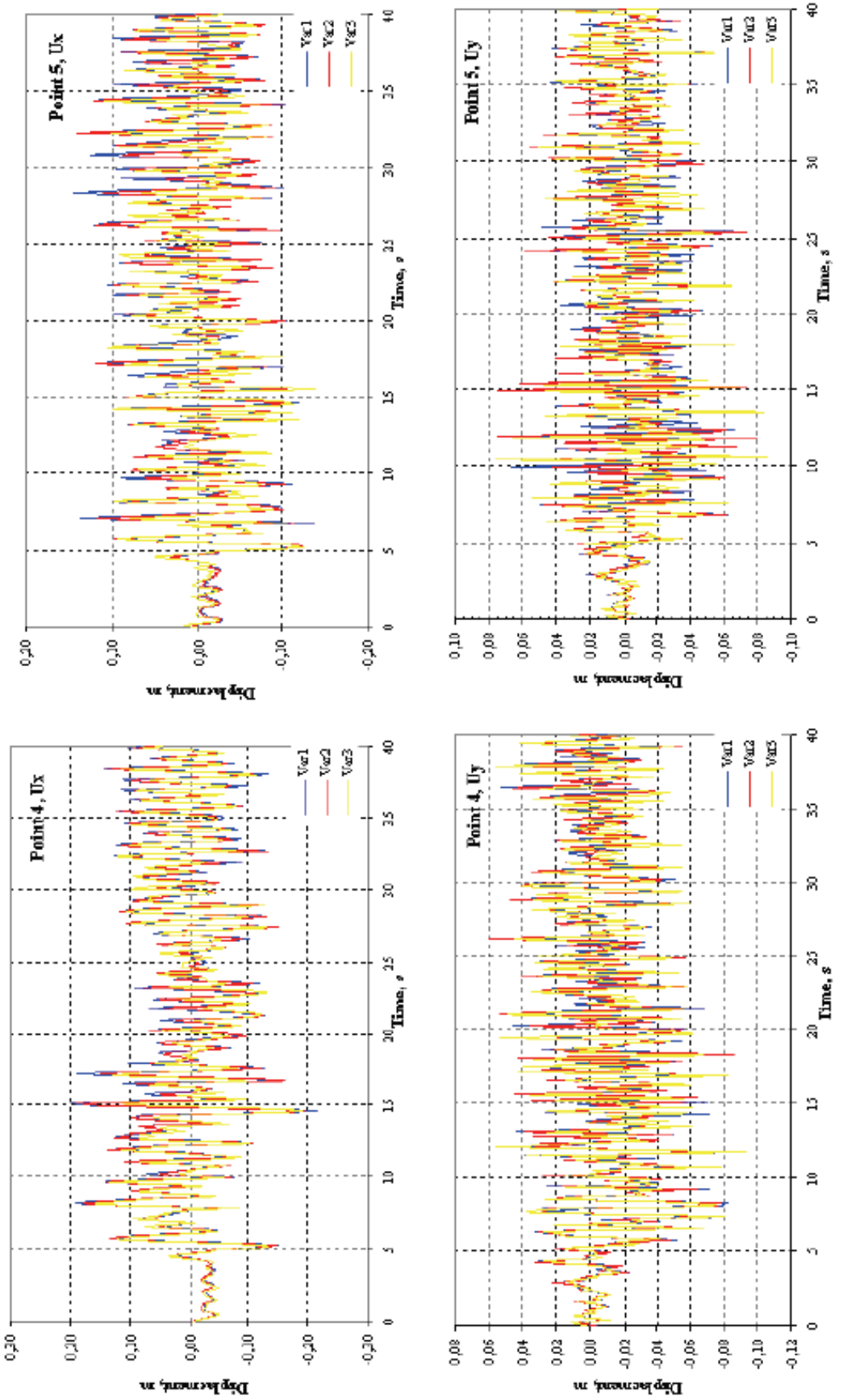

Fig. 7. Seismogram in the points of the section 2: horizontal and vertical component

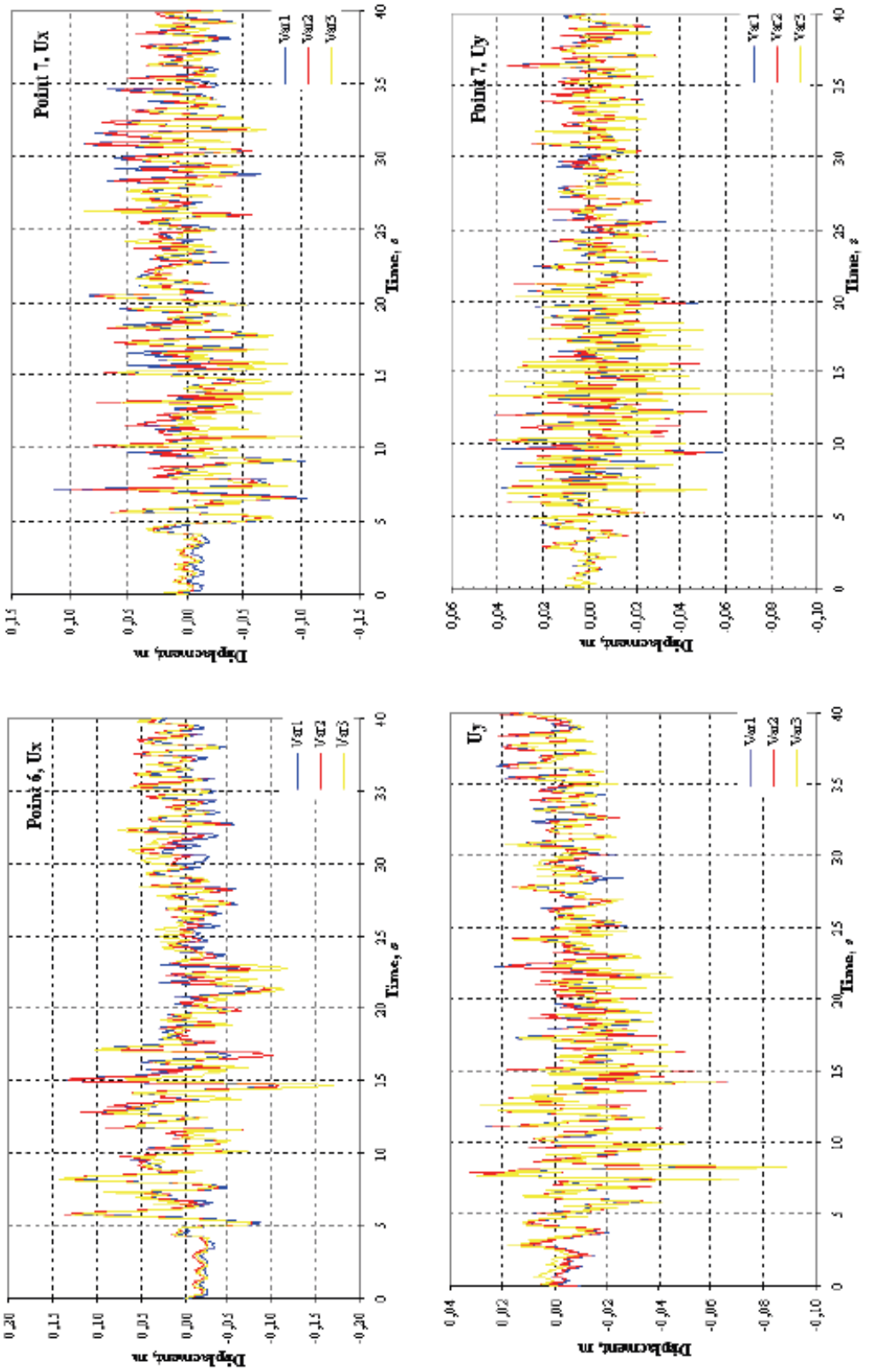

Fig. 8. Seismogram in the points of the section 3: horizontal and vertical component

Three cross-sections and the corresponding points of the cross-sections were chosen to analyze the displacement results. All points are located on the dam upstream side between the face and transition zone.

Fig. 6 shows the changes of the horizontal displacements in time in the selected points of the cross-section 1 (central). The figures demonstrate that displacements are decreasing by height in 3.5 times approximately. One can also note that the third variant gives the greatest displacement value, about 25.3 cm, in the point 1 near the dam crest on the 15.6 second of the earthquake and has got more oscillation amplitude in comparison with the variant 1 where the displacements were of 15.7 cm on the same second (that in comparison with the variant 1 is 1.6 times more). The vertical displacements in the selected points were also considered. They are also decreasing by height in 3 times approximately from the value of 12 cm in the point 1 up to 3.2 cm in the point 3 for the third variant.

Comparing the obtained results in the points 5 and 6 of the cross-section 2 (Fig. 7) it can be seen that the maximum horizontal displacements are about 21.4 cm on the 14.6 second of the earthquake in the point 5 (left bank) whereas in the point 6 (right bank) they are equal to 11.5 cm, these maximum displacements having been obtained for the variant 1. Whereas the maximum values of the vertical displacements are determined in the points 5 and 6 and are of 9.3 cm and 4.5 cm correspondingly for the third variant. The variant 1 solution gives similar displacement data.

The following considered results for the cross-section 3 (Fig. 8) demonstrated the same relationships as for the cross-section 2. Maximum horizontal and vertical displacements were received for the variants 1 and 3. So the maximum horizontal displacements in the point 6 (left bank) were 17 cm on the 14.6 second of the earthquake and at the same moment they were equal to 7.4 cm in the point 7 (the third variant).

Comparing all obtained results one can make the following preliminary conclusions: when the deformation modulus of the downstream dam embankment is 40 MPa (the variant 1) the dam is more oscillating at the banks, the left bank being displaced by greater value than the right bank, whereas when the modulus is equal to 53 MPa (the variant 3) the most displacements are observed in the central dam part.

At seismic impact the concrete face was basically contacted with its foundation because of the hydrostatic reservoir pressure. The face can lose contact with the rockfill in the one third upper part of the face. Here the design solution will be needed to provide strength of this zone.

CONCLUSIONS

- At CFRD designing the special attention should be paid to assigning the material properties for the dam rockfill;
- For the designing the dam site choice is of great importance (i.e. the slope in the place of dam and bank conjugation);
- The full problem statement requires solving a lot of question. It is necessary to develop 3D numerical model, to take into account in the evaluations the geometrical and physical nonlinearity of the CFRD-foundation system.

REFERENCES

1. P. Marques Filho, N.L. de S. Pinto. CFRD dam characteristics learned from experience// Hydropowers & dam, Issue 1, 2005.

2. J. Antunes Sobrinho, L. Vieira Xavier и др. Performance and concrete face repair at Campos Novos// Hydropowers & dam, Issue 2, 2005.

3. A. Frutuoso, A.P. Assis et al. Numerical analysis of concrete face rockfill dam under three-dimensional conditions// Dam and Reservoirs, Societies and Environment in the 21st Century, London, 2006.

4. Lysmer J, Kuhlemleyer RL. Finite dynamic model for infinite media// Journ.Engng.Mech. Div., ASCE 1969; Vol. 95, No EM4: 859-77.

5. Lysmer J, Waas G. Shear waves in plane infinite structures// Journ. Engng. Mech. Div., ASCE 1972; Vol. 98, No EM1: 85-105.

WORKSHOP IN THE PROCESS

TECHNICAL TOUR

On Sunday, 24 June delegates and accompanying persons visited Volhovskaya HPP, one of the oldest HPP in Russia. The first project of utilization of the Volhov River for generation of electrical energy was carried out by G.O.Graftio, the prominent engineer, in 1902. In 1918 the updated project of Volhovskaya HPP was included in the GOELRO Plan and construction of HPP was started. But construction was interrupted because of the Civil War and recommenced only in1921. HPP was put into operation in December, 1926 and its installed capacity was 58 MW at the beginning.
Volhovskaya HPP is run-of-river low-head HPP. HPP consists of:

- spillway concrete dam 212m in length;
- fishway;
- power house 140m in length;
- single-lane single lock with headbay and afterbay;
- water discharge;
- ice protecting wall 256m in length.

During the World War II Volhovskaya HPP provided sieged Leningrad with electric power through submerged cable laid on the bottom of Ladoga Lake. After war the HPP was restored and its capacity was increased to 66 MW. Now the capacity is 83 MW, annual hydro generation – 347 million kW-hours. Capacity of reservoir is 36 million m^3. Waterfront is 450 m in length.
Particular feature of Volhovskaya HPP is its disposition at an angle to river banks.

On the way from Volhovskaya HPP delegates visited the historical and cultural place Staraya Ladoga and had lunch there.